Cellular targets of Kaposi's sarcoma-associated herpesvirus latency-associated nuclear antigen

by

Daniel Royston Hollyman

Supervised by Professor Chris Boshoff and Dr Paul Kellam

Thesis submitted to the University of London

for the degree of Doctor of Philosophy

The Cancer Research UK Viral Oncology Group

Wolfson Institute for Biomedical Research

Department of Oncology

University College London

Gower Street

London WC1E 6BT

ProQuest LLC
789 East Eisenhower Parkway
P.O. Box 1346
Ann Arbor, MI 48106-1346

Abstract

The latency-associated nuclear antigen (LANA1) of Kaposi's sarcoma-associated herpesvirus (KSHV) is a multi-function protein involved in maintenance of the viral episome and has been shown to interact with several proteins including p53 and pRB. It is likely that the multi-functional role of LANA1 exceeds these observations therefore the work in this thesis aimed to study LANA1 at both the transcription and protein-protein interaction level. I developed a lentiviral system for the infection of primary endothelial cells with LANA1, to analyse changes in gene expression profiles by gene expression microarrays. While the system was successfully developed, no significant changes in gene expression could be attributed to LANA1. Subsequently, using the yeast two-hybrid system and large-scale immunoaffinity purification coupled to mass spectrometry, I identified 26 novel binding partners of the KSHV LANA1 complex. The majority of these proteins have functions in splicing or mRNA processing and further analysis lead to the discovery of predominant protein domains. Several of the identified proteins, including heterogeneous nuclear ribonucleoprotein (hnRNP) A1, A2/B1, D and I, constitute members of the human H-complex. hnRNP A1, A2/B1 and D are also implicated in telomere biogenesis. I show that LANA1 binds UP1, the proteolytic derivative of hnRNP A1, which modulates telomere elongation and maintenance. Furthermore, I show an *in vivo* interaction between LANA1 and human telomerase reverse transcriptase (hTERT) and the ability of LANA1 to recover telomerase activity from cell lysates. These findings suggest a function for LANA1 in the maintenance of telomeres and may have important implications for the role of LANA1 in KSHV-related tumours. I propose models for the role of these complexes in splicing and telomere biogenesis.

Acknowledgement

I am very grateful to all of the people that made the completion of this thesis possible. I am indebted to my PhD supervisors Professor Chris Boshoff and Dr Paul Kellam for their support, patience, time and generosity. It would not have been possible to do this PhD without the support and generosity of the postdoctoral fellows and researchers in the laboratory including Tyson Sharp, Hsei-Wei Wang, Heike Laman, Stoyan Radkov and Andy Koumi. I am also very grateful for the support of my project collaborators including Soren Naaby-Hansen, Rainer Cramer, Dick Campbell, Mike O'Hare, Laurent Daviet, Pierre Legrain and Yoshio Endo. The research in this thesis was funded by Cancer Research UK.

Table of Contents

Tables

Figures

Abbreviations

aa	amino acid
AIDS	acquired immune deficiency syndrome
Amp	ampicillin
APS	ammonium persulphate
ARF	alternative reading frame
β-ME	beta-mercaptoethanol
BSA	bovine serum albumin
Cdk	cyclin dependent kinase
CMV	cytomegalovirus
CKI	cyclin dependent kinase inhibitor
DMSO	dimethyl sulphoxide
DNA	deoxyribonucleic acid
DTT	dithiotheritol
EBV	Epstein-Barr virus
EDTA	ethylenediaminetetraacetic acid
EGTA	ethyleneglycol bis-b-aminoethylether N-N-N-N Tetraacetic acid
EHV-2	equine herpesvirus 2
ESI MS/MS	electrospray ionization tandem mass spectrometry
FCS	foetal calf serum
FADD	Fas-associated death domain
FLICE	Fas-associated death domain-like interleukin-1b converting enzyme
FLIP	FLICE-inhibitory proteins
GEM	gene expression microarray
GPCR	G-protein coupled receptor
GST	glutathione-S-transferase
Hdac	histone deacetylase
HEK-293	human embryonic kidney 293
HEPES	N'-(20hydroxyethyl) piperazine N'-(2-ethanesulphonic acid)
HHV-8	human herpesvirus 8
HIV-1	human immunodeficiency virus type 1
HMVEC	human microvascular endothelial cells

HPV	human papillomavirus
HTLV-1	human T-cell leukaemia virus-1
IP	immunoprecipitation
IRF	interferon regulatory factor
KSHV	Kaposi's sarcoma-associated herpesvirus
KS	Kaposi's sarcoma
LANA1	Latent nuclear antigen
LMP	Latent membrane protein
LTR	Long terminal repeat
MALDI-TOF MS	matrix assisted laser desorption ionization – time of flight mass spectrometry
MHV-68	murine herpesvirus 68
MIP	macrophage inflammatory protein
MS	mass spectrometry
Nano-HPLC	Nano-high performance liquid chromatography
NP40	Nonident P 40/IGEPAL CA-630
O/N	overnight
ORF	open reading frame
PAGE	polyacrylamide gel electrophoresis
PCR	polymerase chain reaction
p.i.	post infection
PMSF	phenyl-methyl-sulphonyl fluoride
pRB	retinoblastoma protein
rcf	relative centrifugal force
RLU	relative light units
RNA	ribonucleic acid
RT	room temperature (22°C)
SDS	sodium dodecyl sulphate
Tween	polyoxyethylene-sorbitan monolaurate
UV	ultraviolet
bp	base pair
^{0}C	degrees centigrade
g	gram
kb	kilobase
kDa	kilodalton

Kg	kilogram
M	moles per litre
m	milli
n	nano
rpm	revolutions per minute
μ	micro
V	Volt
v/v	volume for volume
vbcl-2	viral bcl-2
v-cyclin	human herpesvirus 8 encoded cyclin
vIL-6	viral Interleukin-6
wt	wildtype
w/v	weight for volume

Amino acid code

A	Alanine
C	Cysteine
D	Aspartic acid
E	Glutamic acid
F	Phenylalanine
H	Histidine
I	Isoleucine
L	Lysine
M	Methionine
N	Asparagine
P	Proline
Q	Glutamine
R	Arginine
S	Serine
T	Threonine
V	Valine
W	Tryptophan
Y	Tyrosine

For my parents

Chapter 1 Introduction

1.1 Kaposi's sarcoma-associated herpesvirus

In 1994 the discovery of new herpesvirus DNA in Kaposi's sarcoma (KS) biopsies by representational differential analysis (RDA) led to the identification of Kaposi's sarcoma-associated herpesvirus (KSHV, also termed human herpesvirus-8[HHV-8]) (Chang *et al.* 1994). Subsequent characterisation and phylogenic analysis placed KSHV within the gamma-2 herpesviruses, genus *Rhadinovirus* (Moore *et al.* 1996b). Sequencing of the KSHV genome revealed an array of cellular homologues, alongside several unique opening reading frames (ORFs) (Russo *et al.* 1996). KSHV is a lymphotropic gammaherpesvirus that has been implicated in the pathogenesis of several malignancies, other than KS, including multicentric Castleman's disease (MCD) and primary effusion lymphoma (PEL) (Sarid *et al.* 1999).

1.1.1 Kaposi's sarcoma

1.1.1.1 Characteristics

Moritz Kaposi, a Hungarian dermatologist, originally described KS in 1872 (Kaposi 1872). Presenting primarily as vascular skin lesions in men of Mediterranean origin (Fig 1.1), KS remained overshadowed by other human malignancies until its appearance in New York and California in gay men, signalling the start of the AIDS pandemic (Centers for Disease Control 1981). KS occurs in four forms; classic KS (Mediterranean), iatrogenic KS (post-organ transplant), African endemic KS (prevalent before HIV) and AIDS-KS. Classic KS is seen predominantly in elderly men of Mediterranean origin. AIDS-KS is seen in HIV infected individuals whose continuing immunosuppression leads to an inability to control a broad spectrum of diseases.

Fig 1.1

A B

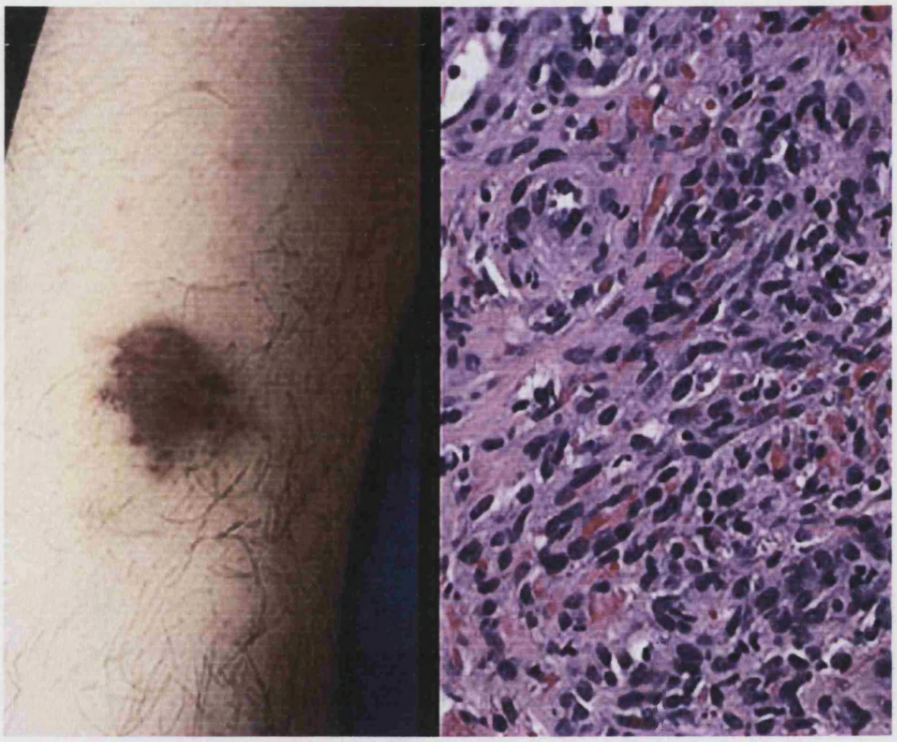

Fig 1.1 – Images of a KS lesion and KS histology
A, A KS lesion showing the characteristic vascular appearance.
B, The spindle cell morphology of KS-related spindle cells.

AIDS-KS is the most common neoplasm in AIDS patients. A further form of KS occurs due to iatrogenic immunosuppression during organ transplantation (Alkan *et al.* 1997;Kedda *et al.* 1996).

1.1.1.2 Histogenesis

The histopathology of KS is unusually complex and involves a wide range of different cell types. KS tissue also shows a high level of infiltration by inflammatory cells. The formation of KS can be divided into three distinct stages of histogenesis; patch, plaque and nodular. The early stage, also termed the patch stage, is characterised by irregular endothelial spaces around normal dermal blood vessels and is associated with a varying level of inflammatory cells. The plaque stage follows, whereby the appearance of characteristic spindle cells is first seen and finally the nodular stage occurs by the expansion of spindle cells through the dermis, culminating in the formation of vascular channels with red blood cells. The precise identity of these spindle cells remains unknown, although they are proposed to derive from the endothelial cell lineage (Boshoff *et al.* 1995a;Dupin *et al.* 1999). However, these spindle cells have also been reported to express cell surface markers of smooth muscle, dendritic cell and macrophage origin (Nickoloff and Griffiths 1989;Sturzl *et al.* 1992), inferring that the cells could represent mesenchymal precursor cells.

1.1.1.3 Epidemiology

The strongest evidence for association between KSHV infection and KS is provided by molecular epidemiological and seroepidemiological surveys. The polymerase chain reaction (PCR) is widely used to detect KSHV and to allow molecular characterisation and phylogenic analysis of the virus. This powerful tool has allowed the creation of a global picture of KSHV infection, allowing comparison with the incidence and risk of disease. Using PCR the link between KS and KSHV was established. KSHV is present in all forms of KS (Ambroziak *et al.* 1995;Boshoff *et al.* 1995b;Dupin *et al.* 1995b), but is

absent from various other skin tumours (Adams *et al.* 1995). KSHV is almost universally present in archival KS biopsies (Cathomas *et al.* 1996;Uthman *et al.* 1996). Seroepidemiological studies of KSHV have been conducted in various areas of the world. A summary of these findings are shown below.

North America and Northern Europe

Serological assays, which detect the presence of anti-KSHV antibodies, provide evidence for close association between KSHV and KS. Homosexual AIDS-KS patients show 88% seroprevalence by immunofluoresence assay (IFA) for KSHV, compared to 30% in homosexual AIDS patients without KS (Gao *et al.* 1996b). No HIV-infected patients with haemophilia or HIV negative blood donors tested positive for anti-KSHV antibodies (Gao *et al.* 1996b). In normal blood donors the incidence of KSHV is low <1%. These data suggest that KSHV may be sexually transmitted (Kedes *et al.* 1996).

Mediterranean Europe

Classic KS is primarily associated with elderly Mediterranean men (Franceschi and Geddes 1995). In Italy a higher prevalence of anti-KSHV latency-associated nuclear antigen (LANA1) antibodies was detected in blood donors than in Northern Europe and North America, which correlates with the increased incidence of KS (Whitby *et al.* 1998). Strikingly, the incidence of KS within Italy strongly mirrors the geographical distribution of KSHV (Whitby *et al.* 1998). Direct comparison between blood donor isolates from North America and Italy again shows a higher incidence of KSHV in Italian donors (Gao *et al.* 1996b). In Israel, the seroprevalence of KSHV also correlates with the incidence of KS in Sephardic and Ashkenazi Jews (Davidivici *et al.* 1999).

Africa

The seroprevalence of KSHV may also vary within a geographical area on the basis of race. In South Africa, a cohort of black cancer patients (no.=3591) was tested for the presence of KSHV antibodies by IFA against LANA1 (Sitas *et al.* 1999). Black cancer patients had a higher seroprevalence of KSHV than Caucasians had within the same area (Sitas *et al.* 1999). Seroprevalence increased with age, number of sexual partners, and decreasing levels of education (Sitas *et al.* 1999). In a small sub-group of cancer patients that had KS, 83% tested positive for KSHV antibodies (Sitas *et al.* 1999).

1.1.1.4 KS and KSHV

The pattern of infection suggested early on in the appearance of KS in AIDS patients that an infectious agent may be involved (Beral *et al.* 1990). While KS was rarely seen in HIV-infected haemophiliac and intravenous drug users, it was more commonly seen in heterosexually acquired HIV patients and most commonly seen in homosexual and bisexual men (Beral 1991). The appearance of KS therefore appeared to be linked to sexual practices, suggesting a role for a sexually-transmitted pathogen (Beral *et al.* 1990). A direct role for KSHV in the aetiology of KS has been proposed, as the presence of KSHV in HIV positive patients is a strong predictive factor for the development of KS (Whitby *et al.* 1995). In the majority of AIDS-KS patients, seroconversion against KSHV occurs prior to the clinical appearance of KS, further supporting a role for the virus in KS aetiology (Gao *et al.* 1996a). KS is a particularly vascular tumour, characterised by the involvement of endothelial blood vessel cells. To play a role in KS formation, KSHV must be able to infect and express viral genes within endothelial cells. This was confirmed when KSHV DNA was detected in KS tumour cells, but not in other non-KS skin tumours (Boshoff *et al.* 1995a;Staskus *et al.* 1997).

1.1.1.5 KS and HIV

AIDS-KS tumour cells express a broad array of cytokines that produce angiogenic, autocrine and paracrine effects (Ensoli *et al.* 1989). Histologically, AIDS-KS tumour cells show evidence of inflammation (Samaniego *et al.* 1995). KSHV encodes a variety of genes with cytokine activities including macrophage inflammatory proteins (vMIPs) and a viral interleukin-6 (vIL-6). The production and subsequent effects of these chemokines may play a significant role in KS pathology, as vMIP-I and vMIP-II both have angiogenic properties (Boshoff *et al.* 1997). The role of vMIPs in angiogenesis during KS and Multicentric Castleman's disease (MCD)(see section 1.1.2) formation may be synergistic with other factors including vascular endothelial growth factor (VEGF) and IL-6 (Boshoff *et al.* 1997).

The epidemiological link between HIV-1 and KS has been well documented, highlighting a strong correlation between HIV and the formation of KS (Sitas *et al.* 1997). Initially it was assumed that the role of HIV in AIDS-KS pathogenesis was limited to the destruction of the immune system. A more direct role for HIV in KS pathogenesis has become apparent. Acute infection of T-cells can lead to the extracellular release of Tat, which can stimulate the growth of vascular spindle cells from HIV positive KS lesions (Barillari *et al.* 1992;Ensoli *et al.* 1993). It has also been proposed that HIV Tat can stimulate the replication of KSHV between 3 and 20 fold, in a wide range of KSHV positive cell lines and in primary cells (Harrington, Jr. *et al.* 1997).

Lymphoproliferative disorders

Although the discovery of KSHV was linked closely to the study of KS (Chang *et al.* 1994), there are other human malignancies associated with KSHV. KSHV is believed to play a central role in the development of two lymphoproliferative disorders; a subset of multicentric Castleman's disease (MCD) and body cavity based primary effusion lymphoma (PEL).

1.1.2 Castleman's disease

1.1.2.1 Characteristics

Castleman's disease (CD) describes a polyclonal lymphoproliferative disorder, with a poorly understood aetiology (Castleman *et al.* 1956).

1.1.2.2 Histogenesis

The clinical formation of CD can be identified as one of two distinct variants. These variants, termed hyaline vascular and plasma cell are identified by their histopathology. The hyaline vascular form is predominant and is usually a localised solitary mass in the mediastinum or retroperitoneum (Boshoff 1999). The systemic plasma cell variant of CD, also termed Multicentric Castleman's disease (MCD), is characterised by general lymphadenopathy and B cell symptoms and can occur in both HIV positive and HIV negative patients (Boshoff and Weiss 1998). The formation of CD and MCD may be cytokine driven. Human IL-6 is detectable at high levels in biopsies, and soluble IL-6 is present in the high levels in the circulating blood of MCD patients.

1.1.2.3 Epidemiology

Detection of KSHV in MCD was first described in biopsies from a cohort of French patients (Soulier *et al.* 1995). All biopsies taken from HIV-positive patients suffering from MCD showed the presence of the

virus (14/14), whereas a lower ratio (7/17) was seen in biopsies from HIV-negative patients (Soulier *et al.* 1995).

1.1.2.4 MCD and KSHV

Following the initial studies by Soulier et al, other groups have since confirmed the presence of KSHV in MCD (Barozzi *et al.* 1996;Dupin *et al.* 1995a). The relationship between KSHV and MCD has been formalized by the discovery that KSHV is associated with a distinct variant of MCD (Dupin *et al.* 2000). Monoclonal antibodies against LANA1 were used for immunohistochemistry studies on MCD revealing an association with micro-lymphoma formation in the mantle zone of B cell follicles (Dupin *et al.* 2000). As KSHV is detectable only in B-cell lineage derived plasmablasts of MCD, the KSHV-related form is termed plasmablastic MCD (Dupin *et al.* 2000). These distinctive plasmablasts are not present in KSHV-negative MCD and may therefore represent a virus specific form of the disease.

Previous reports have hinted at a viral role in the cytokine driven lymphoproliferation of MCD (Peterson and Frizzera 1993). KSHV interleukin-6 (vIL-6) may play a role in the formation of MCD, as levels of cellular IL-6 are high in CD biopsies. Although the presence of KSHV vIL-6 has been confirmed in MCD, its exact role, if any, remains unclear (Parravicini *et al.* 1998).

1.1.2.5 MCD and HIV

During HAART therapy for HIV, KS often spontaneously resolves, leading to the conclusion that immune system control of KS may be important. This is not necessarily the case for MCD disease in HIV-patients. Despite treatment with HAART and lowered HIV viral load, MCD often does not resolve (Dupin *et al.* 2000;Zietz *et al.* 1999).

1.1.3 Body cavity primary effusion lymphoma

1.1.3.1 Characteristics

Primary effusion lymphoma (PEL), previously called body cavity lymphoma, presents as either a pleural or pericardial effusion of B cell origin. Usually confined to AIDS patients, PEL is a rare non-Hodgkin's lymphoma (NHL), which responds poorly to treatment and is rapidly fatal. Initially PEL was defined as an unusual type of effusion lymphoma in AIDS patients and was linked closely with the presence of EBV, but with a distinctive absence of c-myc rearrangements (Karcher *et al.* 1992;Knowles *et al.* 1989;Walts *et al.* 1990). This was unusual as the EBV associated malignancy, Burkitt's lymphoma is characterised by c-myc translocation to the Ig heavy chain locus, leading to overexpression of c-myc, a powerful human oncogene. The presence of KSHV DNA in PEL was first demonstrated by Chang et al (Chang *et al.* 1994) and later in further work by Cesarman et al (Cesarman *et al.* 1995).

1.1.3.2 Histogenesis

Despite a lack of B cell surface antigens, PEL is believed to be derived from a B cell lineage. This is indicated by the presence of clonal immunoglobulin gene rearrangement and the observation of some plasma cell differentiation (Ansari *et al.* 1996;Cesarman *et al.* 1996b;Cesarman *et al.* 1996a). All PEL lacking c-myc translocation events are positive for KSHV and lack p53 alterations (Nador *et al.* 1996).

1.1.3.3 PEL and KSHV

In comparison with KS, KSHV is present in higher copy numbers in PEL and these cells are often co-infected with EBV, suggesting a shared role between KSHV and EBV in PEL formation (Cesarman *et al.* 1995;Otsuki *et al.* 1996). KSHV DNA detected by Southern blot reveals the number of KSHV genomes as 50-150 copies per cell,

considerably higher as compared to KS (Boshoff 1999). Cell lines derived from PELs are largely latent, expressing only a subset of herpesvirus genes and not producing viral particles. However, within PEL a small percentage of lytic cells are observed (Boshoff *et al.* 1998). PEL cells have been shown to release and are dependent on several growth factors *in vitro*. Factors released from KSHV-infected PEL include human IL-10, human IL-6 and viral IL-6 (Jones *et al.* 1999). PEL cells were found to be dependent on human IL-10 and viral IL-6 for proliferation, suggesting an essential role for these factors in PEL development (Jones *et al.* 1999).

1.1.3.4 PEL and HIV

PEL occurs predominantly in advanced stages of HIV-related immunosuppresion, but are occasionally seen in HIV-negative individuals, including women (Komanduri *et al.* 1996;Nador *et al.* 1996;Said *et al.* 1996;Strauchen *et al.* 1997). However PEL, in common with KS, are seen primarily in gay men (Jaffe 1996;Nador *et al.* 1996).

1.2 KSHV transmission

The principle route of transmission for KSHV remains unknown. The epidemiology of KS has always suggested that a sexually transmitted agent may be involved (Beral *et al.* 1990). In normal blood donors the incidence of KSHV is low <1%. Early observations of AIDS patients showed those who acquired HIV via sexual contact, rather than parentally, showed a much higher incidence of KS (Beral *et al.* 1990). Data have shown that a significant proportion of KSHV-infected individuals, who have become immune suppressed due to AIDS, will develop KS (Kedes *et al.* 1996). It has also been shown through epidemiology that infection with KSHV occurs as an adult, not as a child, suggesting a link with the onset of sexual maturity (Blauvelt *et al.* 1997).

Research has been published on the presence of KSHV in semen and prostate samples. One study has shown that semen from HIV positive homosexual males, tested by nested PCR, shows 91% positivity for KSHV, in contrast to 23% in healthy sperm donors. Further testing showed the presence of KSHV in saliva and semen from KS patients (Ambroziak *et al.* 1995). However, other studies have failed to detect the presence of KSHV in semen and prostate from AIDS-KS patients and healthy donors (Corbellino *et al.* 1996;Monini *et al.* 1996). KSHV was only detected in the semen of HIV-infected homosexual men (Lin *et al.* 1995). PCR, and in particular nested PCR, are prone to false positives, which may account for the differences in these studies.

Another suggested route for KSHV is through contact with saliva. Testing of HIV-positive individuals saliva revealed the presence of KSHV (Koelle *et al.* 1997) as did the saliva from HIV-negative Italian classic KS patients (Cattani *et al.* 1999). Further, more recent studies show that KSHV is mainly present in sputum, and epidemiological evidence supports kissing as a major route of transmission (Pauk *et al.* 2000).

1.3 KSHV molecular virology

1.3.1 Viral proteins

KSHV encodes over 85 open reading frames (ORFs) and several of these proteins are unique to the virus (Russo *et al.* 1996). Viral proteins that are unique to KSHV are designated with a K and a number. The unique proteins within KSHV number K1-K15 (Fig 1.2). As with other herpesviruses, the KSHV encoded proteins are classed as lytic or latent as determined by their role in the life cycle of the virus. The main latent proteins of the virus are the viral cyclin (vcyclin), the latency-associated nuclear antigen (LANA1), viral FLICE inhibitory protein (vFLIP), viral interferon regulatory factors (vIRFs) and a transmembrane protein designated K15. The main lytic proteins that could be involved in disease formation are the viral G-protein coupled receptor (vGPCR), viral interleukin-6 (vIL-6) and viral bcl-2 (vbcl-2).

1.3.2 Latent proteins

The main latent transcript of KSHV encodes three proteins; viral cyclin (vcyclin), KSHV FLICE inhibitory protein (v-FLIP) and the latent nuclear antigen (LANA1) (Talbot *et al.* 1999). Two forms of the transcript exist as 1.7kb and 5.32kb transcripts, the smaller of which is a splice variant that lacks LANA1 (Talbot *et al.* 1999). vcyclin is a latently expressed cyclin D homologue which aids in the progression of cells through the cell cycle by forming a stable complex with cellular proteins (Cesarman *et al.* 1996b). The KSHV Flice inhibitory protein (FLIP) is a putative anti-apoptotic protein (Thome *et al.* 1997). The major latency-associated nuclear antigen (LANA1) of KSHV is a nuclear protein that plays an important role in the life cycle of KSHV (see later).

Fig 1.2

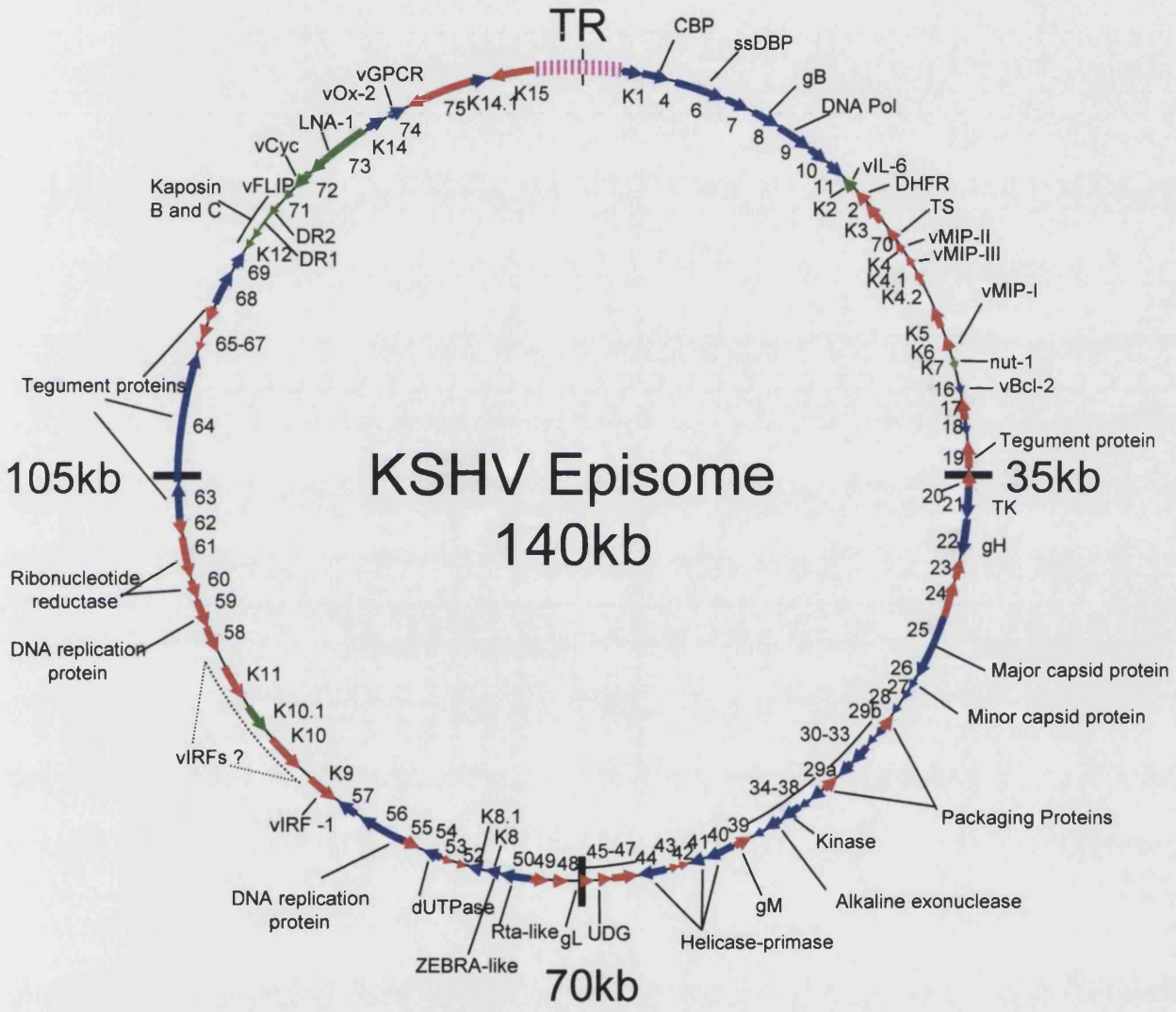

Fig 1.2 – The KSHV viral episome
Adapted from Sharp et al, IUBMB Life, 2000, Feb;49(2):pp97-104
Green arrows – latent proteins
Red arrows – lytic proteins
Blue arrows – structural/replication proteins
TR – Terminal repeats

1.3.2.1 K15

K15, positioned at the far right hand side of the viral genome, was originally identified as a spliced transmembrane protein (Rainbow *et al.* 1998). K15 was further shown to have similarities with Latent Membrane Protein (LMP) 1 and LMP2A of EBV (Glenn *et al.* 1999) and is expressed in one of two forms; predominant (P) and minor (M). P and M forms of K15 are present in 85% and 15% of viral samples, respectively (Hayward 1999). More recently K15 has been shown to be latently expressed and bind HAX-1, a novel anti-apoptotic protein, inferring a role for K15 in blocking apoptosis (Sharp *et al.* 2002).

1.3.2.2 Viral interferon regulatory factor (vIRF)

Cellular interferons are proteins produced by cells in response to viral infections. Three types of interferon are produced: α-interferon, β-interferon and γ-interferon (Challand and Young 1998). Interferon regulating factors are proteins that act as transcription factors. KSHV encodes a homologue of cellular interferon regulatory factor which has been designated vIRF. vIRF is encoded by open reading frame 9 (ORF 9) and has been shown to be a putative viral oncogene (Gao *et al.* 1997). vIRF interferes with normal cellular interferon signaling (Gao *et al.* 1997) via the repression of cellular IRF-1 mediated transcription (Zimring *et al.* 1998). vIRF-2 was identified as a 18kDa protein and was found to interact with cellular IRF-1 and IRF-2, but not IRF-3 (Burysek *et al.* 1999). vIRF-3 was identified as a 73kDa protein with homology to KSHV vIRF-2 and cellular IRF-4 (Lubyova and Pitha 2000). vIRF-3 functions as a dominant negative mutant of IRF-3 and IRF-7, which are essential for the activation of alpha and beta interferon genes (Lubyova and Pitha 2000).

1.3.2.3 Viral cyclin (vcyclin)

Cellular cyclins play an essential role in the regulation of normal cell proliferation and progression through the cell cycle. Dysregulation of a cell's normal proliferation is a major factor in the formation of malignancy. Viruses often exploit the cell cycle to use the cells' replication machinery for replication of viral DNA. There are several types of cyclins including A, D and E, each possessing different roles at different stages of the cell cycle. Cyclin D is particularly important as through an interaction with cyclin-dependent kinase 6 (cdk6) the cyclin D/cdk6 complex phosphorylates pRB. The interaction between D-type cyclin and cdk6 is transient and can be regulated by other cellular proteins termed cyclin-dependent kinase inhibitors (cdki). Active pRB is hypophosphorylated and can interact with E2F, abrogating its function. Through this mechanism pRB performs an essential role as a cell cycle regulator. The phosphorylation of pRB into its hyperphosphorylated form leads to release of E2F and progression of the cell cycle.

KSHV encodes a D-type cyclin homologue (Cesarman *et al.* 1996b), (Chang *et al.* 1996), (Li *et al.* 1997). The co-expression of vcyclin (also called cyclin K) and pRB in a pRB negative cell line (SOAS) resulted in a failure of pRB mediated cell cycle arrest (Chang *et al.* 1996). vcyclin also forms a complex with cdk6 and is capable of phosphorylating both pRB and histone H1 (Godden-Kent *et al.* 1997), however this complex is stable and is not sensitive to inhibition by cdkis (Swanton *et al.* 1997).

Cyclin K also inhibits the growth suppression activities of STAT3 by associating with it via its activation domain and preventing its DNA-binding and transcriptional activities (Lundquist *et al.* 2003).

1.3.2.4 Viral FLIP (vFLIP)

FLIP proteins were originally identified in viruses and therefore designated vFLIPs. They are present in human molluscipoxvirus (Senkevich *et al.* 1996) and in several members of the gamma herpesviruses, including Herpesvirus Saimiri (HVS) and KSHV. Regardless of virus species, the vFLIPs are structurally similar, possessing two death-effector domains. Cellular FLIP protein (FLICE-inhibitory protein) was originally identified as an apoptosis inhibitor mainly expressed in muscular and lymphatic tissues (Irmler *et al.* 1997). Two isoforms were discovered, short ($FLIP_S$) and long ($FLIP_L$), produced by one spliced transcript. KSHV has 'captured' the shorter RNA species. Through their death-effector domains both cellular and viral FLIPs interact with Fas-associated death domain (FADD) to prevent death-receptor mediated apoptosis. vFLIP has more recently been shown to activate IKappaB kinase (IKK) by binding to IKK-gamma (Field *et al.* 2003).

1.3.2.5 Latency-associated nuclear antigen (LANA1)

The structure of LANA1 is unusual and can be divided into three regions on the basis of its amino acids. LANA1 possesses a proline rich amino terminus (aa1-337), which includes the nuclear targeting domain (Piolot *et al.* 2001), an extensive central repeat region that includes a putative leucine zipper and a carboxyl terminus implicated in dimerisation of the protein (Schwam *et al.* 2000) (Fig 1.3). LANA1 and the viral episomes accumulate in heterochromatin-associated nuclear bodies and show a characteristic nuclear stippling pattern in all KSHV infected tumor cells (Dupin *et al.* 1999;Mattsson *et al.* 2002b;Szekely *et al.* 1999). One of the most important roles of LANA1 is in the persistence of the viral episome. Many DNA viruses, including EBV, Human Papilloma virus (HPV) and SV40 employ strategies for the passing on of viral episomes to daughter cells.

Fig 1.3 – Amino acid structure and protein interaction partners of LANA1

A, The structure of the KSHV latent nuclear antigen (LANA1) as predicted from primary amino acid sequence (Adapted from Lim et al, 2001). Interaction partners where precise mapping is unknown are shown underneath.

B, Interaction domains of LANA1. Proteins whose interaction has been mapped to LANA1 domains.

Key:

ATF4 (Activating transcription factor 4)

CREB2 (Cyclic AMP response element binding protein 2)

PRB (Retinoblastoma protein)

SAP30 (Sin3 associated polypeptide 30)

CIR (CBF1 interacting corepressor)

Fig 1.3

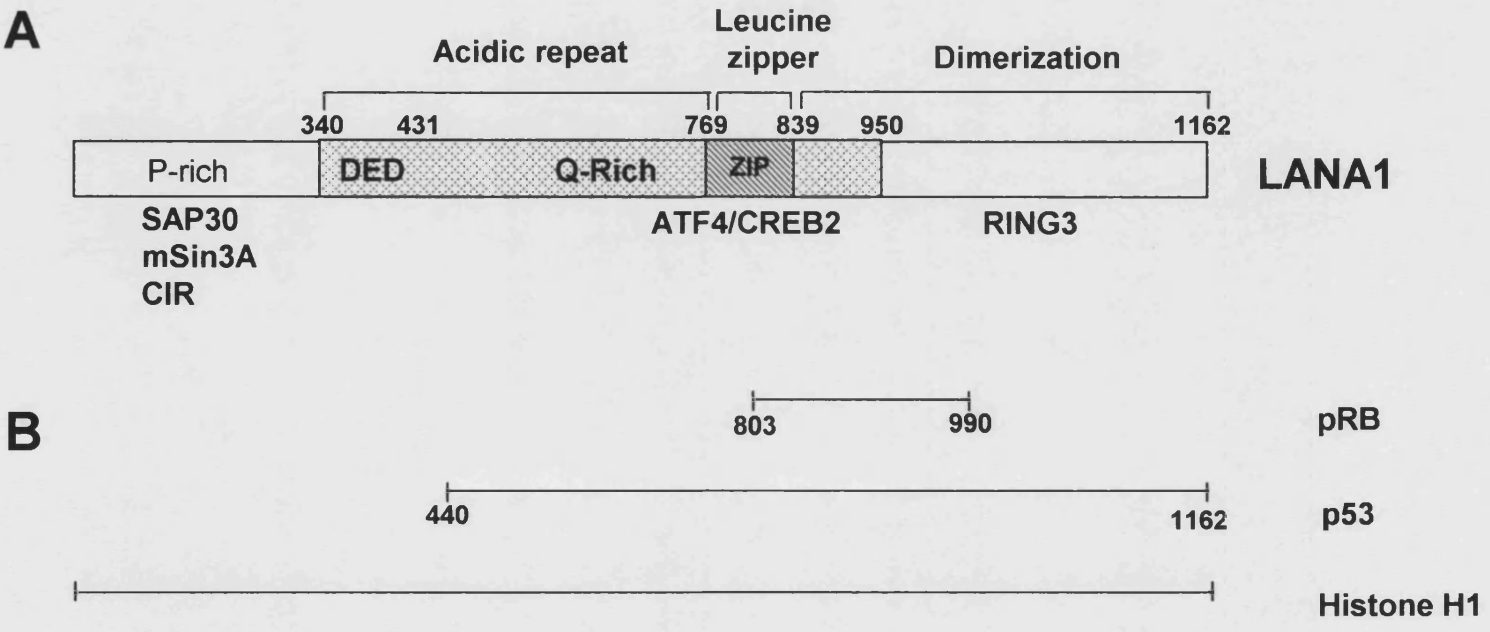
A
Acidic repeat
Leucine zipper
Dimerization
340
431
769
839
950
1162
P-rich
DED
Q-Rich
ZIP
LANA1
SAP30
mSin3A
CIR
ATF4/CREB2
RING3
B
803
990
pRB
440
1162
p53
Histone H1

LANA1 binds to heterochromatin and tethers the viral episome during latent infection, ensuring the virus persists in daughter cells (Ballestas *et al.* 1999;Cotter and Robertson 1999). The interaction of LANA1 with histone H1 is believed to be important for this function. The functional homologue of LANA1 in EBV, EBNA1, is also essential for the maintenance of the viral episome (Yates *et al.* 1985) and has been identified as a histone H1 interacting protein (Aiyar *et al.* 1998). The amino terminus of LANA1 mediates this interaction between amino acids 5-22 (Piolot *et al.* 2001). LANA1 has recently been shown, in a similar role to EBV EBNA1, to mediate the replication of plasmid DNA carrying viral terminal repeats (Grundhoff and Ganem 2003).

LANA1 has been shown to interact with a wide range of proteins and exhibits a wide range of cellular activities. LANA1 has been reported to bind proteins including p53 (Friborg *et al.* 1999), pRB (Radkov *et al.* 2000), RING-3 (Platt *et al.* 1999), ATF4/CREB2 (Lim *et al.* 2000), cAMP response element-binding protein-binding protein (CBP) (Lim *et al.* 2001) and members of the mSIN3 complex (Krithivas *et al.* 2000).

Yeast two-hybrid screening and subsequent confirmatory experiments including *in vitro* and *in vivo* binding assays identified RING3 as an interaction partner of LANA1 (Platt *et al.* 1999). RING3 is a human homologue of the drosophila female sterile hometic (fsh) gene and the interaction with LANA1 leads to phosphorylation of LANA1 (Platt *et al.* 1999). This kinase activity was not however due to RING3 and suggests a further interaction with a cellular kinase as part of the LANA1-RING3 complex (Platt *et al.* 1999).

Several well characterised viral oncoproteins have been shown to bind to p53 and pRB (summarised in Table 1.1).

Table 1.1

	SV40 Large T antigen	papillomavirus		adenovirus		**KSHV LANA1**
		E6	E7	E1A	E1B	
binds p53	+	+	-	-	+	+
binds pRB	+	-	+	+	-	+
binds Histone H1	?	-	+	?	?	+
Episomal maintenance	?	+	+	+	-	+
Transforms primary rodent cells in cooperation with a cellular oncogene	+	+	+	+	+	+

Table 1.1 - Comparison of KSHV LANA1 with other viral oncoproteins. Adapted from Boshoff and Weiss (Boshoff and Weiss 1998).

LANA1 protects against cell death by binding to p53 and thereby inhibiting its pro-apoptotic role (Friborg *et al.* 1999). The interaction between LANA1 and p53 was shown to inhibit the transcriptional activity of p53 (Friborg *et al.* 1999). pRB is an important cellular protein that plays a central role in the regulation of normal cell proliferation (see vcyclin section). As such pRB is targeted by several viral oncoproteins. LANA1 was shown to bind the hypophosphorylated form of pRB and thereby prevent its suppression of E2F and allowing progression of the cell cycle (Radkov *et al.* 2000). Furthermore, LANA1 was shown to transform primary rat embryonic fibroblasts in cooperation with the oncogene Hras (Radkov *et al.* 2000). RING3, which as discussed earlier interacts with LANA1, is also a component of the pRB/E2F complex possibly aiding in the interaction between LANA1 and pRB (Denis *et al.* 2000;Radkov *et al.* 2000).

Yeast two-hybrid was also used to identify ATF4/CREB2 (Lim *et al.* 2000) as a binding partner. Further work showed cAMP response

element-binding protein-binding protein (CBP) to be bound by LANA1 (Lim *et al.* 2001). LANA1 interacts with ATF4/CREB2, a member of the ATF/CREB transcription factor family, via its bZIP domain (Lim *et al.* 2000). Based on previous research that showed a LANA1-mediated repression of NFkB-dependent transcription, the interaction between LANA1 and CBP was tested, as NFkB used CBP as a transcriptional co-activator (Lim *et al.* 2001). An interaction between LANA1 and CBP was confirmed and through this interaction LANA1 repressed not only the transcriptional activity of CBP, but also its histone acetyltransferase (HAT) activity (Lim *et al.* 2001). Through an interaction with the proteins of the mSin3 corepressor complex LANA1 can mediate transcriptional repression (Krithivas *et al.* 2000). Yeast two-hybrid analysis identified SAP30 as an interaction partner, with further interactions between LANA1 and both mSin3A and CIR being demonstrated by glutathione-s-transferase (GST) pulldown assays (Krithivas *et al.* 2000). These interactions were shown to be mediated by amino acids 1-340 (Krithivas *et al.* 2000). LANA1 has been shown to be a potent repressor of various promoters when bound to DNA (Schwam *et al.* 2000). A further interaction with the heterochromatin-associated protein is also suggested to play a role in transcriptional repression (Lim *et al.* 2003).

Using the yeast-two system LANA1 was found to interact with a novel cellular protein, KLIP1 (Pan *et al.* 2003). KLIP1, which contains two leucine zipper motifs, represses herpes simplex virus thymidine kinase promoter activity. The presence of LANA1 prevents this transcriptional repression. This represents evidence of a cellular transcriptional repressor binding to LANA1.

LANA1 has also been shown to be a transcriptional activator of several different promoters including E2F (Radkov *et al.* 2000) and is suggested to contribute to cellular immortalisation by upregulating human telomerase reverse transcriptase (hTERT) , an essential component of the human telomerase complex (Knight *et al.* 2001).

LANA1 has also been shown to alter the transcriptional activity of other viral promoters (Groves *et al.* 2001). LANA1 can activate two major essential EBV latent promoters, the LMP and EBNA C promoters, suggesting a role for LANA1 in the modulation of EBV virus transcription in co-infected B cell lymphoma cells (Groves *et al.* 2001). Human IL-6 (hIL-6), a cytokine directly implicated in the pathogenesis of KSHV-related malignancies, is detected in KS, PEL and MCD, along with the expression of vIL-6 from the viral genome. A link between LANA1 and hIL-6 was shown when upregulation of the hIL-6 promoter was detected in the presence of LANA1 and the AP1 site was found to be required for this activity (An *et al.* 2002).

Recently LANA1 has been shown to modulate the Wnt signaling pathway (Fujimoro *et al.* 2003). β-catenin activates genes containing Tcf and Lef binding sites by forming nuclear complexes with Tcf and Lef transcription factors (Fujimoro *et al.* 2003). Screening interaction partners of LANA1 by yeast two-hybrid revealed GSK-3β as a binding partner. By binding to GSK-3β, a negative regulatory factor of β-catenin, dysregulation of the β-catenin pathway occurs. Dysregulation of the β-catenin pathway is frequently seen in cancers.

An attempt has been made to study the effects of LANA1 on the transcriptome using gene expression microarrays (Renne *et al.* 2001). This study investigated the effects of LANA1 on the activity of several synthetic promoters and found that LANA1 activated synthetic constructs containing ATF, AP1, CAAT and SP1 sites but repressed HIV-LTR and NFkB-dependent reporter genes (Renne *et al.* 2001). Results from gene expression microarrays showed limited modulation of cellular genes, including upregulation of several interferon responsive genes (Renne *et al.* 2001).

Overall LANA1 is a multifunctional protein possibly influencing a large number of cellular functions.

1.3.3 Lytic proteins

1.3.3.1 Viral GPCR (vGPCR)

KSHV GPCR and vcyclin were identified from a PEL-derived virus genomic clone (Cesarman *et al.* 1996b). KSHV GPCR (vGPCR) was confirmed as a signaling receptor with constitutive activity in the phosphoinositide-inositoltriphosphate-protein kinase C signaling pathway with homology to human cellular IL-8 receptors and a GPCR from HVS (Arvanitakis *et al.* 1997). Work on a mouse model encoding the vGPCR showed that transgenic expression in hematopoeitic cells resulted in the formation of angioproliferative lesions (Yang *et al.* 2000). The lesions appeared in several different areas including the skin, heart, skeletal tissue and intestine and resembled KS both in clinical presentation and histology (Yang *et al.* 2000).

1.3.3.2 Viral Interleukin-6 (vIL-6)

Human Interleukin-6 (hIL-6) is a cytokine that is implicated in the survival and replication of B cells. KSHV encodes vIL-6, a protein that has significant sequence similarity to that of hIL-6 (Moore *et al.* 1996a;Nicholas *et al.* 1997).

1.3.3.3 Viral bcl-2 (vbcl-2)

Cellular bcl-2 is a protein that plays a pivotal role in apoptosis. KSHV encodes a bcl-2 gene with sequence similarity to cellular bcl-2, termed vbcl-2, from ORF 16 (Cheng *et al.* 1997;Sarid *et al.* 1997). The KSHV vbcl-2 is expressed during the lytic phase of the virus lifecycle (Sarid *et al.* 1997) (Sarid *et al.* 1998) and can overcome bax-mediated apoptosis (Cheng *et al.* 1997;Sarid *et al.* 1997). It is possible that the vbcl-2 encoded by KSHV may play a role in the survival of tumors via an anti-apoptosis mechanism.

1.3.3.4 K1

ORF K1 is commonly used to subtype KSHV into subtypes A, B, C and D (McGeoch and Davidson 1999;Nicholas *et al.* 1998). These subtypes of KSHV possess between 15-30% amino acid differences within their respective K1 ORFs. The use of K1 to subtype KSHV allows the study of KSHV ethical and geographical distribution. K1 is a transforming protein that contains functional immunoreceptor tyrosine-based activation motifs (ITAMs) (Lee *et al.* 1998b;Lee *et al.* 1998a). Studies have suggested that K1 may be involved in the activation of NFkB signaling (Prakash *et al.* 2002) and K1 has recently been shown to activate the Akt signaling pathway (Tomlinsen and Damania 2004).

1.4 Related viruses

The gammaherpesviruses are a subfamily of herpesviruses characterised by their association with transient and chronic lymphoproliferative disorders due to an ability to induce cell proliferation (Boshoff 1999) (Table 1.2A). The gammaherpesviruses are further subdivided into Lymphocryptovirus and Rhadinovirus on the basis of genome structure. KSHV is a member of the gammaherpesviruses and is classified as a Rhadinovirus. KSHV shares significant homology with other members of this group, which include herpesvirus saimiri (HVS), rhesus rhadinovirus (RRV) and murine herpesvirus 68 (MHV-68) (Neipel *et al.* 1998) (Table 1.2B). In terms of human herpesviruses, KSHV is most similar to Epstein-Barr virus (EBV). Recently, sequences of KSHV-like herpesviruses have been discovered in chimpanzees and in gorillas (Lacoste *et al.* 2000).

The rhadinoviruses as a group have expanded with the discovery of several new viruses that are more closely related to KSHV than HVS or EBV. Newly discovered viruses include retroperitoneal fibromatosis herpesvirus which were isolated from vascular fibroproliferative neoplasm present in two macaque species; *Macaca nemestrina* and *Macaca mulatto* (Rose *et al.* 1997) and Chlorocebus rhadinovirus 1 (Greensill *et al.* 2000). Interestingly, retroperitoneal fibromatosis is histologically similar to KS in humans.

Table 1.2A & B

The human herpesvirus family and subfamily		
Herpesvirus genus	**Example viruses**	**Associated human diseases**
Alphaherpesvirus	Herpes simplex virus type 1	Oral-facial herpes
	Herpes simplex virus type 2	Genital herpes
	Varicella-zoster virus	Chicken pox, Shingles
Betaherpesvirus	Cytomegalovirus	Congenital disease, CMV retinitis
	Human Herpesvirus 6	Febrile illness, exanthem subitum
	Human Herpesvirus 7	Febrile illness
Gammaherpesvirus	Epstein-Barr virus (EBV)	Infectious mononucleosis (IM), Burkitts lymphoma (BL), Nasopharyngeal carcinoma (NPC), AIDS-central nervous system (CNS) lymphoma, post-transplantation lymphoproliferative disease (PTLD)
	Kaposi's sarcoma-associated herpesvirus (KSHV)	Kaposi's sarcoma (KS) Multicentric Castleman's disease (MCD) Primary effusion lymphoma (PEL)
Source: (Timbury 1997)		

KSHV-related herpesviruses		
Virus	**Abbreviation**	**Host species**
Epstein-Barr virus	EBV	Humans
Herpesvirus saimiri	HVS	Squirral monkeys (New World primates)
Herpesvirus ateles	HVA	Spider monkeys (New World primates)
Alcelaphine herpesvirus	AHV-1	Ruminants
Bovine herpesvirus 4	BHV4	Cows
Equine herpesvirus 2	EHV2	Horses
Murine herpesvirus 68	MHV68	Mice, Bank Vole
Retroperitoneal fibromatosis herpesvirus	RFHVMn & RFHVMm	Old World primates
Rhesus monkey rhadinovirus	RRV	Old World primates
Adapted from (Boshoff 1999)		

1.5 Virus mediated gene delivery

1.5.1 Development

In 2000, the field of gene therapy became 10 years old (Mountain 2000). Gene therapy aims to treat disease at the genetic level, thereby treating the cause, not the symptoms of disease. Gene therapy employs many different methods for the introduction of therapeutic DNA to human cells (Mountain 2000). Viruses that have been reverse-engineered as delivery vectors are commonly used. Types of viruses adapted for gene therapy include adenovirus, retrovirus (including lentiviruses), herpesviruses (Elliot and O'Hare 1999) and other less common viruses such as Sendai virus. These viruses share an important common feature of being engineered to be replication deficient; once infection has occurred the viruses do not possess the genetic information to replicate.

1.5.2 Lentiviral vectors

Lentiviruses are increasingly the most widely used type of gene delivery vector. They possess several advantages over other vectors including adenovirus, herpesviruses, vaccinia virus (Carroll and Moss 1997) and even over other members of the retrovirus family (Federico 1990;Verma and Somia 1999).

Initial work on the use of lentiviruses as a vehicle for gene delivery concentrated on the use of a three-construct system. This consisted of a plasmid carrying all of the HIV-1 genes required for production of the virus particles, a plasmid carrying an envelope gene, vesicular stomatitis virus glycoprotein (VSVg) and a plasmid carrying the gene which would ultimately be expressed from the virus positioned with a promoter between two viral long terminal repeats (LTR) (Naldini *et al.* 1996).

Lentiviruses offer greater scope for the infection of mammalian cells as they are able to infect both non-dividing and dividing cells (Fouchier *et al.* 1997). Retroviruses require cellular mitosis for the transport of viral nucleoprotein complexes into the nucleus, whereas lentivirus nucleoprotein complexes are specifically transported in the absence of mitosis (Fouchier *et al.* 1997).

These three plasmids are co-transfected into a packaging cell line, often HEK 293T, from which infectious particles are released. The system is shown in Fig 1.4. These HIV-1 based lentiviruses, when pseudotyped with an envelope coat protein (such as vesicular stomatitis virus glycoprotein, VSVg), can infect a broad range of cells including quiescent haematopoietic progenitor cells (CD34+, CD38-) (Akkina *et al.* 1996;Case *et al.* 1999) and quiescent primary fibroblasts (Reiser *et al.* 1996). The VSVg envelope was employed for this study, as it is able to enter a wide range of cells by means of endocytosis (Superti *et al.* 1987;Yamada and Ohnishi 1986). Comparison of methods has shown the efficiency of the lentivirus system. In tests on human B cell precursor acute lymphoblastic leukemia cells, transfection methods showed a maximum of 12% in Nalm-6 cells, whereas infection with a VSVg-pseudotyped lentivirus gave greater than 90% positive cells (Mascarenhas *et al.* 1998). The lentiviruses were based on the pHR CMV system developed by Naldini et al (Mascarenhas *et al.* 1998;Naldini *et al.* 1996).

Further work has aimed at the ultimate goal of the gene delivery systems: the treatment of human disease at the genetic level, commonly termed gene therapy. HIV-based lentiviruses have been used in studies for the treatment of cystic fibrosis (Goldman *et al.* 1997). Individual organs have also been the target of gene delivery, often with a view to treat diseases specific to them and attempts have included the liver and muscle as target areas (Kafri *et al.* 1997).

Fig 1.4

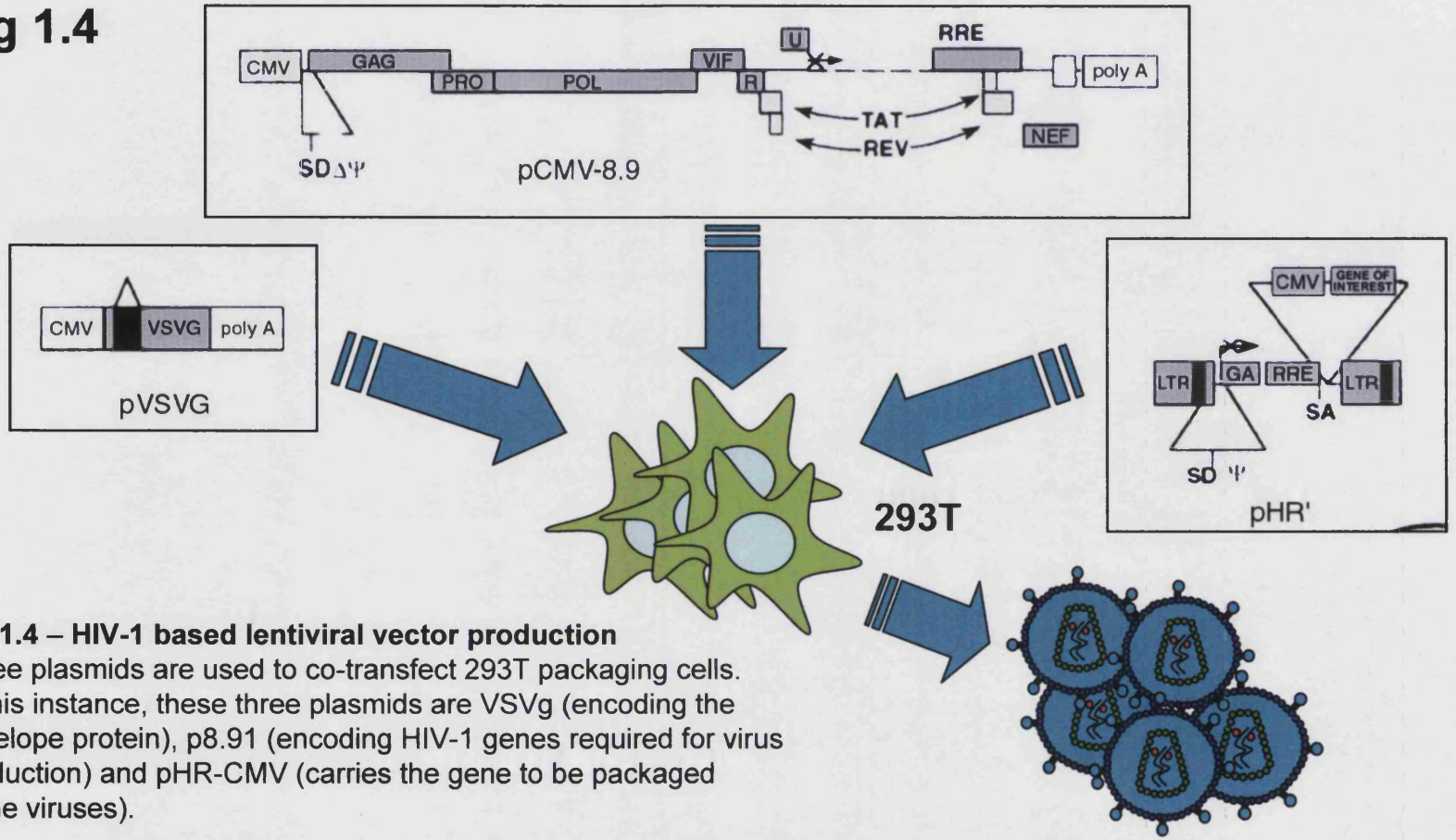

Fig 1.4 – HIV-1 based lentiviral vector production
Three plasmids are used to co-transfect 293T packaging cells. In this instance, these three plasmids are VSVg (encoding the envelope protein), p8.91 (encoding HIV-1 genes required for virus production) and pHR-CMV (carries the gene to be packaged in the viruses).

Development of the lentiviral system has continued since its first use. Although highly efficient and to date safe, the use of human-tropic lentiviruses as the basis for a gene delivery system has raised concerns. Other systems have therefore been developed including a system based on simian immunodeficiency virus (SIV) (White *et al.* 1999). The HIV/SIVpack/G system uses components from both HIV and SIV viruses, and as there is low sequence similarity between the two viruses, there is a reduced risk of recombination (White *et al.* 1999).

Other work has concentrated on the further development of technical aspects. One of the problem areas of the lentivirus-based system is the requirement for multiple transfections of packaging cells, often triple-transfections. To improve this, stable packaging lines have been created that express one or several of the genes required for packaging (Carroll *et al.* 1994;Corbeau *et al.* 1996;Yu *et al.* 1996).

1.6 Gene expression microarrays

1.6.1 Principles and development

Microarray technology developed using the principles of a common molecular biology technique: Southern blotting. Initially gene expression microarrays were constructed from cDNA and bound to a solid surface i.e. nitrocellulose membrane. Currently there are two main forms of gene expression microarray (GEM) available: cDNA arrays and oligonucleotide arrays. Both systems have advantages and disadvantages, often depending on the precise application they are being used for. Microarrays are a means of determining the expression patterns of thousands of different genes at the same time. Essentially, cDNA is created from cellular total RNA or mRNA and labelled either radioactively or with a fluorescent dye. These labelled probes are then hybridised to the array cDNA/oligo supported on a matrix. Scanners are used to convert the signals obtained from specific interactions on the arrays into measured hybridization signals from which software quantifies the levels of each hybridisation. From these data an expression pattern/profile is built up for the cell/tissue tested.

1.6.2 Applications

Gene expression microarray technology has been employed extensively in many different fields of biomedical research. Tissue profiling is now a major application of GEM and has allowed an insight into various malignancies including rhabdomyosarcoma (Khan *et al.* 1998) and T-cell lymphoma (Li *et al.* 2001). GEM technology also allows the identification of disease specific markers that can later be used in the diagnosis of particular diseases.

GEM technology has been applied to investigating the gene profile of endothelial cells under various conditions. The effect of physical stress on endothelial cells has been investigated such as laminar

shear stress (Urbich *et al.* 2000) and blood circulation (Brooks *et al.* 2002). Microarrays have also been used to gain an insight into changes in gene expression in endothelial cells after challenge with various infectious agents including Chlamydia pneumoniae (Coombes and Mahony 2001) and KSHV (Poole *et al.* 2002). This technique has allowed important insight into the viral life cycle. The production of cDNA arrays of viral genes has been employed for viruses including KSHV (Jenner *et al.* 2001) and cytomegalovirus (CMV) (Chambers *et al.* 1999).

1.7 Proteomics

1.7.1 Background

Proteomics, despite a recent drastic increase in the use of proteomics technologies, is not a new field. Proteomics is essentially an amalgamation of several different fields including mass spectrometry, chromatography, protein biochemistry and recent fields such as bioinformatics. The techniques of proteomics offer hope to areas of research previously impossible, as well as enhancing other more traditional areas (Abbott 1999;Pandey and Mann 2000).

1.7.2 Mass spectrometry

The applications of mass spectrometry in biological research have been steadily growing, and have recently expanded greatly. Mass spectrometry, in particular matrix assisted laser desorption ionization – time of flight mass spectrometry (MALDI-TOF) and electrospray ionization tandem mass spectrometry (ESI-MS) have found applications in the study of viruses (Thomas *et al.* 2000). MALDI-TOF MS and ESI MS/MS have gained other wide ranging uses, including structural biology, translational modification detection and drug discovery, because of their abilities to produce accurate protein molecular weight data, thereby allowing timely identification of unknown polypeptides.

1.7.2.1 Mass Spectrometry for the characterization of protein complexes

This is of particular use in the identification of protein-protein interaction studies. There are now an abundance of papers that couple the use of mass spectrometry to either chromatographical methods or immunoprecipitation for the purification of a protein complex that is then identified using mass spectrometry.

Using proteomic techniques several groups have achieved purification and characterisation of protein complexes in both human cells and yeast. In human cells, these include the identification of a novel N-CoR complex (Underhill *et al.* 2000) and the protein complex of SV40 large T antigen (Lanson Jr *et al.* 2000). A novel N-CoR complex which was found to contain members of the mammalian SW1/SNF complex and a co-repressor KAP-1 was purified from HeLa cell nuclear extracts using chromatography and mass spectrometry (Underhill *et al.* 2000). Affinity chromatography and MALDI were used to identify interaction partners of mouse brain profiling I and II, which are involved in the process of actin assembly. Immunoprecipitation methods have been used to identify interaction partners of human $BclX_L$, an apoptosis inhibitor protein (Gygi *et al.* 1999).

Proteomics has also allowed new insights into the interactions of yeast proteins. These include identification of members of splicing complexes (Gottschalk *et al.* 1999), protein complexes involved in motility (Winter *et al.* 1997), the identification of *in vivo* substrates of the chaperonin GroEL, (Houry *et al.* 1999), characterization of the yeast nuclear pore complex (Rout *et al.* 2000) and component analysis of the human CDC5L complex (Ajuh *et al.* 2000).

1.7.2.2. MALDI-TOF MS

Biological mass spectrometry is a biophysical technique that allows the identification of proteins, peptides and nucleic acids. It is often employed as the final step of proteomic techniques i.e. for identification of the members of a purified protein complex. Matrix assisted laser desorption ionization – time of flight mass spectrometry (MALDI-TOF MS) can detect protein molecules at femtomole and subfemtomole levels, that in combination with its ability to analyse complex protein suspensions makes it highly adaptable and sensitive (Thomas *et al.* 2000). MALDI works by desorption and ionization of polypeptides mounted on a matrix, usually in aromatic organic acids

(i.e. 4-methoxy cinnamic acid or 3-hydroxypicolinic acid) (Jackson *et al.* 2000), that leads to formation of a gas phase containing the peptides. This gas phase can then be directed to a mass analyser using electrostatic charge. In MALDI-TOF, the addition of a vacuum tube allows the ions to travel to the detector. The detector then calculates the mass of peptides based on the ion flight time. The resulting data are in the form of estimated peptide molecular weights from which a 'peptide fingerprint' is produced, which can be compared with databases for identification (Thomas *et al.* 2000). Prior to the development of MALDI and ESI-MS, it was not possible to achieve identification of polypeptides greater than 1-2kDa (Jackson *et al.* 2000). A typical protocol will run proteins captured by affinity chromatography on an SDS-PAGE gel, visualise bands by silver staining or Coomassie staining and excise the bands for digestion in trypsin. These proteolytic peptides are then subjected to MALDI-TOF MS and their relative masses determined. By searching databases it is possible to identify the selected proteins. Where identification of a protein is not possible, due to a mixed population of proteins, further analysis by tandem MS (MS/MS) may aid in their identification (Mann *et al.* 2001).

1.7.3 The yeast two-hybrid system

The yeast two-hybrid system is a method of screening for protein-protein interaction partners. It is one of several yeast-based methods including yeast one-hybrid that tests for DNA-protein interactions and yeast three-hybrid that tests RNA-protein interactions. The yeast two-hybrid system provides a method for screening polypeptides (bait) against cDNA or genomic libraries (prey), and is based upon the mechanism of transcriptional activation. In a typical screening experiment, the polypeptide of interest is cloned into a plasmid, next to a DNA-binding domain from a transcription factor (often LexA). The cDNA or genomic library is cloned in frame next to an activation domain of the Gal4 yeast transcription factor. The plasmids are cotransfected into yeast carrying reporter gene constructs and nutritional selection markers (often LacZ and HIS3). If there is no interaction between bait and prey, the yeast cell will not survive in the absence of histidine and will not turn blue (LacZ-). Only in the presence of an interaction between a bait and prey polypeptide will the DNA-binding domain of LexA and the activation domain of Gal4 form a complex to allow transcriptional activation of the genes LacZ/HIS3. Cells containing this interaction will grow in the absence of histidine and appear blue. This method of screening is therefore not suitable for use with transcription factors/DNA-binding proteins. Advances in the yeast two-hybrid system have allowed it to be used for high-throughput screening of protein-protein interaction partners. Work presented later in this thesis, using a high-throughput yeast two-hybrid system, was performed in collaboration with Hybrigenics, Paris. Via these advanced methods, interaction maps have been created for Helicobacter Pylori (Legrain *et al.* 2000;Rain *et al.* 2001) and further advances include two-hybrid systems in bacteria (Legrain and Selig 2000) and the use of high-throughput systems in drug discovery (Legrain and Strosberg 2002).

1.8 Aims of this thesis

This thesis is aimed at furthering our understanding of the LANA1 protein in both its effects on disease relevant primary cells and its interactions with cellular proteins. A particular goal of this thesis was to study LANA1 at a cellular level, identifying true transcriptional targets of LANA1 and provide a global picture of the cellular interaction partners. To achieve this goal, several technical aims needed to be achieved.

Firstly, the development of lentivirus vectors for the delivery of LANA1 to disease relevant primary cells for analysis by gene expression microarrays. I have aimed to develop the lentiviral system to deliver LANA1 to primary human endothelial cells, a cell type implicated as the target of KSHV infection and closely involved in the development of KS. With this method I aimed to achieve high levels of expression in primary cells, aiding in the analysis of the effects of LANA1 on the cellular transcriptome. To analyse the transcriptional effects of LANA1 on a genome-wide scale, I employed gene expression microarray (GEM) technology.

Using this technology I determined the effects of LANA1 on the cellular transcriptome of primary endothelial cells. After delivery of the LANA1 using lentiviruses, RNA was extracted and compared with various controls to determine effects specific to LANA1.

Secondly, the development of protein chromatography and purification methods for the characterisation of a LANA1 native complex by mass spectrometry. To achieve this I used affinity chromatography and immunoaffinity purification coupled to mass spectrometry. The latent nuclear antigen (Rainbow *et al.* 1997) of KSHV is known to interact with several different proteins *in vivo* including p53 (Friborg *et al.* 1999), pRB (Radkov *et al.* 2000), RING-3 (Platt *et al.* 1999), HDAC, mSIN3A (Krithivas *et al.* 2000) and GSK-3β (Fujimuro *et al.*

2003;Fujimuro and Hayward 2003). To discover the overall complex between LANA1 and these various proteins, I have undertaken purification and characterisation of the LANA1 protein complex. Previous work has shown that using a combination of protein purification techniques it is possible to purify a native nuclear protein complex and characterise its individual components using mass spectrometry. For the purification of the LANA1 complex, BC-3 cells (a KSHV positive, EBV negative PEL line) were selected as they show high expression of LANA1 and have suitable growth characteristics for large-scale culture. During the purification of a protein complex the best selection method for an individual protein is affinity chromatography. This method of chromatography employs a specific antibody permanently cross-linked to a stable media i.e. sepharose which can be re-used for many separate purifications. This method allows the specific selection of one protein from a background of thousands of irrelevant cellular proteins. For LANA1 a specific rat monoclonal was selected and used to create an affinity column (Kellam *et al.* 1999). A negative column was also created as a control in purifications.

Chapter 2 Materials and Methods

2.1 Standard methods

2.1.1 Cell culture, transfections & lysis

HEK-293 and HeLa cells were maintained in DMEM + 10% v/v FCS + penicillin/streptomycin (5μg/ml) (Gibco BRL, UK) at 5% CO_2. The PEL cell line BC-3 was maintained at between 10^5–10^6 cells/ml in RPMI + 10% v/v FCS + penicillin/streptomycin (5μg/ml). For large-scale immunoaffinity purification BC-3 cells were washed in PBS and lysed in modified RIPA buffer (50mM Tris pH 8.0, 150mM NaCl, 1% v/v IGEPAL CA-630, 0.1% w/v SDS, 1mM PMSF, 1/100 mammalian protease inhibitor cocktail (Sigma)) with rotation at 4°C for 1h. Lysates were centrifuged at 13,000rpm for 30min in a Beckmann high-speed centrifuge and stored at –80°C. $1x10^5$ HeLa cells were transfected with either 5μg of pHR CMV emp or pHR CMV LANA1 using FuGene 6 according to manufacturer's instructions (Roche Diagnostics, Mannheim, Germany). Cells were lysed in RIPA buffer (50mM Tris pH 8.0, 150mM NaCl, 1% v/v IGEPAL CA-630, 0.5% w/v sodium deoxycholate, 0.1% w/v SDS, 1mM PMSF) 48hrs later and diluted to 50% RIPA with ddH_2O prior to co-immunoprecipitation. CB3 and CB7 cells (a kind gift from B.Chabot, Faculte de Medecine, Universite de Sherbrooke, Canada) were maintained in MEM alpha medium (Gibco BRL) + 10% v/v FCS (Helena Biosciences, UK) + penicillin/streptomycin (5μg/ml) (Gibco BRL). Transfection of CB3 cells is described in the section *TRAP assay*.

2.1.2 PCR

The polymerase chain reaction (PCR) was used for the amplification of DNA fragments or genes for cloning. PCR was performed on a Primus 96-Plus thermocycler (MWG Biotech, UK) under conditions suitable for the particular sequence of DNA being amplified. Polymerase used included Taq polymerase (Promega, Southampton,

UK), Pfu (Promega) and Expand High-Fidelity (Roche). A typical 25µl reaction mixture would include: 100ng each primer, 2.5µl x10 PCR buffer, 1µl polymerase, 1µl of 10mM dNTPs, target DNA and water to 25µl. A typical amplification protocol would be: 30cycles of 95°C 1min, 64°C 1min, 72°C 4mins followed by 1 cycle 72°C 10mins.

2.1.3 Bacterial transformation

Various cell types were used in the course of this thesis. In general the protocol for electroporetic transformation was the same. Cells were thawed on ice and 2-5µl of DNA was added. Cells were shocked at 200ohms, 25mF capacitance and 2kV. Time constants were in the range of 40-50. After electroporation LB was added and cultures were incubated at 37°C with shaking for 1hr. Cultures were then inoculated onto LB+Amp plates and incubated at 37°C overnight.

2.1.4 Agarose gel electrophoresis

Gels were made from agarose (AMRESCO, UK) at between 1-2% in 0.5xTAE buffer (2M Tris pH 8.0, 5mM EDTA, 5.71% v/v Glacial Acetic Acid) and melted in a microwave. 2µl of Ethidium bromide was added (Sigma) per 100ml, gels were poured into casting tanks and run in 0.5xTAE buffer using a mini gel migration trough (MUPID-21). DNA/RNA was visualised and photographed using a Kodak camera system.

2.1.5 DNA gel extraction

Bands selected for gel extraction were cut with a clean scalpel and transferred to a 1.5ml eppendorf. Depending on weight the gel fragment was resuspended and melted by incubation in a 50°C water bath. 1 gel volume of isopropanol was added and the mix was applied to a QIAquick column. Following washes the DNA fragments were eluted into a fresh eppendorf and frozen at –20°C for storage.

2.1.6 DNA ligation

Ligations were performed at 16°C overnight (O/N) followed by electroporation into KC-8 cells. Following electroporation cells were incubated in Luria Broth (LB) lacking ampicillin (Amp) and then plated onto LB + Amp plates. Plates were incubated O/N at 37°C. 20 colonies were selected and 3ml of LB + Amp was inoculated and incubated with shaking at 37°C for 8hrs. Plasmid DNA was extracted from 1.5ml of each culture using a miniprep kit (Promega). Positive clones of pHR CMV LANA1 were selected and confirmed by restriction enzyme digest mapping. A candidate was selected and its sequence confirmed by DNA sequencing.

2.1.7 TA cloning

TA cloning of fresh PCR products was performed using the pcDNA 3.1/V5-His TOPO TA cloning kit (Clontech, UK). PCR was performed and products were subjected to agarose gel electrophoresis. Bands for cloning were rescued from the gel using a Qiagen gel extraction kit (Qiagen, Hilden, Germany). 2μl-4μl of the gel extracted PCR product was added to 1μl of salt solution and 1μl of pcDNA 3.1/V5-His TOPO and adjusted to a final volume of 5μl with sterile H_20. The reaction was mixed and incubated for 5-15mins at RT. Vials of One Shot™ Chemical transformation cells were thawed on ice and 2μl of the 5μl cloning reaction was added, mixed gently and incubated on ice for 15-30mins. The cells were heat-shocked at 42°C for 30secs and transferred to ice. 250μl of pre-warmed SOC (2% w/v Bacto Tryptone, 0.55% w/v Bacto Yeast Extract, 10mM NaCl, 10mM KCl) (Qiagen, Hilden, Germany) was added to each vial followed by incubation of 1hr at 37°C with shaking. The cultures were then spread onto LB+Amp plates and incubated overnight at 37°C.

2.1.8 Plasmid preparation and purification

The small-scale purification of plasmid DNA was performed using Promega minipreps kits. The large-scale purification of plasmid DNA was performed using Maxi™ or Mega™ kits.

For the preparation of minipreps, colonies were selected from LB+Amp streak plates and 3ml of LB+Amp culture was inoculated with a single colony. Cultures were grown at 37°C for 6-7 hours with shaking. 1.5ml of the cultures was centrifuged for 5mins at 5,000rpm in a bench top centrifuge. The culture pellets were resuspended, lysed and neutralised after alkaline protease treatment, according to the kit. The lysates were centrifuged through a spin column and captured plasmid DNA was washed and eluted into Nuclease-free H_20. DNA was either further analysed by restriction enzyme analysis and agarose electrophoresis or stored at –20°C until used.

For Maxi™ and Mega™ preps 3ml cultures were grown as above, and then used to inoculate 500ml of LB+ Amp that was incubated overnight at 37°C with shaking. For high copy number plasmids 500ml of culture was used with a QIAGEN-tip 2500, but for low-copy number plasmids, 2500ml of culture was used. The following day, cultured bacteria were pelleted by centrifugation and either stored at –20°C until processing or used immediately. Cell pellets were resuspended lysed and cleared using reagents from the appropriate kit. A pre-equilibrated QIAGEN-tip column was used to capture the plasmid DNA. The DNA was eluted, precipitated, air dried and redissolved in a suitable volume of TE buffer or MilliQ dH_20. The quantity of DNA was determined using a UV spectrophotometer.

2.1.9 Restriction enzyme analysis

DNA was digested with restriction enzymes to determine correct orientation and size of fragments. Digestions were normally performed in 10μl at 37°C. A typical mix was 1-5μl of miniprep, 2 units of enzyme (1μl), 1μl of BSA and 1μl of 10x buffer. Restriction enzymes were obtained from either Promega or New England Biolabs and used with the buffers supplied by the manufacturer.

2.1.10 Cloning for this thesis

wt LANA1 in pHR CMV construct, hnRNPA1/UP1 and GSTs

Due to a lack of suitable restriction sites within LANA1, amino and carboxyl terminus of LANA1 were prepared separately and ligated into the pHR CMV vector. The N-terminus of LANA1 (aa1-282) was amplified from the parental vector IgH P/E 73cycK13 using PCR with the primers (Forward) aaagtacttgatatcgccaccatggcacccccgggaatgcgc & (Reverse) catggctgtgtcatcacccca. The PCR product was run on a 1% agarose gel and the LANA1 band (850bp) was recovered by gel extraction (Qiagen). Aliquots of the LANA1 fragment were digested with BamHI and EcoRV in preparation for ligation. Restriction digests were run on a 1% gel and the digested LANA1 fragment (aa1-275) was recovered by gel extraction (Qiagen).

The LANA1 fragment (aa275-1162) was prepared by digestion of the parental vector IgH P/E 73cycK13 with BamHI. The BamHI cuts at amino acid 275 in LANA1 and beyond the carboxyl terminus of LANA1. After digestion the fragment (around 4kb) was recovered by gel extraction (Qiagen) and digested with SfoI (2 units) (New England Biolabs) to blunt end the carboxyl terminus. The cut site is situated after the stop codon of LANA1 and before the start of the vcyclin transcript. The final fragment was recovered by gel filtration (Qiagen).

For preparation of the vector, 15μg of lentivirus vector pHR CMV LacZ (a kind gift from Prof. M.Collins, Windeyer Institute, UCL) was cut with

BamH1 (4 units) (Promega) and XhoI (4 units) (Promega) that removes the LacZ insert. The restriction mix was run on a 1% agarose gel and the backbone was recovered using a gel extraction kit (Qiagen). Approximately 2μg of the backbone was blunted using Klenow (22°C 10 mins, 65°C 15 mins) (Promega). After blunting, the vector was dephosphorylated using calf intestinal alkaline phosphatase (Boehringer Mannheim) and again gel purified.
Ligations were performed at 16°C overnight (O/N) followed by electroporation into KC-8 cells. Following electroporation cells were incubated in Luria Broth (LB) lacking ampicillin (amp) and then plated onto LB + amp plates. Plates were incubated O/N at 37°C. 20 colonies were selected and 3ml of LB + amp was inoculated and incubated with shaking at 37°C for 8hrs. Plasmid DNA was extracted from 1.5ml of each culture using a miniprep kit (Promega). Positive clones of pHR CMV LANA1 were selected and confirmed by restriction enzyme digest mapping. A candidate was selected and its sequence confirmed by DNA sequencing.

GST-LANA1 3-263 was created by cutting pHR CMV-LANA1 with *Sma*I (1 unit) and *Nco*I (1 unit) and ligating the fragment into pGEX 6P-1. GST-LANA1 932-1162 was created by PCR using the primers ttgatatcggatccgccaccatggaggagcaggaggtggaaga (forward) and cggaattcgctcgagctattatgtcatttcctgtggaga (reverse). The PCR product was cut using *Bam*HI (1 unit) & *Xho*I (1 unit), cloned into pHR CMV and then subcloned using *Bam*HI & *Xho*I sites into pGEX 6P-1. GST-LANA1 803-981 and GST-LANA1 982-1113 were created as previously described (29).

GST-hnRNP A1 was created by PCR from a human foetal cDNA library using the primers: cgagaggagctgggatccggtatgtctaagtcagagtctcctaaa & gctgccctcgagtccttaaaatcttctgccactgccatagct. UP1-HA was created using the hnRNP A1 forward primer and the reverse primer that

introduces a carboxyl terminal HA tag: cgcctcgagctaagcgtagtctgggacgtcgtatgggtatcgacctctttggctggatga. Both hnRNP A1 and UP1-HA PCR products were TA cloned into pcDNA 3.1/V5 HIS TOPO vectors (Invitrogen, Groningen, The Netherlands). pcDNA 3.1/V5 HIS TOPO hnRNP A1 was digested with *Bam*HI (1 unit) & *Xho*I (1 unit) and ligated into pGEX 6P-1. Sequences of all constructs created were verified on a Beckmann sequencer.

2.1.11 Primary microvascular endothelial culture

Primary human microvascular endothelial cells were obtained from male or female breast tissue (a kind gift from Dr Mike O'Hare, Ludwig Institute of Cancer Research, UCL). Cells were washed with 10mls of pre-warmed DMEM + 10% v/v FCS. The wash media was discarded and 20mls of pre-warmed Trypsin-EDTA was added. Flasks were incubated until rounding of cells was observed under an inverted microscope (1-2mins). Pre-warmed DMEM + 10% v/v FCS (25-30mls) was added into each flask. Trypsinisation of cells was performed as quickly as possible to maintain the stability and quality of the cultured primary endothelial cells. Cell suspension was removed by gentle pipetting to wash the flask surface and transferred to a 15ml Falcon tube. The suspension was centrifuged for 5mins at 22°C at 1200rpm. The cell pellet was resuspended in 10mls of pre-warmed DMEM + 10% v/v FCS +penicillin/streptomycin (5μg/ml). The washing step was repeated. After centrifugation the wash media was gently removed with a pipette and cells were resuspended in 8mls of EGM-2 (Clonetics) + 10% v/v FCS (3 x 2mls for continuing culture and 1 x 2mls for freezing). 3 x 2mls of cell suspension was added into 3 x 18mls of pre-warmed EGM-2 + 10% v/v FCS + penicillin/streptomycin (5μg/ml) in 3 x pre-warmed 75cm^2 flasks. Cultures were then incubated at 37°C in 5% CO_2. 3 x 600μl of cell suspension was added into 3 x cryovials containing 600μl of freezing solution (10ml stock = 1.8ml DMSO + 8.2ml of DMEM+20% v/v FCS) (final concentration of

10% v/v DMSO). Cryovials were placed at -80°C then transferred into liquid nitrogen for long term storage.

2.1.12 Immunofluoresence assay (IFA)

Cells were prepared on glass slides (after storage in 100% ethanol slides were washed twice in PBS/DMEM) in 6 well plates. Infections were carried out on cells grown overnight on slides. Cells were washed (x3) in ice cold PBS. 1ml of 1:1 methanol:acetone (chilled to -20°C) was added to each well for fixation and slide plates were incubated at –20°C for 5mins. Cells were washed (x3) in ice cold PBS. 1ml of blocking buffer (3% w/v BSA, 1mM $MgCl_2$, 1mM $CaCl_2$ in PBS) was added to each well and incubated for 1hr at 22°C. Cells were washed (x3) in ice cold washing buffer (1/10 dilution of blocking solution in PBS). Slides were removed from the plates and transferred to stands to allow addition of antibodies. Primary antibody (LN53/LN72) was added diluted in wash buffer (1:100 - 1:400). Slides were incubated with antibodies for 2hr at 22°C. Cells were washed (x3) in ice cold washing buffer. Secondary antibody (FITC-conjugated rabbit anti-rat IgG [DAKO]) was diluted in wash buffer (1:120/1:240) and incubated on cells for 40mins-1hr at 22°C. Cells were washed (x3) in ice cold washing buffer. Coverslips were mounted on slides using 20μl of 100% glycerol or FITC preservative solution (DAKO). Slides were observed on a fluorescent microscope (NIKON) or stored at 4°C in silver foil.

2.1.13 Tube formation assay

1ml of Matrigel (Clonetics) was aliquoted per well, using cooled pipettes, into a 24 well plate. The Matrigel was allowed to set at room temperature. Primary endothelial cells in EGM-2 were added onto the Matrigel and observed at various times post-seeding for the formation of tubes on the gel surface.

2.1.14 FACS analysis

For a typical experiment in a 6-well dish cells were washed twice in PBS and then trypsinised. Fresh media (DMEM + 10% v/v FCS) was added and cells were transferred to FACS tubes. Cells were washed twice with PBS and resuspended in a suitable volume of PBS (100μl per well of a six well dish). Cells were vortexed prior to analysis on a Beckmann FACS calibur machine. Uninfected cells were used to adjust the FSC/SSC of cells to be analysed. Cells were then run through the FACS and either 5000 or 10000 events were collected. Overlays of infected vs uninfected controls were created using CellQuest software. In some infections cells were gated and the percentage of infection of gated populations was calculated.

2.2 Protein Biochemistry

2.2.1 Western blotting

Protein was separated on 6% or 15% SDS-PAGE gels depending on the size of the protein to be detected. Protein was transferred to Hybond P membrane (Amersham Pharmacia Biotech, Buckinghamshire, UK) and blocked with 5% w/v milk powder in PBS + tween 20 (Sigma, St Louis, MO). LANA1 was detected using anti-LANA1 rat monoclonal (LN53) (1:1000), UP1-HA was detected using an anti-HA mouse monoclonal antibody (Cambridge Biosciences, UK) (1:1000) and hTERT was detected using anti-hTERT rabbit polyclonal (1:500) (Santa Cruz Biotechnology Ltd.). hnRNP A1 was detected using anti-hnRNP A1 mouse monoclonal (2D32) (1:500) (a kind gift from S.Murakami, Kanazawa University, Japan) or anti-hnRNP A1 (4B10) (1:500) (a kind gift from G.Dreyfuss, Howard Hughes Medical Institute). Secondary antibodies used were HRP-conjugated rabbit anti-rat IgG (Santa Cruz Biotechnology Ltd.), HRP-conjugated goat anti-mouse IgG (Jackson Immunoresearch Laboratories Inc, PA, USA) and HRP-conjugated goat anti-rabbit IgG (Santa Cruz Biotechnology Ltd.). Bands were visualised using ECL+ (Amersham Pharmacia Biotech).

2.2.2 Cell culture, lysis & disruption

BC-3 cells were maintained in RPMI-1640 (Gibco BRL) supplemented with 10% v/v FCS and penicillin/streptomycin (5μg/ml) (Gibco BRL). Cell densities were maintained at 10^5 – 10^6/ml. To harvest cells, cultures were centrifuged at approx. 850g (rcf) (4°C) and washed twice in ice-cold PBS. Cell pellets were resuspended in a suitable volume of lysis buffer. For example, low salt buffer (50mM Tris pH 8.0, 50mM NaCl, 1% v/v IGEPAL-CA630, 1mM PMSF, 0.5% v/v protease cocktail [Sigma] in dH_20), buffers up to $2x10^7$ cells/ml so for $2x10^8$ cells, 10ml of this lysis buffer was used. Cell suspension was sonicated for 6 x 10secs, with 10secs cooling in between, followed by

incubation for 1hr with rotation at 4°C. Cell lysates were centrifuged for 30mins at 15,000g (4°C). Supernatant was removed and transferred to a fresh 15ml Falcon tube. At this stage samples were frozen at –80°C. Samples were thawed, filtered through a syringe fitted with a 0.22μm filter and diluted 1:5 in MilliQ dH_20 (final 10mM Tris) and adjusted to pH 7. Samples were then ready for binding to the antibody columns.

2.2.3 Yeast two-hybrid screen (collaboration with Hybrigenics)

The yeast two-hybrid assay was used to identify proteins interacting with the amino terminus of LANA1. Protein target sequences and cDNA plasmids were provided by UCL and yeast two-hybrid screening was performed at Hybrigenics. Amino acids 1-337 of LANA1 and amino acids 893-1129 of LANA1 (see Fig 2.1A & B) were cloned as a C-terminal LexA fusion protein in the pB27 plasmid. The library used for screening was generated from random primed human placental mRNA. The cDNA was cloned into the pP6 plasmid derived from pACT2 and transformed into E.coli DH10B cells. The library was transformed into yeast and 10 million clones were collected, pooled and stored at –80°C. Screening was performed to obtain a minimum of 50 million tested interactions. The screening conditions were optimised for the amino terminus of LANA1. LacZ activity was measured using a semi-quantitative Z-Gal overlay assay for all selected clones. The inserts of positive clones were amplified by PCR and sequenced at their 5' and 3' junctions using a PE3700 sequencer. Sequences were identified by the GenBank database. Clones obtained in different screens against the same library were discounted as false positives.

2.2.4 *In vitro* pulldowns

Briefly, GST fusion protein constructs were transfected into either BL-21 (Promega) or FB-810 (Cancer Research UK) cells and colonies were inoculated into a 50ml LB+Amp culture and incubated overnight

at 37°C with shaking. Cultures were added to 450ml LP+Amp and incubated for a further 3hrs. IPTG was added to the cultures (final 1mM) and incubated at 30°C for 2-3hrs. Cultures were centrifuged and pellets were resuspended in 5ml PBS + lysozyme + PMSF (final 0.1mM) and incubated on ice for 20-30mins. 250µl of 20x Triton-X was added and sonicated followed by centrifugation. Cleared lysates were either frozen at –80°C or incubated with GST beads (Amersham Pharmacia Biotech) for 1hr at 4°C with rotation. Beads were washed extensively in PBS and used in binding assays or stored at –20°C. *In vitro* cleavage of hnRNP A1 was performed according to manufacturers' protocol. GST-hnRNPA1 purified as above was incubated in cleavage buffer with Precission Protease (Amersham Pharmacia Biotech). Cleaved recombinant hnRNP A1 was collected in the supernatant and incubated with the bank of GST-LANA1 proteins in a buffer previously shown to allow hnRNP A1 telomere binding (Dallaire *et al.* 2000).

2.2.5 Co-immunoprecipitations

BC-3 cells used in small-scale co-immunoprecipitation assays were lysed in modified RIPA buffer (50mM Tris pH 8.0, 150mM NaCl, 1% v/v IGEPAL CA-630, 0.1% w/v SDS, 1mM PMSF, Sigma Protease Cocktail) for 1h at 4°C with rotation, centrifuged for 10min at 13,000rpm 4°C and stored at –80°C. 5µg of anti-LANA1 or control antibody was incubated with lysates for 2hr with rotation. 20µl of protein G beads (50:50 slurry) (Amersham Pharmacia Biotech) were added and incubated O/N at 4°C. Beads were washed twice in 50% modified RIPA buffer for 5min with rotation and bound proteins eluted by boiling in 20µl of 2x Laemmli loading buffer (200mM EDTA, 50% v/v glycerol, 0.2% w/v Xylene cyanole, 0.2% w/v Bromophenol Blue). $1x10^6$ HeLa cells were transfected with either 5µg of pHR CMV emp or pHR CMV LANA1 using FuGene 6 according to manufacturer's instructions (Roche Diagnostics, Mannheim, Germany). Cells were lysed in RIPA buffer (50mM Tris pH 8.0, 150mM NaCl, 1% v/v

IGEPAL CA-630, 0.5% w/v sodium deoxycholate, 0.1% w/v SDS, 1mM PMSF) 48hrs later and diluted to 50% RIPA with ddH_2O prior to incubation with 5μg of LANA1 antibody. 20μl of protein G beads (Amersham Pharmacia Biotech) were added and incubated O/N at 4°C. Immune complexes were washed in 50% RIPA and protein eluted in 2x Laemmli loading buffer.

2.2.6 Telomeric Repeat Amplification Protocol (TRAP) assay

$5x10^5$ CB3 cells (a kind gift from B.Chabot) were transiently transfected in 24-well plates with 6μl of DMRIE-C (a low toxicity lipid transfection reagent) and 2μg of pcDNA/V5-HIS TOPO UP1-HA per well. Cells were lysed in CHAPS buffer (+RNasin) and lysates equivalent to $5x10^5$ cells were incubated with either GST alone or GST-LANA1 (982-1113) overnight at 4°C with rotation. Complexes were washed in CHAPS buffer and an aliquot was used to perform a TRAP assay to detect telomerase activity (TRAPeze)(Intergen, UK). 2% and 0.2% of the unbound lysates (FT) and 10% and 1% of the bound protein (PD) was used in the TRAP assay. Dilutions of FT and PD were used to discount the possibility of contaminating inhibitors of telomerase activity. Products were amplified as per the manufacturer's instructions (Intergen). Controls included heat treatment, lysis buffer only (CHAPS) and a telomerase positive control. PCR products were separated on a 12.5% non-denaturing polyacrylamide gel and stained with CYBR Green (Molecular Probes, UK) for 15min at a 1 in 10,000 dilution. Images were detected on a Storm Scanner (Amersham Pharmacia Biotech).

2.2.7 Protein yield determination (BCA assay)

A BCA assay system was purchased from Pierce and used to determine concentration of proteins in various buffers. Standards were prepared using BSA (Sigma, St Louis, MO) in Low salt buffer, RIPA [RadioImmunoProtection Assay] and PBS + 0.1% v/v sodium azide (from 10mg/ml or 20mg/ml at 0.6 step dilutions). 5µl of each standard was added to a 96 well plate with 5µl of each sample and a 5µl blank (RIPA/Low salt buffer or PBS + 0.1% v/v sodium azide). On later experiments an internal control of a known concentration of BSA was used. Assay reagents A and B were prepared at a 1:50 concentration, respectively. The assay plate was incubated at 37°C for 30mins and read at 540nm in a 96–well spectrophotometer.

2.2.8 Antibody purification

To prepare a negative control column, Rat IgG (10mg) technical grade antibody was purchased from Sigma. A 5ml HiTrap Protein G HP column (Amersham Pharmacia Biotech) was equilibrated in 20mM Sodium Phosphate pH 7.0. 5mg of rat IgG was diluted 1:5 in 20mM Sodium Phosphate pH 7.0 and circulated on the column to allow binding. Bound antibody was eluted using 100mM glycine pH 2.7. 1ml fractions were collected and pH neutralised using 1M Tris pH 8.0. Fractions 7-12 were desalted on PD-10 columns (Amersham Pharmacia Biotech) and dried by vacuum centrifugation. Purified Rat IgG was then resuspended in PBS + 0.1% v/v sodium azide. Antibody concentration was determined by BCA assay (4.3mg/ml in 1.5ml = 6.45mg).

2.2.9 Affinity column construction

To construct LANA1 specific affinity columns anti-LANA1 rat monoclonal antibodies were crosslinked to cyanogen bromide activated (CNBr) sepharose 4B media (Amersham Pharmacia Biotech). 5mg (2.4ml) of LN53 (calculated by BCA assay) antibody was dialysed against 1 litre of coupling buffer (0.1M $NaHCO_3$ pH 8.0 +

0.5M NaCl) for 6hrs at 4°C. Fresh coupling buffer was added and the antibody was dialysed O/N at 4°C with gentle stirring. To prepare the CNBr-Sepharose 4B beads for coupling, 0.5g were suspended in 5mls of 1mM HCl. Clumps were removed by gentle mixing. This slurry was added onto a glass-sintered column (15mls) and washed in a total of 100mls of 1mM HCl. 1ml of CNBr-Sepharose 4B slurry was added to 2.4mls of dialysed LN53 and incubated at 4°C O/N with gentle shaking. The next day a glass-sintered column (15mls) was washed with 10mls of coupling buffer. The column was closed and a further 2mls of coupling buffer was added, followed by the overnight coupling reaction (LN53 + CNBr-Sepharose 4B). The column was washed through with 10 volumes of coupling buffer, which was collected for binding efficiency calculation. The remaining active sites on the beads were blocked by 1hr incubation in 0.1M Tris pH 8.0. Fresh 0.1M Tris pH 8.0 was added and incubated for a further 1hr. Beads were then washed in 10mls 0.1M acetate buffer + 0.5M NaCl followed by 10mls 0.1M Tris pH 8.0 + 0.5M NaCl. This process was repeated for 4 cycles. Finally beads were stored at 4°C in preparation for column packing.

A negative column was prepared in a similar manner, except that Rat IgG antibody (Sigma) was purified using a 5ml protein G column (Amersham Pharmacia Biotech). 5mg of purified rat IgG (1.162ml rat IgG + 1.234ml PBS + 0.1% v/v sodium azide) was dialysed against 1litre of coupling buffer (6hrs then replaced buffer for O/N), then coupled to CNBr-Sepharose 4B using the same protocol. Columns were packed at 1ml/min using a dialysis pump at 4°C. Columns were packed in 10mM Tris pH 8.0 and then flushed with 20% ethanol for storage.

2.2.10 AKTA FPLC system operation – affinity columns

Columns were attached to an AKTA FPLC system and equilibrated with buffer (10mM Tris pH 8.0) until baselines were stable. Samples were then circulated through the columns at a suitable flowrate (0.5ml/min), usually overnight. Unbound protein was removed using extensive washes of buffer followed by elution of bound proteins in 100mM glycine pH 2.7. 1ml fractions were collected and equalised with 100µl of 1M Tris pH 8.0. Fractions were then frozen in preparation for desalting and concentration. 1ml aliquots were thawed and diluted to 2.5mls with MilliQ dH_20. PD-10 desalting columns were equilibrated with 25ml MilliQ dH_20 and samples added. Flowthrough was discarded and protein eluted in 3.5mls of MilliQ dH_20. Samples were then centrifuged O/N in vacuum conditions to dry protein. Protein was then resuspended in lysis buffer and stored at –80°C for gel electrophoresis. Identical protocols were followed for both anti-LANA1 (LN53) and control columns (Rat IgG).

2.2.11 Immunoaffinity purification

For immunoaffinity purification, BC-3 cells were washed in PBS and lysed in modified RIPA buffer (50mM Tris pH 8.0, 150mM NaCl, 1% v/v IGEPAL CA-630, 0.1% w/v SDS, 1mM PMSF, Sigma Protease Cocktail) with rotation at 4°C for 1h. Lysates were centrifuged at 13,000rpm for 10min in a Beckmann high-speed centrifuge, filtered through a 0.45µm filter and stored at –80°C. To construct LANA1 specific and control affinity media, 5mg of anti-LANA1 rat monoclonal antibody (LN53) or rat IgG (Sigma, St Louis, MO) were crosslinked to cyanogen bromide (CNBr) activated sepharose 4B media according to the manufacturer's protocol (Amersham Pharmacia Biotech, Buckinghamshire, UK).

For large-scale immunoaffinity purification, 5mg of anti-LANA1 antibody and rat IgG cross linked to CNBr activated sepharose 4B media were incubated with BC-3 cell lysates (diluted to 50% RIPA with

ddH_20) overnight followed by washing in buffer A (25mM Tris pH 8.0, 75mM NaCl, 0.5mM PMSF) and elution of bound proteins in 100mM glycine at pH 2.7. Eluted protein was desalted using PD-10 columns (Amersham Pharmacia Biotech, Buckinghamshire, UK) and centrifuged overnight (O/N) in vacuum conditions to dryness. Proteins were then resuspended in modified RIPA lysis buffer (50mM Tris pH 8.0, 150mM NaCl, 1% v/v IGEPAL CA-630, 0.1% w/v SDS, 1mM PMSF, Sigma Protease Cocktail) and stored at –80°C for gel electrophoresis. Identical protocols were followed for both anti-LANA1 and control experiments. Elutes were separated by 10% SDS-PAGE. Proteins were visualised using Coomassie brilliant blue R-250 staining (BDH laboratories, UK). Bands were excised from the gel, transferred to siliconised tubes and stored at -20°C prior to sample preparation for mass spectrometry.

2.2.12 SDS-PAGE for MALDI-TOF/Nano HPLC

10% gels were poured in a 10cm x 10cm gel (Biorad) and samples loaded. Gels were run at 200V for 5-6hrs and transferred to a 'clean room' for staining and cutting. Gels were stained in Coomassie Brilliant Blue (CBB-R250) [40% v/v Methanol, 10% v/v acetic acid] overnight with rocking followed by destaining over 96hrs [40% v/v Methanol, 1% v/v acetic acid]. Gels were scanned on a Biorad flatbed scanner. Specific polypeptides were selected and prepared for cutting.

2.2.13 MALDI-TOF MS, MALDI-LIFT/PSD MS/MS & nano-HPLC-ESI-CID MS/MS

Mass spectrometry was performed in collaboration with the Ludwig Proteomics group at the Lugwig Institute for Cancer Research and later at the Wolfson Institute for Biomedical Research. Proteins in the excised gel bands were digested using a similar protocol as published elsewhere (Gharbi *et al.* 2002). Briefly, gel pieces were treated using a solution of DTT to reduce protein disulphide bridges (Sigma, St

Louis, MO) prior to alkylation of free cysteines using iodoacetamide (Sigma, St Louis, MO). Proteins were then digested overnight at 37°C using 50ng modified sequencing grade trypsin (Promega, Southampton, UK) per gel band. Following in-gel digestion peptides were recovered using three extractions in 50% v/v acetonitrile, 5% v/v TFA, before complete evaporation in a vacuum centrifuge. The dried tryptic digests were stored at -20°C.

Peptides from the digests were first analysed by MALDI-TOF MS, which was performed upon a Bruker Ultraflex (Bruker Daltonics, Bremen, Germany). α-cyano-4-hydroxycinammic acid (HCCA, Sigma) and 2,5-dihydroxybenzoic acid (DHB, Bruker Daltonics) were used as MALDI matrices. Peptides were resuspended in 5μl 0.1% v/v formic acid and an aliquot of 0.5μl was mixed on-target with 1μl matrix solution before drying and introduction to the mass spectrometer. Peptide mass fingerprinting was carried out using DHB, which was prepared as a saturated aqueous solution.

The mass spectrometer was externally calibrated with the Sequazyme™ calibration mixture 2 (5 peptides in the mass range of 1-6kDa, Applied Biosystems, Framingham, MA) using a quadratic calibration algorithm. Where it was possible, internal calibration of peptide mass fingerprints was carried out using the known masses of two autolytic trypsin peptide ions (*m/z* 842.5100 and 2211.1046) and optionally with the coomassie brilliant blue peak at m/z 804.2777.

Peptide mass fingerprint data were submitted to Mascot (Matrix Sciences, London, UK) and ProteinProspector (UCSF, San Francisco, CA) database search algorithms for peptide mass mapping using the NCBI non-redundant protein database. When internal calibration of the MALDI MS data was possible, a tolerance of 50ppm was used in the searches, otherwise a tolerance of 100ppm was used. All other parameters and criteria for protein identification are described in an

earlier publication (Benvenuti *et al.* 2002b).

Four samples were submitted for tandem mass spectrometric analysis. These were carried out using MALDI-PSD/LIFT MS/MS on the Bruker Ultraflex or by nano-HPLC-ESI-CID MS/MS on a Q-TOF instrument (Micromass, Warrington, Cheshire, UK) coupled to an UltiMate HPLC system with autosampler (LC Packings, Amsterdam, Netherlands) (Minogue *et al.* 2001).

MALDI-PSD/LIFT measurements were carried out using a saturated matrix solution of HCCA in acetone/0.1% TFA (97:3; vol:vol) according to the thin-layer method of Gobom *et al.* (Gobom *et al.* 2001). Peptide ions of strong signal intensity were chosen for MALDI-PSD/LIFT, their fragmentation data automatically processed and submitted to database searching through MS BioTools™ (Bruker Daltonics). Nano-HPLC-ESI-CID measurements were carried out as described previously (Benvenuti *et al.* 2002a) using the remainder of the sample.

Both MALDI-PSD/LIFT and nano-HPLC-ESI-CID data were submitted for searching against the NCBI non-redundant protein database using Mascot. For MALDI-PSD/LIFT data a peptide ion mass tolerance of 0.5Da and a fragment ion mass tolerance of 1Da were chosen. For LC-MS/MS data the mass tolerances were 100ppm for peptide ions and 100mmu for fragment ions. In both cases, where the data significantly matched to more than one peptide of a particular protein, this protein was considered to be a true 'hit'. If the data from only one peptide ion matched a protein but had a significant probability score or if it could not be matched to any protein, these spectra were examined manually. Manual interpretation of MS/MS data was carried out by searching with the main fragment ion masses using ProteinProspector's MS-Tag (UCSF) and/or manual extraction of sequence information from the fragment ion spectrum and submission

of sequence tags to ProteinProspector's MS-Pattern.

2.3 Lentivirus and microarray methods

2.3.1 Virus production (polyethylenimine transfection method)

293T cells were maintained in DMEM + 10% v/v FCS + penicillin/streptomycin (5μg/ml). For virus production cells were seeded at $4x10^6$ in a $75cm^2$ flask or $8x10^6$ in a $150cm^2$ flask the previous day. 15mins prior to cell transfection media was changed (6mls in a $75cm^2$ flask or 12mls in a $150cm^2$). For transfections, plasmids were mixed in the following quantities (Mix 1) (based on $150cm^2$ flask): p8.91 or CRE control 10μg, pHR-CMV-GFP/pHR-CMV-LANA1/pHR-CMV-empty 15μg, pHM-G-VSV-G 5μg and made up to 1400μl with 150mM NaCl. 10mM (200μl) polyethylenimine (PEI) (Sigma) and 1200μl of 150mM NaCl (Mix 2) were combined to make 1400μl. Mix 1 and Mix 2 were incubated at 22°C for 15mins then combined with gentle shaking. The mixture was added into the 293T medium dropwise and incubated for 5 hours at 37°C (5% CO_2). Media was changed (20mls in $150cm^2$ flask) and virus harvested 48hrs later by filtration of media through a 0.45μm filter. For concentration of virus, supernatants were centrifuged at 25,000rpm for 11/2-2hrs at 4°C and virus pellets were resuspended in suitable media (DMEM/EGM-2). Viruses were then stored at –80°C long term or 4°C for short term storage.

2.3.2 RNA extraction

Cells at 48hrs postinfection were washed twice in PBS and total RNA was extracted using an RNeasy kit (Qiagen). Briefly, cells were centrifuged at 1200rpm for 10mins and resuspended in 350μl of RLT buffer (Qiagen) (including β-ME). To homogenise the sample, RLT lysate was transferred onto a QIAshredder (Qiagen) and centrifuged at 13,000rpm for 2mins and the flowthrough collected. 350μl of 70% v/v ethanol was added to the flowthrough and mixed. The 700μl mix was transferred to an RNeasy mini spin column and centrifuged at

13,000rpm for 15secs. 700µl of RW1 buffer (Qiagen) was added to the column and centrifuged at 13,000rpm for 15secs. The column was transferred to a fresh collection tube and 500µl of RPE was added, followed by centrifugation at 13,000rpm. This was repeated but centrifuged for 2mins. The column was transferred to a new eppendorf and eluted at 13,000rpm for 1min using 30µl of RNase-free H_2O. This was repeated with a further 30ml of RNase-free H_2O. RNA yield was quantified by UV spectrophometry and quality was determined by electrophoresis on a 1% agarose gel. Total RNA was stored at –80°C.

2.3.3 p24 quantification by ELISA

24hrs prior to the assay, High bind white plates were coated with 100µl per well of 5mg/ml D7320 anti-p24 antibody in 0.1M $NaHCO_3$ (Aalto bioreagents, Dublin). Wells were washed with LBS and blocked with LBS+2% w/v milk powder w/v for 1hr at RT. 80µl of virus supernatant + 20µl of PBS containing 5% v/v Empigen BB detergent (Surfachem Ltd, UK) was prepared. This was then diluted further at either 1 in 20 or 1 in 200 by the addition of PBS + 5% v/v Empigen BB detergent. A dilution series of p24 protein in LBS + 0.05% v/v Empigen was included on the plate. After blocking plates were washed in LBS and 100µl of each sample added. Plates were incubated for 4hrs at RT and then washed twice in LBS. Secondary anti-p24 antibody conjugated with alkaline phophatase (EH12E1-AP) was diluted to 0.5µg/ml in 4% w/v milk powder + 20% v/v sheep sera + 0.5% v/v Tween 20 in LBS and incubated on the plates for 1hr. Plates were washed 5 times with LBS+0.5% v/v Tween 20 and then exposed to 100 µl of alkaline phosphatase substrate Lumi-Phos Plus (Aureon Biosystems). Plates were incubated in the dark for 30mins at 37°C. Plates were read using Stingray software (Dazdaq, UK) and a Lucy 1 luminometer (Athos-Labtech) giving data in RLU.

2.3.4 Microarray hybridisation and analysis

GF211 array filters were purchased from Research Genetics/Invitrogen (Groningen, The Netherlands) and prehybridised according to the manufacturers' specifications. Initially membranes were washed with boiling 0.5% w/v SDS followed by incubation in 5ml of MicroHyb solution (Research Genetics). 5μg Cot-1 DNA and 5μg Poly dA was added and incubated for 2hrs at 42°C. For preparation of probe, 2μg of Oligo dT was added to 4-5μg total RNA in of DEPC dH_20 (10μl total) and placed at 70°C for 10min followed by incubation on ice. 6μl of 5X First Strand Buffer (Life Technologies), 1ml DTT (0.1M Life Technologies), 1.5μl dNTP mix (20mM dATP, dGTP, dTTP), 1.5μl Reverse Transcriptase (Superscript II, Life Technologies) and 10μl ^{33}PdCTP were added to the Oligo dT/RNA mix and incubated for 90mins at 37°C. The probe was denatured by boiling and added to the pre-hybridised membranes and incubated for 16hrs at 42°C. Membranes were washed twice at 50°C in 2X SSC, 1% w/v SDS and once at 55°C in 0.5X SSC, 1% w/v SDS at 20mins per wash. Membranes were then exposed to phosphor imager screens and scanned using a Storm PhosphoImager (Amersham Pharmacia Biotech). Microarray experiments were performed in duplicate. Images were imported into Pathways software (Research Genetics) and raw intensities were exported to Excel. Raw intensities were normalised against mean values for each data set and a list of candidate genes were selected that were >3 fold over background and showed >1.4 fold up/down regulation. The Pathways image for each gene was checked for misalignment and false positives were discounted.

Fig 2.1A LANA1 amino termini sequences used for Hybrigenics yeast two-hybrid screening

Orf 73 Latent nuclear antigen (LANA1)

Sequence from: 8648..12037 (reverse complement of original sequence)

ORF 73 N-terminus (as DNA sequence): ATG (1) to ACA (1011)

> Expected PCR DNA: 1011bp

> Expected Protein: 337aa (1-337aa)

1 (START)

atggcgccccgggaatgcgcctgaggtcgggacggagcaccggcgcgcccttaacgagag
gaagttgtaggaaacgaaacaggtctccggaaagatgtgaccttggcgatgacctacatctaca
accgcgaaggaagcatgtcgccgactccgtcgacggccgggaatgtggaccccacaccttgc
ctataccaggaagtcccacagtgttcacatccgggctgccagcatttgtgtctagtcctactttacc
ggtggctcccattccttcacccgctcccgcaacacctttacctccaccggcactcttacccccgt
aaccacgtcttcctccccaatccctccatcccatcctgtgtctccggggaccacggatactcattct
ccatctcctgcattgccacccacgcagtctccagagtcttctcaaaggccaccgctttcaagtcct
acaggaaggccagactcttcaacacctatgcgtccgccaccctcgcagcagactacacctcca
cactcacccacgactcctccacccgagcctccctccaagtcgtcaccagactctttagctccgtct
accctgcgtagcctgagaaaaagaaggctatcgtccccccaaggtccctctacactaaaccca
atatgtcagtcgcccccagtctctcccctagatgtgacttcgccaaccgtagtgtgtacccccat
gggccacagagtccccgatctacgtgggatcatccagcgatggcgatactccgccacgccaa
ccgcctacatctcccatctccataggatcatcatccccgtctgagggatcctggggtgatgacac
agccatgttggtgctccttgcggagattgcagaagaagcatccaagaatgaaaaagaatgttcc
gaaaataatcaggctggcgaggataatggggacaacgagattagcaaggaaagtcaggttga
caaggatgacaatgacaataaggatgatgaggaggagcaggag**aca**

337

Fig 2.1B LANA1 carboxyl termini sequences used for Hybrigenics yeast two-hybrid screening

ORF 73 C-terminus (as DNA sequence): GAA (2677) to 3390 (TAA)

>Expected PCR DNA: 714bp

>Expected protein: 237aa (893-1129aa) (excluding STOP codon)

893

gaacagcaggagcaggagacggtggaagagcccataatcttgcacgggtcgtcatccgagg
acgaaatggaagtggattaccctgttgttagcacacatgaacaaattgccagtagcccaccagg
agataatacaccagacgatgacccacaacctggcccatctcgcgaataccgctatgtactcag
aacatcaccaccccacagacctggagttcgtatgaggcgcgttccagttacccacccaaaaaa
gccacatccaagataccaacaaccaccggtcccttacagacagatagatgattgtcctgcgaa
agctaggccacaacacatcttttatagacgctttttgggaaaggatggaagacgagatccaaag
tgtcaatggaagtttgcagtgatttttttggggcaatgacccatacggacttaaaaaattatctcagg
ccttccagtttggaggagtaaaggcaggccccgtgtcctgcttgccccaccctggaccagacca
gtcgcccataacttattgtgtatatgtgtattgtcagaacaaagacacaagtaagaaagtacaaat
ggcccgcctagcctgggaagctagtcacccccctggcaggaaacctacaatcttccatagttaag
tttaaaaagcccctgccattaacccagccaggggaaaaccaaggtcctggggactctccacag
gaaatgaca**taa**

1130 (STOP)

Table 2.1 Antibodies used in this thesis

Primary

Protein Target	Antibody name/Ref	Species	Type	Source	Academic reference
LANA1	LN53	Rat	Mono	P.Kellam	(Kellam *et al.* 1999)
LANA1	LN72	Rat	Mono	P.Kellam	(Kellam *et al.* 1999)
hnRNPA1	2D32	Mouse	Mono	S.Murakami	-
hnRNPA1	4B10	Mouse	Mono	G.Dreyfuss	-
PABP1	-	Mouse	Mono	G.Dreyfuss	-
hTERT	sc-7212	Rabbit	Poly	Santa Cruz	-
GST	sc-459	Rabbit	Poly	Santa Cruz	-
CD31	-	Mouse	Mono	Chemicon	-

Secondary

Protein Target	Antibody Ref Code	Species	Conjugate	Source
Anti-rat IgG	F0234	Rabbit	FITC	DAKO
Anti-mouse IgG	R0480	Goat	RPE	DAKO
Anti-rabbit IgG	sc-2054	Goat	HRP	Santa Cruz
Anti-rat IgG	sc-2006	Rabbit	HRP	Santa Cruz

Table 2.2 Cell line information

Cell line	Source	Cell type	Features	Adherent/ suspension
DG75	Burkitt's lymphoma	B-cell	EBV transformed (EBV-negative)	Suspension
BCP-1	PEL	B-cell	KSHV positive	Suspension
BC-3	PEL	B-cell	KSHV positive	Suspension
HEK-293	Human embryonic kidney	Fibroblast	Adenovirus E1A & E1B	Adherent
HEK-293T	Human embryonic kidney	Fibroblast	Adenovirus E1A & E1B & SV40 large T antigen	Adherent
HeLa	Cervical	Epithelial	HPV E6 & E7	Adherent
CB3	Mouse erythroleukaemia	Erythrocyte progenitor	Retrovirus insertion	Suspension
CB7	Mouse erythroleukaemia	Erythrocyte progenitor		Suspension

Table 2.3 Primers used for PCR/RT-PCR

Target	**5'/3'**	**Oligo sequence**
LANA1 aa1-282	**5'**	aaagtacttgatatcgccaccatggcacccccgggaatgcgc
LANA1 aa1-282	**3'**	catggctgtgtcatcacccca
hnRNP A1	**5'**	cgagaggagctgggatccggtatgtctaagtcagagtctcctaaa
hnRNP A1	**3'**	gctgccctcgagtccttaaaatcttctgccactgccatagct
UP1	**5'**	cgagaggagctgggatccggtatgtctaagtcagagtctcctaaa
UP1	**3'**	cgcctcgagctaagcgtagtctgggacgtcgtatgggtatcgacct ctttggctggatga

Chapter 3 Results

HIV-1 based lentivirus infection of human primary endothelial cells

Chapter aims: The aim of this chapter was to develop an HIV-1 based lentivirus vector carrying KSHV LANA1 and demonstrate its use in both primary cells and cell lines.

3.1 Phenotypic analysis of primary endothelial cells

Primary endothelial cells were obtained from a donor and sorted by Dr Mike O'Hare, UCL. Prior to use in gene delivery and gene expression microarray experiments cells were checked for phenotype and viability. Staining with anti-CD31 antibody, observation of cells in continuous culture and functional activity in a tube formation assay were used to achieve this. Cells maintained the characteristic 'cobble stone' phenotype up to passage 15, at which point culture of cells was stopped (senescence usually occurs between passages 15-20). Staining of cells in culture with anti-CD31 antibody showed characteristic expression of CD31 at cell-to-cell contact (Fig 3.1A). The functional ability of the endothelial cells to form artificial blood vessels in a tube formation assay was tested. This assay allows the 'health' of the cells to be judged as low passage endothelial form tubes very quickly after seeding on Matrigel. Cells began forming tubes at 2hrs post seeding and this continued until the assay was stopped at 24hrs (Fig 3.1B). The formation of correct junctions is observable. While fibroblasts may possess tube formation activity and express CD31, they have a very different phenotype in culture and are easily distinguishable from primary endothelial cells. Fibroblasts have an elongated, streaming phenotype as compared to a cobblestone phenotype for endothelial cells. From these data I concluded that the cells obtained were of endothelial origin and were suitable for further experiments.

Fig 3.1 – Phenotypic analysis of primary HMVEC.

A, CD31 staining of primary endothelial cells. Primary human microvascular endothelial cells (HMVEC) were seeded onto glass slides as described in Material and Methods. Cells were fixed and permeabilised and incubated with anti-CD31 primary antibody and anti-mouse-RPE conjugated secondary antibody. Secondary antibody only controls were included which showed no staining. Cells were visualized and images obtained from a Leica microscope. CD31 can be seen at cell-cell junctions as is typical for healthy primary endothelial cells.

B, Tube formation assay on primary endothelial cells. Cells were seeded into 24 well plates previously coated with Matrigel. Cell morphology was observed at various times post-seeding and photographed using a Nikon microscope and digital camera.

Fig 3.1

A

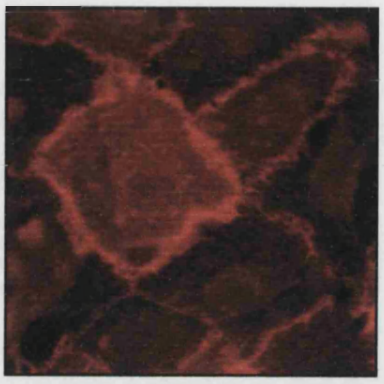

B

1hr post-seeding:
Limited pre-tubule formation is observed (most cells are still round after attachment)

2hr post-seeding:
More advanced pre-tubule formation is observed (most cells are now tubular)

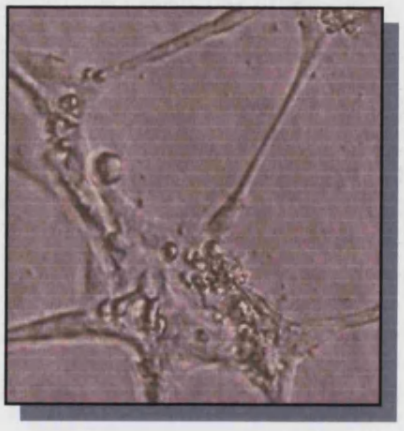

16hr post-seeding:
Mature tube formation is observed

24hr post-seeding:
Mature tube formation is complete

3.2 pHR CMV GFP infects cell lines

The pHR CMV-based virus system was selected to achieve my aim (Naldini *et al.* 1996). Initial testing of the pHR CMV-based lentivirus system concentrated on the infection of cell lines. If successful, further work would be undertaken of infection of primary cell lines with GFP and cloning of LANA1 into the system to allow delivery of LANA1 to cells. Virus was produced by the three plasmid transient transfection of HEK-293T cells (Naldini *et al.* 1996). HEK-293T cells (abbreviated to 293T from here on) are derived from human embryonic kidney cells but have been infected with adenovirus and SV40. They therefore express adenovirus E1A, E1B and SV40 large-T antigen. They are commonly used as packaging cells for the pHR CMV-based system as they are simple to grow, easy to transfect and the pHR CMV plasmids contain an SV40 origin of replication. Virus supernatant produced from these cells was concentrated by ultracentrifugation and used to infect DG75 (EBV negative Burkitts lymphoma cell line), BCP-1 (KSHV positive PEL cell line) and HEK-293. Control virus was produced by replacing the p8.91 plasmid with a plasmid expressing CRE. This was done to control for non-specific uptake and expression of GFP protein. As GFP protein is produced and released into the viral supernatant, this is a concern. Cells mock-infected with these controls should therefore not show expression of GFP. A high level of infection and good expression of GFP was seen in all cells tested (except primary B cells – see section 3.3) (Fig 3.2). This initial data showed that the lentivirus system was producing viable HIV-1 based viruses carrying the GFP transgene and was suitable for use in several types of cell line. The expression of any introduced gene can have aberrant effects on cells. I therefore tested the stability of GFP expression in cells up to 8 days/3 passages post-infection. HeLa cells were seeded at $5x10^5$ and infected the following day with 100μl of ultracentrifuge concentrated GFP virus and control (CRE transfected packaging cells). Cells were examined by FACS analysis for percentage of GFP expression at 48hrs, 120hrs

Fig 3.2 - pHR CMV GFP lentivirus infections of various cell types (72 hrs post infection). pHR CMV GFP virus was prepared in parallel with a GFP-CRE packaging control. Various cell types were infected with virus or control, and GFP was visualized at 72hrs post-infection using a confocal microscope.

Fig 3.2

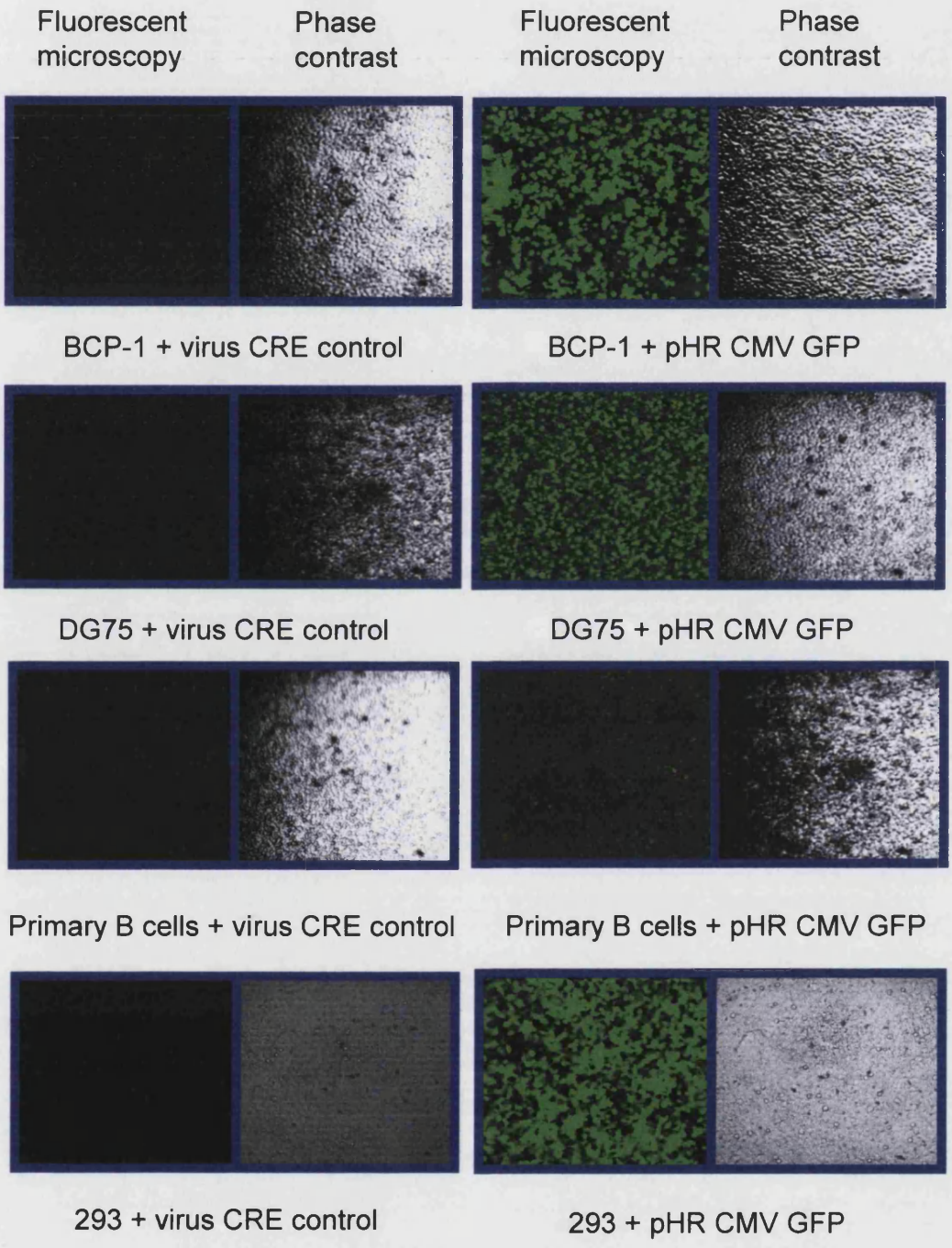
Fluorescent microscopy
Phase contrast
Fluorescent microscopy
Phase contrast
BCP-1 + virus CRE control
BCP-1 + pHR CMV GFP
DG75 + virus CRE control
DG75 + pHR CMV GFP
Primary B cells + virus CRE control
Primary B cells + pHR CMV GFP
293 + virus CRE control
293 + pHR CMV GFP

and 192hrs post-infection (Fig 3.3). Percentage of infected cells was determined by comparison with the CRE control. Percentage of infection was calculated as around 82% at 48hrs and throughout subsequent passages. These data show that the expression of GFP is stable and has no effect on the health of the cells. From this I also concluded that the GFP expression seen was due to infection and not short-term non-specific uptake of GFP protein.

3.3 Infection and stability of GFP expressing virus in primary endothelial cells

The lentiviral system, driven by the cytomegalovirus (CMV) promoter is capable of infection and driving GFP expression in several different types of primary and transformed cells lines, both adherent and suspension (Fig 3.2). The results show, however, that the system or this particular promoter is not suitable for infection of primary B-cells. Initial work concentrated on optimization of the lentiviral system in endothelial cells using GFP virus. The experiments for expression of GFP virus were controlled by a negative packaging control. In parallel with the production of virus using VSVg, p8.91 and pHR CMV GFP, flasks were transfected with VSVg, CRE plasmid and pHR CMV GFP. This control was needed, as it is possible for GFP protein to be endocytosed by cells. This is potentially a problem with primary endothelial cells as under certain conditions endothelial cells can act as professional antigen presentation cells and display proteins via the MHC-II pathway. GFP expression was never seen either by fluorescent microscopy or by FACS in CRE packaged controls during normal infections. However, the addition of polybrene as a reagent leads to an increased background in GFP-CRE controls (Fig 3.4). Due to this increased background and high levels of infection without the addition of polybrene, its use in subsequent infections was stopped. Primary endothelial cells were infected with a titration of GFP virus to determine the maximum percentage of

Fig 3.3 - Stability of GFP virus expression in HeLa cells. HeLa cells were seeded at $5x10^5$ and infected the following day with 100µl of ultracentrifuge concentrated GFP virus and control (CRE transfected packaging cells). Cells were examined by FACS analysis for percentage of GFP expression at 48hrs, 120hrs and 192hrs post-infection (Fig 3.3). Percentage of infection was determined by comparison with the CRE control. Percentage of infection was calculated as around 82% at 48hrs and throughout subsequent passages.

Fig 3.3

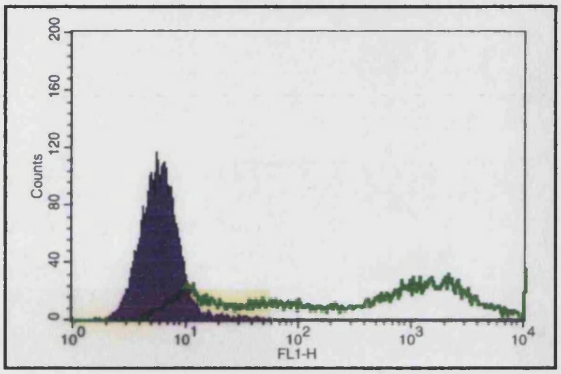

48hrs
82.91%

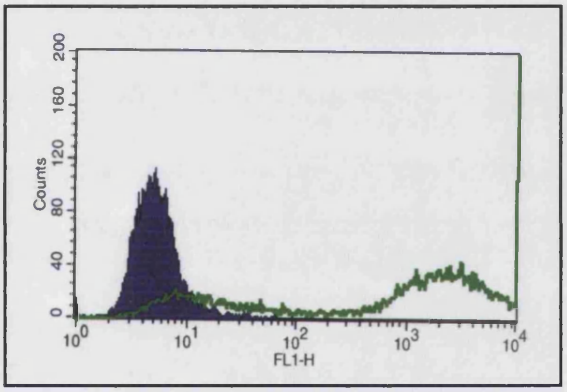

120hrs
81.33%

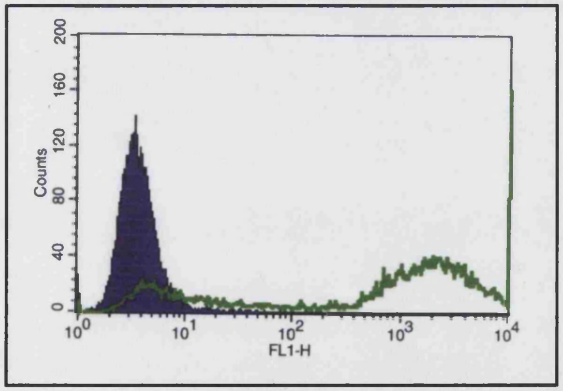

196hrs
81.33%

Fig 3.4 - The effects of polybrene on pHR CMV GFP infection of primary endothelial cells. pHR CMV GFP virus was prepared in parallel with a GFP-CRE packaging control. Virus supernatant was centrifuged at 25,000rpm for 11/2 hrs at 4°C. Concentrated virus was resuspended in 500μl of EGM-2 (per 20ml supernatant) and stored at –80°C. Primary endothelial cells were seeded at $2x10^4$ per well (6 well plate) and infected 4 days later. 100μl of virus or control was added per well. 72hrs later cells were observed using a confocal microscope. Polybrene was added to 3 wells, with 1μl of EGM-2 added to the other 3 wells.

Fig 3.4

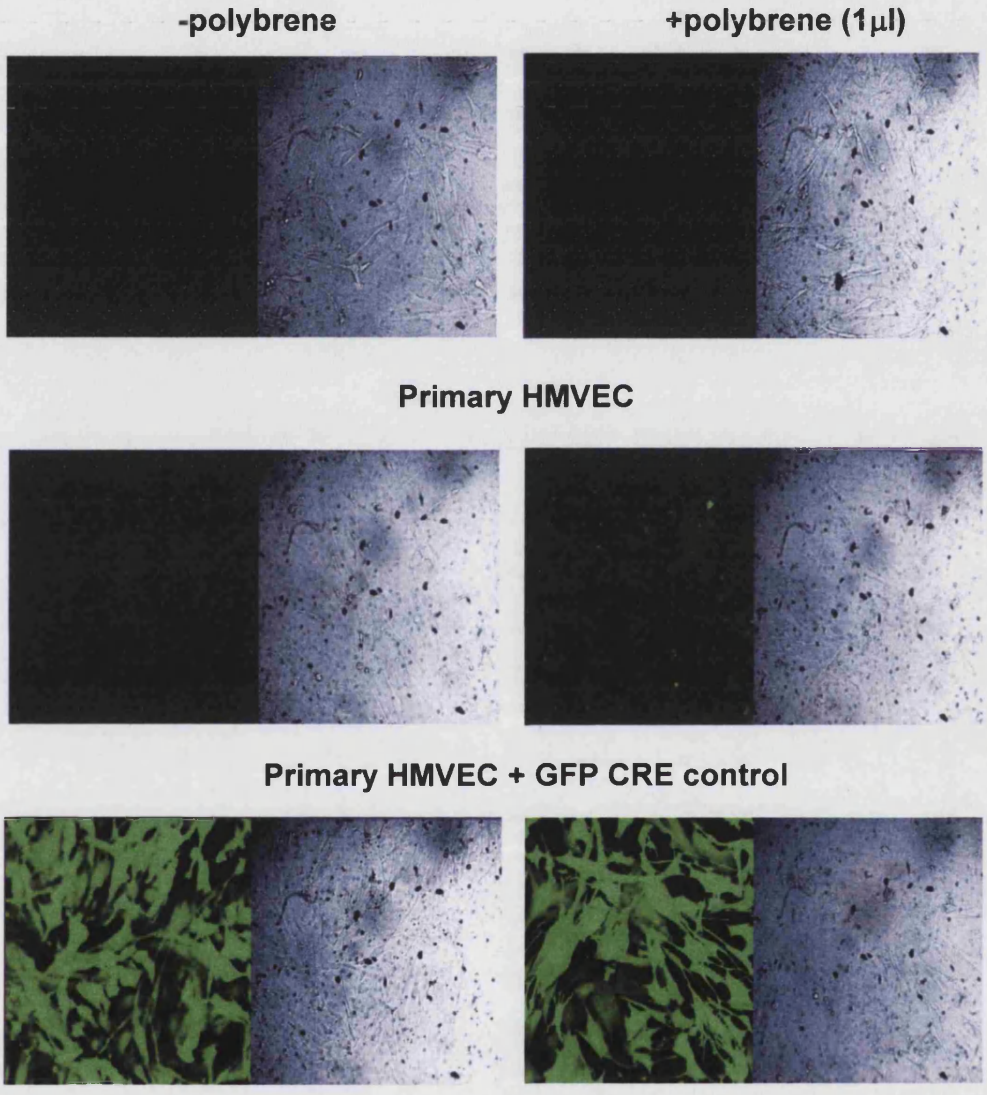
-polybrene
+polybrene (1μl)
Primary HMVEC
Primary HMVEC + GFP CRE control
Primary HMVEC + pHR CMV GFP

endothelial cells that were infectable. $1x10^4$ HMVEC were seeded in a 24well plate and infected the following day with a titration (1μl, 10μl, 100μl, 1000μl and 1000μl CRE control) of unconcentrated GFP virus. Infected cells were infected and examined by FACS analysis at 10 days post-infection after 3 passages. Overall, unconcentrated pHR CMV GFP virus is capable of high levels of infection in primary endothelial cells. >90% is practically possible, and the infection is stable over passaging as shown by FACs on 3rd passage HMVEC (Fig 3.5). Furthermore the data suggest correct integration of pHR CMV GFP allowing long-term expression and no aberrant effects on infected cells (Fig 3.5).

Fig 3.5 - The stability of pHR CMV GFP lentivirus in primary HMVEC. Primary human male microvascular endothelial cells (HMVEC) at passage 6 were seeded at $1x10^4$ in 24 well plate (1ml per well) in EGM-2 media 12 hours prior to infection. Media were removed from the cells and virus was added in amounts of 1000μl unconcentrated pHR CMV GFP-CRE (negative control), 1μl, 10μl, 100μl and 1000μl unconcentrated pHR CMV GFP. All infections were adjusted to 1000μl with DMEM + 10% FCS + antibiotics if necessary. Virus was left on cells for 5hrs then replaced with fresh EGM-2. At passage 8, cells were trypsinised and washed twice in PBS for FACS. FACS data were gated against pHR CMV GFP-CRE.

Fig 3.5

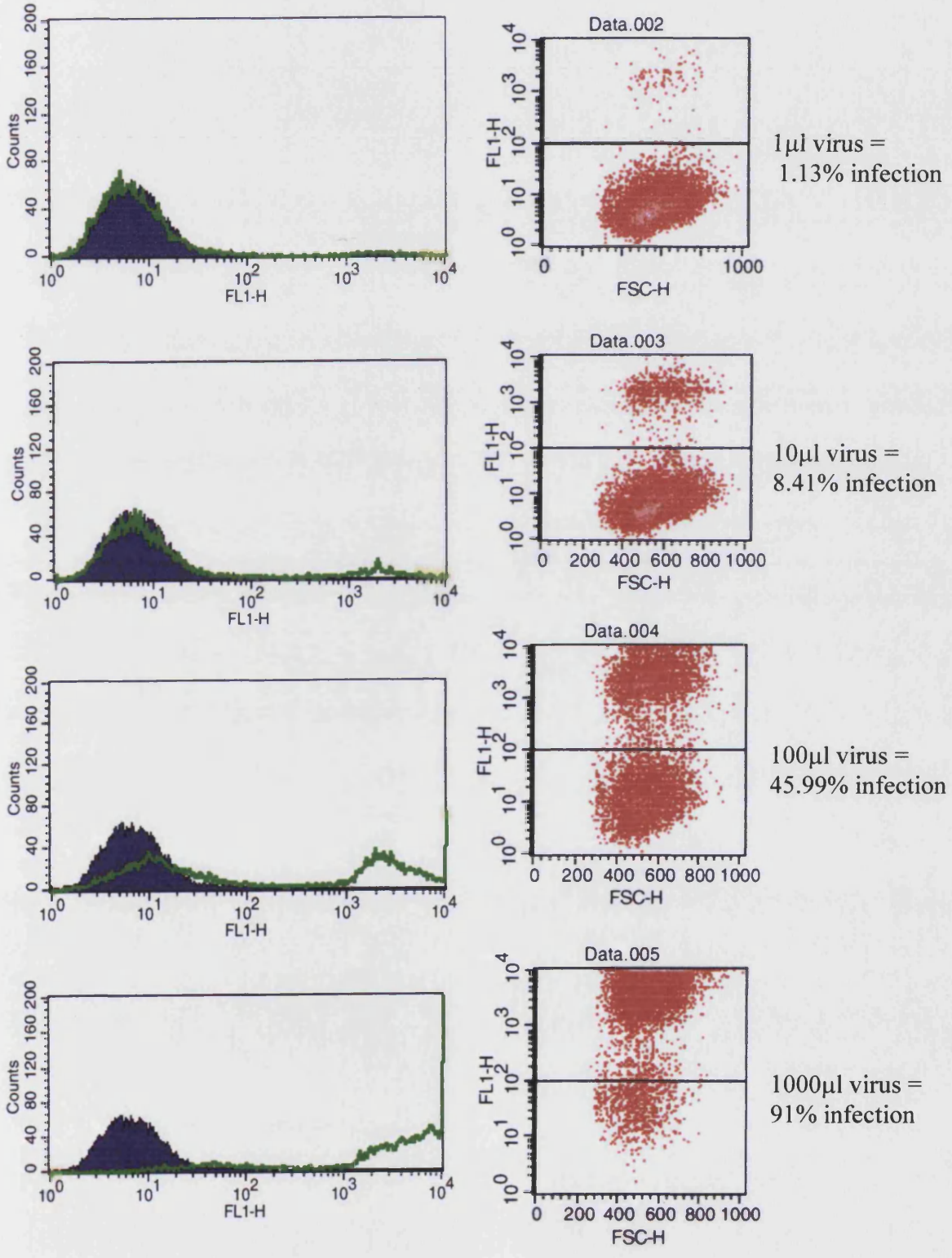
Counts
FL1-H
Data.002
FSC-H
1µl virus =
1.13% infection
Data.003
10µl virus =
8.41% infection
Data.004
100µl virus =
45.99% infection
Data.005
1000µl virus =
91% infection

3.4 pHR-CMV-LANA1 lentivirus infects cell lines

LANA1 was introduced into the pHR CMV LacZ vector as detailed in Materials and Methods. Briefly, LANA1 amino terminus was amplified by PCR and the carboxyl terminus was created by restriction digest of the parental vector IgH P/E 73cycK13, followed by three way cloning into the pHR CMV backbone from which LacZ had been removed. LANA1 is a large protein with a predicted molecular weight of 160kDa, but LANA1 actually runs during electrophoresis as a doublet at around 222/234 (Rainbow *et al.* 1997) or 220/235kDa (Kellam *et al.* 1997). The cloned pHR CMV LANA1 was confirmed by restriction mapping and DNA sequencing. For the production of LANA1 carrying HIV-1 based lentiviruses, 293T cells were transiently transfected with the pHR CMV LANA1 plasmid or an empty vector (pHR CMV emp), VSVg and p8.91. Supernatants were collected at 48hrs post transfection and stored at –80°C. The 293T cells were lysed in RIPA and subjected to western blotting using an anti-LANA1 antibody (Fig 3.6A). The cells showed good expression of LANA1 at 48hrs post-transfection indicating that the cloning and expression of LANA1 had been successful (Fig 3.6A). Syncytial formation is observed in cells transfected to produce LANA1 virus, indicating the expression of the VSVg construct (Fig 3.6B).

The kinetics of LANA1 expression at 24, 48 and 72hrs post-infection was observed by western blotting of infected DG75 cells (Fig 3.6C). LANA1 expression was detected at 48 and 72hrs post-infection, but was either low or not expressed at 24hrs (Fig 3.6C). These data indicated that the best time points for LANA1 expression is 48 and 72hrs post-infection. It is possible that the low expression of LANA1 at 24hrs is due to the time required for infection, integration and expression of the pHR CMV-based viruses.

Fig 3.6 - LANA1 lentivirus production and testing. **A**, WB on 293T cells for LANA1. HEK-293T cells were transiently transfected with 15 μg of pHR CMV LANA1 or pHR CMV emp, 10μg of p8.91 and 5μg of VSVg. Cells were lysed in RIPA buffer at 48hrs post-transfection and protein was separated on a 6-12% SDS-PAGE gel. Proteins were transferred to nitrocellulose membranes and blotted with anti-LANA1 antibody followed by anti-Rat HRP. Bands were visualized using ECL+ and ECL film. **B** , Formation of VSVg induced syncytia at 48hrs post transfection. Post-transfection 293T show the formation of syncytia due to the expression of VSVg. **C** , Kinetics of LANA1 expression 24-72hrs post infection. DG75 cells were infected with LANA1 lentivirus or CRE packaging control supernatant. Cells were lysed at 24, 48 and 72hrs post-infection. Expression of LANA1 post-infection is observed at 48 and 72hrs.

Fig 3.6

A

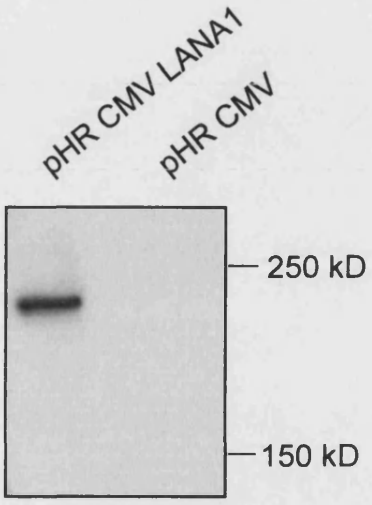

B

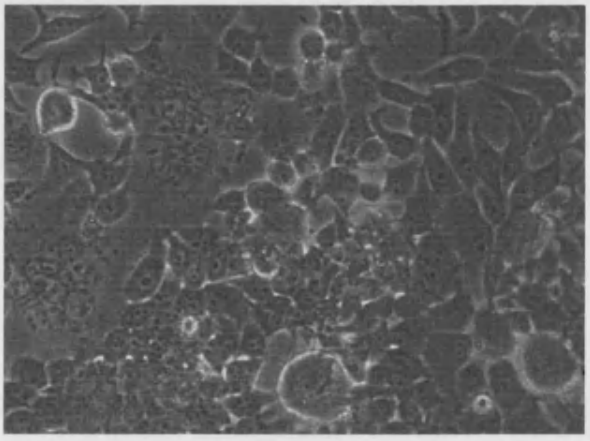

C

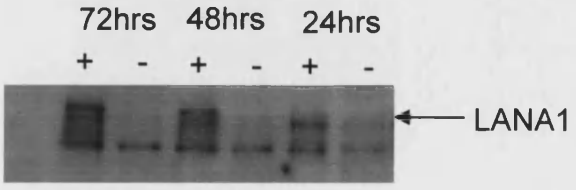

The expression pattern of LANA1 in cell lines post-infection was tested using HeLa cells. LANA1 carrying virus, along with a CRE packaging control was used to infect cells. The pattern of LANA1 by western blotting was compared to endogenous LANA1 in BC-3 cells to ensure correct processing of LANA1 expressed from the lentiviral construct. BC-3 and HeLa-LANA1 cells were lysed in RIPA buffer and a titration of cell number was used for western blotting. LANA1 expressed from infected HeLa cells shows the same pattern by western blotting as endogenous LANA1 from BC-3 cells (Fig 3.7A). These data showed that LANA1 was being processed correctly.

As mentioned earlier, LANA1 is a large protein that acts as both a transcriptional activator and repressor. To test that over expression of LANA1 was not having an aberrant effect on cells, the stability of LANA1 in HeLa cells was observed over time by western blotting. HeLa cells at passage 1,2 and 3 post-infection with pHR CMV LANA1 or CRE control were lysed and LANA1 was detected by western blotting. LANA1 expression is seen at 3 passages post-infection indicating stability of the transgene (Fig 3.7B).

For initial experiments viruses were produced in parallel with a packaging control, in which the p8.91 plasmid was substituted with a CRE expressing plasmid. The data in this section show that no specific uptake and expression of LANA1 was seen in control infections. For later use [in gene expression microarray experiments], a pHR CMV empty plasmid was packaged as a negative, to control for the effects of viral infection on primary endothelial cells.

Fig 3.7 - LANA1 expression and stability in Hela and primary endothelial cells. **A**, LANA1 patterning by Western blot in HeLa cells. BC-3 and pHR CMV LANA1 /LANA1-CRE control virus infected HeLa cells were lysed in RIPA buffer. Various amounts of protein were separated on a 6-12% SDS-PAGE at 120V. Proteins were transferred to a Hybond-P membrane over night at 0.1A in MeOH transfer buffer. Membranes were blocked in PBS+Tween+milk powder and probed with anti-LANA1 LN72 rat monoclonal diluted 1:1000 in 10% blocking buffer for 2hrs. After washing anti-Rat HRP (Santa Cruz) was incubated with the membranes for 1hr and bands were visualized after incubation with ECL+ (Amersham Pharmacia Biotech) and exposure to ECL film (Amersham Pharmacia Biotech). The patterning of LANA1 expressed from the lentivirus matches that seen in BC-3, indicating that the virus is expressing correctly. **B**, LANA1 expression in Hela cells is stable over 3 passages. $5x10^5$ HeLa cells were infected with concentrated LANA1 lentivirus and CRE packaging control. Cells were maintained in culture over three passages and a proportion lysed in RIPA buffer for analysis by western blotting. Proteins were separated on 6-12% gradient SDS-PAGE gel and detected by anti-LANA1 monoclonal antibody. Expression of LANA1 is evident up to passage three. **C**, LANA1 expression in primary HMVEC is stable over 4 passages. $8x10^4$ primary HMVEC at passage 5 were infected with 10μl, 100μl or 1000μl of unconcentrated LANA1 lentivirus. Cells were maintained in culture until passage 9 and lysates were prepared in RIPA buffer at each passage. Protein was separated on a 6-12% SDS-PAGE gradient gel and LANA1 was detected using anti-LANA1 monoclonal antibody. Expression of LANA1 is evident up to passage 9 (4 passages post-infection).

Fig 3.7

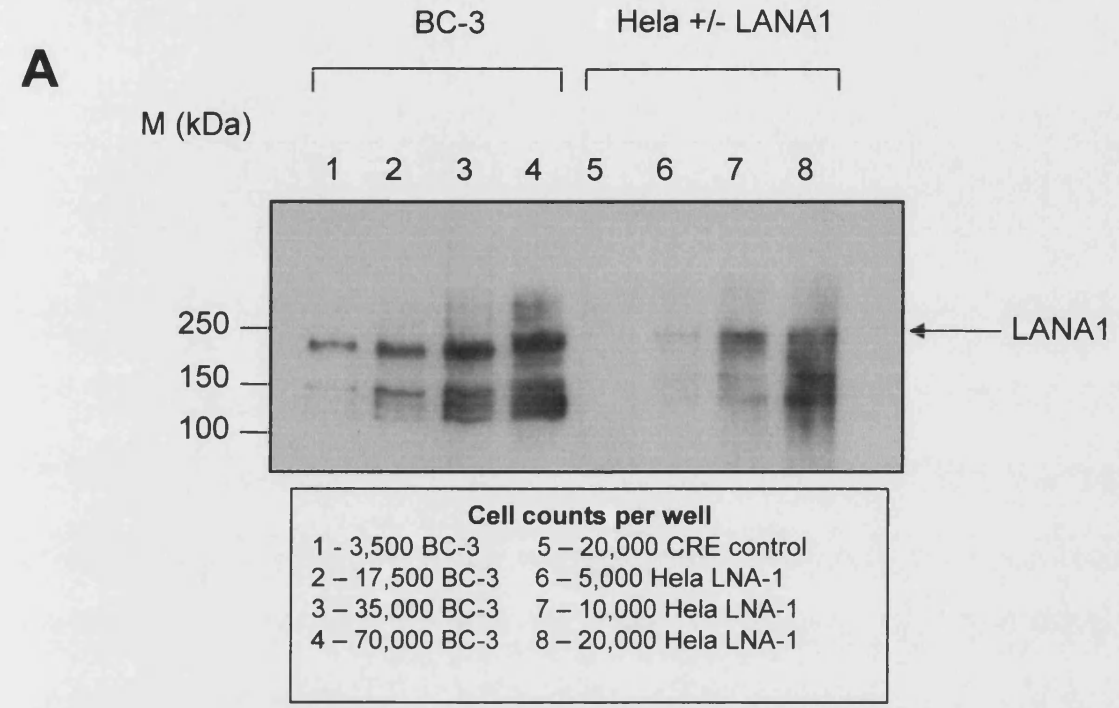
A
BC-3
Hela +/- LANA1
M (kDa)
1 2 3 4 5 6 7 8
250
150
100
LANA1
Cell counts per well
1 - 3,500 BC-3
2 – 17,500 BC-3
3 – 35,000 BC-3
4 – 70,000 BC-3
5 – 20,000 CRE control
6 – 5,000 Hela LNA-1
7 – 10,000 Hela LNA-1
8 – 20,000 Hela LNA-1

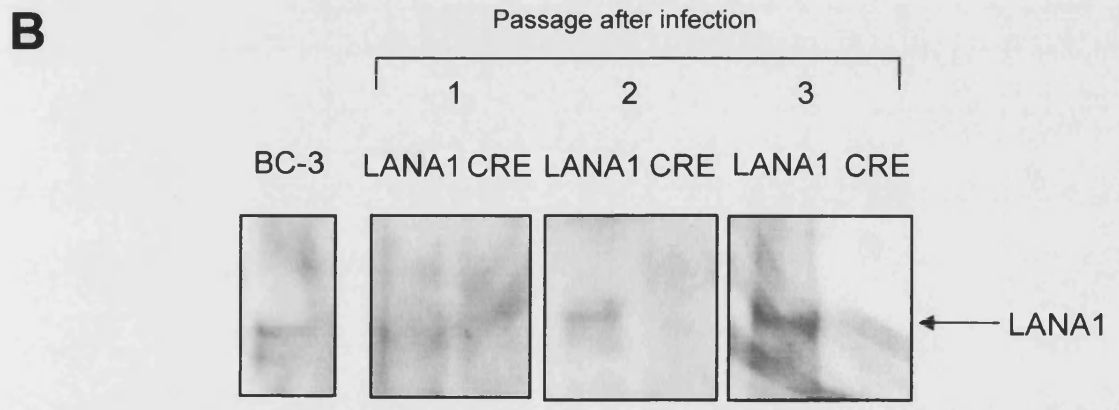
B
Passage after infection
1 2 3
BC-3 LANA1 CRE LANA1 CRE LANA1 CRE
LANA1

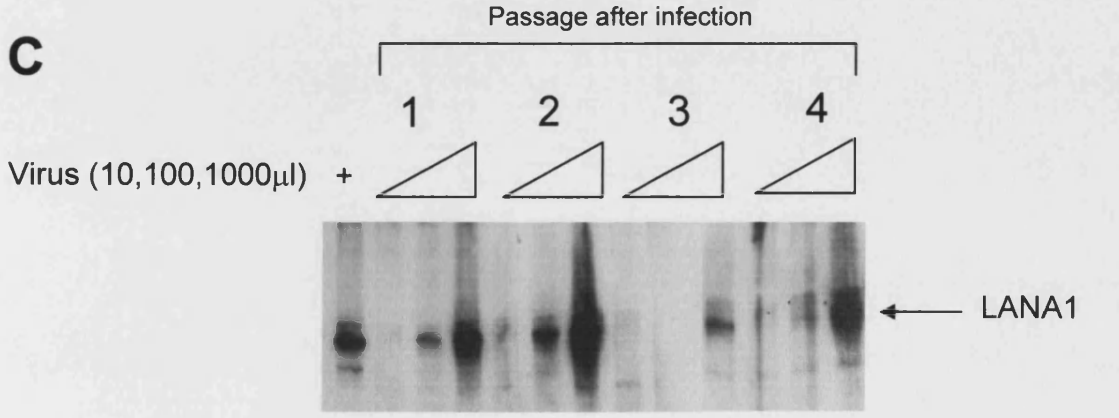
C
Passage after infection
1 2 3 4
Virus (10,100,1000µl) +
LANA1

3.5 pHR-CMV-LANA1 lentivirus infects primary HMVEC

LANA1 shows characteristic patterning by western blot (Fig 3.7A) of a doublet at 220-235kDa, similar to endogenous expression of LANA1 in KSHV-infected PEL cells (BC-3). I next tested the infection of primary endothelial cells with the LANA1 virus. Endothelial cells were infected and expression of LANA1 was monitored by western blotting over several passages. The expression of LANA1 is high and LANA1 is stable over at least 4 passages (Fig 3.7C). This data indicated that the infection of primary cells was possible, LANA1 was expressing and the expression was stable over time indicating no growth disadvantage for cells expressing LANA1.

KSHV LANA1 has previously been shown to be a nuclear protein that associates with heterochromatin-nuclear bodies and shows a characteristic nuclear stippling by immunofluoresence assay (Szekely *et al.* 1999). Although my data showed that the system was expressing LANA1, I also wanted to confirm the cellular localization of LANA1 after infection with this virus. To achieve this I used immunofluoresence assay with an anti-LANA1 antibody. Primary endothelial cells were grown on pre-sterilised glass cover slips in 6-well plates. After infection, cells were incubated with anti-LANA1 antibody and visualized using fluorescent microscopy. The results of LANA1 staining in endothelial cells are seen in Fig 3.8. Detection of pHR CMV LANA1 in primary HMVEC 72hrs after infection reveals the characteristic nuclear localization and stippling (Fig 3.8A) and association with cellular DNA during mitosis (Fig 3.8B). Co-staining of LANA1 and CD31, an endothelial cell marker, was also undertaken (Fig 3.8C). Overall, these data showed that good infection of endothelial cells was possible with the LANA1 virus and that LANA1 behaved in a phenotypically correct manner.

Fig 3.8 – Cellular localization of LANA1. **A**, Primary microvascular endothelial cells were plated in 6 well plates containing glass cover slips. Cells were seeded at 8 $x10^4$ per well the evening before infection with virus. Cells were infected either with 1ml of pHR CMV LANA1 (LANA1+) or 1ml of LANA1 CRE (LANA1-) control. 48hrs p.i. cells were subjected to IFA protocol using LN53 as the primary and anti-Rat FITC (DAKO) as the secondary antibody. Cells were visualized and photographed on a Nikon fluorescent microscope. **B**, LANA1 associates with condensed chromatin during mitosis. **C**, Primary endothelial cells were grown on glass cover slips and infected with LANA1 lentivirus. Cells were fixed, permeabilised and co-stained with anti-LANA1 rat monoclonal (1:1000) and anti-CD31 mouse monoclonal (1:500). Secondary antibodies used were anti-rat FITC (1:120) and anti-mouse RPE (1:100).

Fig 3.8

A

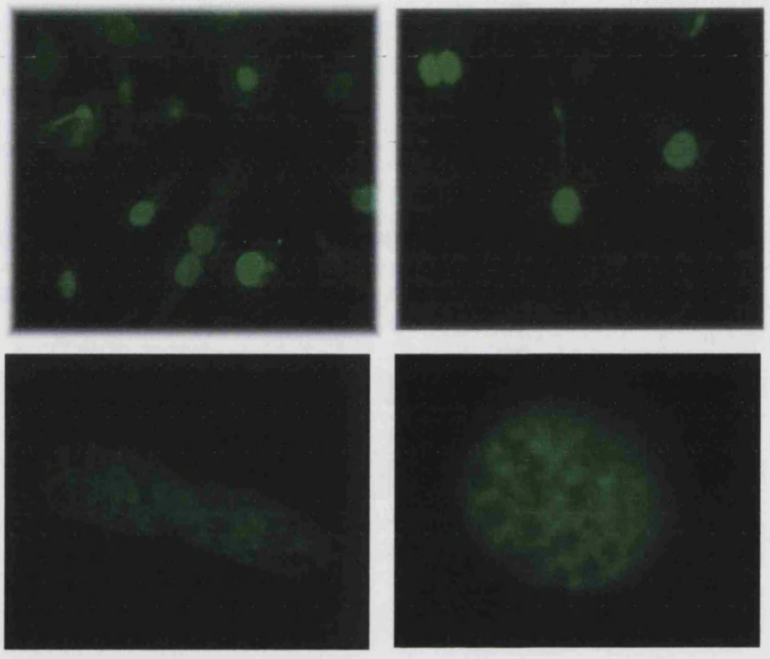

B

C

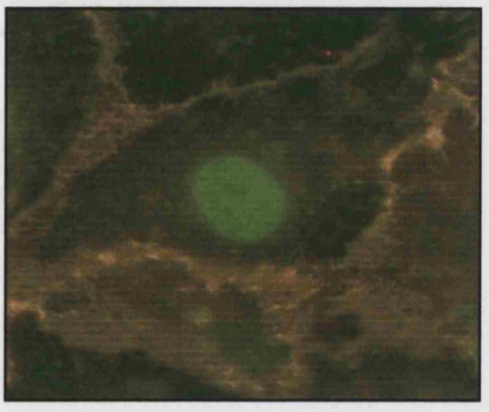

3.6 Discussion and conclusion

In this chapter I have developed a reliable method for the delivery of viral genes to transformed cell lines and to primary endothelial cells. Other groups have utilized the system for delivery of transgenes to endothelial cells, including LacZ (Totsugawa *et al.* 2002), eGFP (Wang *et al.* 2000) and the non-catalytic fragment of matrix metalloproteinase 2 (PEX) (Pfeifer *et al.* 2000). The pHR CMV GFP system has been used to infect a range of cells including CD34+ CD38- human hematopoietic cells (Case *et al.* 1999). The data contained in this chapter represent the first study to use a lentiviral system for the delivery of a viral oncogene to primary endothelial cells.

The lentiviral system, although eventually reliable and robust, was initially problematic. Careful considerations when using the system include the preparation of plasmid DNA, the density and age of packaging cells and the transfection of packaging cells. Together, these areas represent the main reasons for either sub-optimal results or failure of the lentiviral systems. In the whole however, once these technical aspects have been learnt, the lentivirus system is a powerful and flexible tool that will no doubt continued to be developed and used in an increasing number of laboratories.

The delivery of LANA1 to primary endothelial cells using the lentiviral system resulted in a characteristic phenotype and localization of LANA1 protein. This is important in any system, allowing results obtained to be interpreted as being directly relevant to disease state. LANA1 and the viral episomes accumulate in heterochromatin-associated nuclear bodies ensuring the virus persists in daughter cells (Ballestas *et al.* 1999;Cotter and Robertson 1999) and show a characteristic nuclear stippling pattern in all KSHV infected tumour cells (Dupin *et al.* 1999;Mattsson *et al.* 2002a;Szekely *et al.* 1999). The characteristic nuclear stippling and association of LANA1 with

DNA in dividing cells were observed by IFA on LANA1 virus infected endothelial cells.

Overall, the data in this chapter show that LANA1 can be delivered effectively to primary cells and cell lines using a lentiviral based system and no aberrant effects are seen as a result. The expression of LANA1 is high, phenotypically correct and stable. The results show that the lentiviral system is a robust tool that could be applied to several different technical problems in modern biological research. The system was developed specifically for the delivery of LANA1 to primary endothelial cells but could be adapted for other viral genes. Areas include the delivery of viral genes to stem cells and the delivery of small interfering RNA (siRNA) to primary cells. This would be of particular interest in silencing KSHV genes from infected primary cell lines to study the effects of viral genes in a more relevant context. In the context of primary endothelial, the lentiviral delivery system may be an excellent way of delivering genes to cells for screening by chorioallantoic membrane assay (CAM) in which the cell growth and invasion potential of cells can be assessed.

In the next chapter I describe the use of the lentivirus system to study the effects of LANA1 on primary endothelial cells using gene expression microarrays.

Chapter 4 Results

Effects of LANA1 on primary endothelial cells determined by gene expression microarray

Chapter aims: The aim of this chapter was to use the HIV-1 based lentivirus to determine the effects of LANA1 on the transcriptome of primary endothelial cells thereby identifying novel cellular transcriptional targets.

4.1 Optimization of cell culture and RNA extraction

Several considerations were important for the design of the microarray experiment. Firstly, primary endothelial cells are difficult to culture at a large scale, therefore the required amount of material for the microarray experiments (RNA) had to be calculated. Secondly, primary endothelial cells express a different array of genes depending on their cell density. It was decided that array analysis should take place on cells infected with lentivirus that had not yet reached confluent culture. It is known that upon confluence endothelial cells change their expression pattern from angiogenic to vascular homeostasis. I therefore designed experiments to determine suitable seeding conditions that would provide a sufficient amount of RNA, without the cells reaching confluence after infection. Primary endothelial cells were seeded in varying concentrations in $25cm^2$ flasks. Cell populations were examined at 24hrs and 72hrs post seeding (Fig 4.1). In the previous chapter I showed that expression of LANA1 was strong at 48hrs post-infection. Based on this, infection with lentivirus would be carried out at 24hrs post seeding and RNA extracted at 72hrs post seeding, the equivalent of 48hrs post infection. The data show that the best seeding conditions are $2x10^5$ in $25cm^2$ flask (Fig 4.1), as this allows good cell growth, but remain sub-confluent at the equivalent of 48hrs post-infection. RNA test extractions were performed to ensure that sufficient quantities of RNA could be recovered (Fig 4.2). Cells seeded at $2x10^5$ provided 14.4μg

of high quality RNA (260/280 = 1.935). As microarrays would be performed in duplicates, these parameters were therefore deemed suitable.

Fig 4.1

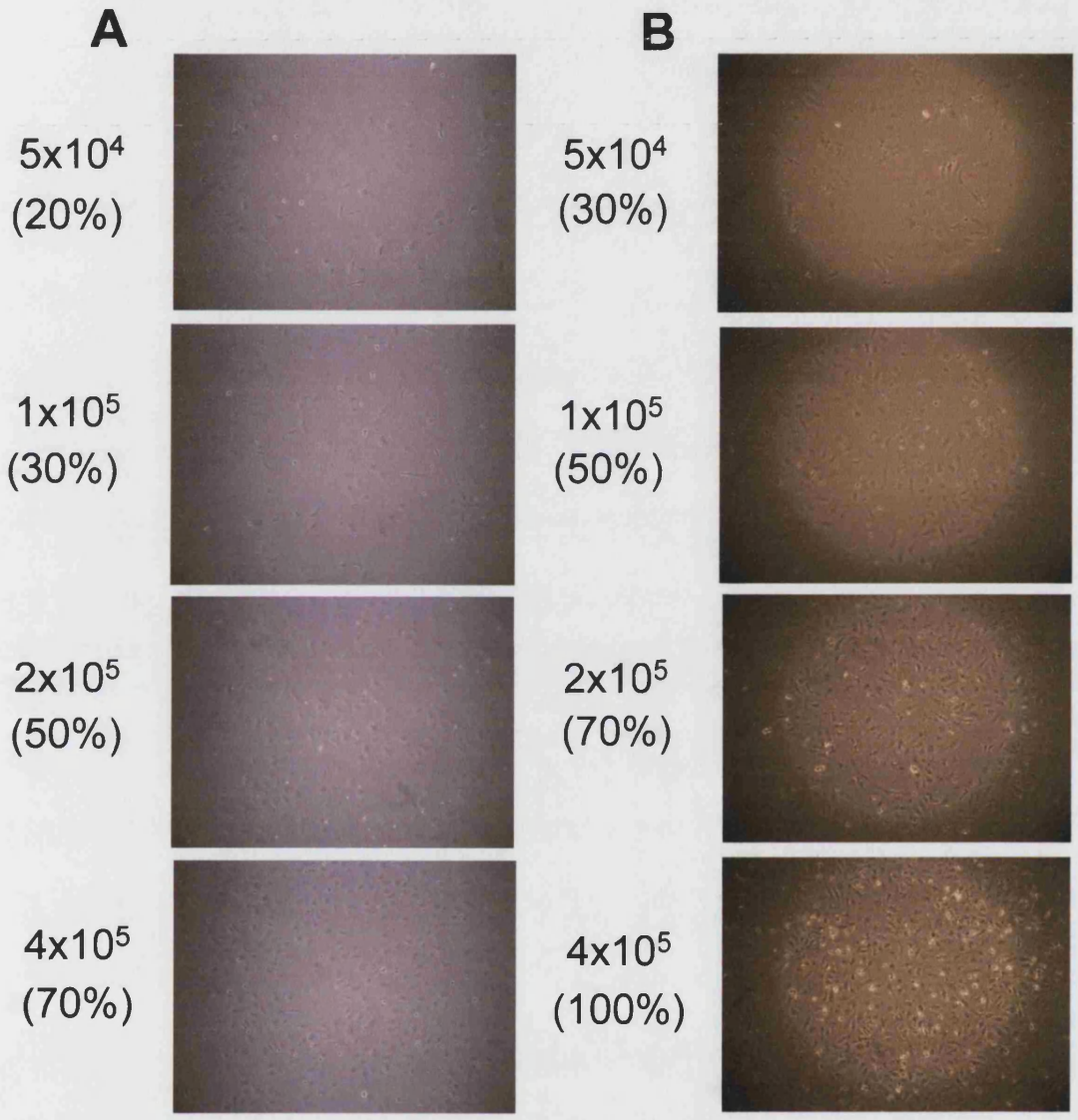

Fig 4.1 Test seeding of primary endothelial cells
Primary microvascular endothelial cells were seeded at passage 8 at concentrations ranging from $5x10^4$ to $4x10^5$ in $25cm^2$ flasks suspended in EGM-2 media.
A, Photographs were taken on the next day post seeding (24hrs) and
B, at 72hrs post seeding. Percentages of confluence were calculated and are shown in brackets.

Fig 4.2

A

Seeded	Final	RNA yield	260/280
$5x10^4$	$1.14x10^5$	2.4μg	5.5
$1x10^5$	$1.98x10^5$	2.4μg	2.7
$2x10^5$	$3.6x10^5$	14.4μg	1.935
$4x10^5$	$9.36x10^5$	12.72μg	1.827

B

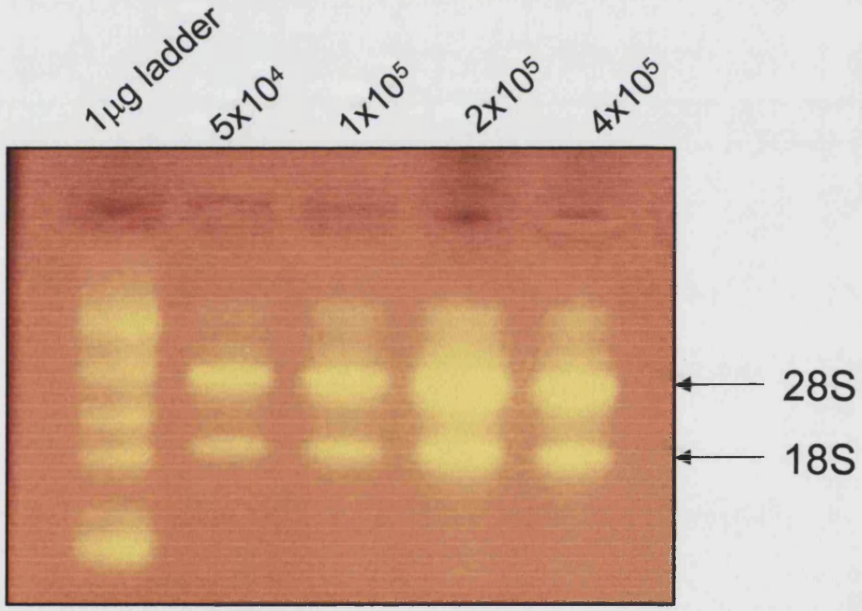

Fig 4.2 Endothelial test seeding RNA extraction
Total RNA was extracted from primary endothelial cells seeded at various cell densities. **A**, Total quantities of RNA obtained from each cell density at the equivalent of 48hrs post-infection. **B**, 1% agarose gel of extracted total RNA.

4.2 Equalisation of viral infections and infection data at 48hrs post infection

During the course of virus preparations it became evident that different pHR CMV transgene inserts produced varying quantities of virus. This was considered a problem for the controls during the microarray analysis. As gene expression microarray technology is sensitive, unequal amounts of virus put onto cells in terms of LANA1 vs control may have quenched significantly up or down regulated transcripts. To solve this problem, virus preparations were quantified prior to infection of primary endothelial cells. The size of insert cloned into the pHR CMV backbone correlated with the yield of virus. Using GFP as a guide, viruses were equalised in terms of p24 quantity. A quantity of GFP virus that had previously given high levels of infection was selected and other viruses equalised to this figure. Quantities of p24 for each virus produced were calculated using a p24 ELISA (Fig 4.3 A). From the p24 ELISA results it was evident that there was an inverse relationship between the size of the insert cloned into the pHR CMV vector and the quantity of p24 protein in viral supernatants (Fig 4.3 B). A quantity of GFP virus was calculated from p24 values to achieve as close to 100% infection of cells as possible. 78 ng of p24 for each virus was added to cells for RNA extraction for analysis by gene expression microarray. At 48hrs post-infection, GFP infected cells were analysed by FACS and showed greater than 97% infection (Fig 4.4 A). This indicated that the expression of LANA1 viruses should be high in the primary endothelial cells. To confirm this, LANA1 was detected by western blotting of cell lysates at 48hrs post-infection. LANA1 expression was detected in only the LANA1 infected cells (Fig 4.4 B). RNA was extracted from the infected cells at 48hrs post-infection and quantity and quality were determined by UV spectrophotometry. Data are shown for total RNA yield and quality based on two extractions for each sample (Fig 4.5).

Fig 4.3

A

Size of gene insert	p24 ng/ml
0kb	115
1.1kb	39.7
1.5kb	26.7
3.1kb	18.8

B

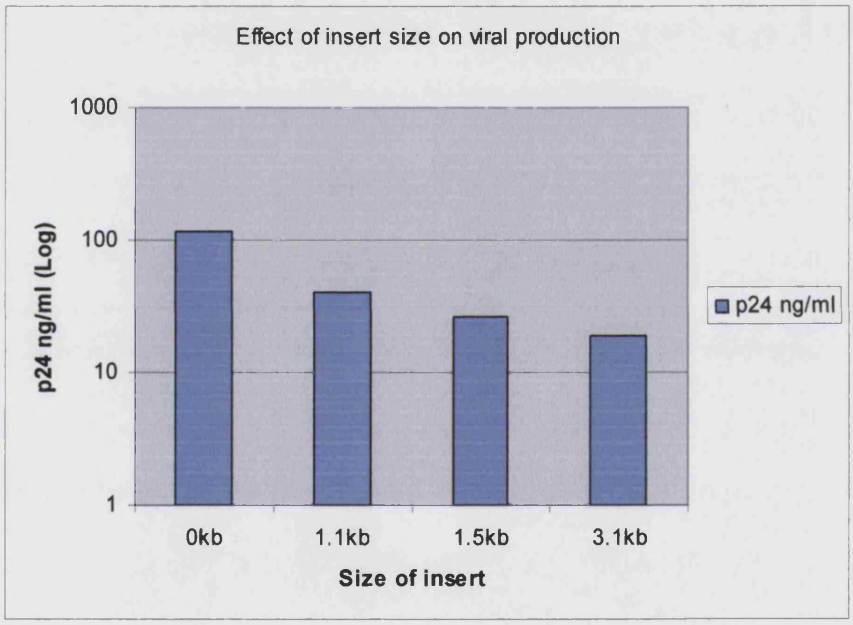

Fig 4.3 Quantification of viruses using p24 ELISA
A, Viruses were produced by the transient transfection of 293T cells. Supernatants from the packaging cells, which contain released virus, were used in a p24 ELISA to determine the quantity of virus as protein quantity. Quantities of protein are shown for each of the viruses tested.
B, the relationship between insert size in kb and quantity of produced virus.

Fig 4.4

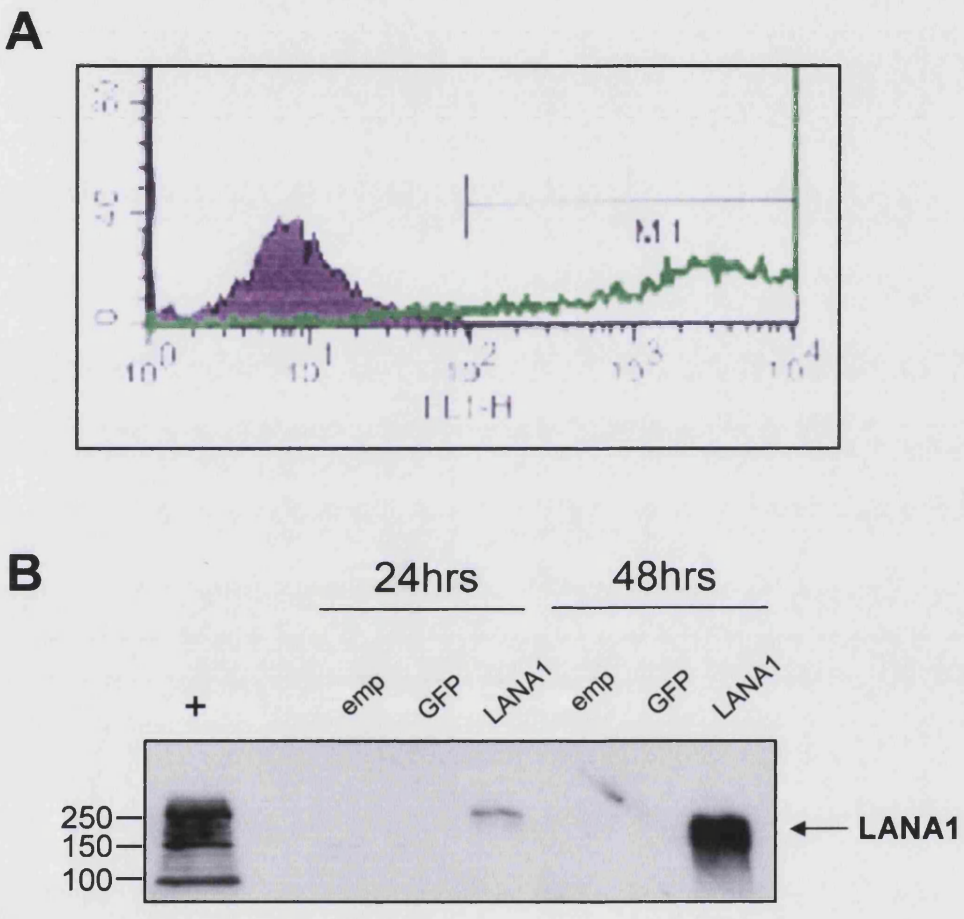

Fig 4.4 FACS data and LANA1 expression from primary endothelial cells for gene expression microarray analysis
A, FACS analysis was performed at 48hrs post-infection on pHR CMV GFP lentivirus infected primary endothelial cells. Percentage of infection was calculated as 97%. **B**, Cells infected with various viruses in parallel with gene expression microarray experiments were lysed in RIPA buffer, separated by SDS-PAGE and subjected to western blotting with anti-LANA1 antibody. Expression of LANA1 is clearly visible at 24 and 48hrs post-infection.

Fig 4.5

A

RNA yield/quality 48hr p.l.

Lane #	Sample	Yield (μg)	260/280
1	Norm 1	12	1.142
2	Norm 2	18.6	2.480
3	Empty 1	33.24	1.928
4	Empty 2	4.5	0.000
5	LANA1 1	35.7	2.087
6	LANA1 2	3.6	6.000

B

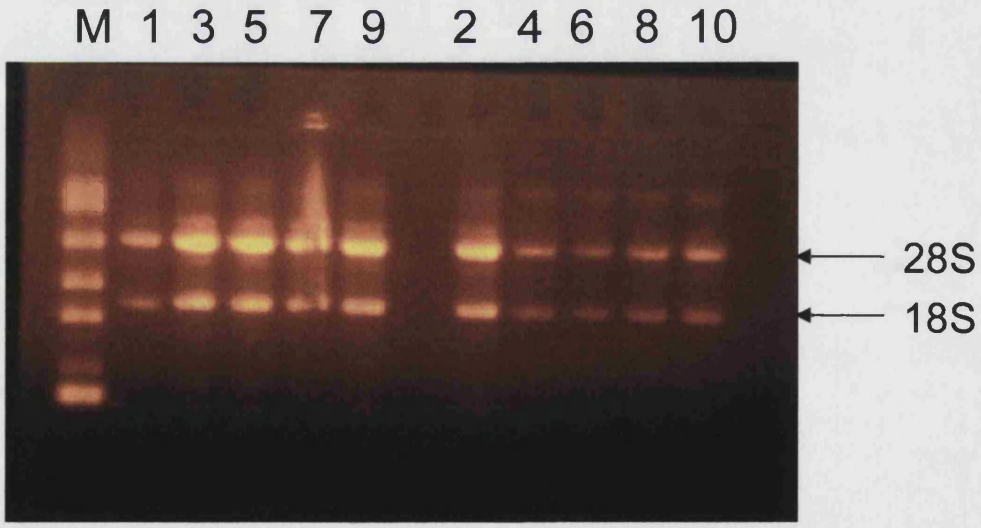

Fig 4.5 Total RNA extraction for gene expression microarrays
A, Total quantity and quality of total RNA obtained from lentivirus infected cellsat 48hrs post-infection. **B**, 1% agarose gel of extracted total RNA.

4.3 Analysis of GEM data

Data from duplicate microarray hybridisations were obtained from a Storm scanner (Amersham Pharmacia Biotech) as .gif files and were imported into Research Genetics Pathways software. Initially data analysis was attempted by using software derived normalisation. This however did not provide good distribution figures for the data, so the data were exported as raw intensity values into MS Excel. In MS Excel data were normalised by the average total array values. The normalised average intensities for each duplicate set of arrays was plotted and correlation between the normalised data were determined to be $R^2 = 0.9884$.

A list of potential genes was generated with a cut-off fold change of +/- 1.4 for LANA1 vs Emp (control). This list was used to cross-reference back to array figures, in order to confirm that each data spot was correctly aligned and not a false positive. Many of the genes identified were of low signal intensity. Using this method over 90% of target genes that could be visualized on the Pathways software, were discounted as false positives. This most often occurred where Pathways software had misinterpreted 'bleed' from a strong spot signal in close proximity (Fig 4.6). The problem was determined not to be caused by misalignment during import of the array images. Due to this, the final list of genes includes only those that were able to be checked manually against images. Genes whose low signal was not visible for checking were excluded from the final list. All genes initially selected are in Appendix 1. A final list of up/down regulated genes was created from this manual selection and curation of data. Figure 4.7 B shows the final list of genes selected as having a good fold change, t-test value <0.05 and visible correctly aligned cDNA spot. Figure 4.7 A shows the Pathways™ images in a representative experiment for each spot.

Fig 4.6

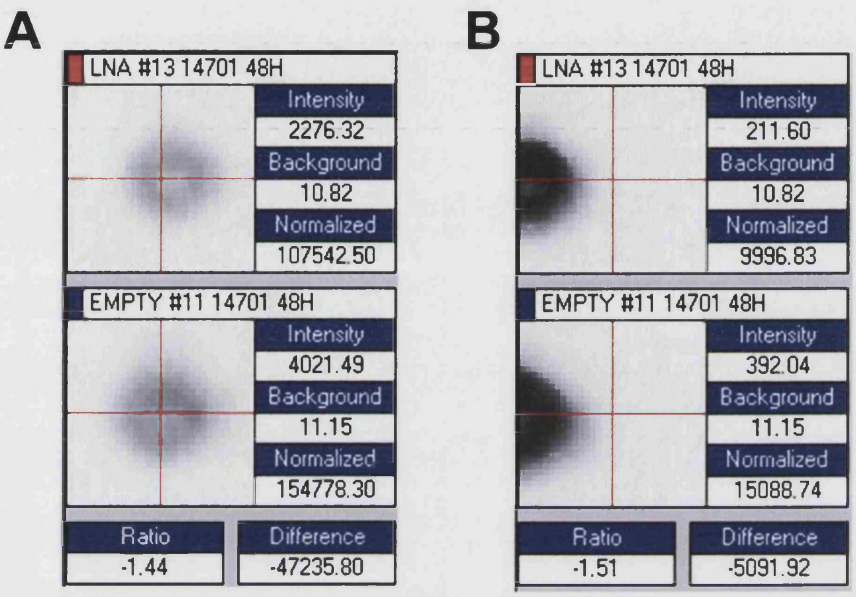

Fig 4.6 Alignment of cDNA spots on GF211 research genetics microarrays
A, shows a correctly aligned data point. **B**, shows a misaligned false positive. Where spot intensities were sufficient for manual checking, approximately 90%+ software selected where false positives, often due to strong intensities of surrounding cDNA spots.

Fig 4.7

A

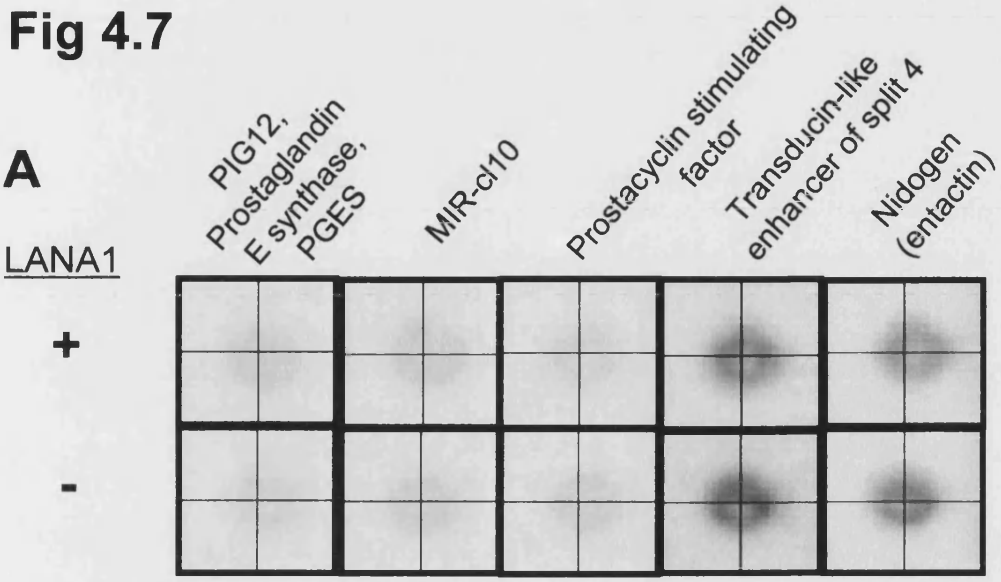

B

Gene name	Ratio	Fold	ttest	Accession
Prostacyclin-stimulating factor	0.644241	-1.55	0.044394	T53298
MIR-10	1.433614	+1.43	0.034453	H54023
Nidogen	0.722972	-1.38	0.049286	AA709414
Transducin-like enhancer of split	0.709209	-1.41	0.017366	AA704492
Prostaglandin E synthase (PIG12)	1.500	+1.5		AA436163

Fig 4.7 Gene expression microarray images and data for LANA1 target genes

A, Images of cDNA spots were captured from PathwaysTM software.
B, Genes determined as true targets of LANA1 based on manual screening of PathwaysTM images, ttest and fold change.

From the manually curated microarray data, few changes were observed in gene expression patterns due to LANA1 expression. Overall 5 genes could be confirmed by manual curation (real image) and had fold changes +/- 1.4 fold. Genes of particular interest in regard to endothelial cells are discussed below.

Prostacyclin-stimulating factor, as its name suggests, stimulates the synthesis of prostacyclin. It is a potent vasodilator, antithrombotic and antiplatelet agent (Smyth and Fitzgerald 2002). Research has shown that prostacyclin-stimulating factor produced by fibroblast cells can stimulate the synthesis of prostacyclin (PGI2) in endothelial cells (Masakado *et al.* 1994). PGI2 is released from healthy endothelial cells (Gryglewski *et al.* 2002). Prostacyclin-stimulating factor localizes in endothelial cells and smooth muscle cells and may play a role in vascular homeostasis (Umeda *et al.* 1996).

Prostaglandin E synthase (PGES), also designated PIG12 and MGST1-L1 is a membrane associated protein. Although its change in expression is not statistically significant, it showed a good fold change and is possibly relevant to LANA1 induced gene expression changes in endothelial cells. It is part of a protein superfamily involved in eicosanoid and glutathione metabolism (MAPEG family)(Jakobsson *et al.* 1999). High expression of PIG12 is detectable in lung carcinoma (A549) and human ovarian cancer (HeLa) cell lines(Jakobsson *et al.* 1999). PGES converts cyclooyxgenase (COX)-derived prostaglandin (PG)H2 into PGE2 (Jakobsson *et al.* 1999). In common with prostacyclin-stimulating factor, prostaglandin E is released from healthy endothelial cells (Gryglewski *et al.* 2002).

4.4 Discussion and conclusion

In this chapter, I attempted to use the ability of the lentivirus system to deliver LANA1 to primary cells, and interrogate the functions of LANA1 on the cellular transcriptome using gene expression microarrays.

The results from the gene expression microarray analysis of the effects of LANA1 on primary endothelial cells were disappointing and show little change in the gene expression pattern. Post-infection, LANA1 positive cells gene expression appears to differ little as compared to normal primary endothelial cells or an infection control (pHR CMV emp). Previous work has been published that attempted to identify the cellular targets of LANA1 in transformed B-cells. Stable cell lines expressing LANA1 were created and the gene expression profile was compared with LANA1 negative cells (Renne *et al.* 2001). Findings from this work were limited as no significant changes in known genes were observed. LANA1 did however alter the expression of several ESTs (Renne *et al.* 2001). The study investigated the effects of LANA1 on the activity of several synthetic promoters and found that LANA1 activated synthetic constructs containing ATF, AP1, CAAT and SP1 sites but repressed HIV-LTR and NFkB-dependent reporter genes (Renne *et al.* 2001). Results from gene expression microarrays showed limited modulation of cellular genes, including upregulation of several interferon responsive genes (Renne *et al.* 2001).

Previously LANA1 has been shown to be a potent regulator of promoter activity, acting as both a transcriptional activator and repressor (An *et al.* 2002;Knight *et al.* 2001;Radkov *et al.* 2000). However, these results have been obtained from artificial systems such as promoter reporter assays which are several times more sensitive than detection of changes in cellular transcripts by methods such as RT-PCR or gene expression microarrays. The promoters known to be transcriptionally activated by LANA1 include E2F

(Radkov *et al.* 2000), human telomerase reverse transcriptase (hTERT) (Knight *et al.* 2001) and the hIL-6 promoter via the AP1 site (An *et al.* 2002).

Other work undertaken in our laboratory also attempted to compare the gene expression profile of LANA1 transformed rat embryonic fibroblasts (S.Radkov, unpublished data)(Radkov *et al.* 2000) with control cells but this also showed no significant changes in gene expression profile due to LANA1 expression (S.Radkov, unpublished data).

I attempted to improve on work with LANA1 and gene expression microarrays by using several new methods. There was concern that the specific effects of LANA1, which may be quite subtle, were being lost in the large changes of gene expression in transformed cells. Also cell types used were not necessarily relevant to KS, and it has been noted previously that the transcriptional activity of LANA1 is cell type specific (Knight *et al.* 2001). To answer these concerns, I used disease relevant un-transformed primary endothelial cells. The levels of LANA1 gene expression were also a concern as low levels of transfection may have lead to a diluted effect of LANA1-mediated gene expression change. I employed a lentiviral gene delivery system to achieve infection of greater than 95% of cells. However, despite these changes, little data were derived from the GEM experiments. There are several possible reasons for this.

Firstly, the choice of the gene expression microarray system may not have been ideal. While gene expression microarrays are sensitive, the majority of LANA1 transcriptional activation/repression studies have been performed using promoter constructs that express reporter genes. This is a much more sensitive assay than the detection offered by cDNA GEM technology.

The specific type of GEM used in these experiments, cDNA arrays, may also have not been suitable. Problems encountered with the work on microarrays were mainly concerned with the analysis of data and interpretation of array images with the Research Genetics software. False positives were common using the software resulting in the need for lengthy manual checking of data with primary images.

The field of gene expression microarray production has grown considerably and there are now new alternatives to the traditional methods of cDNA microarrays. Most promising appears to be the use of oligo based array technology such as that employed by the Affymetrix system. The improvements in technology result in not only greater sensitive and reproducibility, but also greater confidence in data due to extensive internal controls. Future work could involve the use of the existing delivery and expression methods used for this work, coupled to the use of the new generation of oligo microarray systems. This may allow better sensitivity of detecting LANA1 mediated gene expression changes.

Secondly, it is possible that the endothelial cells are not suitable for such experiments. In the formation of KS and other associated KSHV malignancies, LANA1 may act in concert with other viral genes. Future work could study the effects of LANA1 when co-expressed with vcyclin and/or vFLIP, as occurs in KSHV infected cells. The transcriptional effects of LANA1 may also be due to subtle cellular changes, not present in the primary endothelial cells used here.

Overall, despite attempts to analyse the transcriptional effects of LANA1, my results have not shown any significant change in gene expression that could be attributed to LANA1. As few changes were seen, I could conclude that it is likely the main functions of LANA1 are not mediated through transcriptional regulation. However, I believe that further work is required before this conclusion should be reached.

In the next chapter of this thesis I looked at another possible route of LANA1 function; protein-protein interactions.

Chapter 5 Results

Characterisation of a LANA1 complex

Chapter aims: The aim of this chapter was to develop methods for the capture of a LANA1 native complex from KSHV infected B-cells and identify the binding partners of LANA1 using mass spectrometry. In parallel, the yeast two-hybrid system was used to identify direct interaction partners allowing comparison of candidate proteins and protein interaction domains between the two methods.

5.1 Construction and testing of LN53 and control columns

Previous studies on the protein-protein interactions of KSHV LANA1 have concentrated on the use of the yeast two-hybrid system to identify individual direct partners (Fujimoro *et al.* 2003;Fujimuro *et al.* 2003;Fujimuro and Hayward 2003;Platt *et al.* 1999). Here I sought to study LANA1 at the protein complex level, therefore identifying both direct and indirect binding proteins.

Initial work on the purification of a LANA1 complex concentrated on the construction of a suitable LANA1-specific column. Several methods are available for the capture and purification of proteins from a cell lysate. One method is to produce the proteins as a fusion, often with a glutathione-s-transferase (GST) moiety and use an anti-GST column to capture the recombinant fusion protein from bacteria. Mammalian cell lysate is then circulated over this column and proteins that bind to the immoblilised fusion protein are rescued from the lysate. This method does however have its disadvantages. Fusion proteins produced in bacteria will often bind to bacterial proteins and these can interfere with later mass spectrometry identification. This can be improved by ectopically expressing the fusion protein in mammalian cells. However, the addition of a GST moiety may alter the biochemical or structural properties of a protein and therefore alter its binding partners. As a high level of non-specific interactions occur

with this method, it is often necessary to construct several columns with increasing amounts of fusion protein immobilized on them. Proteins that are identified as increasing in yield with increasing amounts of fusion protein can therefore be identified as specific. This is time consuming and not very cost effective. In addition, this method often only captures directly interacting proteins and not a native protein complex.

A method that is more specific and captures not only direct but indirect interaction partners is antibody affinity chromatography. This uses protein specific antibodies to bind proteins from cells lysates. There are two methods normally used: If no specific antibody is available, the protein is tagged, commonly with an HA or MYC tag, and ectopically expressed in cells. An anti-HA or anti-MYC column is then used to bind the proteins from cell lysates. This method is more suitable as the proteins are captured from cells *in vivo* and all binding partners can be identified. It still has the disadvantage however that the tag may interfere or change the proteins' binding characteristics.

When available, the second and preferential method for protein capture is to use either a monoclonal or polyclonal protein specific antibody to capture complexes in a native form. This is the method I developed for use in this study.

To enable the capture of a native protein complex from KSHV latently infected B-cells I employed affinity chromatography. Specific anti-LANA1 antibody was cross-linked to CNBr media, in parallel with a non-specific rat IgG control. While it is possible to bind antibody to, for example, protein G beads, this method is not permanent and loss of antibody occurs at the elution stage. By cross linking the antibody to CNBr beads I was able to reuse the antibody media (antibody + CNBr) repeatedly.

During construction, both columns (LN53 & Rat IgG) bound over 98% of the antibody coupled to them. Loss of antibody was calculated from flowthrough after binding. The BCA protein assay was used for quantification against known standards (see Materials and Methods). The results show that both the rat IgG and LN53 columns contain greater than 4.9mg of control antibody or anti-LANA1 antibody, respectively (Fig 5.1). The anti-LANA1 and control CNBr beads were packed into columns.

Initial work with the columns concentrated on the conditions for optimum capture of LANA1 from cell lysates, while maintaining as high a degree of stringency as possible. Different methods of physical disruption (sonication, dounce homogenization or no mechanical disruption) were employed to release LANA1 from BC-3 cells. LANA1 was immunoprecipitated using anti-LANA1 rat monoclonal and the captured immunocomplexes were examined by western blotting (Fig 5.2). Results showed that cells in low salt buffer disrupted with sonication gave the best results (Fig 5.2). Low salt buffer and sonication were therefore initially employed to allow gentle lysis of cells for column work.

The elution of proteins from an affinity column is often as important as the method of capture. There are several methods available to elute proteins including an increase in salt (often used in combination with a step or gradient elution), the use of an antibody specific eluting peptide, or pH. For this study I used a low pH method: 100mM glycine (pH 2.7). This method is often used because it provides rapid elution with the majority of the protein eluting at once. This makes concentration of the samples easier and more convenient.

Fig 5.1

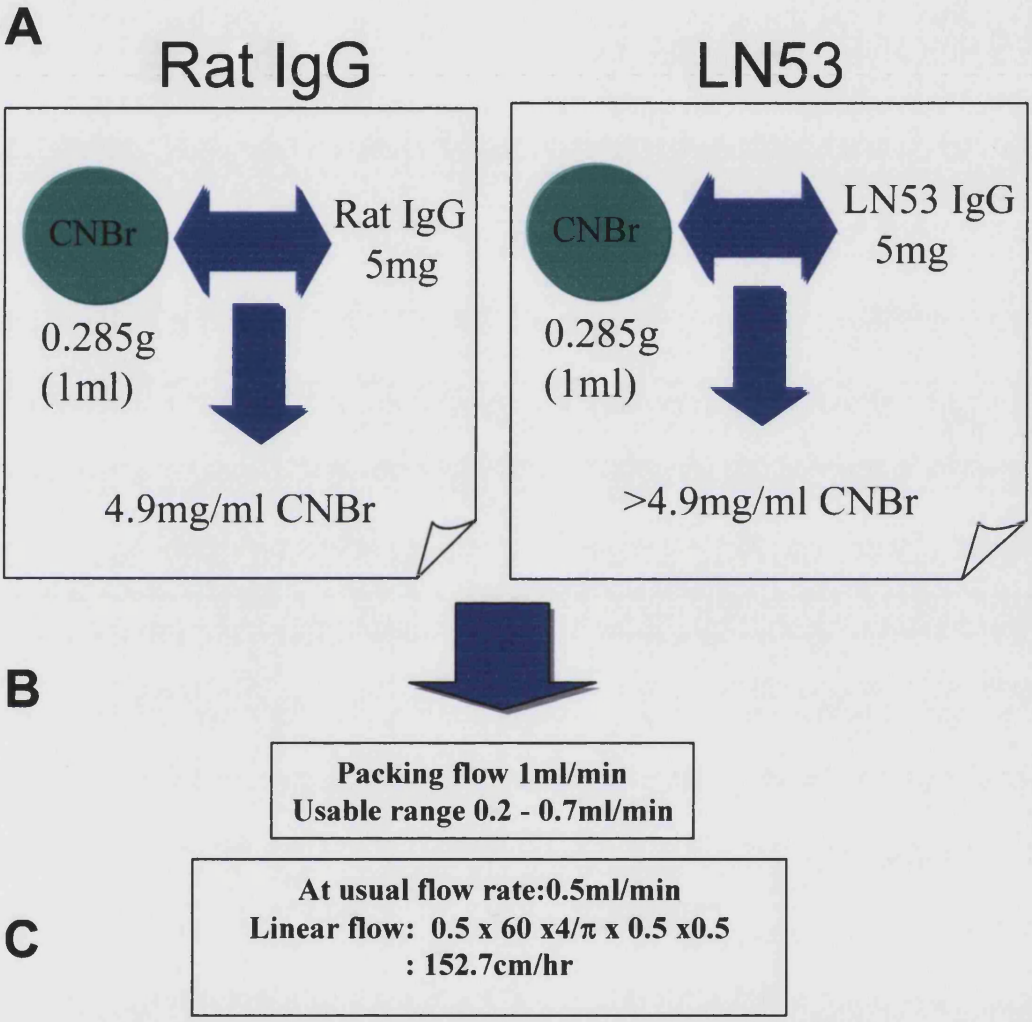

Fig 5.1 - Affinity column statistics
LANA1 specific and non-specific control columns were constructed by cross-linking of purified antibodies to CNBr activated sepharose 4B media. A & B - Media was packed into HR 5/5 columns at 1ml/min flowrate. The efficiency of coupling was calculated by BCA assay on concentration of unbound antibody **C** – Usable flow rate was calculated.

Fig 5.2

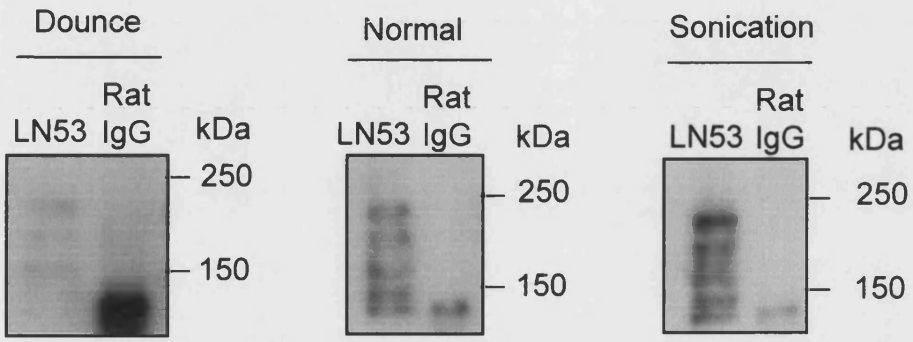

Fig 5.2 - Immunoprecipitation of LANA1 from low salt buffer lysed cell extracts

BC-3 cells were lysed in low salt buffer using various methods of physical disruption and immunoprecipitated with anti-LANA1 antibody. Cells were washed in PBS then resuspended in Low salt buffer at $1x10^7$/ml. Lysates were subjected to either sonication, Dounce homogenisation or no physical disruption. Lysates were precleared with 50µl of protein G beads for 1hr at 4°C. Rat IgG or LN53 antibody (5µg) was added per IP for 2 ½ hrs at 4°C. 50µl of protein G beads were added and allowed to bind overnight at 4°C with rotation. Beads were washed 3 times with low salt buffer, resuspended in Lamelli loading buffer and boiled at 95°C for 5mins. Proteins were then separated on a 6-12% SDS-PAGE gel, transferred to Hybond-P membranes (Amersham Pharmacia Biotech) and proteins detected with 1:1000 LN72 antibody. The resulting western blot shows that the most efficient method for extracting LANA1 protein for immunoprecipitation is by sonication in low salt buffer.

5.2 Enrichment of LANA1 from BC-3 cells

The anti-LANA1 column was tested for an ability to capture LANA1 from BC-3 cells lysate. I used an AKTA explorer FPLC system that allowed the development of chromatographic methods. Conditions for the running of the columns had previously been calculated to be between 0.5-0.7ml/min as determined by the type of media, the size of the columns and the packing conditions. Initially the columns were run at 0.7ml/min. BC-3 cells were lysed in low salt buffer with sonication and prior to binding were diluted with MilliQ dH_20 and adjusted to pH 7. Columns were pre-equilibrated in 10mM Tris-HCL pH 8. After binding, washing and elution, protein was detected by the AKTA system and aliquoted. The resulting chromatograph showed the elution of two distinct peaks (Fig 5.3A). The first peak may contain weakly associated non-specific proteins, perhaps bound to the column media, which were not removed by washing. Western blot analysis of fractions shows strong positive band at 220-235kDa for LANA1 using an anti-LANA1 antibody (Fig 5.3B). When compared to the positive control (BC-3 cells) despite a far higher BC-3 protein quantity the LANA1 signals in the purified fractions are higher, indicating enrichment i.e. 1.4μg vs 0.4μg (Fig 5.3B). The strongest LANA1 signal correlated with the two protein peaks eluted from the column. The second peak may contain proteins associated with the antibody and may therefore be specific. It was decided in future experiments to attempt to separate the two peaks by decreasing the size of the fractions. Coomassie staining of column-eluted protein reveals a distinct pattern different to that seen in pre-bound extracts (Fig 5.3C). This patterning indicates the purification of certain proteins and a reduction in others. These data showed that LANA1 was purified from BC-3 cells by the column. Although preliminary, the Coomassie blue banding pattern also suggested co-purification of associated proteins. LANA1 is purified from BC-3 extracts by the CNBr LN53 column. To further investigate column specificity, a negative control column (rat IgG) was used to perform a control purification.

Fig 5.3 – LANA1 is purified from BC-3 extracts by the CNBr LN53 column. **A**, Binding and elution of LANA1 from CNBr LANA1 column $2.3x10^8$ BC-3 cells were lysed in low salt buffer as described in materials and methods. After column equilibration, lysate was bound for 3 1/2hrs at 0.7ml/min. After washing, bound proteins were eluted in 100mM glycine pH 2.7 and neutralised with 1M Tris pH 8.0. An example chromatograph is shown, demonstrating the presence of two distinct protein peaks. Samples were desalted on PD-10 columns, concentrated by spin-vac and resuspended in low salt buffer. **B**, Detection of LANA1 in CNBr-LN53 column fractions using anti-LANA1 rat monoclonal antibody. 5μl from each fraction (100μl total per fraction) was separated on a 6-12% SDS-PAGE gel and run for 2hrs at 120V. 5μl of pre-bound BC-3 lysate was used as a positive control. Proteins were transferred to a Hybond-P membrane over night at 0.1A in MeOH transfer buffer. Membranes were blocked in PBS+Tween+milk powder and probed with anti-LANA1 LN72 rat monoclonal diluted 1:1000 in 10% blocking buffer for 2hrs. After washing, anti-Rat Hrp (Santa Cruz) was incubated with the membranes for 1hr and bands were visualised after further washing with ECL+ (Amersham Pharmacia Biotech) and ECL film (Amersham Pharmacia Biotech). Membranes were stained with coomassie blue and air-dried at 22°C. **C**, A distinct protein pattern is revealed by coomassie staining on column elutes. 8μl of each column fraction and pre-bound BC-3 were run on a 6-12% SDS PAGE gel. Protein was visualised by staining with coomassie blue. A distinct banding pattern is seen in column elutes when compared with pre-bound BC-3 lysate.

Fig 5.3

A

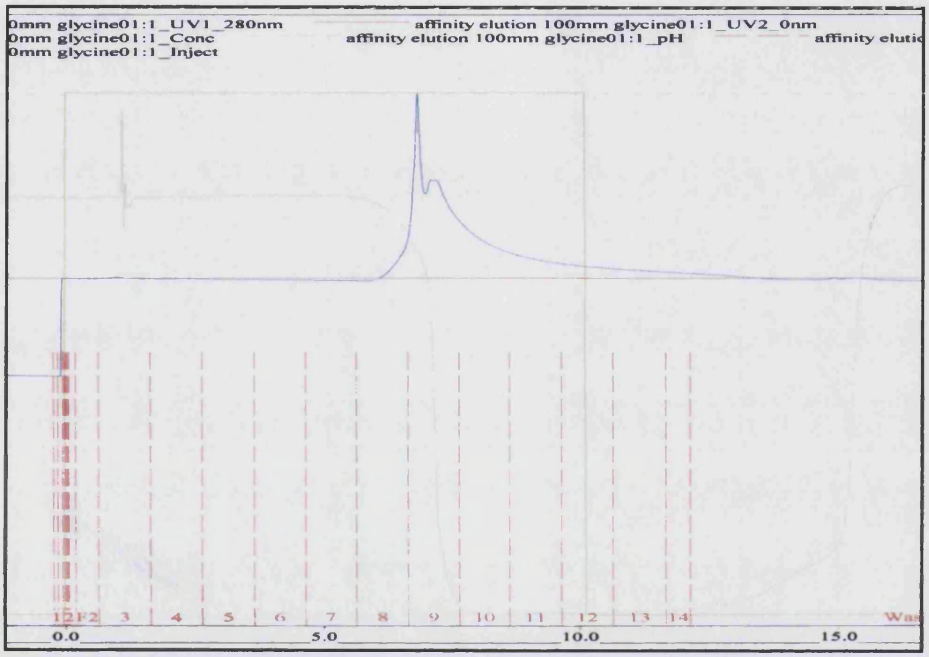
0mm glycine01:1_UV1_280nm
0mm glycine01:1_Conc
0mm glycine01:1_Inject
affinity elution 100mm glycine01:1_UV2_0nm
affinity elution 100mm glycine01:1_pH
affinity elutic
1 F2 3 4 5 6 7 8 9 10 11 12 13 14
0.0
5.0
10.0
15.0

B

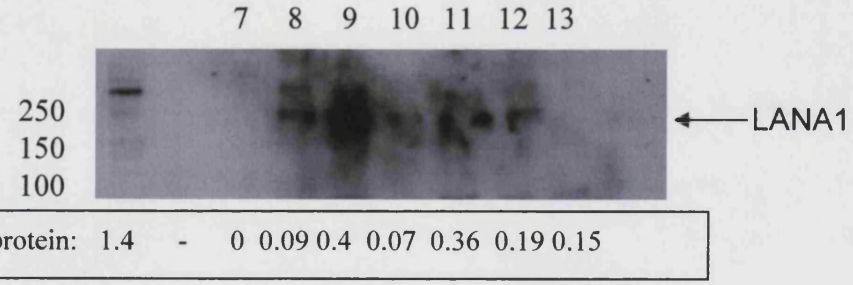
7 8 9 10 11 12 13
250
150
100
LANA1
µg protein: 1.4 - 0 0.09 0.4 0.07 0.36 0.19 0.15

C

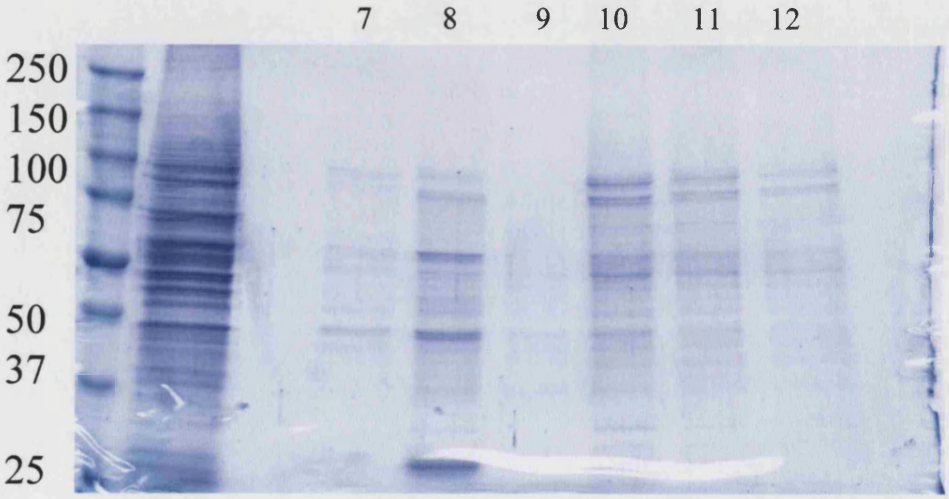
7 8 9 10 11 12
250
150
100
75
50
37
25

This was important as the peaks may have been non-specific and resulted from retardation of protein after passage over the column. A control of CNBr beads alone could have been used, but it was decided that an antibody control was preferable. Ideally, the antibody would have been an isotype control, but this was not available at the time. Fig 5.4 shows the results of this control column as compared to a new purification on the anti-LANA1 column. This experiment achieved separation of the two peaks into separate fractions. Two peaks are again seen in the anti-LANA1 column (LN53) elutes (Fig 5.4B) whereas only one peak is seen in elutes from the control column (rat IgG) (Fig 5.4A). Western blot analysis showed that strong LANA1 signal was associated with the second smaller eluted peak (Fig 5.4B). This further reinforces the previous result showing specific elution of enriched LANA1 from the LN53 column. The rat IgG column shows little enrichment of LANA1, although some may be present due to the low salt and non-stringent conditions used.

The above data provide evidence that the second peak is specific and contains LANA1. At this point it was unclear if LANA1 elutes prior to its interacting proteins, or after the proteins bound to it. On this basis fractions 8, 9 and 10 were analysed by SDS-PAGE and coomassie blue staining, to identify unique proteins. Any unique proteins, found in the anti-LANA1 column but not the control column would be selected for identification by MALDI-TOF MS. Unfortunately, the gel revealed no specific bands (data not shown).

Western blot analysis of concentrated fractions from the columns showed good recovery of LANA1 from cells. These data, in combination with the observation that the negative column does appear to recover a small amount of BC-3 from cells (Fig 5.4B), lead to the conclusion that the experimental conditions may not be optimal. The protein eluted from the LN53 and Rat IgG columns was high for the purification of a protein that probably represents >0.01% of total cell protein.

Fig 5.4 - Purification of LANA1 complex from BC-3 cells using a CNBr-LN53 column and a control CNBr-Rat IgG column. **A & B**, BC-3 cells (c.4x10^8) were lysed in low salt lysis buffer (50mM Tris, 50mM NaCl, 1% IEGAL-CA 630, 1mM PMSF, 0.5% protease inhibitor [Sigma]) and disrupted by sonication. Lysates were rotated for 1hr at 4°C, diluted 1:5 in MilliQ dH_20 and adjusted to pH 7 prior to binding. Rat IgG (A) and LN53 (B) and columns (stored in 20% EtOH) were equilibrated in 10mM Tris pH 8.0 on an AKTA FPLC Explorer system. Lysates were bound overnight by circulation at 0.5ml/min. Columns were washed in 10mM Tris pH 8.0 until baselines were at 0mAu. Protein was then eluted from the columns using 100mM glycine pH 2.7 over a 5 column volume 100% gradient. 1ml fractions were collected and neutralised with 100µl of 1M Tris pH 8.0. After elution Rat IgG column (A) has 1 peak, whereas LN53 column (B) shows 2 peaks. Protein eluted from each column was desalted, dried by centrifugation and resuspended in modified RIPA buffer. Protein was separated on a 6% SDS-PAGE gel and LANA1 was detected by western blotting with anti-LANA1 rat monoclonal (LN53) (shown beneath chromatographs). LANA1 was enriched in fraction 8 which corresponds to peak 2 on the chromatographs (Fig 5.4B).

Fig 5.4

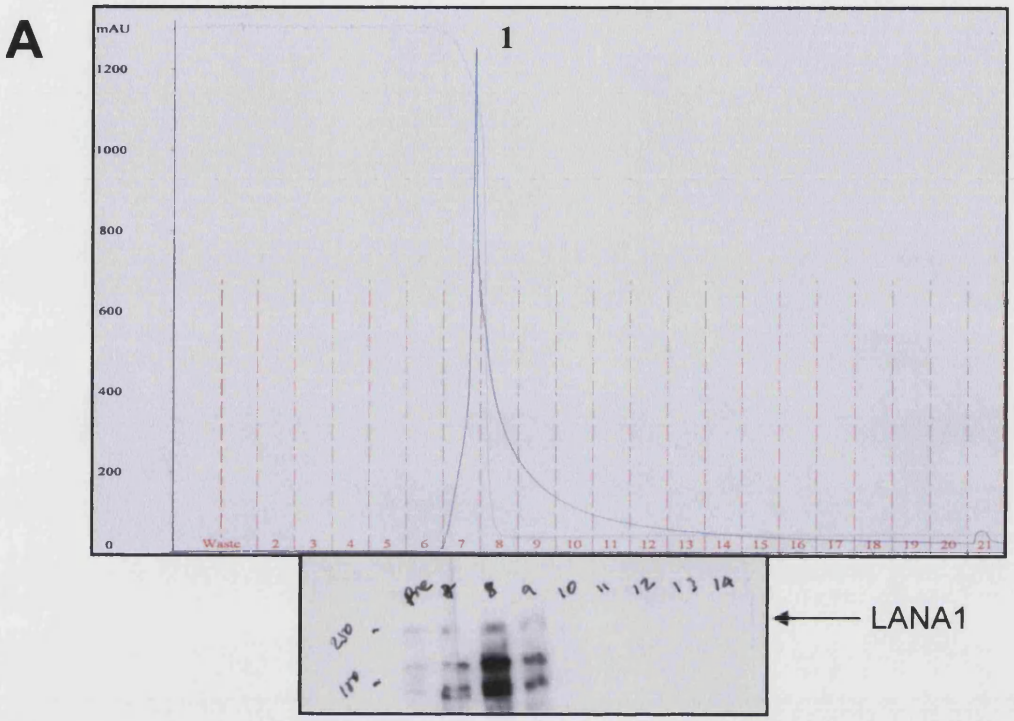
A
mAU
1200
1000
800
600
400
200
0
1
Waste
2
3
4
5
6
7
8
9
10
11
12
13
14
15
16
17
18
19
20
21
Pre
8
9
10
11
12
13
14
230
150
LANA1

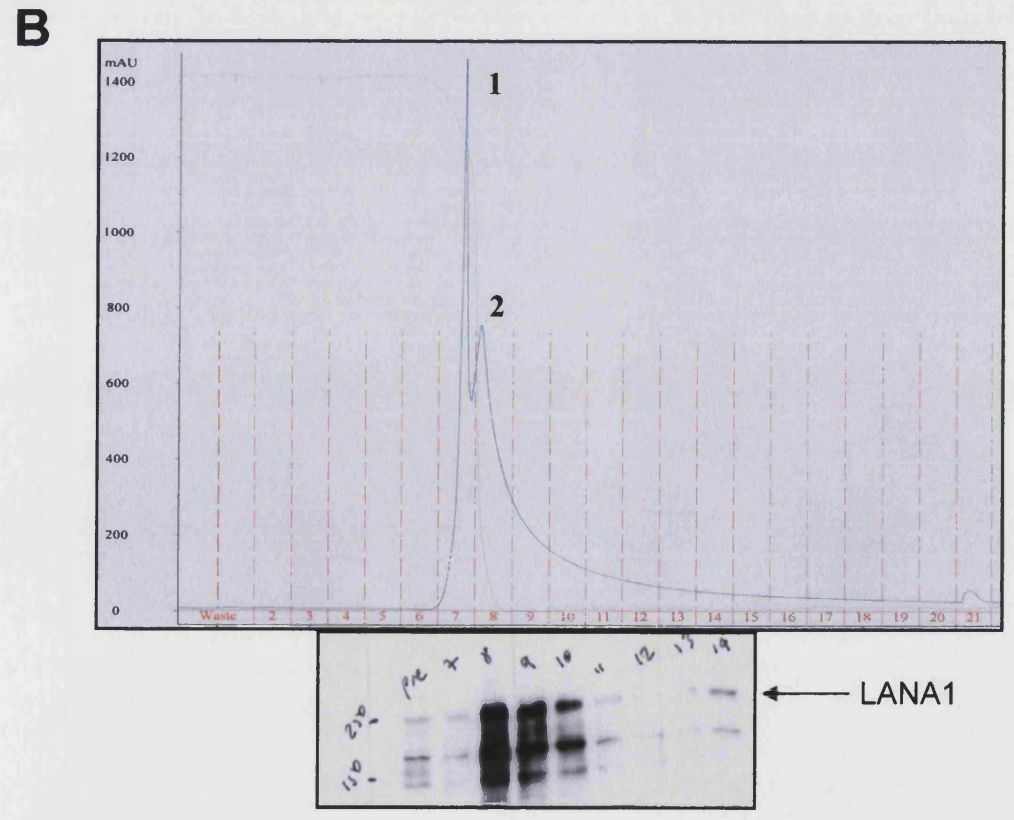
B
mAU
1400
1200
1000
800
600
400
200
0
1
2
Waste
2
3
4
5
6
7
8
9
10
11
12
13
14
15
16
17
18
19
20
21
Pre
7
8
9
10
11
12
13
14
230
150
LANA1

This result calls into question the stringency of the purification. A possible criticism of any protein complex purification strategy is specificity. How can it be certain that proteins eluted from the columns are actually part of the complex? Initial purifications have been undertaken with BC-3 cells lysed and disrupted in non-stringent conditions. Low salt buffer was used with sonication possibly resulting in non-specific interactions. The columns were run at low salt levels (10mM Tris pH 8.0), which may have possibly lead to non-specific protein interactions with the columns/captured LANA1. The adjustment of cell lysates to pH 7 may have also been a factor.

The purification was repeated using more stringent conditions in which a modified RIPA buffer (150mM NaCl, 50mM Tris pH 8.0, 0.1% SDS, 1mM PMSF, protease inhibitors) was used to lyse cells. RIPA buffer is commonly used for such experiments as its composition closely matches the cytoplasm of a mammalian cell. The affinity columns were then equalised in Buffer A (75mM NaCl, 25mM Tris pH 8.0 0.5mM PMSF) and lysates were diluted to 50% RIPA prior to binding. For these experiments cell lysates were not pH adjusted.

Columns were again run on AKTA FPLC systems. Results were significantly different from those obtained with the low salt buffer. The chromatographs showed elution of a specific peak relating in position post-elution to the second peak on the low salt lysate columns (Fig 5.5A & B). Under these more stringent conditions (50% RIPA) the first peak containing a large quantity of protein was markedly absent, despite a similar number of cells being used. This indicated a more selective capture of proteins. As the eluted protein levels were so low, there was concern that proteins had simply not bound to the columns. To investigate this immunodepletion of LANA1 was demonstrated by western blotting of lysates both pre and post circulation over the columns (Fig 5.5C). LANA1 was absent from the lysates passed over the LN53 column, but the quantity of LANA1 as compared to pre-

bound lysates did not change after circulation over the control rat IgG column. Overall, these data provided evidence for the total depletion of LANA1 from cell lysates by a specific method. By increasing the stringency of binding and washing on the columns I had reduced background and efficiently removed LANA1 from BC-3 cell lysates.

The post-elution 1ml fractions from the LN53 column (fractions 15-26) (Fig 5.5A & B) were pooled, desalted, vacuum centrifuged and resuspended in 100% modified RIPA. The corresponding fractions from the rat IgG column were processed in parallel. Unfortunately insufficient protein was eluted for western blot analysis. Protein was diluted in loading buffer and loaded onto a 10% SDS-PAGE gel and separated overnight. Following staining and destaining, the gel was scanned and specific bands observed (Fig 5.6). A total of 3 bands in the rat IgG column elutes and 27 bands in the LN53 column elutes were observed. Bands 1-27 from the LN53 column elutes were selected for identification by MALDI-TOF MS (Fig 5.6).

Fig 5.5 - Capture of LANA1 from 50% RIPA BC-3 cell lysates using affinity columns. **A & B**, $6x10^8$ BC-3 cells were lysed in modified RIPA buffer and diluted to 50% RIPA in dH20. Columns were equilibrated in 25mM Tris, 75mM NaCl and 0.5mM PMSF. Lysates were circulated O/N, washed and eluted in low pH glycine (pH 2.7). Aliquots 15-26 were pooled, desalted, concentrated and resuspended in RIPA buffer. Equal quantities for BC-3 cell lysates were circulated over a Rat-IgG control column (**A**) and an anti-LANA1 (LN53) column (**B**). Fig 5.5 shows the presence of a greater reduced peak in the same area as the second peak on Fig 5.4, indicating greater specificity of purification. As these peaks correspond in terms of time after elution, they are comparable. The proteins were used to run an SDS-PAGE gel for identification of proteins by MALDI-TOF MS. **C**, Immunodepletion of LANA1 from pre- and post-affinity lysates. Cell lysates before and after circulation over affinity columns were tested for the presence of LANA1 by western blotting. LANA1 is completely removed by passage over the anti-LANA1 affinity column, but not by passage over the control (Rat IgG) column.

Fig 5.5

A

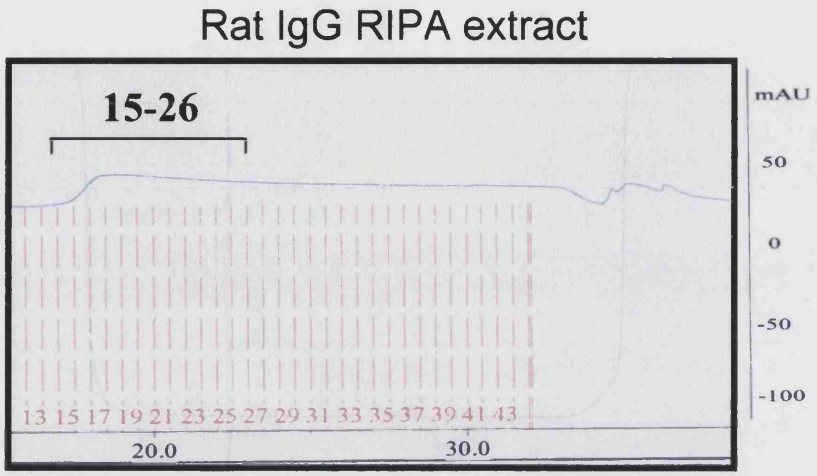
Rat IgG RIPA extract
15-26
mAU
50
0
-50
-100
13 15 17 19 21 23 25 27 29 31 33 35 37 39 41 43
20.0
30.0

B

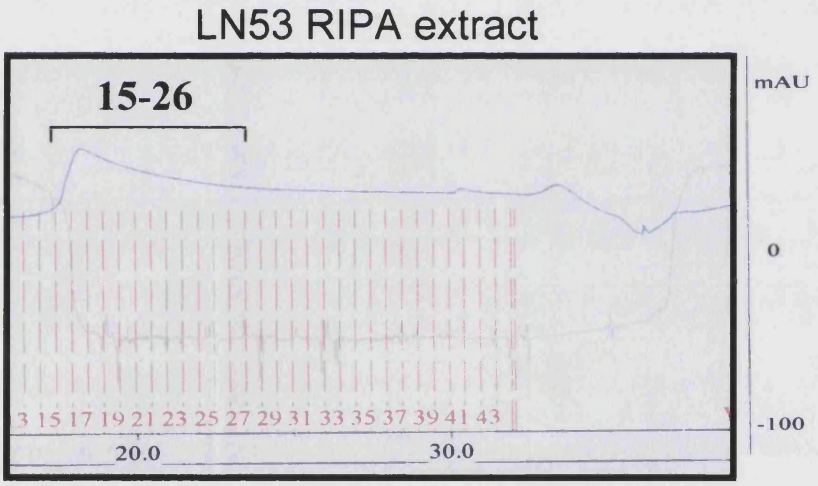
LN53 RIPA extract
15-26
mAU
0
-100
3 15 17 19 21 23 25 27 29 31 33 35 37 39 41 43
20.0
30.0

C

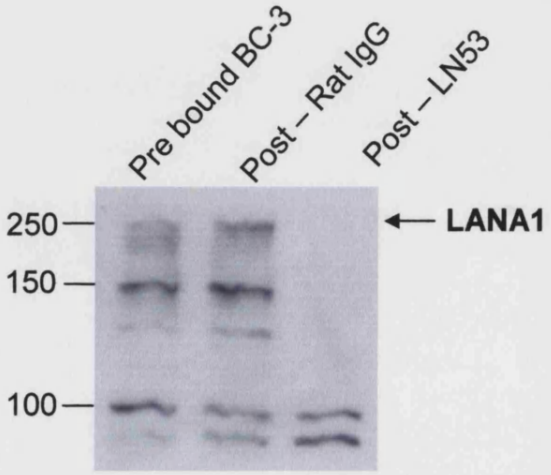
Pre bound BC-3
Post – Rat IgG
Post – LN53
250
150
100
LANA1

Fig 5.6 - SDS-PAGE of affinity captured LANA1 complex. Proteins eluted from anti-LANA1 and rat IgG columns under 50% RIPA binding conditions were separated by SDS-PAGE electrophoresis on a 10% gel. Proteins from affinity chromatography experiments (Fig 5.5 A&B) were separated on a 10% SDS-PAGE gel and run until the dye front was lost. The gel was then stained with Coomassie Brilliant Blue and destained over several days. Protein bands were excised and identified by mass spectrometry (see Materials and Methods).

Fig 5.6

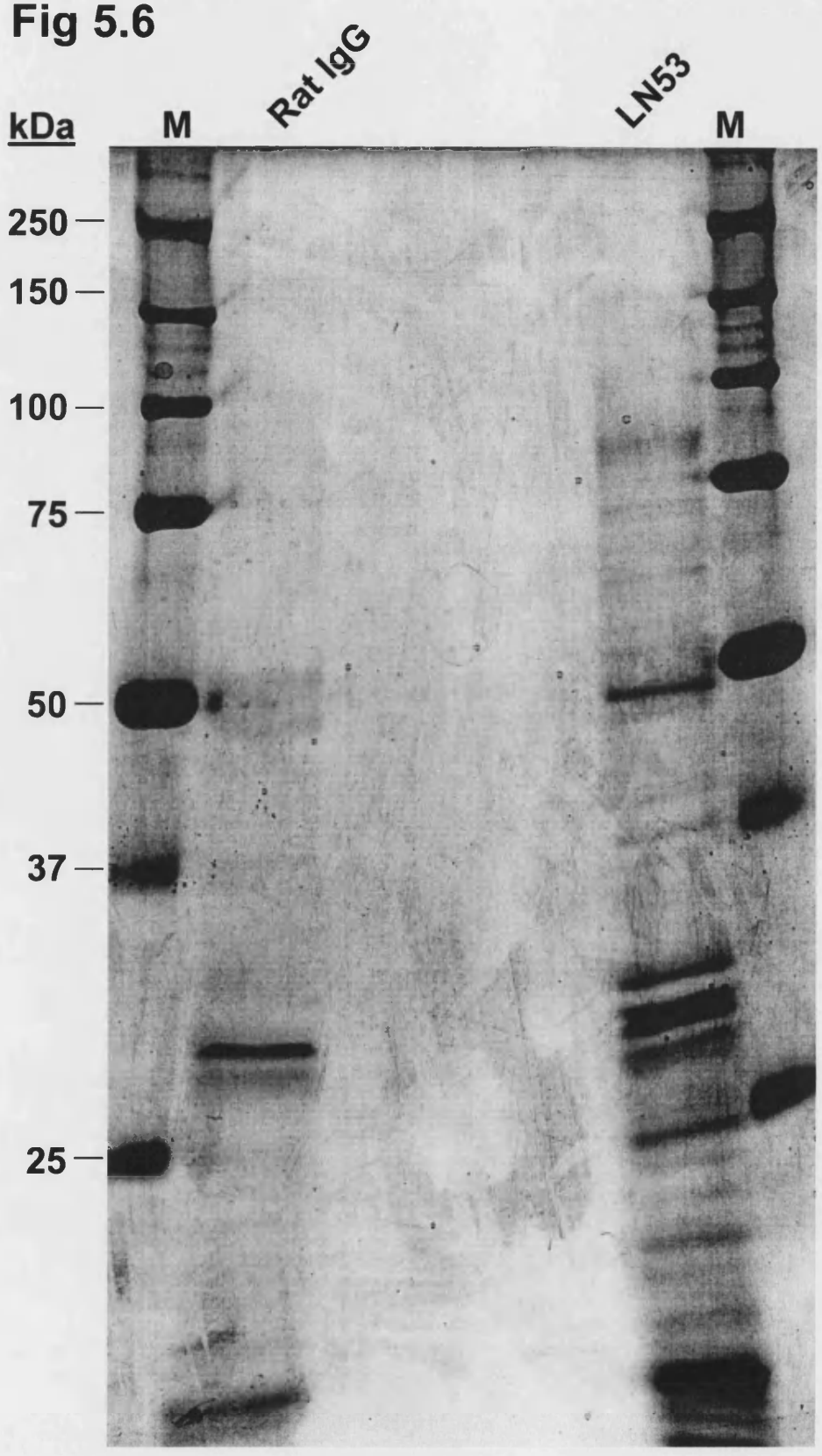

5.3 Identification of LANA1 complex members

After excision and tryptic digestion polypeptides were identified by MALDI-TOF MS, MALDI-PSD/LIFT MS/MS and nano-HPLC-ESI-CID MS/MS. The proteins identified as interacting with the LANA1 column from the affinity chromatography method are listed in Table 5.1. The table shows data from both MALDI-TOF and protein MS/MS identification methods. From this initial data, novel interaction partners of LANA1 were identified. These included polyadenylate binding protein 1 (PABP1), heterogeneous nuclear ribonucleoprotein A1 (hnRNP A1), galectin-3, HSP73 and histone H1. The presence of keratin was assumed to be due to contamination. Rat IgG antibody was also identified having co-eluted with proteins from the column.

When identifying gel bands from 1-D gels it is possible that there is a mixed population that is difficult to identify using MALDI-TOF MS. In these cases the use of protein sequencing allows the identification of mixed protein populations. Several of the most abundant polypeptides were identified by Nano-HPLC ESI MS/MS (Table 5.1). Several members of histone H1 were found to co-migrate in bands with other proteins and therefore share the same polypeptide number (Table 5.1). LANA1 has been previously shown to bind histone H1, and via this interaction maintain the KSHV viral episome (Ballestas *et al.* 1999;Cotter and Robertson 1999). Histone H1 family members 4 and 5 were identified, but no other histones i.e. H2A, H2B, H3, H4 were immunoprecipitated. Previously it has been shown that LANA1 can be co-immunoprecipitated with histone H1 but not histones 3 or 4 (Cotter and Robertson 1999).

Table 5.1

Polypeptide number	Protein Name	NCBI Accession	Identification method			
			MALDI-TOF	MALDI LIFT /PSD MS/MS	CID ESI MS/MS	Nano-HPLC ESI MS/MS
pp24.5	Cleavage and polyadenylation specific factor 5, 25kDa subunit		x			
pp27	Galactose-specific lectin	AAA88086	x			
pp27.5	Galactose-specific lectin	AAA88086	x			
pp27.5	Histone H1 family, member 4	NP_005312				x
pp28	Small nuclear ribonuclear nucleoprotein polypeptide A	NP_004587	x			x
pp28	Histone H1 family, member 5	NP_005313				x
pp29.5	Heterogeneous nuclear ribonucleoprotein A1	NP_002127	x			x
pp30	Heterogeneous nuclear ribonucleoprotein A1	NP_002127	x			x
pp49	IgG-2C Chain C region (rat)	P20762	x			x
pp65	Keratin contamination		x			
pp72	Polyadenylate-binding protein 1 (PABP1)	P11940*	x			
pp74	HSP73	NP_006588	x			

Table 5.1 LANA1 column interacting proteins captured by affinity chromatography and identified by MALDI-TOF mass spectrometry (MS) and/or nano-HPLC-ESI-CID MS/MS. Proteins are referenced by their polypeptide size (pp) as compared with molecular weight size markers and by NCBI accession numbers. Proteins identified were of human origin unless otherwise stated.

The data at this point provided the identifications of 9 LANA1 column interacting proteins. I was able to discount the identification of rat IgG as contamination from the experimental method, as well as keratin, which is a common contamination of mass spectrometry gels. At this point a general trend in the types of protein identified became apparent. Of the remaining 7 proteins, 6 have roles in cellular splicing/transport of mRNA. One of these proteins (hnRNP A1), also has a role in telomere biogenesis. Furthermore, a large proportion of the identified proteins have either a nuclear localization, or are known to shuttle between the cytoplasm and the nucleus. As LANA1 is known to have a nuclear localization this data reinforces the likelihood of a real interaction. I will give a brief overview of the most interesting proteins in regard to LANA1:

Cleavage and polyadenylation specific factor 5 (CPSF-5) is a member of a complex required for 3' cleavage and subsequent polyadenylation of RNA. It is also commonly termed the "pre-mRNA cleavage factor Im (25kDa) and was identified as a co-purifying polypeptide with CF I_m activity (Ruegsegger *et al.* 1996). Subsequently it was cloned and characterised as possessing no known structural motifs (Ruegsegger *et al.* 1998). Recently, the purification and characterization of the human spliceosome using proteomics has revealed many interesting new interactions (Zhou *et al.* 2002). Among these was the presence of cleavage factor Im, 25kDa subunit (CPSF-5) (Zhou *et al.* 2002).

Galactose-specific lectin is also termed Galectin-3 and as its name suggests is a galactose-specific lectin which binds IgE antibody. Its localization is normally nuclear, but changes to cytoplasmic in malignancies such as carcinomas. Galectin-3 has been characterised as interacting with several important cellular proteins including bcl-2 (Akahani *et al.* 1997;Yang *et al.* 1996) and Gemini4 (Park *et al.* 2001). Galectin-3 has been shown to be present in SMN-containing complexes which complement the H/E splicing complex by the addition of functional snRNPs (Pellizzoni *et al.* 1998).

Polyadenylate binding protein (PABP1) is a 72kDa protein that contains four RNA-binding domains (RRM). PABP1 is a versatile and important protein involved in cellular activities including translation initiation, mRNA deadenylation, mRNP maturation, and RNA stability. It is also known to shuttle between the nucleus and the cytoplasm, aiding in the formation and transport of mRNPs (Afonia *et al.* 1998).

Heterogeneous nuclear ribonucleoprotein A1 (hnRNP A1) is an abundant member of the H-complex. Its functions include mRNA splicing, mRNA transport and a role in the biogenesis of telomeres.

5.4 Immunoaffinity purification

While the methods for LANA1 purification using affinity chromatography had proved successful, it was decided to attempt a different method of purification. The AKTA FPLC system was originally used as it was predicted that the purification of a LANA1 complex would require several steps, including affinity chromatography, ion-exchange and gel filtration. This type of method had been used successfully by other groups to purify a native protein complex. It was evident, however, from the affinity chromatography experiments that the capture of LANA1 by a single step was sufficient. This was judged by the percentage of LANA1 captured (100%) and the difference between specific and control columns protein bands (9:1 respectively). This one step allowed a lower quantity of starting material (cell lysate) to be used, therefore making the system convenient in terms of cell culture. Subsequently purification experiments were undertaken using the media from the columns (LN53 & ratIgG antibodies). This new method was termed large-scale immunoaffinity purification. This employed the same reagents as the affinity chromatography, but the experiment took the form of a large-scale immunoprecipitation, not involving the use of an FPLC system. In brief, cell lysates were circulated over the antibody media, immunocomplexes were washed and bound protein eluted using the same buffers as previously. As elution was in one tube, no pooling of samples was required. Eluted protein was desalted and concentrated as before. As this was a change in protocol from the affinity chromatography method, the capture of LANA1 from cell lysates was again checked. This was done by western blotting on both pre and post-bound fractions and on washed beads, which should contain bound LANA1 immunocomplexes (Fig 5.7). Equal amounts of pre-circulated BC-3 lysate and BC-3 lysates passed over both the positive and negative beads were subjected to western blotting with anti-LANA1 antibody to confirm immunodepletion and immunoprecipitation (sampled prior to elution) of LANA1 (Fig 5.7A & B).

Fig 5.7 - Immunoprecipitation/Immunodepletion of LANA1 from BC-3 extract by large scale immunoaffinity. **A**, Western blotting on pre- and post-binding lysates shows that LANA1 was removed completely from cell lysates by the anti-LANA1 CNBr beads. **B**, Eluted proteins from either the anti-LANA1 or control rat IgG were subjected to western blotting. LANA1 was detected in proteins eluted from the anti-LANA1 large-scale immunoaffinity purification only.

Fig 5.7

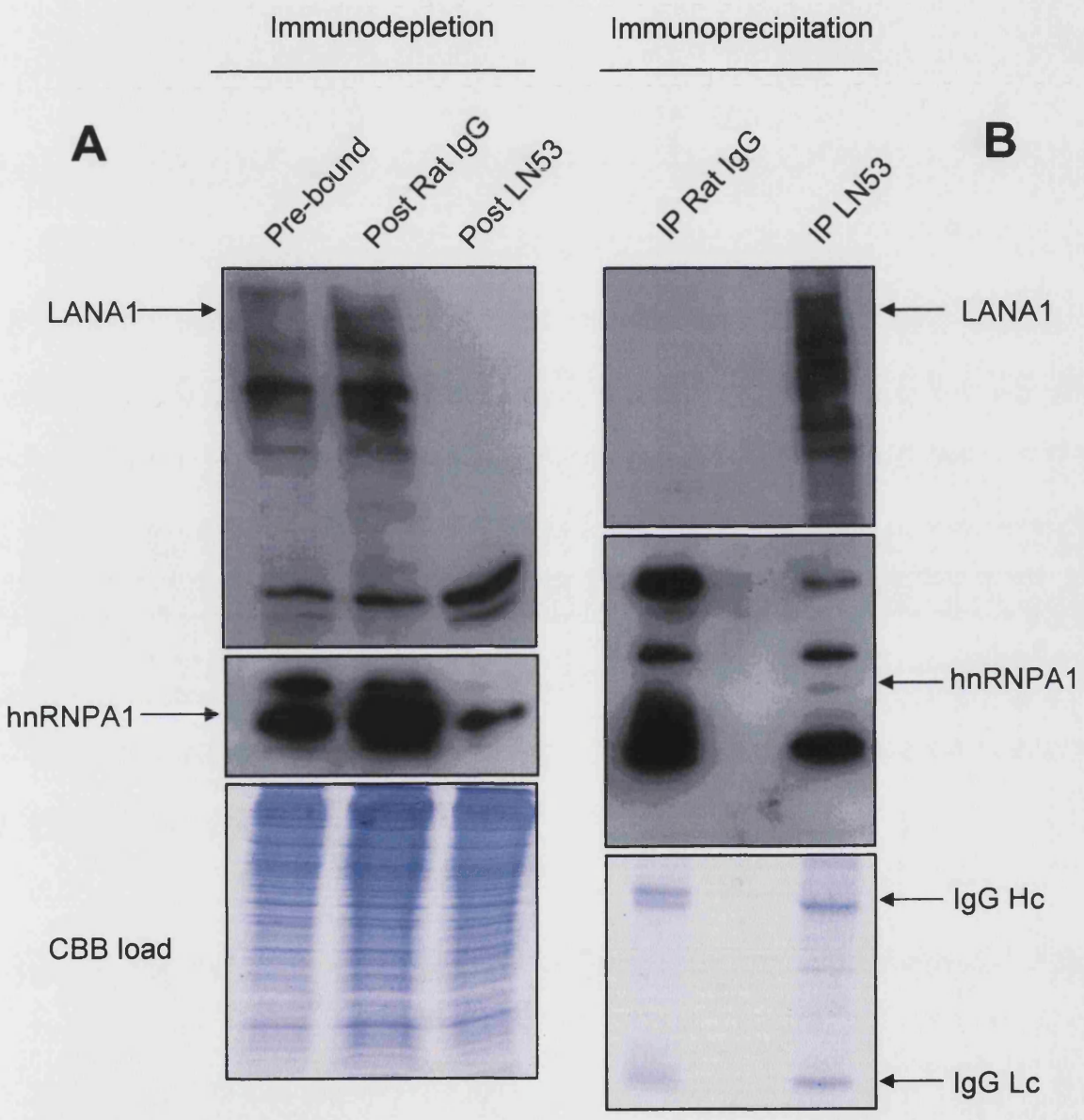
Immunodepletion
Immunoprecipitation
A
B
Pre-bound
Post Rat IgG
Post LN53
IP Rat IgG
IP LN53
LANA1
hnRNPA1
CBB load
LANA1
hnRNPA1
IgG Hc
IgG Lc

LANA1 is immunoprecipitated only by the anti-LANA1 beads (Fig 5.7B) and the efficiency of the large-scale immunoprecipitation was high as all LANA1 was efficiently removed from circulated lysates (Fig 5.7A). From these data I was confident that the native complex of LANA1 had been purified. The percentage of LANA1 removed from cell lysates was again 100% showing a high level of efficiency. The ratio of proteins that co-purified with LANA1 as compared to the negative control was acceptable and the system was therefore suitable for the identification of proteins interacting directly/indirectly with LANA1.

During these experiments hnRNP A1 was used a control for the immunoprecipitation of the LANA1 complex as it had been identified as an interaction partner by affinity chromatography. High levels of immunoprecipitation of LANA1 and hnRNP A1 are observed by the LN53 columns whereas the Rat IgG column does not immunoprecipitate LANA1 and subsequently hnRNP A1 (Fig 5.7B). Western blotting for immunodepletion shows that although 100% of LANA1 is captured from $3x10^8$ BC-3 cells a more subtle decrease in levels of hnRNP A1 are observed (Fig 5.7A). This is likely due to the relative abundance of each protein. hnRNP A1 is one of the most abundant nuclear proteins in cells, whereas LANA1 is a virally encoded protein with relatively low levels of expression. Proteins for identification by mass spectrometry were again separated on a 10% SDS-PAGE gel and bands visualised by Coomassie brilliant blue staining (Fig 5.8). Improvements in the processing methods for the samples resulted in an increased number of identified interaction partners. Table 5.2 lists the proteins identified. Positive identification was again obtained for Histone H1, hnRNP A1 and PABP1. Further proteins identified included human p32, several other hnRNP proteins, cyclophilin and galactose-specific lectin. As with the affinity chromatography method, several proteins co-migrated on the gels and required identification by MS/MS. Overall, 25 proteins (excluding rat

Ig protein and keratin) were identified using immunoaffinity purification, of which 6 were confirmed by earlier data from my affinity chromatography experiments. The functions for each of the 25 identified proteins, where known, are shown in Table 5.3.

hnRNP proteins

The data obtained from the affinity chromatography experiments showed hnRNP A1 was a LANA1 binding protein. The immuno affinity purification data replicates these data, but also identifies hnRNP AB, hnRNP A2/B1, hnRNP D and hnRNP I (polypyrimidine tract binding protein). Some of these proteins are members of the H-complex present within mammalian cells (Table 5.4). As evident from the table, HSP73, also identified as a LANA1 column interacting protein, is a further member of the complex.

Fig. 5.8 - Large-scale immunoaffinity purification of a native LANA1 complex. $3x10^8$ BC-3 cells were lysed in RIPA, diluted to 50% and passed over either an anti-LANA1 (LN53) or control IgG CNBr beads. Immune complexes were washed and protein was eluted with 100mM glycine pH 2.7. Eluted proteins were pooled, desalted, vacuum dried and resuspended in RIPA buffer. Protein was separated on a 10% SDS-PAGE gel and stained with coomassie brilliant blue. Molecular markers are shown on each side of the gel. Bands were excised, subjected to tryptic digestion and identified by mass spectrometry.

Fig 5.8

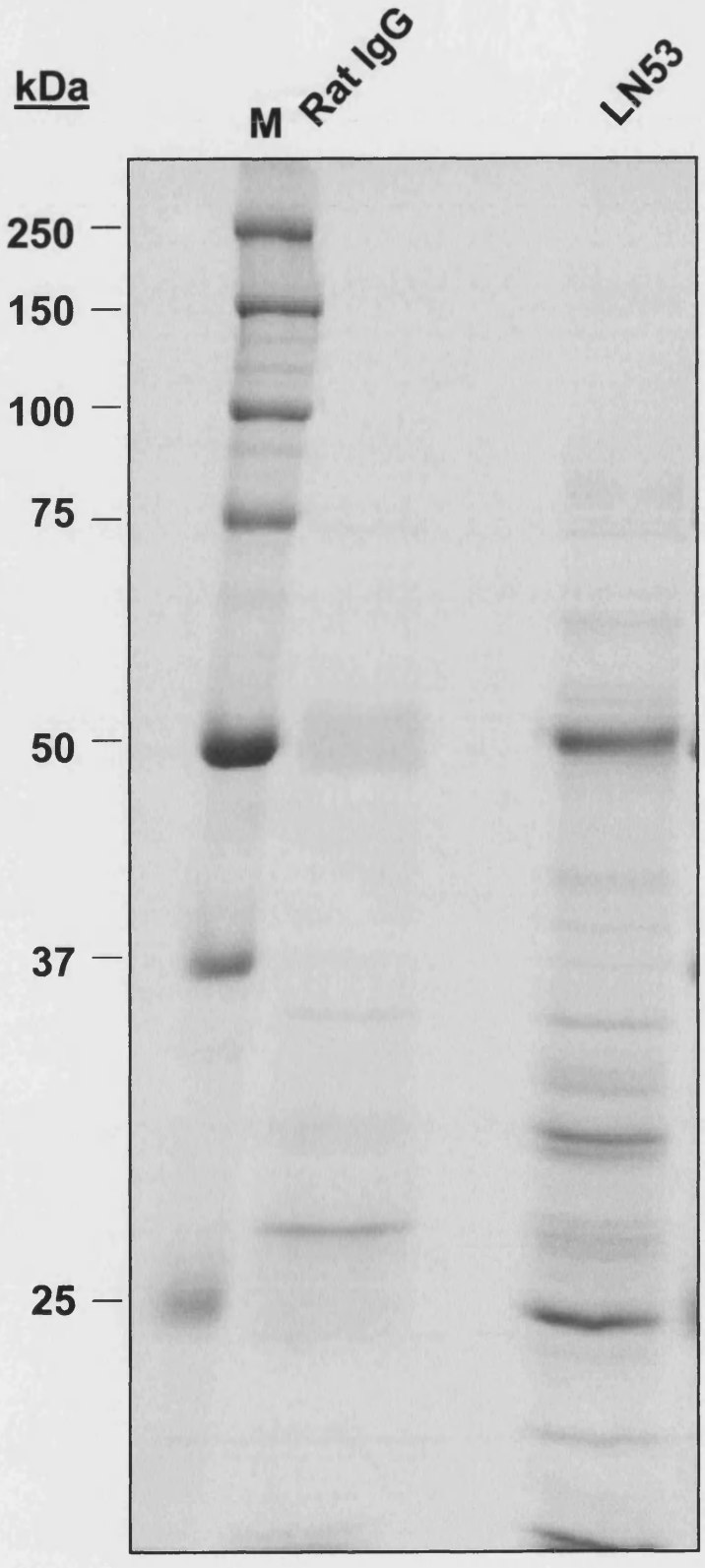

Table 5.2. LANA1 column interacting proteins captured by immunoaffinity purification and identified by MALDI-TOF mass spectrometry (MS), MALDI-PSD/LIFT tandem mass spectrometry (MS/MS) and nano-HPLC-ESI-CID MS/MS. Proteins are referenced by their polypeptide size (pp) as compared with molecular weight size markers and by NCBI accession numbers. Where homology lead to more than one protein entry match from the database search, a representative NCBI accession number is given and marked (*). Proteins identified were of human origin unless otherwise stated.

Table 5.2

Polypeptide number	Protein Name	NCBI Accession	Identification method		
			MALDI-TOF	MALDI LIFT /PSD MS/MS	CID ESI MS/MS
pp15	Cyclophilin	AAA35733*	x	x	
pp20	Stromal cell derived factor 2-like 1	XP_096152	x		
pp20	Ribosomal protein	AAB00969*	x		
pp25	Ig kappa chain (rat)	AAA41395*	x		
pp27	Galactose-specific lectin	AAA88086*	x		x
pp27	Endoplasmic reticulum lumenal protein 28	NP_06808			x
pp27	Heterogeneous nuclear ribonucleoprotein A2/B1	NP_112533*	x		x
pp27	PYM protein	NP_115721*	x		x
pp27.5	Galactose-specific lectin	AAA88086*	x		
pp27.5	Heterogeneous nuclear ribonucleoprotein A2/B1	NP_112533*	x		
pp28	FK-506-binding protein 3	NP_002004	x		
pp28	Galactose-specific lectin	AAA88086*	x	x	
pp31.5	Transcriptional activator ALY	AAD096608*	x		
pp32	Small nuclear ribonuclear nucleoprotein polypeptide A	NP_004587			x
pp32	Similar to heterogeneous nuclear ribonucleoprotein A1	XP_015697*			x
pp32	bZIP enhancing factor	NP_005773			x
pp32	Complement component 1, p32 splicing factor S	NP_001203*			x
pp32	Histone H1	JX0087*			x
pp32	Ig gamma-2c chain C region (rat)	121056			x
pp34.5	Heterogeneous nuclear ribonucleoprotein A1	NP_002127	x		
pp35	Heterogeneous nuclear ribonucleoprotein A1	NP_002127*	x		
pp36	Annexin A2	AAH23990*	x		
pp36	Apex nuclease	S47521*	x		
pp37	Heterogeneous nuclear ribonucleoprotein A/B	XP_038946	x		
pp39	Heterogeneous nuclear ribonucleoprotein D	NP_002129*	x		
pp41	Heterogeneous nuclear ribonucleoprotein D	NP_002129*	x		
pp50	IgG-2C Chain C region (rat)	P20762	x		
pp52	IgG-2C Chain C region (rat)	P20762	x		
pp52	Similar to DKFZP564M2423	AAH03049	x		
pp54	Polypyrimidine tract binding protein (PTB) (Heterogeneous nuclear ribonucleoprotein I)	NP_114368*	x		
pp54	IgG-2C Chain C region (rat)	P20762	x		
pp62	Splicing factor 3a, subunit 2, 66kDa	NP_009096*	x		
pp74	HSP73	NP_006588	x		
pp75	Polyadenylate-binding protein 1 (PABP1)	P11940*	x		
pp76	Keratin contamination		x		
pp24	Nuclear RNA helicase, DECD variant of DEAD box family	XP_031276*	x		
pp24	Ig kappa chain	AAA41395*	x		
pp24	PDGF associated protein	NP_055706	x		

pp26	Heterogeneous nuclear ribonucleoprotein A2/B1	NP_002128*	x		
pp26	Galactose-specific lectin	AAA88086	x		

Table 5.3

Protein Name	NCBI Accession	Function	Localisation
Cyclophilin	AAA35733	peptidyl-prolyl cis-trans isomerase	ER
Stromal cell-derived factor 2-like1	XP_096152	-	-
Ribosomal protein	AAB00969	Cellular ribosomes	ER
Galactose-specific Lectin	AAA88086	Galactose-specific lectin which binds IgE.	Nuclear; (Cytoplasmic in adenomas and carcinomas)
Heterogeneous nuclear ribonucleoprotein A2	NP_002128	Involved in pre-mRNA processing. Member of ribonucleosomal complexes	Nuclear Component of ribonucleosomes
Hypothetical protein MGC13064	NP_115721	-	-
FK506-binding protein 3	NP_002004	FK506/Rapamycin binding protein	
Transcriptional coactivator ALY	AAD09608	Mediator of the TCRalpha enhancer complex	Nuclear
Heterogeneous nuclear ribonuclearprotein A1	NP_002127	Member of ribonucleosomal complexes. Modulation of splice site selection. Packages pre-mRNA into hnRNP complexes Transport of poly A+ mRNA from the nucleus to the cytoplasm.	Nuclear; Nuclear/cytoplasmic shuttling protein
Annexin A2	AAH23990	Plasminogen receptor	Cell surface
bZIP enhancing factor	NP_005773	Transcriptional co-activator	Nuclear
Apex nuclease	S47521	-	-
Heterogeneous nuclear ribonceloprotein A/B	XP_038946	RNA splicing	Nuclear/Cytoplasmic
Nuclear ribonucleoprotein D	. NP_002129	Binds to RNA containing AU-rich elements.	Nuclear; Member of ribonucleosomal complexes.
Similar to DKFZP564M2423	AAH03049	-	-
Polypyrimidine tract binding protein (PTB) (also hnRNP I)	. NP_114368	Involved in pre-mRNA splicing. Binds to the polypyrimidine tract of introns. May promote the binding of U2 snRNP to pre-mRNA.	Nuclear
Splicing Factor 3a, subunit 2, 66kD (SAP62)	NP_009096	Subunit of the splicing factor SF3a required for 'A' complex formation. May anchor U2 snRNP to the pre-mRNA. Possibly also involved in the 'E' complex assembly.	Nuclear; A main component of the SF3A complex (SF3A3/SAP61, SF3A2/SAP62, SF3A1/SAP114). The U2 snRNP ribonucleoprotein complex is formed by the binding of SF3A to SF3B and a 12S RNA unit.
HSP73 Identical to HSP71 (P11142)	NP_006588	Heat shock protein involved in protein folding. May also act as an ATPase	-
Polyadenylate-binding protein	P11940	Binds mRNA at the polyA tail	Cytoplasmic; Nuclear/cytoplasmic shuttling protein
Nuclear RNA helicase, DECD variant of DEAD box	XP_031276	-	-

family			
PDGF associated protein	NP_055706	Signal transduction/cell proliferation	
snRNP U1A	NP_004587	Member of the spliceosome complex	Nuclear
PYM protein	NP_115721	-	-
Histone H1	JX0087	Essential for the condensation of nucleosome chains into higher order structures	Nuclear
Human p32	NP_001203	RNA splicing, binds SF2	Mitochondrial/Nuclear

Table 5.3

Pooled functional annotation data for all proteins identified as interacting directly/indirectly with LANA1 by affinity chromatography and immunoaffinity purification.

Table 5.4

Spliceosome proteins	**Identification method**
U1 specific proteins	
U1 A	Immunoaffinity purification
Cyclophilin	Immunoaffinity purification
Cleavage factor Im, 25kDa subunit	Immunoaffinity purification

H-complex components	**Identification method**
hnRNP A1	Immunoaffinity purification
hnRNP A2/B1	Immunoaffinity purification
hnRNP D	Immunoaffinity purification
hnRNP I/PTB	Immunoaffinity purification
HSP73	Immunoaffinity purification

Table 5.4 – Spliceosome and H-complex members identified as interacting directly/indirectly with LANA1.

5.5 LANA1 interactions identified by yeast two-hybrid screening

To complement the immunoaffinity purification data I sought to confirm and identify further direct protein-protein interaction partners of LANA1, using a yeast two-hybrid screening system. Two areas of LANA1 were selected as bait – amino acids 1-337 and 893-1130. Unfortunately, the carboxyl terminus of LANA1, aa893-1130, were toxic in yeast. Screens with the amino terminus of LANA1, aa1-337, identified interactions with several novel proteins (Appendix II). One of these proteins, SAF-B, contains a RRM domain in common with many other proteins identified by immunoaffinity purification and mass spectrometry.

SAF-B, also termed HAP, heat-shock protein (HSP27) estrogen response element and tata box-binding protein (HSP27 ERE-TATA-binding protein) is a 849 amino acid with a predicted molecular weight of 96,696 Da (Renz and Fackelmayer 1996). Purified SAF-B migrates at 150kDa on denaturing SDS-PAGE due to a high number of charged amino acids (Renz and Fackelmayer 1996). SAF-B binds to S/MAR-DNA, which are regions of DNA that are A T rich sequences. Several proteins have been identified as S/MAR-DNA binding proteins, including SAF-A (hnRNP U) (Fackelmayer *et al.* 1994) and Histone H1 (Izaurralde *et al.* 1989). The relevance of an interaction between SAF-B and LANA1, in the context of the large-scale immunopurification data are discussed later.

The raw data and summary data for SAF-B are shown in Table 5.5 and Fig 5.9A, respectively. Two clones of SAF-B were identified by yeast two-hybrid screening and corresponded to aa341-825 and aa357-777. Both of the clones sequences overlapped with the RRM domain of SAF-B, which is located at aa409-480 (Fig 5.9A).

Table 5.5

Contig number	Contig member	Sequence I.D.	Percentage match vs Genbank sequence	Protein name	Function
Contig918363	2	gi|4506778|ref|NM_002967.1| Homo sapiens scaffold attachment factor B (SAFB), mRNA	97.9	SAF-B Hsp27 ERE-TATA-binding protein (HET)	Scaffold attachment
Contig918358	2	gi|4506778|ref|NM_002967.1| Homo sapiens scaffold attachment factor B (SAFB), mRNA	99.5	SAF-B	Scaffold attachment

Table 5.5 - Identification of SAF-B as a LANA1 interacting protein using yeast two-hybrid analysis. LANA1 (aa1-337) was used as bait for a yeast two-hybrid screen. Several interacting partners were identified and are listed in appendix II. Details of SAF-B are shown.

Fig. 5.9 - LANA1 protein-protein interaction domains. **A**, SAF-B was identified as binding to the amino terminus of LANA1 (aa1-337) by yeast two-hybrid analysis. Data show independent clones rescued. **B**, Several proteins identified as directly/indirectly interacting with LANA1 share common RNA-binding domains (RRM/RBD domains). Domain data were obtained from the NCBI.

Fig 5.9

A

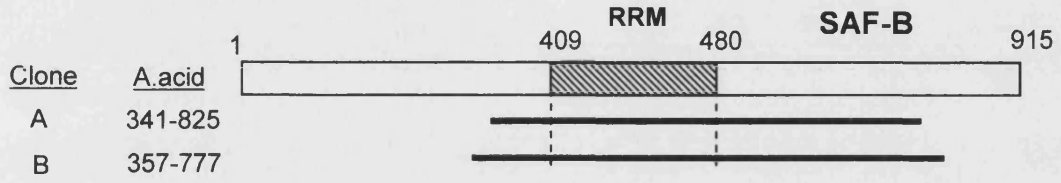

B

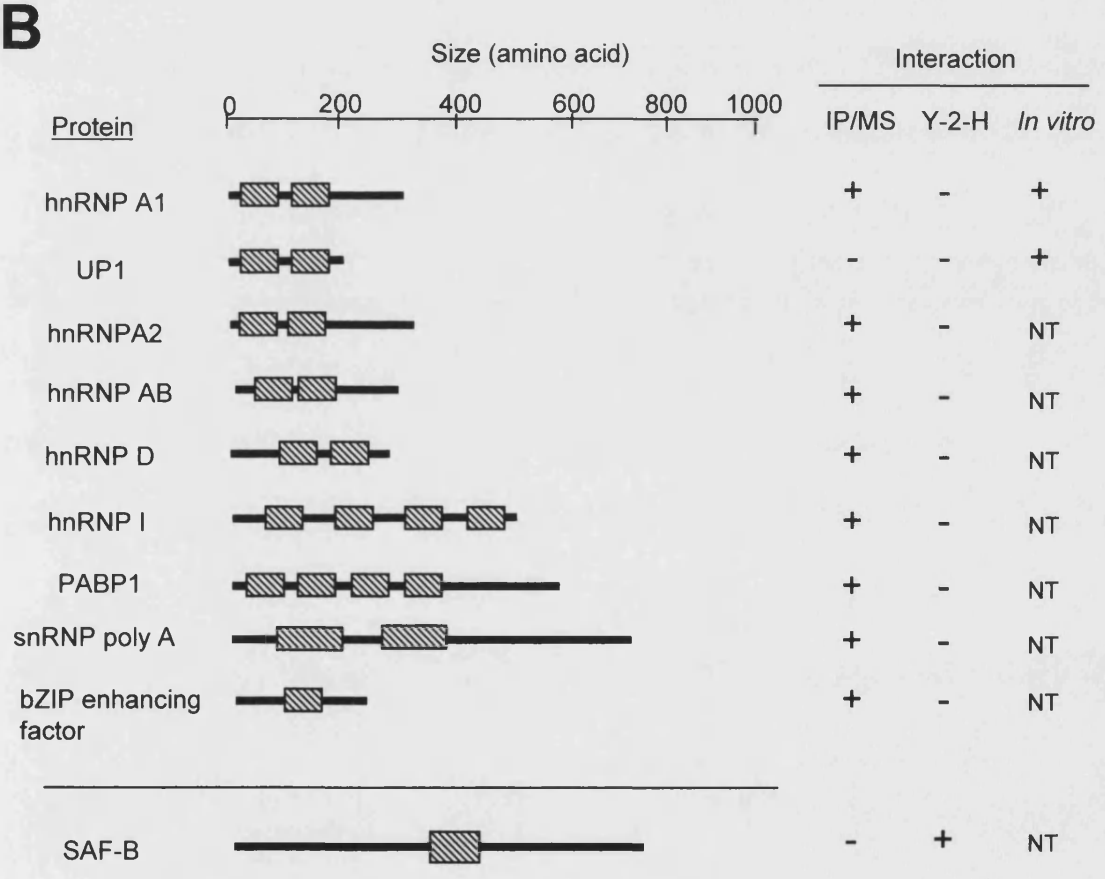

RRM/RBD RNA binding domain

NT = Not tested

Protein-protein interaction domain: RRM domain

SAF-B contains an RNA binding domain in common with many of the other novel LANA1 interaction proteins, which are summarized in Fig 5.9B. The RNA-recognition motif (RRM), also termed RNA binding domain (RBD) and ribonucleoprotein consensus sequence (RCS), is common among many hnRNPs and proteins involved in splicing (Xu *et al.* 1997).

Overall the data obtained by both methods of interaction screening revealed the RRM domain as a common target for LANA1. From the pooled data 9 novel interaction partners of LANA1 were identified which had at least one RRM domain. However, the proteins hnRNP A1, hnRNP A2/B1 and hnRNP D all also contain an RGG site, located in the carboxyl terminus. The interaction between LANA1 and the RRM sites will be developed in Chapter 6.

5.6 Discussion and conclusion

Biological experiments are becoming increasingly global in cellular scale. Previously protein-protein interactions were often studied at a one-to-one scale. Techniques that fall under the recently popular field of proteomics were successfully used to obtain and characterise the native LANA1 complex.

KSHV is an infectious agent directly implicated in the etiopathogenesis of several important human malignancies including KS, MCD and PEL (Cesarman *et al.* 1995;Chang *et al.* 1994;Soulier *et al.* 1995). Of all KSHV proteins, LANA1 is one of the few proteins expressed in all tumor cells, interacts with a broad spectrum of important cellular proteins and acts as both a transcriptional activator and repressor. In this work I sought to identify further novel interactions of LANA1 that may have direct relevance to pathology. By employing a protein complex capture method and a yeast two-hybrid system I identified several novel LANA1 complex proteins.

The work presented in this chapter represents the first attempt to purify a native LANA1 complex. When employing a novel method it is important to obtain data that overlaps with previous knowledge in the field. As techniques differ from group to group and lab to lab it is not possible to recreate the conditions for several experiments in one. In the case of LANA1, more than 10 groups have reported LANA1 interacting proteins often using different methods. In this chapter I report the confirmation of data from two such groups publishing on two ORF73 interacting proteins; Histone H1 and cellular p32 (the latter was identified as an HVS ORF73 interacting protein)(Hall *et al.* 2002). These results not only show that the techniques employed for the capture and analysis of the LANA1 complex in this chapter were sound, but that greater confidence can be placed on the identification of novel LANA1 complex proteins.

Recently the publication of an extensive characterisation of the human spliceosome was achieved (Zhou *et al.* 2002). This paper identified all previously known spliceosome components and also identified 58 new proteins. Among these proteins were several members identified as binding to LANA1, both by the Hybrigenics data and complex purification.

Coupled with yeast two-hybrid data I have identified not only several new interaction partners of LANA1, but also novel interaction domains. The RRM domain was identified by as an interaction domain by both yeast two-hybrid and the immunoaffinity purification work. The large proportion of the novel interaction partners of LANA1 described here have common protein domains. The hnRNPs, PABP1 and several others all contain RRM motifs (also termed RBD), protein domains required for RNA binding (Fig 5.9B).

As mentioned earlier, SAF-B was identified as interacting with LANA1 by yeast two-hybrid. Identification of SAF-B as a direct protein-protein interaction partner was interesting as literature searches on SAF-B revealed further interaction partners. SAF-B is known to bind directly to two proteins I identified here, by immunoaffinity purification, as interacting with a LANA1 complex; hnRNP A1 and hnRNP D (Arao *et al.* 2000;Weighardt *et al.* 1999). The specificity of this interaction and the confirmation of direct protein-protein interactions with this domain are explored further in Chapter 6.

More recently evidence has emerged of an important role for several hnRNPs at the telomeres of mammalian cells (Ford *et al.* 2002). The telomerase complex whose components include hTR, telomerase reverse transcriptase (hTERT) and several associated ribonucleoproteins including hnRNP A1, C1/C2 and D, maintains mammalian telomeres. Telomerase activity is frequently upregulated in human tumors and extended telomeres are associated with lifespan

extension (Hahn and Weinberg 2002). Both hnRNP A1 and its proteolytic derivative, UP1, were found to bind telomere sequences and UP1 was found to be sufficient for the maintenance of mammalian telomeres *in vivo* (LaBranche *et al.* 1998). hnRNP A1 and UP1 also protect mammalian telomeres from degradation by endonucleases and exonucleases (Dallaire *et al.* 2000). I identified here hnRNP A1, A2/B1 and D as LANA1 complex proteins (Fig 5.9). Telomere related protein Interactions identified by yeast two-hybrid and proteomics techniques, and their novelty, are highlighted in Fig 5.10. This suggests a role for LANA1 in the biogenesis of telomeres and is expanded upon in Chapter 6. The interaction of LANA1 with several hnRNPs and splicing factors suggests a role for LANA1 in the modulation of cellular and viral RNA splicing. The herpesviruses interact with a wide range of proteins involved in splicing and RNA metabolism. Human cytomegalovirus (CMV) immediate early protein 2 (IE2) has been reported to bind hnRNP A1 (Wang *et al.* 1997) and in common with LANA1, IE2 has also been shown to bind pRB and p53 (Hagemeier *et al.* 1994;Speir *et al.* 1994). SAP62, a subunit of the splicing factor SAF3a and a member of the U2 snRNP complex was identified here as a LANA1 complex protein. In herpes simplex virus (HSV-1) the multifunctional protein ICP27 (also termed IE63) binds to SAP145, another member of the SAF3a splicing complex (Bryant *et al.* 2001). Via this interaction, ICP27 has been shown to inhibit cellular RNA splicing. A further interaction partner of ICP27, the cellular protein p32 (Bryant *et al.* 2000) was also identified here as a KSHV LANA1 complex protein (Table 5.3). As p32 plays a role in cellular splicing and as it is targeted by ICP27, HSV-1 can further deregulate normal splicing functions. Herpesvirus saimiri (HVS) ORF73, a homologue of KSHV LANA1, was recently shown to interact with p32 by yeast two-hybrid (Hall *et al.* 2002).

Fig. 5.10 Interactions identified and/or confirmed in this thesis. By using two independent methods of interaction screening (yeast two-hybrid and large scale immunoaffinity purification) I identified several novel binding partners of LANA1. Proteins shown are either related to telomere biogenesis or share common RRM domains. Published interactions between proteins and/or telomeres and telomerase are shown.

Fig 5.10

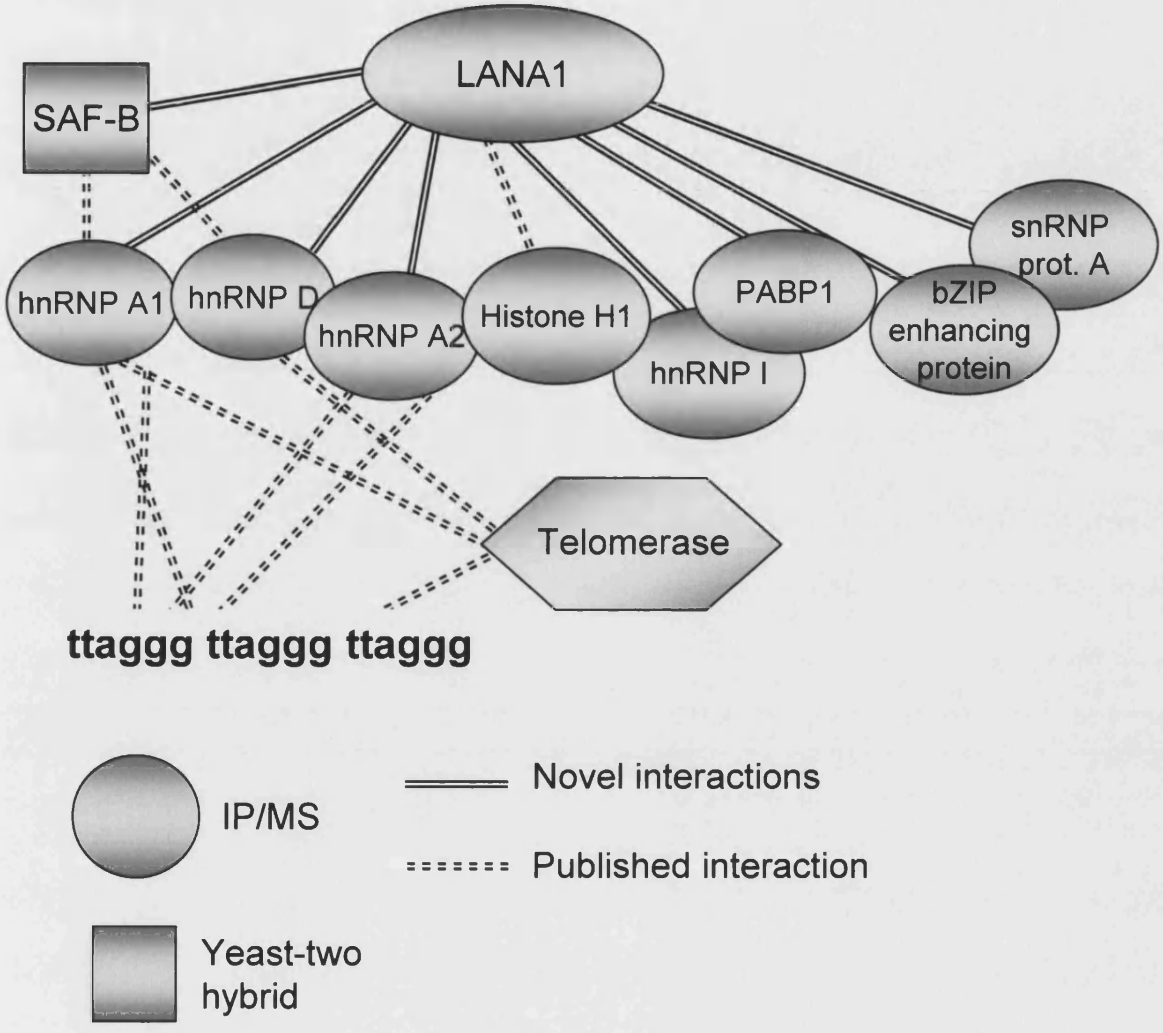
LANA1
SAF-B
snRNP prot. A
hnRNP A1
hnRNP D
hnRNP A2
Histone H1
PABP1
bZIP enhancing protein
hnRNP I
Telomerase
ttaggg ttaggg ttaggg
IP/MS
Novel interactions
Published interaction
Yeast-two hybrid

It is tempting to propose that interactions with cellular splicing factors may allow LANA1 to modulate KSHV transcripts and perhaps its own post-transcriptional modification. This is particularly relevant as LANA1 mRNA levels appear to be tightly regulated. LANA1 is transcribed with vcyclin and vFLIP on a polycistronic transcript (Talbot *et al.* 1999). Two forms of the transcript exist as 1.7kb and 5.32kb transcripts, the former of which is a splice variant that lacks LANA1 and is increased by *n*-butyrate treatment (Talbot *et al.* 1999). Talbot *et al* suggest that changes in the relative levels of each transcript after *n*-butyrate treatment may be due to levels of hnRNP A1 and SF2. As LANA1 is located at the viral episome in KSHV-infected cells, the recruitment of hnRNP A1 by LANA1 may favour the selection of the distal splice site and increase the relative levels of the 1.7kb transcript. This presents a novel post-transcriptional mechanism for the control of LANA1 protein levels within KSHV infected cells.

A possible criticism of this work is that several proteins previously identified as interacting with LANA1 were not confirmed, for example p53 and pRB. While this is disappointing, it is perhaps not unexpected. During different phases in the cell cycle and stages in cell proliferation, interactions often change. Depending on which stage the cells are lysed at will identify interactions at that particular time-point. This was a consideration during the planning of this work and it was decided to use a heterogeneous population of cells. I have successfully identified many proteins using this method. It is possible that interactions with p53 and pRB are cell-cycle dependent and so would need more detailed protocols for capture of the complex containing them. Future work could aim to identify cell-cycle specific LANA1-related complexes, using synchronised cells lysed at various times after induction of the cell cycle.

Several of the proteins identified using this method are highly abundant in mammalian cells, including hnRNP A1 and PABP1. In

Hela cells, hnRNPA1 is present at 70 x 10^6 molecules per cell (Kiledjian *et al.* 1994). The techniques used in the chapter to identify protein-protein interactions may have been limited by the level of starting material.

A further possibility is the stringency of the purification step. Initial work concentrated on the use of a low salt buffer to capture the LANA1 complex, but this buffer proved difficult to use as too many proteins co-purified with LANA1. Using this buffer it would not have been possible to identify specific LANA1 complex proteins. Therefore, the loss of some weakly interacting proteins may have been the price for the identification of strong and specific interacting proteins.

It was also interesting that LANA1 was not identified as an eluting protein from the columns. This could be due to several different factors. Firstly, the low abundance of LANA1 in BC-3 cells, in relation to other identified proteins (the hnRNPs and histones), may have resulted in insufficient material for identification. Secondly, the high molecular weight and unusual biochemical structure of LANA1 may have resulted in LANA1 precipitating out of solution during the elution (due to low pH) or protein concentrating steps (due to vacuum drying). When beads were tested prior to elution and concentration of protein, high levels of LANA1 were detectable. The lack of LANA1 identification by MS is therefore likely to be due to the nature of LANA1.

Overall, I have identified many new interaction partners of LANA1 using proteomic analysis. The majority of these new interaction partners have a role in cellular splicing. Proteins are either involved in the formation of the human spliceosome (CPSF-5, cyclophilin) or form part of the H-complex (hnRNPA1, A2/B1, D, I and HSP73). It is possible that by interacting with a broad range of proteins involved in spliceosome formation, RNA splicing and RNA transport, LANA1 may

modulate cellular splicing. Alternatively, the formation and recruitment of such factors to the viral episome would be beneficial to the life-cycle of the virus, enabling the preferential processing of viral transcripts. Further studies will elucidate these putative functions of LANA1.

Chapter 6 Results

hnRNP A1 is part of a native LANA1 complex

Chapter aims: The aim of this chapter was to further confirm and investigate the protein-protein interaction data for LANA1. Further experiments were undertaken in an attempt to understand the functional implications of the interaction data.

6.1 Conformation of interacting proteins

To confirm interactions identified from the columns, immunoprecipitations, GST-pulldown assays and for some interacting proteins, functional assays were performed. From the combined Hybrigenics (Paris, France) and IP/MALDI results common interaction domains became obvious. The majority of proteins interacting with LANA1 from the columns possessed at least one RNA binding domain (RRM/RBD), with several possessing multiple motifs up to a maximum of 4. A selected number of proteins were chosen for further analysis. These were hnRNP A1, PABP1 and galactose specific lectin (Galectin-3). A bank of GST-LANA1 constructs were used to screen for the interaction domains on LANA1.

Galectin-3, Galactose specific lectin, also termed Galectin-3 is a multi-functional protein with roles in several different areas of the cellular life cycle (Liu *et al.* 2002). Galectin-3 has been shown to protect cells from anoikis, cell death induced by loss of anchorage. Despite Galectin-3 being pulled down by the columns, no specific interaction was seen when BC-3 cell lysates were incubated with GST-LANA1 constructs. This may be due to the interaction domain for Galectin-3 being in the central region of LANA-1, an area which I was unable to successfully express as a GST- fusion protein, probably due to its highly repetitive nature. I also encountered difficulties when trying to confirm the interaction via small-scale immunoprecipitation, as Galectin-3 runs at the same size as the rat light chain (25kDa).

Despite these problems, Galectin-3 was repeatedly identified by mass spectrometry and is therefore likely to be a true interaction partner.

PABP1, The polyadenylate binding protein 1 is a 70 kDa protein that functions in RNA metabolism by binding the polyA+ tail of mature mRNA. It has a predominately cytoplasmic distribution, although it shuttles between the cytoplasm and the nucleus. To confirm the interaction of PABP1 with LANA1, BC-3 cells and immunaffinity purification lysates performed as stated in Materials and Methods were subjected to western blotting with mouse anti-PABP1 antibody (a kind gift from Professor Gideon Dreyfuss). The western blot shows the specific co-immunoprecipitation of PABP1 with LANA1 in BC-3 cells (Fig 6.1A).

hnRNP A1 and UP1, The implication of hnRNP A1 as a regulator of telomere length was shown when both hnRNP A1 and its proteolytic N-terminal derivative UP1 were found to bind telomere sequences and found to be required for the maintenance of mammalian telomeres *in vivo* (LaBranche *et al.* 1998). hnRNP A1 and UP1 protect mammalian telomeres from degradation by endonucleases and exonucleases (Dallaire *et al.* 2000). To confirm the interaction between hnRNP A1 and LANA1 as revealed by affinity chromatography, I used *in vitro* pulldown and *in vivo* co-immunoprecipitation assays.

6.2 hnRNP A1 co-immunoprecipitates with LANA1 *in vivo*

To further characterise the interaction of LANA1 with hnRNPA1/UP1, co-immunoprecipitation assays were performed. BC-3 cells were lysed in RIPA buffer, diluted to 50% RIPA and bound to either 5μg of anti-LANA1 antibody or a control antibody. After washing, beads were resuspended in 2x Laemmli loading buffer, proteins were separated by SDS-PAGE and detected by Western blotting.

Fig. 6.1 - Confirmatory small scale immunoprecipitations. **A**, PABP1 co-immunoprecipitates from BC-3 lysates with LANA1. To detect PABP1, protein was eluted from CNBr beads used for the large-scale immunoaffinity purification and separated on a 6% SDS-PAGE gel. PABP1 was detected using anti-PABP1 (1:500). **B**, hnRNP A1 was detected by western blotting after small scale immunoprecipitation from BC-3 cells. Both PABP1 and hnRNP A1 co-immunoprecipitated with LANA1 confirming the large-scale immunoaffinity purification data. **C**, hnRNPA1 co-immunoprecipitates with LANA1 from HEK-293 cells. HEK-293 cells were transfected with pHR CMV LANA1 or empty vector. Lysates were incubated with anti-LANA1 antibody and washed repeatedly. hnRNPA1 was detected with anti-hnRNPA1 mouse monoclonal (1:500). hnRNPA1 was immunoprecipitated only from HEK-293 cells transfected with LANA1.

Fig 6.1

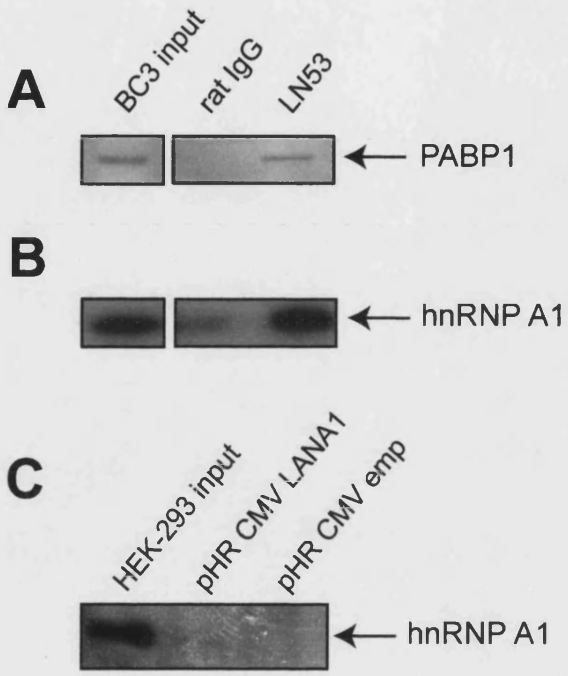
A
BC3 input
rat IgG
LN53
PABP1
B
hnRNP A1
C
HEK-293 input
pHR CMV LANA1
pHR CMV emp
hnRNP A1

hnRNP A1 co-immunoprecipitates with LANA1 from BC-3 cells lysed in RIPA (Fig 6.1B). As all *in vivo* co-immunoprecipitation experiments had so far been carried out in KSHV infected cells, there was a possibility that another KSHV protein or transcript may be either required for the interaction between LANA1 and hnRNPA1 or involved in stabilization of the interaction. To investigate this possibility, *in vivo* binding assays were performed on HEK-293 cells, which contain no KSHV genes. HEK-293 cells were transfected with pHR CMV LANA1 or pHR CMV EMP and lysed in RIPA buffer. LANA1 was immunoprecipitated from the cell lysates and bound proteins were separated by gel electrophoresis. hnRNPA1 was detected by western blotting. hnRNPA1 was found to co-immunoprecipitate only from HEK-293 cells transfected with LANA1, indicating that LANA1 alone is sufficient for this interaction (Fig 6.1C).

6.3 LANA1 binds hnRNP A1 *in vitro.*

To further confirm and map the interaction between hnRNP A1 and LANA1, as revealed by large-scale immunoaffinity purification, I used *in vitro* pulldown assays. A series of GST-LANA1 fusion proteins were used to confirm and map the interaction of LANA1 with hnRNP A1 (Fig 6.2A). RIPA lysates from BC-3 cells were diluted to 50% with ddH20 and incubated with the bank of GSTs. I detected binding of hnRNP A1 to GST-LANA1 (aa3-236), GST-LANA1 (aa982-1113) and GST-LANA1 (aa932-1162), but not GST-LANA1 (aa803-981) (Fig 6.2B). Similar to the *in vivo* experiments, I sought to show that the *in vivo* interaction of LANA1 with hnRNPA1 was not dependent on the presence of other KSHV proteins or transcripts. To investigate this, *in vitro* binding assays were performed on HEK-293 cells, which contain no KSHV genes. hnRNP A1 is also pulled-down by GST-LANA1 in KSHV negative mammalian cells, indicating that LANA1 alone is sufficient for the formation of this complex (Fig 6.2C).

Fig. 6.2 LANA1 interacts with hnRNP A1. **A**, GST-LANA1 constructs used for *in vitro* binding studies. **B**, A bank of GST-LANA1 proteins were incubated with BC-3 cell RIPA lysates diluted to 50%. Protein bound was washed, eluted in loading dye and hnRNP A1 was detected by western blotting. Minimum domains for the binding of LANA1 to hnRNP A1 were found both at the amino (aa3-236) and carboxyl ends (aa982-1113). **C**, GST-LANA1 binds hnRNPA1 in HEK-293 cells. HEK-293 cells were lysed in RIPA buffer, diluted to 50% RIPA with ddH20 and incubated with a bank of GST-LANA1 constructs. LANA1 binds hnRNPA1 in 293 cells, indicating that no other viral transcript or protein is required for this interaction. **D**, BC-3 CHAPS lysates were incubated with equal amounts of either GST or GST-hnRNP A1 proteins. Protein bound was washed, eluted in loading dye and separated on a 6% SDS-PAGE gel. LANA1 was detected using anti-LANA1 rat monoclonal (1:1000). Only GST-hnRNP A1 and not GST alone recovered LANA1.

Fig 6.2

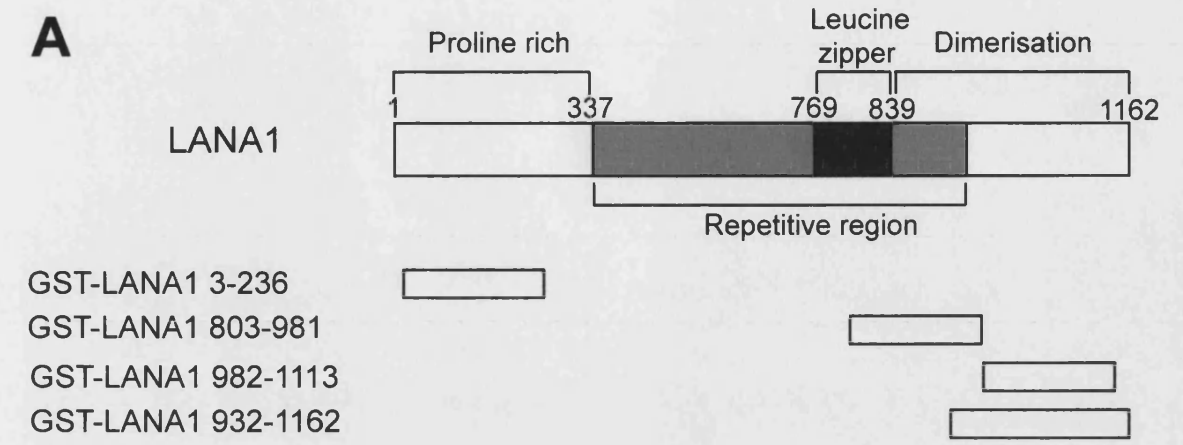
A
Proline rich
Leucine zipper
Dimerisation
1
337
769
839
1162
LANA1
Repetitive region
GST-LANA1 3-236
GST-LANA1 803-981
GST-LANA1 982-1113
GST-LANA1 932-1162


B
BC3 input
GST
GST-LANA1 3-236
GST-LANA1 803-981
GST-LANA1 982-1113
GST-LANA1 932-1162
hnRNP A1
*predicted size

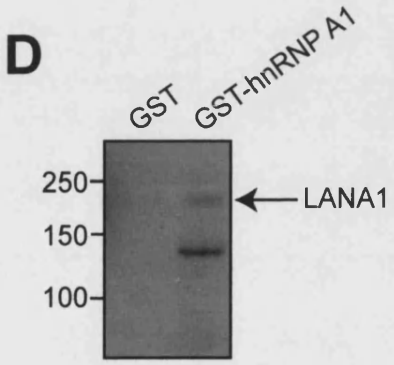
D
GST
GST-hnRNP A1
250
150
100
LANA1

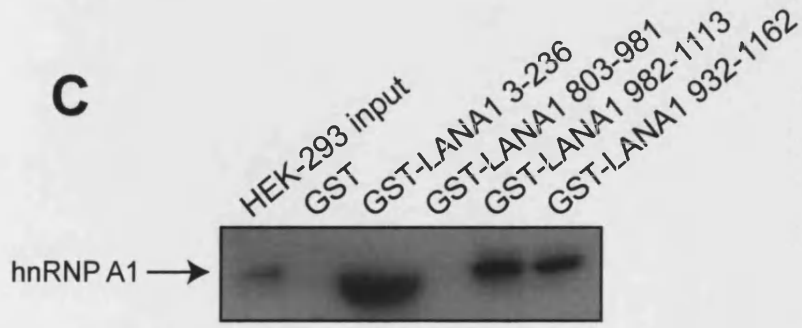
C
HEK-293 input
GST
GST-LANA1 3-236
GST-LANA1 803-981
GST-LANA1 982-1113
GST-LANA1 932-1162
hnRNP A1

These data confirm the immunoaffinity purification data and map the interaction domains of hnRNP A1 at the amino terminus (aa3-236) and the carboxyl terminus (982-1113).

In reciprocal experiments, I sought to show that recombinant hnRNP A1 could pull down LANA1 from cell lysates. BC-3 cells were lysed in CHAPS buffer and incubated with GST or GST-hnRNP A1. After binding overnight, the beads were washed twice in CHAPS buffer and bound proteins eluted with 2x Laemmli loading buffer. Protein was separated by SDS-PAGE and subjected to western blotting using anti-LANA1 antibody. LANA1, was pulled-down by GST-hnRNP A1, but not the GST control (Fig 6.2D).

6.4 LANA1 binds UP1, the proteolytic derivative of hnRNP A1, *in vitro.*

UP1 consists of the first 196 amino acids of hnRNP A1 (Fig 6.3A) and unlike full length, has no function in splicing (Mayeda *et al.* 1994;Riva 1986). Recombinant UP1 pulls down telomerase activity from cell lysates (LaBranche *et al.* 1998). As LANA1 interacts with hnRNP A1, I next tested if UP1 is also bound by LANA1. HEK-293 cells were transfected with HA tagged UP1 and lysed in RIPA buffer. Lysates were incubated with my bank of LANA1 GSTs. This revealed that UP1-HA binds LANA1 in the same regions as hnRNP A1 (Fig 6.3B). Along with the previous data, this shows that both the amino and carboxyl terminus of LANA1 can bind hnRNP A1 and UP1. As UP1 possesses no splicing activity it suggested that the interaction with LANA1 may be involved in telomere biogenesis. This hypothesis was reinforced by the *in vivo* interaction data that showed interactions with other proteins that have been proposed to play a role in telomere regulation: hnRNP D and hnRNP A2/B1.

Fig. 6.3 LANA1 interacts with UP1. **A**, The structure of hnRNP A1 and its proteolytic derivative, UP1. **B**, LANA1 interacts with UP1-HA. 293 cells transfected with UP1-HA were lysed in RIPA buffer, diluted to 50% and incubated with a bank of GST-LANA1 proteins. Protein bound was detected using anti-HA mouse monoclonal antibody (1:1000). In common with hnRNP A1, the minimum domains for the binding of LANA1 to UP1-HA were found both at the amino (aa3-236) and carboxyl termini (aa982-1113). **C**, GST-hnRNP A1 pre- and post-cleavage with Precission Protease. Protein was separated on a 15% gel and stained with coomassie brilliant blue. hnRNPA1 is seen as a 34kDa band. **D**, GST-hnRNP A1 was cleaved of its GST moiety and incubated with a bank of GST-LANA1 proteins. hnRNP A1 was detected with anti-hnRNP A1 antibody. Recombinant hnRNP A1 interacted with LANA1 in the same regions as endogenous hnRNP A1.

Fig 6.3

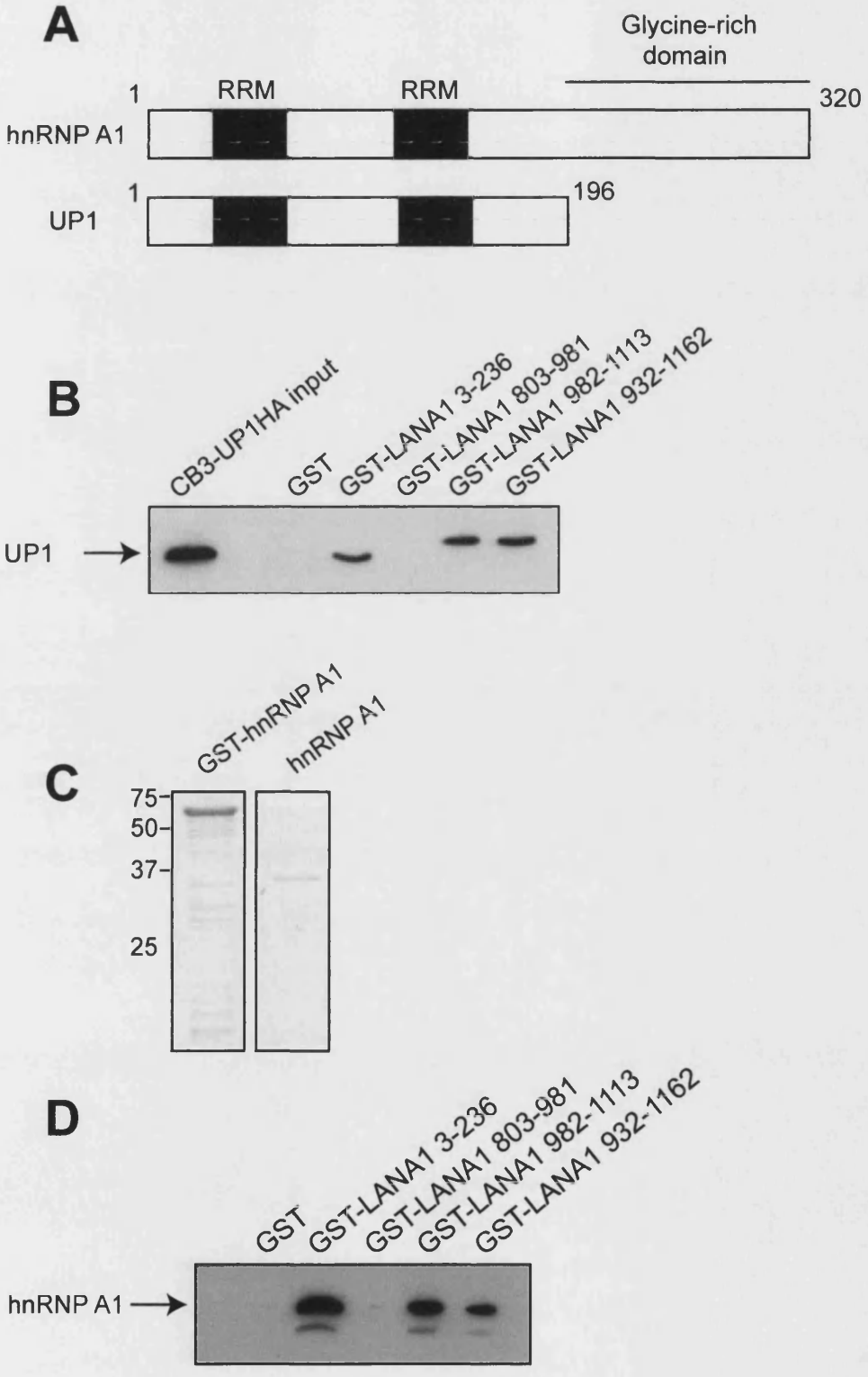
A
Glycine-rich domain
1
RRM
RRM
320
hnRNP A1
1
196
UP1
B
CB3-UP1HA input
GST
GST-LANA1 3-236
GST-LANA1 803-981
GST-LANA1 982-1113
GST-LANA1 932-1162
UP1
C
GST-hnRNP A1
hnRNP A1
75
50
37
25
D
GST
GST-LANA1 3-236
GST-LANA1 803-981
GST-LANA1 982-1113
GST-LANA1 932-1162
hnRNP A1

Previous work by another group has shown that hnRNP A1 can bind to a viral protein, immediate early gene 2 (IE2) of human cytomegalovirus (CMV) (Wang *et al.* 1997). The interaction between IE2 and hnRNP A1 was found to be located between amino acids 99 and 490, indicating that regions within both the amino and carboxyl terminus of IE2 mediate the interaction with hnRNP A1(Wang *et al.* 1997).

6.5 Direct protein-protein interaction

As hnRNP A1 is a DNA and RNA binding protein it is possible that mammalian DNA or RNA may mediate the interaction with LANA1, which is known to bind histone H1 and tether KSHV episome to cellular DNA. To investigate this I prepared GST-hnRNP A1 and cleaved off the GST moiety using Precission Protease (Fig 6.3C). This recombinant protein was incubated with the bank of GST-LANA1 in a HEPES buffer (Dallaire *et al.* 2000). Under these buffer conditions, hnRNP A1 and UP1 have been shown to bind an artificial telomere sequence (Dallaire *et al.* 2000). Recombinant hnRNP A1 bound to the same regions of LANA1 as native hnRNP A1/UP1 indicating that mammalian DNA/RNA transcripts did not mediate the interaction (Fig 6.3D). Furthermore it is possible that under these conditions LANA1 and hnRNP A1 may form a complex on mammalian telomeres.

6.6 LANA1 and the telomerase complex

In mammalian cells, hnRNP A1 recruits telomerase activity. Telomerase activity has been shown to be recruited by UP1 in mouse cells (LaBranche *et al.* 1998) and telomerase activity can be recovered by immunoprecipitation of hnRNP A1 from human cells (Ford *et al.* 2002). The telomerase holoenzyme consists of several proteins including TEP1, La, p23, Hsp 90 and hTERT. As LANA1 associates with hnRNP A1/UP1, I sought to establish if LANA1 forms a complex with the telomerase holoenzyme. To determine this I used

the human telomerase reverse transcriptase (hTERT) as a protein target.

6.7 LANA1 binds hTERT *in vivo*

HeLa cells were transfected with 5μg of pHR CMV LANA1 or pHR CMV. Cells were lysed 48hrs post-transfection and lysates were subjected to immunoprecipitation with anti-LANA1 monoclonal antibody (LN53). hTERT was detected using anti-hTERT rabbit polyclonal (Santa Cruz Biotechnology Ltd.). hTERT immunoprecipitated from HEK-293 cells with anti-hTERT rabbit polyclonal and was used for size comparison. hTERT was found to only co-immunoprecipitate with LANA1 from transfected HeLa cells (Fig 6.4A). In reciprocal experiments I sought to co-immunoprecipitate LANA1 with hTERT from BC-3 cells. BC-3 cells were lysed in CHAPS buffer and incubated with 5μg of either anti-hTERT rabbit polyclonal or 5μg of anti-GST polyclonal antibody. LANA1 co-immunoprecipitated with hTERT using an anti-hTERT antibody in BC-3 cells, although this interaction appeared very weak (Fig 6.4B). I have previously found that the expression of hTERT in BC-3 cells is not detectable in cell lysates, indicating that the expression of hTERT in these cells may be very low. This may account for the very low amounts of LANA1 recovered. These data represent several forms of evidence for an interaction between LANA1 and the hTERT protein. While a physical interaction between LANA1 and hTERT suggests a role in telomere biogenesis, these data do not show that the hTERT, when bound by LANA1, is part of a functional telomerase complex.

Fig 6.4 **A**, hTERT co-immunoprecipitates with LANA1 from HeLa cells. HeLa cells were transfected with 5μg of pHR CMV LANA1 or pHR CMV. Cells were lysed 48hrs post-transfection and lysates were subjected to immunoprecipitation with anti-LANA1 monoclonal antibody. hTERT was found to co-immunoprecipitate only from HeLa cells transfected with LANA1 and not the vector only. **B**, hTERT antibody immunoprecipitates LANA1. BC-3 cells were lysed in CHAPS buffer and incubated with 5μg of either anti-hTERT rabbit polyclonal or 5μg of anti-GST polyclonal antibody. Bound protein was separated by SDS-PAGE and LANA1 was detected by western blotting. LANA1 is co-immunoprecipitated by hTERT but not GST antibodies.

Fig 6.4

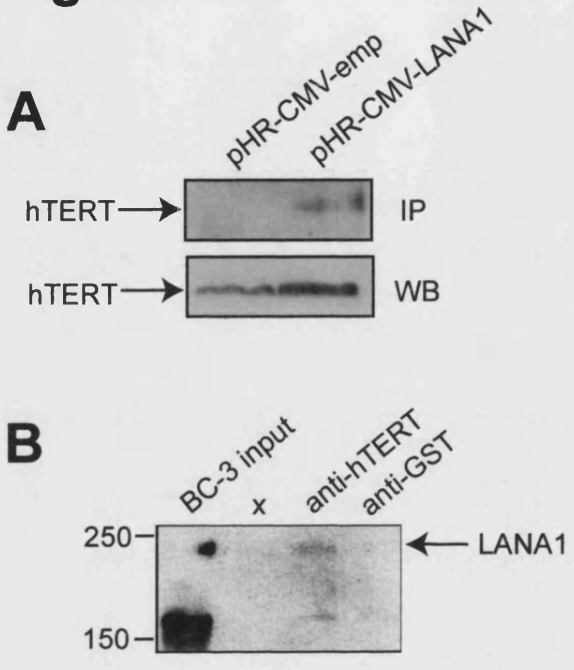
A
pHR-CMV-emp
pHR-CMV-LANA1
hTERT
IP
hTERT
WB
B
BC-3 input
+
anti-hTERT
anti-GST
250
150
LANA1

6.8 LANA1 binds a functional telomerase complex

While physical interaction between LANA1 and hTERT is strong evidence that LANA1 may recruit a telomerase complex, merely demonstrating an interaction does not show that the hTERT is part of a functional telomerase complex. The most common method of showing a functional telomerase holoenzyme complex is by using a Telomerase Repeat Amplification Protocol (TRAP) assay. In this assay cell lysates that possess telomerase activity extend an artificial telomere *in vitro*. This extended telomere is then amplified using PCR with telomere specific primers. The result is a DNA ladder for a positive result and a blank lane for a negative result. The TRAP assay contains several controls including telomerase positive cells, false positive and heat treatment controls. To show that LANA1 recruits a functional telomerase complex, CB3 cells were chosen, as these cells lack endogenous hnRNP A1 (LaBranche *et al.* 1998). The CB3 cells were transfected with UP1-HA and a pulldown using GST and GST-LANA1 982-1113 was used to capture a functional telomerase complex (Fig 6.5). CB3 cells lack hnRNP A1 due to retroviral insertion downstream of the gene (Fig 6.5A) (Ben-David *et al.* 1992). CB3 cells were transfected with pcDNA-UP1-HA and lysed in CHAPS buffer. The expression of UP1 was detected using an anti-HA antibody (Fig 6.5B). As I had already shown that LANA1 can interact with hTERT, telomerase activity would show that LANA1 was interacting not only with the hTERT protein, but likely interacting with it as part of a complex. The results show that the region of LANA1 that binds UP1/hnRNP A1 can pulldown telomerase activity from CB3-UP1-HA cells (Fig 6.5C). Therefore UP1 is sufficient to mediate an interaction between LANA1 and telomerase. Input lysate was assayed for activity at two different dilutions. This was done to show that the cell lysate did not contain inhibitors of telomerase activity. Telomerase inhibitory products can be present in cell lysates and may lead to a false negative result. If this is the case, by diluting the sample, the detected TRAP activity would have increased in

Fig 6.5 - LANA1 and telomerase. **A**, CB3 cells lack hnRNP A1. Cell lysates from CB3, CB7, NIH-3T3 and BC-3 cells were tested for hnRNP A1 expression using anti-hnRNP A1 mouse monoclonal antibody (4B10) (1:500). CB3 cells show an absence of hnRNP A1 protein expression. **B**, CB3 cells were transfected with UP1-HA using DMRIE-C. Lysates were separated on a 15% SDS-PAGE gel and subjected to western blotting using an anti-HA mouse monoclonal antibody. **C**, GST-LANA1 can pulldown telomerase activity from cell lysates. CB3 cells were transfected with UP1-HA and lysates were incubated with either GST (lanes 1-4) or GST-LANA1 (982-1113) (lanes 5-8). After washing, unbound protein (FT) (lanes 1,2 and 5,6) and pulled-down protein (PD) (lanes 3,4 and 7,8) were used in a TRAP assay. PCR products were separated on a 12.5% non-denaturing polyacrylamide gel and stained with 1 in 10,000 dilution of CYBR green stain. Step dilutions (1/10 dilution) of both unbound and pulled down fractions were included to discount the possibility of TRAP assay inhibiting contaminants. Lane 9 shows the PCR contamination control and lane 11 a heat-treated cell lysate control. Lane 10 shows the telomerase positive control included in the kit. Telomerase activity was pulled down only by GST-LANA1 and not GST alone.

Fig 6.5

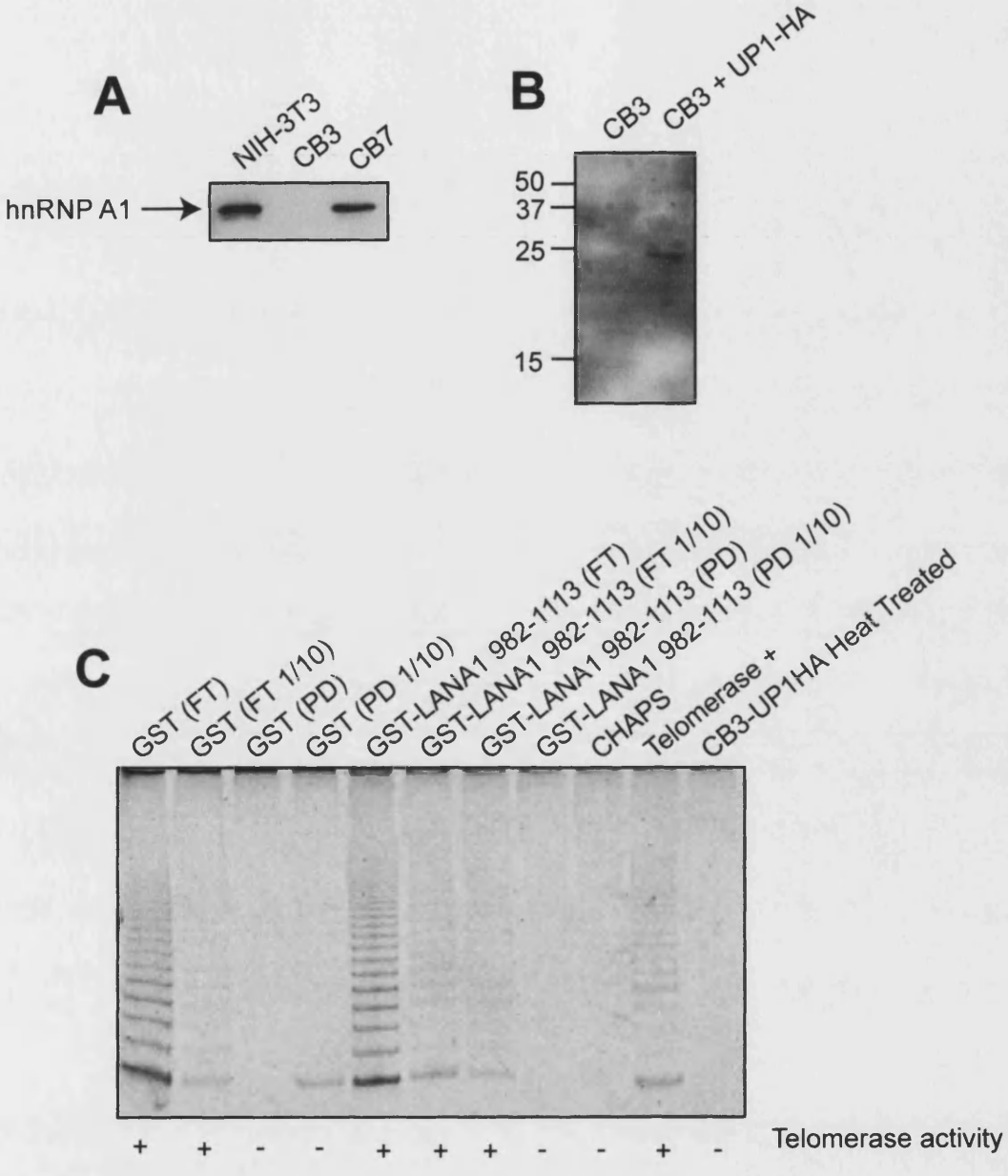
A
NIH-3T3
CB3
CB7
hnRNP A1
B
CB3
CB3 + UP1-HA
50
37
25
15
C
GST (FT)
GST (FT 1/10)
GST (PD)
GST (PD 1/10)
GST-LANA1 982-1113 (FT)
GST-LANA1 982-1113 (FT 1/10)
GST-LANA1 982-1113 (PD)
GST-LANA1 982-1113 (PD 1/10)
CHAPS
Telomerase + CB3-UP1HA Heat Treated
+ + - - + + + - - + -
Telomerase activity

strength. This was not seen and by diluting the lysates, the TRAP activity was decreased. Therefore I am confident that the result is a true negative and indeed telomerase activity was only pulled down by recombinant LANA1.

6.9 Discussion and conclusion

hnRNPs are a large conserved family of proteins playing a role in mRNA splicing, mRNA export, mRNA localisation and polyadenylation (Dreyfuss *et al.* 2002;Krecic and Swanton 1999). hnRNP proteins associate with pre-mRNA to form the H-complex that is an essential part of the spliceosome. More recently evidence has emerged of an important role for several hnRNPs at the telomeres of mammalian cells (Ford *et al.* 2002). The telomerase complex whose components include hTR, telomerase reverse transcriptase (hTERT) and several associated ribonucleoproteins including hnRNP A1, C1/C2 and D, maintains mammalian telomeres. Telomerase activity is frequently upregulated in human tumors and extended telomeres are associated with lifespan extension (Hahn and Weinberg 2002). Both hnRNP A1 and its proteolytic derivative, UP1, were found to bind telomere sequences and UP1 was found to be sufficient for the maintenance of mammalian telomeres *in vivo* (LaBranche *et al.* 1998). hnRNP A1 and UP1 also protect mammalian telomeres from degradation by endonucleases and exonucleases (Dallaire *et al.* 2000). I identified here hnRNP A1, A2/B1 and D as LANA1 interacting proteins (Chapter 5). In this chapter I sought to confirm the interaction of PABP1 and hnRNPA1 using several binding assays. Results in this chapter confirmed the large-scale *in vivo* data presented in Chapter 5.

hnRNP A2/B1 has been shown to bind to the TTAGGGn sequence of human telomeres (McKay and Cooke 1992). Via this interaction hnRNP A2/B1 offers *in vitro* protection against nuclease activity and increases telomerase function (Kamma *et al.* 2001). hnRNP D has also been shown to bind the G-rich telomere strand of telomeres (Eversole and Maizels 2000). Furthermore, it was shown that hnRNP D could recover the telomerase holoenzyme from human cell lysates (Eversole and Maizels 2000). These previously published data, along with my interaction data for LANA1 and hnRNPA1, led me to investigate a putative role for LANA1 in telomere biogenesis.

As hnRNP A1/UP1 is known to bind the active telomerase complex, I sought to test the ability of LANA1 to bind members of the telomerase complex. I demonstrated the ability of LANA1 to bind a functional telomerase complex *in vitro* in CB3 cells transfected with HA tagged UP1 (Fig 6.5). This suggests that LANA1 may form a complex with telomerase and that UP1 is sufficient for this interaction. However, I cannot discount that this interaction is aided by the LANA1/hnRNP D complex. Further to this I sought to show an interaction with a member of the telomerase complex by co-immunoprecipitation. hTERT, a member of the telomerase holoenzyme, co-immunoprecipitates with LANA1 from HeLa cells. It is currently unclear if the physical interaction of LANA1 with hnRNP A1/UP1 and hnRNP D enhances the recruitment of telomerase to telomeres or if the interaction with LANA1 enhances physical protection at the telomeres afforded by hnRNP A1/UP1, hnRNP D and hnRNP A2. As LANA1 binds both the telomere binding hnRNP A1, hnRNP A2/B1 and hnRNP D and telomerase-associated hnRNP A1 and hnRNP D, it is attractive to propose that LANA1 may act as a bridge to aid in recruitment of telomerase to the telomeres.

A major role for LANA1 in the life cycle of KSHV is the maintenance of the viral episome. It has previously been shown that LANA1 maintains viral episomes via binding to histone H1. The mammalian histone H1 family contains at least 7 subtypes. In this study two subtypes of histone H1 co-immunoprecipitated with LANA1; histone 1.4 and histone H1.5, H2B and H2A, respectively (see Chapter 5). In common with LANA1, EBNA1 of EBV is involved in the maintenance of the viral episome. It has recently been shown that the OriP/dyad symmetry element of EBV binds to several telomere related proteins (Deng *et al.* 2002). It is possible that the interactions with hnRNP A1, A2 and D may also have a role in the persistence of KSHV viral episomes.

The data presented suggest the formation of a LANA1 complex

including various hnRNPs, histone H1 and components of the spliceosome complex. Together with previously published data that LANA1 can upregulate the hTERT promoter (Knight *et al.* 2001), I propose that LANA1, by binding to hnRNP A1/UP1 and hnRNP D, aids in the recruitment of the telomerase complex. Both hnRNP A1 and D have been shown to rescue telomerase activity from cell lysate. This suggests a scenario whereby LANA1 aids in the immortilisation of primary infected cells (e.g. B cells) through the activation and recruitment of the telomerase complex to telomeres. Furthermore the physical protection offered by hnRNP A1/UP1, hnRNP D and hnRNP A2 to telomeres may be increased in the presence of LANA1. By binding to these proteins LANA1 may increase their relative half-life and increase their protective capability.

In conclusion, I have used large-scale immunoaffinity purification linked to mass spectrometry to identify several novel interaction partners of LANA1. Domain analysis has revealed a predominance of proteins possessing at least one RRM domain, and I propose that this represents a protein-protein interaction target for LANA1. I show that LANA1 may have a direct role in the biogenesis of telomeres by recruitment of the active telomerase complex.

Chapter 7 Discussion and Conclusion

The work described in this thesis was set out with distinct aims to be achieved. These included both technical problems to be overcome and scientific questions to be answered. The major aims of my project work are listed below:

7.1 Virus-mediated LANA1 delivery to primary cells
7.2 Transcriptional targets of LANA1 in primary cells
7.3 Purification of a native LANA1 complex
7.4 Identification of novel protein interaction partners of LANA1
7.5 Insight into novel cellular functions of LANA1

7.1 Virus mediated LANA1 delivery to primary cells

The use of primary cells for the study of single proteins is gaining popularity. This is due to the increasing availability of primary cells, progress in primary cell culture and the continuing development of gene delivery systems. I aimed to develop a tool for the study of LANA1 in primary endothelial cells. This was done to allow a sensitive study of LANA1 in primary cells that have not undergone many of the genetic alterations associated with cell lines. Using the pHR CMV based system I cloned and developed the expression of LANA1 in test cell lines, before studying primary endothelial cells. I have demonstrated the use of the lentiviral system for the delivery of LANA1 to primary cells, and characterised the expression of LANA1 in terms of cellular localization, DNA association and stability.

Lentiviruses carrying this gene successfully infected primary cells. These infected cells were positive for LANA1 by western blot and show characteristic patterns of expression. Nuclear localisation is seen during staining by IFA and LANA1 localises to chromatin during

mitosis, a known function of LANA1. I aimed to show an application of the system by linking it with gene expression microarray technology.

7.2 Transcriptional targets of LANA1 in primary cells

The results from the gene expression microarray experiments on LANA1 expressing endothelial cells were disappointing. Expression of LANA1 in the primary endothelial cells was high and predicted at over 90% infection. However, no significant phenotypic or transcriptomic changes were seen in primary cells infected with LANA1 lentivirus. Furthermore, the GEM technology, in particular the software used, provided problems. Despite these problems, these lack of genetic changes were not totally unexpected. Despite many reports of LANA1 effects on cellular promoters (An *et al.* 2002;Knight *et al.* 2001;Radkov *et al.* 2000), these effects are usually detected by *in vitro* reporter assays and have rarely been demonstrated at a physiological level i.e. by RT-PCR or Northern blot. It is likely that the main function of LANA1 is not via transcriptional regulation, but through protein-protein interactions or other protein dysregulations.

7.3 Purification of a native LANA1 complex

Many groups have used small-scale immunoprecipitation to demonstrate and identify protein-protein interaction partners of LANA1. These studies often involve yeast two-hybrid screens followed by interaction mapping with GST constructs. I undertook the first large scale proteomic analysis of LANA1, to identify a native LANA1 complex in primary effusion lymphoma cell lines. Through the development of techniques in both affinity chromatography and large-scale immunoprecipitation, I achieved purification of the complex, and demonstrated its separation into the individual protein components. The different methods for the purification of LANA1 provided overlapping results, increasing confidence in the data. To complement this and identify common protein interaction domains, I used a yeast two-hybrid screen.

7.4 Identification of novel protein interaction partners of LANA1

Proteins that co-purified with LANA1 by affinity chromatography and large-scale immunoprecipitation were identified, after separation, by mass spectrometry. Some of these proteins, including Histone H1 and p32 have previously been identified as LANA1 interaction partners i.e. p32 interaction with HVS ORF73 (Hall *et al.* 2002). The majority of the interaction partners identified were novel. These proteins include amongst them several important splicing proteins, as well as proteins involved in RNA metabolism and transport. Among these was hnRNP A1 which not only functions in 5' site selection, but has also been implicated in the biogenesis of mammalian telomeres.

The novel interactions identified by both the yeast two-hybrid and large scale IP/MS approaches have proved to be non-overlapping but complementary. Using both methods, LANA1 complex interacting proteins with common domains were identified. This implies that to achieve an overall view of the protein-protein interactions of a gene, several different approaches should be utilised. Through the use of these different approaches, new putative cellular functions for LANA1 have been identified. Proteins identified have roles in splicing and telomere biogenesis suggesting that LANA1 may affect one or both of these areas of the cellular life cycle.

7.5 Insight into novel cellular functions of LANA1

Taken together the two broad approaches used in this thesis have provided an interesting insight into the global effects of LANA1 on the cellular proteome. The work in this thesis suggests that the main roles of LANA1 are achieved by way of protein-protein interactions. I have confirmed a role for LANA1 in episome maintenance via an association with Histone H1 and provided insight into further roles for LANA1 in both RNA splicing and telomere biogenesis.

References

Abbott,A. (1999) The promise of proteomics. *Nature* **402**, 703-720.

Adams,V., Kempf,W., Schmid,M., Muller,B., Briner,J. and Burg,G. (1995) Absence of herpesvirus-like DNA sequences in skin cancers of non-immunosuppressed patients. *Lancet* **346**, 1715.

Afonia,E., Stauber,R. and Pavlakis,G.N. (1998) The human poly(A)-binding protein 1 shuttles between the nucleus and the cytoplasm. *J Biol Chem* **273**, 13015-13021.

Aiyar,A., Tyree,C. and Sugden,B. (1998) The plasmid replicon of EBV consists of multiple cis-acting elements that facilitate DNA synthesis by the cell and a viral maintenance element. *EMBO J* **17**, 6394-6403.

Ajuh,P., Kuster,B., Panov,K., Zomerdijk,J.C.B.M., Mann,M. and Lamond,A.I. (2000) Functional analysis of the human CDC5L complex and identification of its components by mass spectrometry. *EMBO J* **19**, 6569-6581.

Akahani,S., Nangia-Makker,P., Inohara,H., Kim,H.R.C. and Raz,A. (1997) Galectin-3: A novel antiapoptotic molecule with a functional BH1 (NWGR) domain of Bcl-2 family. *Cancer Res* **57**, 5272-5276.

Akkina,R.K., Walton,R.M., Chen,M.L., Li,Q.-X., Planelles,V. and Chen,I.S.Y. (1996) High-efficiency gene transfer into CD34+ cells with a human immunodeficiency virus type 1-based retroviral vector pseudotyped with vesicular stomatitis virus envelope glycoprotein G. *J Virol* **70**, 2581-2585.

Alkan,S., Karcher,D.S., Ortiz,A., Khalil,S., Akhtar,M. and Ali,M.A. (1997) Human herpesvirus-8/Kaposi's sarcoma-associated herpesvirus in organ transplant patients with immunosuppression. *Br J Haematol* **96**, 412-4.

Ambroziak,J.A., Blackbourn,D.J., Herndier,B.G., Glogau,R.G., Gullett,J.H., McDonald,A.R., Lennette,E.T. and Levy,J.A. (1995) Herpes-like sequences in HIV-infected and uninfected Kaposi's sarcoma patients. *Science* **268**, 582-583.

An,J., Lichtenstein,A.K., Brent,G. and Rettig,M.B. (2002) The Kaposi sarcoma-associated herpesvirus (KSHV) induces cellular interleukin 6 expression: role of the KSHV latency-associated nuclear antigen and the AP1 response element. *Blood* **99**, 649-654.

Ansari,M.Q., Dawson,D.B., Nador,R., Rutherford,C., Schneider,N.R., Latimer,M.J., Picker,L., Knowles,D.M. and McKenna,R.W. (1996) Primary body cavity-based AIDS-related lymphomas. *Am J of Clin Path* **105**, 221-

229.

Arao,Y., Kuriyama,R., Kayama,F. and Kato,S. (2000) *Arch Biochem Biophys* **380**, 228-236.

Arvanitakis,L., GerasRaaka,E., Varma,A., Gershengorn,M.C. and Cesarman,E. (1997) Human herpesvirus KSHV encodes a constitutively active G-protein- coupled receptor linked to cell proliferation. *Nature* **385**, 347-349.

Ballestas,M.E., Chatis,P.A. and Kaye,K.M. (1999) Efficient persistence of extrachromosomal KSHV DNA mediated by latency-associated nuclear antigen. *Science* **284**, 641-644.

Barillari,G., Buonaguro,L., Fiorelli,V., Hoffman,J., Michaels,F., Gallo,R.C. and Ensoli,B. (1992) Effects of cytokines from activated immune cells on vascular cell growth and HIV-1 gene expression. Implications for AIDS-Kaposi's sarcoma pathogenesis. *J Immunol* **149**, 3727-34.

Barozzi,P., Luppi,M., Masini,L., Marasca,R., Savarino,M., Morselli,M., Ferrari,M.G., Bevini,M., Bonacorsi,G. and Torelli,G. (1996) Lymphotropic herpesvirus (EBV, HHV-6, HHV-8) DNA sequences in HIV negative Castleman's disease. *J Clin Pathol Mol Pathol* **49**, M232-M235.

Ben-David,Y., Bani,M.R., Chabot,B., De Koven,A. and Bernstein,A. (1992) Retroviral insertions downstream of the heterogeneous nuclear ribonucleoprotein A1 gene in erythroleukaemia cells:evidence that A1 is not essential for cell growth. *Mol Cell Biol* **12**, 4449-4455.

Benvenuti,S., Cramer,R., Bruce,J., Waterfield,M.D. and Jat,P.S. (2002a) Identification of novel candidates for replicative senescence by functional proteomics. *Oncogene* **21**, 7609.

Benvenuti,S., Cramer,R., Quinn,C.C., Bruce,J., Zvelebil,M., Corless,S., Bond,J., Yang,A., Hockfield,S., Burlingame,A.L., Waterfield,M.D. and Jat,P.S. (2002b) Differential proteome analysis of replicative senescence in rat embryo fibroblasts. *Mol. Cell. Proteomics* **1**, 280-292.

Beral, V. (1991) Epidemiology of Kaposi's sarcoma. In *Cancer, HIV and AIDS* ed. Beral,V., Jaffe,H.W. and Weiss,R.A. pp. 5-22. New York: Cold Spring Harbor Laboratory Press.

Beral,V., Peterman,T.A., Berkelman,R.L. and Jaffe,H.W. (1990) Kaposi's sarcoma among persons with AIDS: a sexually transmitted infection? *Lancet* **335**, 123-128.

Blauvelt,A., Sei,S., Cook,P.M., Schulz,T.F. and Jeang,K.-T. (1997) Human herpesvirus-8 infection occurs following adolescence in the United States. *J Infec Dis* **176**, 771-774.

Boshoff, C. (1999) Kaposi's sarcoma-associated herpesvirus. In *Cancer Surveys: Infections and Human Cancer* ed. Newton,R., Beral,V. and Weiss,R.A. pp. 157-190. Cold Spring Harbor Press.

Boshoff,C., Endo,Y., Collins,P.D., Takeuchi,Y., Reeves,J.D., Schweickart,V.L., Saini,M., Sasaki,T., Williams,T.J., Gray,P.W., Moore,P.S., Chang,Y. and Weiss,R.A. (1997) Angiogenic and HIV inhibitory functions of KSHV-encoded chemokines. *Science* **278**, 290-293.

Boshoff,C., Gao,S.-J., Healy,L.E., S.,M., Thomas,A.J., Coignet,L., Warnke,R.A., Strauchen,J.A., Matutes,E., Kamel,O.W., Moore,P.S., Weiss,R.A. and Chang,Y. (1998) Establishment of a KSHV positive cell line (BCP-1) from peripheral blood and characterizing its growth in vivo. *Blood* **91**, 1671-1679.

Boshoff,C., Schulz,T.F., Kennedy,M.M., Graham,A.K., Fisher,C., Thomas,A., McGee,J.O., Weiss,R.A. and O'Leary,J.J. (1995a) Kaposi's sarcoma-associated herpesvirus infects endothelial and spindle cells. *Nature Medicine* **1**, 1274-8.

Boshoff, C. and Weiss, R. A. (1998) Kaposi's sarcoma-associated herpesvirus. In *Advances in Cancer Research* ed. Vande Woude,G. and Klein,G. pp. 57-86. San Diego: Academic Press.

Boshoff,C., Whitby,D., Hatziioannou,T., Fisher,C., van der Walt,J., Hatzakis,A., Weiss,R. and Schulz,T. (1995b) Kaposi's-sarcoma-associated herpesvirus in HIV-negative Kaposi's sarcoma. *Lancet* **345**, 1043-4.

Brooks,A.R., Lelkes,P.I. and Rubanyi,G.M. (2002) Gene expression profiling of human aortic endothelial cells exposed to disturbed flow and steady laminar flow. *Physiol Genomics* **9**, 27-41.

Bryant,H.E., Matthews,D.A., Wadd,S., Scott,J.E., Kean,J., Graham,S., Russell,W.C. and Clements,J.B. (2000) Interaction between herpes simplex virus type 1 IE63 protein and cellular protein p32. *J Virol* **74**, 11322-11328.

Bryant,H., Wadd,S., Lamond,A., Silverstein,S. and Clements,J. (2001) Herpes simplex virus IE63 (ICP27) protein interacts with spliceosome-associated protein 145 and inhibits splicing prior to the first catalytic step. *J Virol* **75**, 4376-85.

Burysek,L., Yeow,W.S. and Pitha,P.M. (1999) Unique properties of a second human herpesvirus 8-encoded interferon regulatory factor (vIRF-2). *J Hum Virol* **2**, 19-32.

Carroll,M. and Moss,B. (1997) Host range and cytopathogenicity of the highly attenuated MVA strain of vaccinia virus: propagation and generation of recombinant viruses in non-human mammalian cell line. *Virology* **238**, 198-211.

Carroll,R., Lin,J.-T., Dacquel,E.J., Mosca,J.D., Burke,D.S. and St Louis,D.C. (1994) A human immunodeficiency virus type 1(HIV-1)-based retroviral vector system utilizing stable HIV-1 packaging cell lines. *J Virol* **68**, 6047-6051.

Case,S.S., Price,M.A., Jordan,C.T., Yu,X.J., Wang,L., Bauer,G., Haas,D.L., Xu,D., Stripecke,R., Naldini,L., Kohn,D.B. and Crooks,G.M. (1999) Stable transduction of quiescent CD34+CD38- human hematopoietic cells by HIV-1 based lentivirus systems. *Proc Natl Acad Sci* **96**, 2988-2993.

Castleman,B., Iverson,L. and Menendez,V.P. (1956) Localized mediastinal lymph-node hyperplasia resembling thymoma. *Cancer* **9**, 822-830.

Cathomas,G., McGandy,C.E., Terracciano,L.M., Itin,P.H., De Rosa,G. and Gudat,F. (1996) Detection of herpesvirus-like DNA by nested PCR on archival skin biopsy specimens of various forms of Kaposi sarcoma. *Journal of Clinical Pathology* **49**, 631-633.

Cattani,P., Capuano,M., Cerimele,F., La Parola,I.L., Santangelo,R., Masini,C., Cerimele,D. and Fadda,G. (1999) Human herpesvirus 8 seroprevalence and evaluation of nonsexual transmission routes by detection of DNA in clinical specimens fom human immunodeficiency virus-seronegative patients from central and southern Italy, with and without Kaposi's sarcoma. *J Clin Microbiol* **37**, 1150-1153.

Centers for Disease Control (1981) Kaposi's sarcoma and pneumocystis pneumonia among homosexual men-New York City and California. *MMWR* **30**, 305.

Cesarman,E., Chang,Y., Moore,P.S., Said,J.W. and Knowles,D.M. (1995) Kaposi's sarcoma-associated herpesvirus-like DNA sequences in AIDS-related body-cavity-based lymphomas. *N Engl J Med* **332**, 1186-91.

Cesarman,E., Nador,R.G., Aozasa,K., Delsol,G., Said,J.W. and Knowles,D.M. (1996a) Kaposi's sarcoma-associated herpesvirus in non-AIDS-related lymphomas occuring in body cavities. *Am J Pathol* **149**, 53-57.

Cesarman,E., Nador,R.G., Bai,F., Bohenzky,R.A., Russo,J.J., Moore,P.S., Chang,Y. and Knowles,D.M. (1996b) Kaposi's sarcoma-associated herpesvirus contains G protein-coupled receptor and cyclin D homologs which are expressed in Kaposi's sarcoma and malignant lymphoma. *J Virol* **70**, 8218-23.

Challand, R. and Young, R. J. (1998) *Antiviral chemotherapy.* Oxford University Press.

Chambers,J., Angulo,A., Amartunga,D., Guo,H., Jiang,Y., Wan,J.S., Bittner,A., Frueh,K., Jackson,M.R., Peterson,P.A., Erlander,M.G. and Ghazal,P. (1999) DNA microarrays of the complex human cytomegalovirus genome: profiling kinetic class with drug sensitivity of viral gene expression.

J Virol **73**, 5757-5766.

Chang,Y., Cesarman,E., Pessin,M.S., Lee,F., Culpepper,J., Knowles,D.M. and Moore,P.S. (1994) Identification of herpesvirus-like DNA sequences in AIDS-associated Kaposi's sarcoma. *Science* **266**, 1865-1869.

Chang,Y., Moore,P.S., Talbot,S.J., Boshoff,C.H., Zarkowska,T., Godden,K., Paterson,H., Weiss,R.A. and Mittnacht,S. (1996) Cyclin encoded by KS herpesvirus. *Nature* **382**, 410.

Cheng,E.H.Y., Nicholas,J., Bellows,D.S., Hayward,G.S., Guo,H.G., Reitz,M.S. and Hardwick,J.M. (1997) A Bcl-2 homolog encoded by Kaposi sarcoma-associated virus, human herpesvirus 8, inhibits apoptosis but does not heterodimerize with Bax or Bak. *Proc Natl Acad Sci USA* **94**, 690-694.

Coombes,B.K. and Mahony,J.B. (2001) cDNA array analysis of altered gene expression in human endothelial cells in response to Chlamydia pneumoniae infection. *Infect Immun* **69**, 1420-7.

Corbeau,P., Kraus,G. and Wong-Staal,F. (1996) Efficient gene transfer by a human immunodeficiency virus type 1 (HIV-1)-derived vector utilizing a stable HIV packaging cell line. *Proc Natl Acad Sci* **93**, 14070-14075.

Corbellino,M., Bestetti,G., Galli,M. and Parravicini,C. (1996) Absence of HHV-8 in prostate and semen. *N Engl J Med* **335**, 1237.

Cotter,M. and Robertson,E. (1999) The latency-associated nuclear antigen tethers the Kaposi's sarcoma-associated herpsvirus to host chromosomes in body cavoty-based lymphoma cells. *Virology* 254-265.

Dallaire,F., Dupuis,S., Fiset,S. and Chabot,B. (2000) Heterogeneous Nuclear Ribonucleoprotein A1 and UP1 Protect Mammalian Telomeric Repeats and Modulate Telomere Replication in Vitro. *J Biol Chem* **275**, 14509-14516.

Davidivici,B., Karakis,I., Bourboulea,D., Ariad,S., Sarov,B. and Boshoff,C. (1999) The seroepidemiology of HHV-8 among Israeli Jews. *submitted.*

Deng,Z., Lezina,L., Chen,C., Shtivelband,S., So,W. and Lieberman,P. (2002) Telomeric proteins regulate episomal maintenance of Epstein-Barr Virus origin of plasmid replication. *Molecular Cell* **9**, 493-503.

Denis,G.V., Vaziri,C., Guo,N. and Faller,D.V. (2000) RING3 kinase transactivates promoters of cell cycle regulatory genes through E2F. *Cell Growth Differ* **11**, 417-424.

Dreyfuss,G., Kim,V.N. and Kataoka,N. (2002) Messenger-RNA-binding proteins and the messages they carry. *Nature Reviews (Molecular Cell Biology)* **3**, 195.

Dupin,N., Diss,T.L., Kellam,P., Tulliez,M., Du,M.Q., Sicard,D., Weiss,R.A., Isaacson,P.G. and Boshoff,C. (2000) HHV-8 is associated with a

plasmablastic variant of Castleman disease that is linked to HHV-8-positive plasmablastic lymphoma. *Blood* **95**, 1406-1412.

Dupin,N., Fisher,C., Kellam,P., Ariad,S., Tulliez,M., Franck,N., Van Marck,E., Salmon,D., Gorin,I., Escande,J.-P., Weiss,R.A., Alitalo,K. and Boshoff,C. (1999) Distribution of HHV-8 positive cells in Kaposi's sarcoma, multicentric Castleman's disease, and primary effusion lymphoma. *Proc Natl Acad Sci USA* **96**, 4546-4551.

Dupin,N., Gorin,I., Deleuze,J., Agut,H., Huraux,J.M. and Escande,J.P. (1995a) Herpes-like DNA sequences, AIDS-related tumors, and Castleman's disease. *N Engl J Med* **333**, 798-9.

Dupin,N., Grandadam,M. and Calvez,V. (1995b) Herpes-like DNA sequences in patients with Mediterranean Kaposi's sarcoma. *Lancet* **345**, 761-762.

Elliot,G. and O'Hare,P. (1999) Live-cell analysis of Green Fluorescent Protein-Tagged Herpes Simplex Virus Infection. *J Virol* **73**, 4110-4119.

Ensoli,B., Buonaguro,L., Barillari,G., Fiorelli,V., Gendelman,R., Morgan,R.A., Wingfield,P. and Gallo,R.C. (1993) Release, uptake, and effects of extracellular human immunodeficiency virus type 1 Tat protein on cell growth and viral transactivation. *J Virol* **67**, 277-87.

Ensoli,B., Nakamura,S., Salahuddin,S.Z., Biberfeld,P., Larsson,L., Beaver,B., Wong,S.F. and Gallo,R.C. (1989) AIDS-Kaposi's sarcoma-derived cells express cytokines with autocrine and paracrine growth effects. *Science* **243**, 223-6.

Eversole,A. and Maizels,N. (2000) In vitro properties of the conserved mammalian protein hnRNP D suggest a role in telomere maintenance. *Mol and Cell Biol* **20**, 5425-5432.

Fackelmayer,F., Dahm,K., Renz,A., Ramsperger,U. and Richter,A. (1994) Nucleic-acid-binding properties of hnRNP-U/SAF-A, a nuclear-matrix protein which binds DNA and RNA in vivo and in vitro. *European Journal of Biochemistry* **211**, 749-757.

Federico,M. (1990) Lentiviruses as gene delivery vectors. *Current Opinion in Biotechnology* **10**, 448-453.

Field,N., Low,W., Daniels,M., Howell,S., Daviet,L., Boshoff,C. and Collins,M. (2003) KSHV vFLIP binds to IKK-(gamma) to activate IKK. *J Cell Sci* **116**, 3721-3728.

Ford,L., Wright,W. and Shay,J. (2002) A model for heterogeneous nuclear ribonucleoproteins in telomere and telomerase regulation. *Oncogene* **21**, 580-583.

Fouchier,R.A., Meyer,B.E., Simon,J.H., Fischer,U. and Malim,M.H. (1997) HIV-1 infection of non-dividing cells: evidence that the amino-terminal basic region of the viral matrix protein is importatn for Gag processing but not for post-entry import. *EMBO J* **16**, 4531-4539.

Franceschi,S. and Geddes,M. (1995) Epidemiology of classic Kaposi's sarcoma, with special reference to Mediterranean population. *Tumori* **81**, 308-314.

Friborg,J.J., Kong,W., Hottiger,M.O. and Nabel,G.J. (1999) p53 inhibition by the LANA protein of KSHV protects against cell death. *Nature* **402**, 889-894.

Fujimuro,M. and Hayward,S.D. (2003) The latency-associated nuclear antigen of Kaposi's sarcoma-associated herpesvirus manipulates the activity of glycogen synthase kinase-3 beta. *J Virol* **77**, 8019-8030.

Fujimuro,M., Wu,F.Y., ApRhys,C., Kajumbula,H., Young,D.B., Hayward,G.S. and Hayward,S.D. (2003) A novel viral mechanism for dysregulation of beta-catenin in Kaposi's sarcoma-associated herpesvirus latency. *Nat Med* **9**, 300-306.

Gao,S.J., Kingsley,L., Hoover,D.R., Spira,T.J., Rinaldo,C.R., Saah,A., Phair,J., Detels,R., Parry,P., Chang,Y. and Moore,P.S. (1996a) Seroconversion to antibodies against Kaposi's sarcoma-associated herpesvirus-related latent nuclear antigens before the development of Kaposi's sarcoma. *New Engl J Med* **335**, 233-241.

Gao,S.J., Kingsley,L., Li,M., Zheng,W., Parravicini,C., Ziegler,J., Newton,R., Rinaldo,C.R., Saah,A., Phair,J., Detels,R., Chang,Y. and Moore,P.S. (1996b) KSHV antibodies among Americans, Italians and Ugandans with and without Kaposi's sarcoma. *Nature Medicine* **2**, 925-8.

Gao,S.-J., Boshoff,C., Jayachandra,S., Weiss,R.A., Chang,Y. and Moore,P.S. (1997) KSHV ORF K9 (vIRF) is an oncogene which inhibits the interferon signalling pathway. *Oncogene* **15**, 1979-1985.

Gharbi,S., Gaffney,P., Yang,A., Zvelebil,M.J., Cramer,R., Waterfield,M.D. and Timms,J.F. (2002) Evaluation of two-dimensional differential gel electrophoresis for proteomic expression analysis of a model breast cancer cell system. *Mol. Cell. Proteomics* **1**, 91-98.

Glenn,M., Rainbow,L., Aurade,F., Davidson,A. and Schulz,T. (1999) Identification of a spliced gene from Kaposi's sarcoma-associated herpesvirus encoding a protein with similarities to latent membrane proteins 1 and 2A of Epstein-Barr virus. *J Virol* **73**, 6953-6963.

Gobom,J., Schuerenberg,M., Mueller,M., Theiss,D., Lehrach,H. and Nordhoff,E. (2001) alpha-cyano-4-hydroxycinnamic acid affinity sample preparation. A protocol for MALDI-MS peptide analysis in proteomics. *Anal. Chem.* **73**, 434-438.

Godden-Kent,D., Talbot,S.J., Boshoff,C., Chang,Y., Moore,P., Weiss,R.A. and Mittnacht,S. (1997) The cyclin encoded by Kaposi's sarcoma-associated herpesvirus (KSHV) stimulates cdk6 to phosphorylate the retinoblastoma protein and Histone H1. *J Virol* **71**, 4193-4198.

Goldman,M.J., Lee,P.S., Yang,J.S. and Wilson,J.M. (1997) Lentiviral vectors for gene therapy of cystic fibrosis. *Hum. Gene Ther.* **8**, 2261-2268.

Gottschalk,A., Neubauer,G., Banroques,J., Mann,M., Luhrmann,R. and Fabrizio,P. (1999) Identification by mass spectrometry and functional analysis of novel proteins of yeast [U4/U6.U5] tri-snRNP. *EMBO J* **18**, 4535-4548.

Greensill,J., Sheldon,J.A. and Renwick,J.A. (2000) Two distinct gamma-2 herpesviruses in African green monkeys: a second gamma-2 herpesvirus lineage among Old World primates? *J Virol* **74**, 1572-1577.

Groves,A.K., Cotter,M.A., Subramanian,C. and Robertson,E.S. (2001) The latency-associated nuclear antigen encoded by kaposi's sarcoma-associated herpesvirus activates two major essential Epstein-Barr virus latent promoters. *J Virol* **75**, 9446-9457.

Grundhoff,A. and Ganem,D. (2003) The latency-associated nuclear antigen of Kaposi's sarcoma-associated herpesvirus permits replication of terminal repeat-containing plasmids. *J Virol* **77**, 2779-2783.

Gryglewski,R.J., Uracz,W., Chlopicki,S. and Marcinkiewicz,E. (2002) Bradykinin as a major endogenous regulator of endothelial function. *Pediatr Pathol Mol Med* **21**, 279-290.

Gygi,S.P., Han,D.K.M., Gingras,A.C., Sonenberg,N. and Aebersold,R. (1999) Protein analysis by mass spectrometry and sequence database searching: tools for cancer research in the post-genomic era. *Electrophoresis* **20**, 310-319.

Hagemeier,C., Caswell,R., Hayhurst,G., Sinclair,J. and Kouzarides,T. (1994) Functional interaction between the HCMV IE2 transactivator and the retinoblastoma protein. *EMBO J* **13**, 2897-2903.

Hahn,W. and Weinberg,R. (2002) Modelling the molcular circuitry of cancer. *Nature Cancer Reviews* **2**, 331-341.

Hall,K.T., Giles,M.S., Calderwood,M.A., Goodwin,D.J., Matthews,D.A. and Whitehouse,A. (2002) The Herpesvirus Saimiri Open Reading Frame 73 Gene Product Interacts with the Cellular Protein p32. *J Virol* **76**, 11612-11622.

Harrington,W., Jr., Sieczkowski,L., Sosa,C., Chan a Sue,S., Cai,J.P., Cabral,L. and Wood,C. (1997) Activation of HHV-8 by HIV-1 tat [letter]. *Lancet* **349**, 774-5.

Hayward, G. S. (1999) KSHV strains: the origins and global spread of the virus. In *Seminars in Cancer Biology: Kaposi's sarcoma-associated herpesvirus* ed. Weiss,R.A. and Boshoff,C. pp. 187-199. London: Academic Press.

Houry,W.A., Frishman,D., Eckerskorn,C., Lottspeich,F. and Hartl,F.U. (1999) Identification of in vivo substrates of the chaperonin GroEL. *Nature* **402**, 147-154.

Irmler,M., Thome,M., Hahne,M., Schneider,P., Hofman,K., Steiner,V., Bodmer,J.L., Schroter,M., Burns,K., Mattmann,C., Rimoldi,D., French,L.E. and Tschopp,J. (1997) Inhibition of death receptor signals by cellular FLIP. *Nature* **388**, 190-195.

Izaurralde,E., Kas,E. and Laemmli,UK. (1989) Highly preferential nucleation of histone H1 assembly on scaffold-associated regions. *J Mol Biol* **210**, 573-585.

Jackson,P.E., Scholl,P.F. and Groopman,J.D. (2000) Mass spectrometry for genotyping: an emerging tool for molecular medicine. *Mol Med Today* **6**, 271-276.

Jaffe,E.S. (1996) Primary body cavity-based AIDS-related lymphomas. *Am J Pathol* **105**, 141-143.

Jakobsson,P.J., Thoren,S., Morgenstern,R. and Samuelsson,B. (1999) Identification of human prostaglandin E synthase: a microsomal, glutathione-dependent, inducible enzyme, constituting a potential novel drug target. *Proc Natl Acad Sci* **96**, 7220-7225.

Jenner,R.G., Alba,M.M., Boshoff,C. and Kellam,P. (2001) Kaposi's sarcoma-associated herpesvirus latent and lytic gene expression as revealed by DNA arrays. *Journal of Virology* **75**, 891-902.

Jones,K.D., Aoki,Y., Chang,Y., Moore,P.S., Yarchoan,R. and Tosato,G. (1999) Involvement of interleukin-10 (IL-10) and viral IL-6 in the spontaneous growth of Kaposi's sarcoma-associated herpesvirus infected primary effusion lymphoma cells. *Blood* **94**, 2871-2879.

Kafri,T., Blomer,U., Peterson,D.A., Gage,F.H. and Verma,I.M. (1997) Sustained expression of genes delivered directly into liver and muscle by lentiviral vectors. *Nature Genetics* **17**, 314-317.

Kamma,H., Fujimoto,M., Fujiwara,M., Matsui,M., Horiguchi,H., Hamasaki,M. and Satoh,H. (2001) Interaction of hnRNP A2/B1 isoforms with telomeric ssDNA and the in vitro function. *Biochem Biophis Res Commun* **280**, 625-630.

Kaposi,M. (1872) Idiopathisches multiples pigmentsarcom der haut. *Arch. Dermatol und Syphillis* **4**, 265-273.

Karcher,D.S., Dawkins,F. and Garrett,C.T. (1992) Body cavity-based non-Hodgkin's lymphoma (NHL) in HIV-infected patients: B-cell lymphoma with unusual clinical, immunophenotypic, and genotypic features. *Lab Invest* **92**, 80a.

Kedda,M.A., Margolius,L., Kew,M.C., Swanepoel,C. and Pearson,D. (1996) Kaposi's sarcoma-associated herpesvirus in Kaposi's sarcoma occurring in immunosuppressed renal transplant recipients. *Clin Transplant* **10**, 429-31.

Kedes,D.H., Operskalski,E., Busch,M., Kohn,R., Flood,J. and Ganem,D. (1996) The seroepidemiology of human herpesvirus 8 (Kaposi's sarcoma-associated herpesvirus): distribution of infection in KS risk groups and evidence for sexual transmission. *Nature Medicine* **2**, 918-24.

Kellam,P., Boshoff,C., Whitby,D., Matthews,S., Weiss,R.A. and Talbot,S.J. (1997) Identification of a major latent nuclear antigen (LNA-1) in the human herpesvirus 8 (HHV-8) genome. *J Hum Virol* **1**, 19-29.

Kellam,P., Bourboulia,D., Dupin,N., Talbot,S., Boshoff,C. and Weiss,R.A. (1999) Characterising monoclonal antibodies against KSHV latent nuclear antigen (LNA-1). *J Virol* **73**, 5149-5155.

Khan,J., Simon,R., Bittner,M., Chen,Y., Leighton,S.B., Pohida,T., Smith,P.D., Jiang,Y., Gooden,G.C., trent,J.M. and Meltzer,P.S. (1998) Gene expression profiling of alveolar rhabdomyosarcoma with cDNA microarrays. *Cancer Res* **58**, 5009-5013.

Kiledjian, M., Burd, C. G., Gorlach, M., Portman, D. S. and Dreyfuss, G. (1994) Structure and function of hnRNP proteins. In *RNA-protein interactions* ed. Nagai,K. and Mattaj,I.W. pp. 127-141. Oxford University Press.

Knight,J.S., Cotter,M.A. and Robertson,E.S. (2001) The latency-associated nuclear antigen of Kaposi's sarcoma-associated herpesvirus transactivates the telomerase reverse transcriptase promoter. *J Biol Chem* **276**, 22971-22978.

Knowles,D.M., Inghirami,G., Ubriaco,A. and Dalla-Favera,R. (1989) Molecular genetic analysis of three AIDS-associated neoplasms of uncertain lineage demonstrates their B-cell derivation and the possible pathogenetic role of the Epstein-Barr virus. *Blood* **73**, 792-799.

Koelle,D.M., Huang,M.-L., Chandran,B., Vieira,j., Piepkorn,M. and Corey,L. (1997) Frequent detection of Kaposi's sarcoma-associated herpesvirus (human herpesvirus-8) in saliva of human immunodeficiency virus-infected men: clinical and immunologic correlates. *J Infect Dis* **176**, 94-102.

Komanduri,K.V., Luce,J.A., McGrath,M.S., Herndier,B.G. and Ng,V.L. (1996) The natural history and molecular heterogeneity of HIV-associated primary malignant lymphomatous effusions. *J Acquir Immune Defic Syndr Hum Retrovirol* **13**, 215-26.

Krecic,A.M. and Swanton,M.S. (1999) hnRNP complexes: composition, structure and function. *Curr Opin Cell Biol* **11**, 363-371.

Krithivas,A., Young,DB., Liao,G., Greene,D. and Hayward,SD. (2000) Human herpesvirus 8 LANA interacts with proteins of the mSin3 corepressor complex and negatively regulates Epstein-Barr virus gene expression in dually infected PEL cells. *J Virol* **74**, 9637-45.

LaBranche,H., Dupuis,S., Ben-David,Y., Bani,M.R., Wellinger,R.J. and Chabot,B. (1998) Telomere elongation by hnRNPA1 and a derivative that interacts with telomeric repeats and telomerase. *Nature Genetics* **19**, 199-202.

Lacoste,V., Mauclere,P., Dubreuil,G., Lewis,J., Courbot,M.C.G. and Gessain,A. (2000) KSHV-like herpesviruses in chimps and gorillas. *Nature* **407**, 151-152.

Lanson Jr,N.A., Egeland,D.B., Royals,B.A. and Claycomb,W.C. (2000) The MRE11-NBS-RAD50 pathway is perturbed in SV40 large T antigen-immortalized AT-1, AT-2 and HL-1 cardiomyocytes. *Nucleic Acid Research* **28**, 2882-2892.

Lee,H., Guo,J., Li,M., Choi,J.-K., DeMaria,M., Rosenzweig,M. and Jung,J.U. (1998a) Identification of an immunoreceptor tyrosine-based activation motif of K1 transforming protein of Kaposi's sarcoma-associated herpesvirus. *Mol and Cell Biol* **18**, 5219-5228.

Lee,H., Veazey,R., Williams,K., Li,M., Guo,J., Neipel,F., Fleckenstein,B., Lackner,A., Desrosiers,R.C. and Jung,J.U. (1998b) Deregulation of cell growth by the K1 gene of Kaposi's sarcoma-associated herpesvirus. *Nature Medicine* **4**, 435-440.

Legrain,P., Jestin,J.L. and Schachter,V. (2000) From the analysis of protein complexes to proteome-wide linkage maps. *Curr Opin Biotechnol* **11**, 402-407.

Legrain,P. and Selig,L. (2000) Genome-wide protein interaction maps using two-hybrid systems. *FEBS letters* **480**, 32-36.

Legrain,P. and Strosberg,D. (2002) Protein interaction domain mapping for the selection of validated targets and lead compounds in the anti-infectious area. *Curr Pharm Des* **8**, 1189-1198.

Li,M., Lee,H., Yoon,D.W., Albrecht,J.C., Fleckenstein,B., Neipel,F. and Jung,J.U. (1997) Kaposi's sarcoma-associated herpesvirus encodes a functional cyclin. *J Virol* **71**, 1984-91.

Li,S., Ross,D.T., Kadin,M.E., Brown,P.O., Wasik,M.A. and Wasik,M.A. (2001) Comparative genome-scale analysis of gene expression profiles in T cell lymphoma cells during malignant progression using a complementary

DNA microarray. *Am J Pathol* **158**, 1231-1237.

Lim,C., Gwack,Y., Hwang,S., Kim,S. and Choe,J. (2001) The transcriptional activity of cAMP reponse element-binding protein-binding protein is modulated by the latency associated nuclear antigen of Kaposi's sarcoma-associated herpesvirus. *J Biol Chem* **276**, 31016-31022.

Lim,C., Lee,D., Seo,T., Choi,C. and Choe,J. (2003) Latency-associated nuclear antigen of Kaposi's sarcoma-associated herpesvirus functionally interacts with heterochromatin protein 1. *J Biol Chem* **278**, 7397-7405.

Lim,C., Sohn,H., Gwack,Y. and Choe,J. (2000) Latency-associated nuclear antigen of Kaposi's sarcoma-associated herpesvirus (human herprevirus-8) binds ATF4/CREB2 and inhibits its transcriptional activation activity. *J Gen Virol* **81**, 2645-2652.

Lin,J.C., Lin,S.C., Mar,E.C., Pellett,P.E., Stamey,F.R., Stewart,J.A. and Spira,T.J. (1995) Is Kaposi's-sarcoma-associated herpesvirus detectable in semen of HIV-infected homosexual men? *Lancet* **346**, 1601-2.

Liu,F.-T., Patterson,R.J. and Wang,J.L. (2002) Intracellular functions of galectins. *Biochimica et biophysica acta* **1572**, 263-273.

Lubyova,B. and Pitha,P.M. (2000) Characterization of a novel human herpesvirus 8-encoded protein, vIRF-3, that shows homology to viral and cellular interferon regulatory factors. *J Virol* **74**, 8194-8201.

Lundquist,A., Barre,B., Bienvenu,F., Hermann,J., Avril,S. and Coqueret,O. (2003) Kaposi sarcoma-associated viral cyclin K overrides cell growth inhibition mediated by oncostatin M through STAT3 inhibition. *Blood* **101**, 4070-4077.

Mann,M., Hendrickson,R.C. and Pandey,A. (2001) Analysis of proteins and proteomes by mass spectrometry. *Annu Rev Biochem* **70**, 437-73.

Masakado,M., Umeda,F., Yamauchi,T., Ishii,H., Ono,Y. and Nawata,H. (1994) Human fibroblast cells produce a factor that stimulates prostacyclin synthesis by vascular endothelial cells. *Thrombosis Research* **76**.

Mascarenhas,L., Stripecke,R., Case,S.S., Xu,D., Weinberg,K.I. and Kohn,D. (1998) Gene delivery to human B-precursor acute lymphoblastic leukaemia cells. *Blood* **92**, 3537-3545.

Mattsson,K., Kiss,C., Platt,G.M., Simpson,G.R., Kashuba,E., Klein,G., Schulz,T.F. and Szekely,L. (2002a) *J Gen Virol* **83**, 179-188.

Mattsson,K., Kiss,C., Platt,G.M., Simpson,G.R., Kashuba,E., Klein,G., Schulz,T.F. and Szekely,L. (2002b) *J Gen Virol* **83**, 179-188.

Mayeda,A., Munroe,S.H., Caceres,J.F. and Kramer,A.R. (1994) Function of

conserved domains of hnRNP A1 and other hnRNP A/B proteins. *EMBO J* **13**, 5483-5495.

McGeoch, D. J. and Davidson, A. J. (1999) The descent of human herpesvirus 8. In *Seminars in Cancer Biology: Kaposi's sarcoma-associated herpesvirus* ed. Boshoff,C. and Weiss,R. Academic Press.

McKay,S. and Cooke,H. (1992) hnRNP A2/B1 binds specifcally to single stranded vertebrate telomeric repeat TTAAGGGn. *Nucleic Acid Research* **20**, 6461-6464.

Minogue,S., Anderson,J.S., Waugh,M.G., dos Santos,M., Corless,S., Cramer,R. and Hsuan,J.J. (2001) Cloning of a human type II phosphatidylinositol 4-kinase reveals a novel lipid kinase family. *J Biol Chem* **276**, 16635-16640.

Monini,P., De Lellis,L. and Cassai,E. (1996) Absence of HHV-8 in prostate and semen (letter). *New England Journal of Medicine* **335**, 1239.

Moore,P.S., Boshoff,C., Weiss,R.A. and Chang,Y. (1996a) Molecular mimicry of human cytokine and cytokine response pathway genes by KSHV. *Science* **274**, 1739-1744.

Moore,P.S., Gao,S.J., Dominguez,G., Cesarman,E., Lungu,O., Knowles,D.M., Garber,R., Pellett,P.E., McGeoch,D.J. and Chang,Y. (1996b) Primary characterization of a herpesvirus agent associated with Kaposi's sarcoma. *J Virol* **70**, 549-58.

Mountain,A. (2000) Gene therapy: the first decade. *TIBTECH* **18**, 119-128.

Nador,R.G., Cesarman,E., Chadburn,A., Dawson,D.B., Ansari,M.Q., Said,J. and Knowles,D.M. (1996) Primary effusion lymphoma: a distinct clinicopathologic entity associated with the Kaposi's sarcoma-associated herpes virus. *Blood* **88**, 645-56.

Naldini,L., Blomer,U., Gallay,P., Ory,D., Mulligan,R., Gage,F., Verma,I. and Trono,D. (1996) In vivo delivery and stable transduction of nondividing cells by a lentiviral vector. *Science* **272**, 263-267.

Neipel,F., Albrecht,J.C. and Fleckenstein,B. (1998) Human herpesvirus 8 - the first human Rhadinovirus. *J Natl Can Inst* **23**, 73-77.

Nicholas,J., Jian-Chao,Z., Alcendor,D.J., Ciufo,D.M., Poole,L.J., Sarisky,R.T., Chiou,C.-J., Zhang,X., Wan,X., Guo,H.-G., Reirz,M.S. and Hayward,G.S. (1998) Novel organizational features, captured cellular genes, and strain variability within the genome of KSHV/HHV-8. *J Natl Can Inst* **23**, 79-88.

Nicholas,J., Ruvolo,V.R., Burns,W.H., Sandford,G., Wan,X., Ciufo,D., Hendrickson,S.B., Guo,H.G., Hayward,G.S. and Reitz,M.S. (1997) Kaposi's

sarcoma-associated human herpesvirus-8 encodes homologues of macrophage inflammatory protein-1 and interleukin-6. *Nature Medicine* **3**, 287-92.

Nickoloff,B.J. and Griffiths,C.E. (1989) Factor XIIIa-expressing dermal dendrocytes in AIDS-associated cutaneous Kaposi's sarcomas. *Science* **243**, 1736-7.

Otsuki,T., Kumar,S., Ensoli,B., Kingma,D.W., Yano,T., Stetler Stevenson,M., Jaffe,E.S. and Raffeld,M. (1996) Detection of HHV-8/KSHV DNA sequences in AIDS-associated extranodal lymphoid malignancies. *Leukemia* **10**, 1358-62.

Pan,H.Y., Zhang,Y.J., Wang,X.P., Deng,J.H., Zhou,F.C. and Gao,S.J. (2003) Identification of a novel cellular transcriptional repressor interacting with the latent nuclear antigen of Kaposi's sarcoma-associated herpesvirus. *J Virol* **77**, 9858-9868.

Pandey,A. and Mann,M. (2000) Proteomics to study genes and genomes. *Nature* **405**, 837-845.

Park,J.W., Voss,P.G., Grabski,S., Wang,J.L. and Patterson,R.J. (2001) Association of galectin-1 and galectin-3 with Gemin4 in complexes containing the SMN protein. *Nucl Acid Research* **29**, 3595-3602.

Parravicini,C., Corbellino,M., Paulli,M., Magrini,U., Lazzarino,M., Moore,P.S. and Chang,Y. (1998) Expression of a virus-derived cytokine, KSHV vIL-6, in HIV seronegative Castleman's disease. *Am J Pathol* **6**, 1517-1522.

Pauk,J., Huang,M.L., Brodie,S.J., Wald,A., Koelle,D.M., Schaker,T., Celum,C., Selke,S. and Corey,L. (2000) Mucosal shedding of human herpesvirus 8 in men. *New Engl J Med* **343**, 1369-1377.

Pellizzoni,L., Kataoka,N., Charroux,B. and Dreyfuss,G. (1998) A novel function for SMN, the spinal muscular atrophy disease gene product, in pre-mRNA splicing. *Cell* **95**, 615-624.

Peterson,B.A. and Frizzera,G. (1993) Multicentric Castleman's disease. *Semin Oncol* **20**, 636-647.

Pfeifer,A., Kessler,T., Silletti,S., Cheresh,D.A. and Verma,I.M. (2000) Suppression of angiogenesis by lentiviral delivery of PEX, a noncatalytic fragment of matrix metalloproteinase 2. *Proc Natl Acad Sci* **97**, 12227-12232.

Piolot,T., Tramier,M., Coppey,M., Nicolas,J.C. and Marechal,V. (2001) Close but distinct regions of human herpesvirus 8 latency-associated nuclear antigen 1 are responsible for nuclear targeting and binding to human mitotic chromosomes. *J Virol* **75**, 3948-3959.

Platt,G.M., Simpson,G.R., Mittnacht,S. and Schulz,T.F. (1999) Latent nuclear antigen of Kaposi's sarcoma-associated herpesvirus interacts with RING3, a homolog of the Drosophila female sterile homeotic (fsh) gene. *J Virol* **12**, 9789-9795.

Poole,L.J., Yu,Y., Kim,P.S., Zheng,Q.Z., Pevsner,J. and Hayward,G.S. (2002) Altered patterns of cellular gene expression in dermal microvascular endothelial cells infected with Kaposi's sarcoma-associated herpesvirus. *J Virol* **76**, 3395-420.

Prakash,O., Tang,Z.Y., Peng,X., Coleman,R., Gill,J., Farr,G. and Samaniego,F. (2002) Tumorigenesis and aberrant signaling in transgenic mice expressing the human herpesvirus-8 K1 gene. *J Natl Cancer Inst* **94**, 926-935.

Radkov,S.A., Kellam,P. and Boshoff,C. (2000) The latent nuclear antigen of Kaposi sarcoma-associated herpesvirus targets the retinoblastoma-E2F pathway and with the oncogene Hras transforms primary rat cells. *Nature Medicine* **10**, 1091-2.

Rain,J.C., Selig,L., De Reuse,H., Battaglia,V., Reverdy,C., Simon,S., Lenzen,G., Petel,F., Wojcik,J., Schachter,V., Chemama,Y., Labigne,A. and Legrain,P. (2001) The protein-protein interaction map of Helicobacter pylori. *Nature* **409**, 211-215.

Rainbow, L., Glenn, M. A., Davidson, A. J. and Schulz, T. F. Identification of a spliced KSHV/HHV-8 gene predicted to encode a latency associated membrane protein. 1998. Stockholm.
Ref Type: Conference Proceeding

Rainbow,L., Platt,G.M., Simpson,G.R., Sarid,R., Gao,S.J., Stoiber,H., Herrington,C.S., Moore,P.S. and Schulz,T.F. (1997) The 222- to 234-kilodalton latent nuclear protein (LNA) of Kaposi's sarcoma-associated herpesvirus (human herpesvirus 8) is encoded by orf73 and is a component of the latency-associated nuclear antigen. *J Virol* **8**, 5915-21.

Reiser,J., Harmison,G., Kluepfel-Stahl,S., Brady,R.O., Karlsson,S. and Schubert,M. (1996) Transduction of nondividing cells using pseudotypes defective high-titer HIV type 1 particles. *Proc Natl Acad Sci U S A* **93**, 15266-15271.

Renne,R., Barry,C., Dittmer,D., Compitello,N., Brown,P.O. and Ganem,D. (2001) Modulation of cellular and viral gene expression by the latency-associated nuclear antigen of kaposi's sarcoma-associated herpesvirus. *J Virol* **75**, 458-468.

Renz,A. and Fackelmayer,F. (1996) Purification and molecular cloning of the scaffold attachment factor B (SAF-B), a novel human nuclear protein that specifically binds to S/MAR-DNA. *Nucl Acid Research* **24**, 843-849.

Riva,S. (1986) Mammalian single-stranded DNA binding protein UP1 is derived from the hnRNP core protein A1. *EMBO J* **5**, 2267-2273.

Rose,T.M., Strand,K.B., Schultz,E.R., Schaefer,G., Rankin Gw,Jr., Thouless,M.E., Tsai,C.C. and Bosch,M.L. (1997) Identification of two homologs of the Kaposi's sarcoma-associated herpesvirus (human herpesvirus 8) in retroperitoneal fibromatosis of different macaque species. *J Virol* **71**, 4138-4144.

Rout,M.P., Aitchison,J.D., Suprapto,A., Hjertaas,K., Zhao,Y. and Chait,B.T. (2000) The yeast nuclear pore complex: composition, architecture and transport mechanism. *The Journal of Cell Biology* **148**, 635-651.

Ruegsegger,U., Beyer,K. and Keller,W. (1996) Purification and characterisation of human cleavage factor Im involved in the 3' end processing of messenger RNA precursors. *J Biol Chem* **271**, 6107-6113.

Ruegsegger,U., Blank,D. and Keller,W. (1998) Human pre-mRNA cleavage factor Im is related to spliceosomal SR proteins and can be reconstituted in vitro from recombinant subunits. *Molecular Cell* **1**, 243-253.

Russo,J.J., Bohenzky,R.A., Chien,M.C., Chen,J., Yan,M., Maddalena,D., Parry,J.P., Peruzzi,D., Edelman,I.S., Chang,Y. and Moore,P.S. (1996) Nucleotide sequence of the Kaposi sarcoma-associated herpesvirus (HHV8). *Proc Natl Acad Sci USA* **93**, 14862-14867.

Said,J.W., Tasaka,T., Takeuchi,S., Asou,H., de Vos,S., Cesarman,E., Knowles,D.M. and Koeffler,H.P. (1996) Primary effusion lymphoma in women: Report of two cases of Kaposi's sarcoma herpes virus-associated effusion-based lymphoma in human immunodeficiency virus-negative women. *Blood* **88**, 3124-3128.

Samaniego,F., Markham,P.D., Gallo,R.C. and Ensoli,B. (1995) Inflammatory cytokines induce AIDS-Kaposi's sarcoma-derived spindle cells to produce and release basic fibroblast growth factor and enhance Kaposi's sarcoma-like lesion formation in nude mice. *J Immunol* **154**, 3582-92.

Sarid,R., Flore,O., Bohenzky,R.A., Chang,Y. and Moore,P.S. (1998) Transcription mapping of the Kaposi's sarcoma-associated herpesvirus (human herpesvirus 8) genome in a body cavity-based lymphoma cell line (BC-1). *J Virol* **72**, 1005-1012.

Sarid, R., Olsen, S. J. and Moore, P. S. (1999) Kaposi's sarcoma-associated herpesvirus: epidemiology, virology and molecular biology. In *Adv Virus Research* pp. 139-232.

Sarid,R., Sato,T., Bohenzky,R.A., Russo,J.J. and Chang,Y. (1997) Kaposi's sarcoma-associated herpesvirus encodes a functional bcl-2 homologue. *Nature Medicine* **3**, 293-8.

Schwam,D.R., Luciano,R.L., Mahajan,S.S., Wong,L. and Wilson,A.C. (2000) Carboxy terminus of Human Herpesvirus 8 latency associated nuclear antigen mediates dimerisation, transcriptional repression, and targeting to nuclear bodies. *J Virol* **74**, 8532-8540.

Senkevich,T.G., Bugert,J.J., Sisler,J.R., Koonin,E.V., Darai,G. and Moss,B. (1996) Genome sequence of a human tumorigenic poxvirus: Prediction of specific host response-evasion genes. *Science* **273**, 813-816.

Sharp,T.V., Wang,H.W., Koumi,A., Hollyman,D., Endo,Y., Ye,H., Du,M.Q. and Boshoff,C. (2002) K15 protein of Kaposi's sarcoma-associated herpesvirus is latently expressed and binds to HAX-1, a protein with antiapoptotic function. *J Virol* **72**, 802-816.

Sitas,F., Bezwoda,W.R., Levin,V., Ruff,P., Kew,M.C., Hale,M.J., Carrara,H., Beral,V., Fleming,G., Odes,R. and Weaving,A. (1997) Association between human immunodeficiency virus type 1 infection and cancer in the black population of Johannesburg and Soweto, South Africa. *Br J Cancer* **75**, 1704-1707.

Sitas,F., Carrara,H., Beral,V., Newton,R., Reeves,G., Bull,D., Jentsh,U., Pacella-Norman,R., Bourboulia,D., Whitby,D., Boshoff,C. and Weiss,R. (1999) Antibodies against human herpesvirus-8 in black South African patients with cancer. *N Engl J Med* **340**, 1863-1871.

Smyth,E.M. and Fitzgerald,G.A. (2002) Human prostacyclin receptor. *Vitam Horm* **65**, 149-165.

Soulier,J., Grollet,L., Oksenhendler,E., Cacoub,P., Cazals Hatem,D., Babinet,P., d'Agay,M.F., Clauvel,J.P., Raphael,M. and Degos,L. (1995) Kaposi's sarcoma-associated herpesvirus-like DNA sequences in multicentric Castleman's disease. *Blood* **86**, 1276-80.

Speir,E., Modali,R., Huang,E.S., Leon,M.B., Shawl,F., Finkel,T. and Epstein,S.E. (1994) *Science* **265**, 391-394.

Staskus,K.A., Zhong,W., Gebhard,K., Herndier,B., Wang,H., Renne,R., Beneke,J., Pudney,J., Anderson,D.J., Ganem,D. and Haase,A.T. (1997) Kaposi's sarcoma-associated herpesvirus gene expression in endothelial (spindle) tumor cells. *J Virol* **71**, 715-719.

Strauchen,J.A., Hauser,A.D., Burstein,D.A., Jimenez,R., Moore,P.S. and Chang,Y. (1997) Body cavity-based malignant lymphoma containing Kaposi's sarcoma-associated herpesvirus in an HIV-negative man with previous Kaposi's sarcoma. *Ann Intern Med* **125**, 822-825.

Sturzl,M., Brandstetter,H. and Roth,W.K. (1992) Kaposi's sarcoma: A review of gene expression and ultrastructure of KS spindle cells in vivo. *AIDS Research and Human Retroviruses* **8**, 1753-1764.

Superti,F., Seganti,L., Ruggeri,F.M., Tinari,A., Donelli,G. and Orsi,N. (1987) Entry pathway of vesicular stomatitis virus into different host cells. *J Gen Virol* **68**, 387-99.

Swanton,C., Mann,D.J., Fleckenstein,B., Neipel,F., Peters,G. and Jones,N. (1997) Herpesviral cyclin/Cdk6 complexes evade inhibition by CDK inhibitor proteins. *Nature* **390**, 184-187.

Szekely,L., Kiss,C., Mattsson,K., Kashuba,E., Pokrovskaja,K., Juhasz,A., Holmvall,P. and Klein,G. (1999) Human herpesvirus-8-encoded LNA-1 accumulates in heterochromatin-associated nuclear bodies. *J Gen Virol* **80**, 2889-2900.

Talbot,S., Weiss,R.A., Kellam,P. and Boshoff,C. (1999) Transcriptional analysis of human herpesvirus-8 (HHV-8) open reading frames 71, 72, 73, K14 and 74 in a primary effusion lymphoma cell line. *Virology* **257**, 84-94.

Thomas,J.J., Bakhtiar,R. and Siuzdak,G. (2000) Mass spectrometry in viral proteomics. *Accounts of Chemical Research* **33**, 179-187.

Thome,M., Schneider,P., Hofmann,K., Fickenscher,H., Meini,E., Neipel,F., Mattmann,C., Burns,K., Bodmer,J.L., Schroter,M., Scaffidl,C., Krammer,P.H., Peter,M.E. and Tschopp,J. (1997) Viral FLICE-inhibitory proteins (FLIPs) prevent apoptosis induced by death receptors. *Nature* **386**, 517-521.

Timbury, M. C. (1997) *Notes on Medical Virology.* Churchill Livingstone.

Tomlinsen,C.C. and Damania,B. (2004) The K1 protein of Kaposi's sarcoma-associated herpesvirus activates the Akt signaling pathway. *J Virol* **78**, 1918-1927.

Totsugawa,T., Kobayashi,N., Okitsu,T., Noguchi,H., Watanabe,T., Matsumura,T., Maruyama,M., ujiwara,T., Sakaguchi,M. and Tanaka,N. (2002) Lentiviral transfer of the LacZ gene into human endothelial cells and human bone marrow mesenchymal stem cells. *Cell Transplant* **11**, 481-488.

Umeda,F., Ono,Y., Masakado,M., Seiguchi,N., Yamauchi,T., Hashimoto,T. and Nawata,H. (1996) Prostacyclin-stimulating factor, novel protein, and diabetic angiopathy. *Diabetes* **45**, 111-113.

Underhill,C., Qutob,M.S., Yee,S.P. and Torchia,J. (2000) A novel N-CoR complex contains components of the mammalian SW1/SNF complex and the corepressor KAP-1. *J Biol Chem* **275**, 40463-40470.

Urbich,C., Walter,D.H., Zeiher,A.M. and Dimmeler,S. (2000) Laminar shear stress upregulates integrin expression: role in endothelial cell adhesion and apoptosis. *Circulation Research* **87**, 683-9.

Uthman,A., Brna,C., Weninger,W. and Tschachler,E. (1996) No HHV8 in

non-Kaposi's sarcoma mucocutaneous lesions from immunodeficient HIV-positive patients. *Lancet* **347**, 1700-1.

Verma,I.M. and Somia,N. (1999) Gene therapy - promises, problems and prospects. *Nature* **389**, 239-242.

Walts,A.E., Shintaku,P. and Said,J.W. (1990) Diagnosis of malignant lymphoma in effusions from patients with AIDS by gene rearrangement. *Am J Clin Pathol* **194**, 170-175.

Wang,X., Appukuttan,B., Ott,S., Patel,R., Irvine,J., Song,J., Park,J.H., Smith,R. and Stout,J.T. (2000) Efficient and sustained transgene expression in human corneal cells mediated by a lentiviral vector. *Gene Ther* **7**, 196-200.

Wang,Y.F., Chen,S.C., Wu,F.Y. and Wu,C.W. (1997) The interaction between the human cytomegalovirus immediate-early gene 2 (IE2) and heterogeneous ribonucleoprotein A1. *Biochem Biophis Res Commun* **232**, 590-594.

Weighardt,F., Cobianchi,F., Cartegni,L., Chiodi,I., Villa,A., Riva,S. and Biamonti,G. (1999) A novel hnRNP protein (HAP/SAF-B) enters a subset of hnRNP complexes and relocates in nuclear granules in response to heat shock. *J Cell Sci* **112**, 1465-1476.

Whitby,D., Howard,M.R., Tenant Flowers,M., Brink,N.S., Copas,A., Boshoff,C., Hatzioannou,T., Suggett,F.E., Aldam,D.M., Denton,A.S., Miller,R.F., Weller,I.V.D., Weiss,R.A., Tedder,R.S. and Schulz,T.F. (1995) Detection of Kaposi sarcoma associated herpesvirus in peripheral blood of HIV-infected individuals and progression to Kaposi's sarcoma. *Lancet* **346**, 799-802.

Whitby,D., Luppi,M., Barozzi,P., Boshoff,C., Weiss,R.A. and Torelli,G. (1998) HHV-8 seroprevalence in blood donors and lymphoma patients from different regions of Italy. *J Natl Can Inst* **90**, 395-397.

White,S.M., Renda,M., Nam,N.-Y., Klimatcheva,E., Zhu,Y., Fisk,J., Halterman,M., Rimel,B.J., Federoff,H., Pandya,S., Rosenblatt,J.D. and Planelles,V. (1999) Lentivirus vectors using human and simian immunodeficiency virus elements. *J Virol* **73**, 2832-2840.

Winter,D., Podtelejnikov,A.V., Mann,M. and Li,R. (1997) The complex containing actin-related proteins Arp2 and Arp3 is required for the motility and integrity of yeast actin patches. *Current Biology* **7**, 519-529.

Xu,R.M., Jokhan,L., Cheng,X., Mayeda,A. and Krainer,A.R. (1997) Crystal structure of human UP1, the domain of hnRNP A1 that contains two RNA-recognition motifs. *Structure* **5**, 559-570.

Yamada,S. and Ohnishi,S. (1986) Vesicular stomatitis virus binds and fuses

with phospholipid domain in target cell membranes. *Biochemistry* **25**, 3703-8.

Yang,R.Y., Hsu,D.K. and Liu,F.T. (1996) Expression of galectin-3 modulates T-cell growth and apoptosis. *Proc Natl Acad Sci* **93**, 6737-6742.

Yang,T.Y., Chen,S.C., Leach,M.W., Manfra,D., Homey,B., Wiekowski,M., Sullivan,L., Jenh,C.H., Narula,S.K., Chensue,S.W. and Lira,S.A. (2000) Transgenic expression of the chemokine receptor encoded by human herpesvirus 8 induces an angioproliferative disease resembling Kaposi's sarcoma. *J. Exp. Med* **Feb 7**, 445-454.

Yates,J.L., Warren,N. and Sugden,B. (1985) Stable replication of plasmids derived from Epstein-Barr virus in various mammalian cells. *Nature* **313**, 812-815.

Yu,H., Rabson,A.B., Kaul,M., Ron,Y. and Dougherty,J.P. (1996) Inducible human immunodeficiency virus type 1 packaging cell lines. *J Virol* **70**, 4530-4537.

Zhou,Z., Licklider,L., Gygi,S. and Reed,R. (2002) Comprehensive proteomics analysis of the human splicesome. *Nature* **419**, 182-185.

Zietz,C., Bogner,J.R., Goebel,F.-D. and Lohrs,U. (1999) An unusual cluster of cases of Castleman's disease during highly active antiretroviral therapy for AIDS. *N Engl J Med* **340**, 1923-1924.

Zimring,J.C., Goodbourn,S. and Offerman,M.K. (1998) Human herpesvirus 8 encodes an interferon regulatory factor (IRF) homolog that represses IRF-1-mediated transcription. *J Virol* **72**, 701-707.

Appendix I

empty 1	e2	l1	l2	ratio	ttest	acc	title
13.30672	13.27797	18.41907	18.44686	1.386735	1.51E-05	AA164705	CDW52 antigen (CAMPATH-1 antigen)
15.20304	15.34875	21.65868	21.89598	1.425601	0.000458	AA873762	HZF-16
27.26385	27.54928	36.25798	36.54165	1.328142	0.0005	AA424344	Uroporphyrinogen decarboxylase
88.12307	87.61793	77.92646	77.76206	0.885898	0.000701	AA436440	Basigin
17.83748	17.79554	20.80198	20.95899	1.171974	0.000703	N68443	MAX protein
18.36169	18.43814	15.63076	15.77147	0.853326	0.000879	AA398400	Human mRNA for calponin, complete cds
13.79947	13.55885	18.82985	19.17822	1.389269	0.001577	AA045326	Human density enhanced phosphatase-1 mRNA, complete cds
20.66354	20.44225	25.65029	25.2486	1.238241	0.002186	AA479781	Radixin
9.592435	10.11996	15.16342	15.38861	1.549889	0.002788	AA464595	Human malignant melanoma metastasis-suppressor (KiSS-1) gene, mRNA, complete cds
15.4912	15.36009	22.22726	21.55005	1.418978	0.002836	W73474	Homo sapiens microsomal glutathione S-transferase 2 (MGST2) mRNA, complete cds
20.01637	20.15265	23.36158	23.02767	1.154851	0.003345	H22944	Human nicotinamide nucleotide transhydrogenase mRNA
21.05991	21.25085	23.64352	23.88126	1.123232	0.003403	R32450	H.sapiens mRNA for aminopeptidase
16.67458	16.07608	25.02258	24.2343	1.503997	0.003576	AA430615	Human (clone pA3) protein disulfide isomerase related protein (ERp72) mRNA, complete cds
16.03116	15.8201	18.79769	19.11125	1.190186	0.003871	H45668	Homo sapiens Kruppel-like zinc finger protein (EZF) mRNA, complete cds
14.67512	15.13913	19.1997	18.92034	1.278584	0.004225	R91950	Cytochrome b-5
15.20759	15.6199	19.85703	20.34545	1.304111	0.004616	AA441933	64 KD AUTOANTIGEN D1
18.07452	17.73585	20.22764	20.24353	1.130152	0.00525	AA700604	Sorbitol dehydrogenase
15.57746	15.16059	20.44917	19.88292	1.312123	0.005329	AA130714	Placental growth factor, vascular endothelial growth factor-related protein
22.66632	23.22876	28.95136	28.30956	1.247648	0.00559	H05820	Human MRL3 mRNA for ribosomal protein L3 homologue (MRL3 = mammalian ribosome L3)
30.53137	32.06693	47.62756	49.95596	1.558885	0.006296	AA190941	Homo sapiens Trio mRNA, complete cds
18.45828	18.96692	21.97852	22.17715	1.179838	0.006518	AA629542	Brush-1
55.66715	52.09753	30.64695	28.68337	0.550554	0.007001	AA457034	V-myb avian myeloblastosis viral oncogene homolog-like 2
65.01237	63.37514	54.36969	53.83341	0.842785	0.007207	-	-
15.97752	16.76128	21.43998	21.13728	1.300514	0.007214	W72473	PHOSPHATIDYLINOSITOL 3-KINASE CATALYTIC SUBUNIT, ALPHA ISOFORM
49.96148	52.62606	72.77754	70.52356	1.396867	0.007268	-	-

□π

69.49569	69.22483	45.95855	49.71757	0.689704	0.007579	AA482117	H.sapiens mRNA for ras-related GTP-binding protein
15.39213	15.60444	23.74598	22.3923	1.488496	0.00809	AA293778	HETEROGENEOUS NUCLEAR RIBONUCLEOPROTEIN L
20.12498	20.29628	25.81949	26.9412	1.305271	0.008351	AA156940	Homo sapiens TFAR19 mRNA, complete cds
57.52414	59.58008	69.07539	69.56082	1.18387	0.009488	-	-
12.44213	13.00347	15.68017	15.95108	1.243093	0.010001	AA418907	Cytochrome P450, subfamily I (aromatic compound-inducible), polypeptide 1
66.4003	67.10946	57.60919	55.66881	0.848462	0.010267	-	-
11.77128	11.55882	12.74224	12.8286	1.096045	0.010314	AA732983	Homo sapiens PIGCP1 pseudogene
14.5714	14.2199	17.01347	17.48804	1.198331	0.010528	H25510	Human PMS6 mRNA (yeast mismatch repair gene PMS1 homologue), partial cds (C-terminal region)
99.90622	96.25692	75.30943	71.54414	0.74863	0.01112	AA281057	Ribosomal protein S17
17.66237	17.35934	20.80651	20.23311	1.171834	0.011416	R70505	Human P2U nucleotide receptor mRNA, complete cds
59.7543	57.99488	77.25603	74.07996	1.28524	0.011485	-	-
121.6806	128.8426	169.9972	177.7004	1.387886	0.011514	AA482243	CYTOCHROME C OXIDASE POLYPEPTIDE VIA-LIVER PRECURSOR
16.79687	17.0432	23.18093	21.97387	1.334359	0.011648	T62865	Homo sapiens aflatoxin aldehyde reductase AFAR mRNA, complete cds
18.53819	19.81571	24.9366	24.83823	1.297777	0.012354	AA465386	Human Gu protein mRNA, partial cds
10.82521	12.156	18.87275	18.03996	1.606212	0.012461	T67004	Endothelin 3
38.58499	39.17729	35.52683	35.92338	0.918829	0.012513	AA488626	Human ubiquitin-homology domain protein PIC1 mRNA, complete cds
55.94726	54.9831	64.52419	62.89338	1.148627	0.012948	-	-
13.59496	13.53406	17.8711	19.00537	1.3593	0.01331	AA448711	AU RNA-binding protein/enoyl-Coenzyme A hydratase
36.75335	34.67892	26.58254	25.7672	0.732858	0.01337	T71209	Human abnormal beta-hexosaminidase alpha chain (HEXA) mRNA, partial cds
20.34348	21.13715	25.67194	24.95156	1.220413	0.013467	AA293453	Human homeobox protein (PHOX1) mRNA, 3' end
16.52724	17.57	23.03076	24.15742	1.383929	0.013475	AA683058	H.sapiens mRNA for BS69 protein
11.52672	12.67201	18.45761	17.65112	1.492175	0.013552	N26026	Homo sapiens survival of motor neuron protein interacting protein 1 (SIP1) mRNA, complete cds
25.782	26.54238	35.97141	34.02242	1.337691	0.01373	AA480906	Human protein kinase C-binding protein RACK7 mRNA, partial cds
53.69269	50.54551	28.97499	32.93946	0.593971	0.014004	AA598884	Homo sapiens (clone CC6) NADH-ubiquinone oxidoreductase subunit mRNA, 3' end cds
14.59747	15.48924	21.34266	22.77467	1.466339	0.014151	H72030	Homo sapiens nuclear domain 10 protein (ndp52) mRNA, complete cds
12.43127	12.1412	18.6627	17.30535	1.463754	0.014513	T99793	Human meningioma-expressed antigen 11 (MEA11) mRNA, partial cds
15.87071	15.85887	21.54811	23.17317	1.409451	0.015289	AA598578	Homo sapiens mRNA for A+U-rich element RNA binding factor, complete cds
25.36253	24.02741	32.94517	31.55737	1.305985	0.015853	AA453293	Phosphodiesterase 4B, cAMP-specific (dunce (Drosophila)-homolog phosphodiesterase E4)
50.23563	47.83924	63.488	66.83817	1.328844	0.015923	-	-
66.24687	65.40199	74.73863	77.21168	1.154209	0.01617	-	-
11.55567	12.79928	17.72252	18.64369	1.493175	0.016199	AA026918	Fumarate hydratase

53.92576	57.14814	69.88094	72.32212	1.280256	0.016451	H05140	Human mRNA for SMP-30 (senescence marker protein-30), complete cds
12.86548	14.62357	20.4356	20.83379	1.501303	0.016684	AA436372	Zinc finger protein 151 (pHZ-67)
28.49691	29.85522	34.42642	34.28532	1.177536	0.016937	AA099169	Phosphofructokinase, muscle
32.53625	32.15033	38.85101	37.37872	1.178447	0.016945	AA476438	H.sapiens mRNA for rat HREV107-like protein
24.69849	25.17236	28.71903	29.74994	1.172408	0.016971	W80637	Human mRNA for apolipoprotein E receptor 2, complete cds
90.45049	87.08226	102.1153	101.4187	1.146459	0.017052	AA284856	Human adult heart mRNA for neutral calponin, complete cds
14.24826	15.08713	21.44584	20.06228	1.414951	0.017213	H97488	Human N-ethylmaleimide-sensitive factor mRNA, partial cds
4688.674	4573.114	3113.995	3454.545	0.709209	0.017366	AA704492	Transducin-like enhancer of split 4, homolog of Drosophila E(sp1)
14.68872	15.14573	18.73253	19.81891	1.292179	0.017794	N98563	Human retinoic acid- and interferon-inducible 58K protein RI58 mRNA, complete cds
25.88621	25.13954	29.21631	30.09014	1.162285	0.018727	AA411324	H.sapiens IL-13Ra mRNA
18.17923	16.24179	24.74663	24.14883	1.420512	0.019063	H22856	Glutamic-oxaloacetic transaminase 1, soluble (aspartate aminotransferase 1)
21.76521	22.48985	26.39549	27.56171	1.219232	0.019445	N74285	Human Cdc5-related protein (PCDC5RP) mRNA, complete cds
19.3807	17.56778	26.94249	25.65107	1.423429	0.019647	R33642	Glutathione-S-transferase pi-1
23.73213	22.25659	35.72379	32.85917	1.4913	0.019739	AA598637	Human stimulator of TAR RNA binding (SRB) mRNA, complete cds
67.74911	66.11601	52.3737	55.68933	0.807253	0.019908	-	-
18.86224	18.22088	23.87179	25.52371	1.332021	0.020092	N32146	V-rel avian reticuloendotheliosis viral oncogene homolog
180.5052	171.141	137.5591	142.0633	0.795181	0.020187	AA082943	H.sapiens mRNA for cyclin G1
54.54853	51.04049	65.78516	64.88877	1.237571	0.020205	-	-
12.75173	13.12567	15.69013	16.5254	1.244929	0.020218	AA621155	Homo sapiens MutS homolog (MSH5) mRNA, complete cds
20.45996	19.71406	24.0624	25.14662	1.224897	0.020564	AA478043	Interferon regulatory factor 1
46.41784	46.84649	50.11507	49.31993	1.066163	0.020765	AA418689	DNA-DIRECTED RNA POLYMERASE II 14.4 KD POLYPEPTIDE
19.52725	17.67888	26.56574	28.4214	1.477906	0.021016	AA282936	Human putative M phase phosphoprotein 1 (MPP1) mRNA, partial cds
14.6239	14.67654	17.14706	18.00899	1.199847	0.021063	AA405989	Homo sapiens Fas-binding protein Daxx mRNA, complete cds
39.69598	37.63849	29.45587	30.89316	0.780364	0.021143	AA448207	Deoxycytidylate deaminase
12.8691	15.51423	24.24758	26.15563	1.775803	0.021242	AA476490	Homo sapiens thyroid receptor interactor (TRIP4) mRNA, 3' end of cds
26.89934	24.39725	34.0213	34.58425	1.337429	0.021256	AA056465	Human 54 kDa protein mRNA, complete cds
17.83125	18.53786	25.12595	23.45843	1.335869	0.021282	AA262504	Human EYA3 homolog (EYA3) mRNA, complete cds
14.79707	14.8974	18.33965	19.56612	1.276526	0.02173	AA054321	H.sapiens HCG I mRNA
28.9034	25.67394	40.84458	38.84707	1.46016	0.022106	AA490996	Human interferon-gamma induced protein (IFI 16) gene, complete cds
60.55528	64.00571	78.42178	82.85077	1.294728	0.022599	-	-
14.3999	13.11793	18.74286	19.85839	1.402773	0.022711	T65736	Human selenium-binding protein (hSBP) mRNA, complete cds

21.28581	19.38037	26.60932	27.34843	1.326846	0.022837	R59927	Human mRNA for cytochrome c oxidase subunit VIc
14.3109	14.79715	17.19406	18.01471	1.209589	0.023586	T72604	Human cytochrome c-1 gene, complete cds
41.16101	44.66186	22.9877	27.3213	0.586196	0.023735	AA026626	Chymotrypsin-like
69.79562	70.95867	45.92272	36.90624	0.588465	0.023758	AA461456	Collagen, type V, alpha
23.68785	23.7127	30.96185	28.99143	1.264822	0.023769	AA432143	Human melanocyte-specific gene 1 (msg1) mRNA, complete cds
24.36188	26.48693	36.13774	33.96506	1.378652	0.024021	AA448685	Deoxycytidine kinase
11.37659	12.43146	15.18768	15.36424	1.28326	0.024241	N30191	PROCHOLECYSTOKININ PRECURSOR
9.228586	10.56549	15.4967	17.0134	1.642415	0.02436	T66980	Egf-like module containing, mucin-like, hormone receptor-like sequence 1
53.52706	53.18936	60.28094	58.39839	1.1121	0.024621	AA136707	Homo sapiens lysyl hydroxylase isoform 2 (PLOD2) mRNA, complete cds
30.15636	29.47201	33.54459	34.7601	1.145507	0.024887	AA171463	Homo sapiens sorting nexin 2 (SNX2) mRNA, complete cds
62.5688	63.54845	66.07406	66.34295	1.049952	0.025032	-	-
32.0239	30.95701	48.85646	44.1262	1.476363	0.025142	AA431440	H.sapiens hnRNP-E2 mRNA
12.90496	13.73191	17.15693	18.35297	1.333111	0.02582	H20856	DNA repair helicase ERCC3
12.70051	12.6018	16.32587	17.76424	1.347312	0.025877	AA454570	Human clone lambda 5 semaphorin mRNA, complete cds
19.6614	17.69535	25.00189	26.11934	1.36846	0.025947	R91550	Human arginine-rich protein (ARP) gene, complete cds
11.64626	12.03606	13.78392	13.36779	1.146497	0.025963	AA233738	Transforming growth factor, beta 2
18.3875	20.0991	26.13914	28.07849	1.40874	0.025987	T98472	Casein kinase 2, alpha 1 polypeptide
54.51549	53.40671	68.74448	64.67831	1.236287	0.026245	-	-
16.275	17.69464	21.77907	22.81955	1.312896	0.026343	AA873056	Replication protein A (E coli RecA homolog, RAD51 homolog)
80.08463	82.29562	90.2593	88.62492	1.101638	0.02665	R71093	Human mRNA for collagen binding protein 2, complete cds
15.66785	15.1374	18.92866	18.0474	1.200317	0.026678	N68159	Human multidrug resistance-associated protein homolog (MRP5) mRNA, partial cds
20.859	21.6589	27.19119	29.40274	1.331061	0.026797	AA487588	Human mRNA for ORF, Xq terminal portion
18.73655	19.67545	22.8395	22.23996	1.173578	0.026798	AA449738	Homo sapiens protein 4.1-G mRNA, complete cds
45.3586	48.58246	56.84154	58.37243	1.22645	0.02701	-	-
68.63759	70.3948	64.19332	63.42236	0.917885	0.027107	-	-
31.25305	26.90025	46.87265	52.20721	1.70377	0.027154	AA598776	Human p55CDC mRNA, complete cds
67.85542	63.72649	53.01953	50.83924	0.789309	0.027214	-	-
16.36995	18.14875	22.61176	22.49222	1.306653	0.027214	AA454819	EXTRACELLULAR SIGNAL-REGULATED KINASE 1
22.47479	22.69051	27.97646	26.43292	1.204672	0.027268	R17765	Biotinidase
10.97317	12.28621	15.8445	15.4785	1.346682	0.027406	R77517	Human CDK inhibitor p19INK4d mRNA, complete cds
20.95607	20.58239	25.9527	24.48499	1.214241	0.027763	W04674	Homo sapiens mRNA for cytochrome b5, partial cds

13.24626	16.0133	24.24163	22.95284	1.612959	0.027766	AA709143	H.sapiens mRNA for TTF-I
14.53086	14.11347	16.74931	17.64094	1.200595	0.028124	T98019	Human Br140 mRNA, complete cds
15.11686	16.15493	18.73582	19.23424	1.214195	0.028305	R55490	Human phospholipase c delta 1 mRNA, complete cds
82.05017	88.51693	111.2574	106.3696	1.275903	0.028412	AA702254	Major histocompatibility complex, class II, DN alpha
13.31261	13.34946	15.3432	14.74962	1.128675	0.028761	AA676590	Homo sapiens TTAGGG repeat binding factor 2 (hTRF2) mRNA, complete cds
13.53515	15.01674	18.47763	18.75114	1.303899	0.028851	AA757754	Homo sapiens mRNA for dihydropyrimidinase related protein 4, complete cds
32.17749	33.25982	28.15446	26.65073	0.837522	0.029049	H85355	ATPase, Ca++ transporting, cardiac muscle, slow twitch 2
45.75406	46.19835	43.57596	42.68773	0.938134	0.029152	AA670438	UBIQUITIN CARBOXYL-TERMINAL HYDROLASE ISOZYME L1
22.6785	21.41181	31.72049	29.07421	1.378868	0.029489	AA032090	Homo sapiens actin-related protein Arp2 (ARP2) mRNA, complete cds
9.530775	11.5589	17.40649	16.44489	1.605116	0.029569	T73558	Human DNase1-Like III protein (DNAS1L3) mRNA, complete cds
18.6771	18.99872	20.5869	20.15266	1.081318	0.029729	H29475	Homo sapiens pyruvate dehydrogenase kinase isoenzyme 2 (PDK2) mRNA, complete cds
14.57061	15.54405	17.75203	17.97358	1.186319	0.03023	R83224	Human ras inhibitor mRNA, 3' end
83.10598	78.548	62.84057	66.39386	0.799451	0.030341	W46577	H.sapiens mRNA for ESM-1 protein
84.66875	76.44045	56.2244	51.40948	0.66808	0.030344	AA448396	Heat shock 10 kD protein 1 (chaperonin 10)
37.48755	38.34005	45.39497	43.26732	1.169262	0.030444	H57136	Human phospholemman chloride channel mRNA, complete cds
14.15599	14.98015	18.04261	19.24852	1.279892	0.030615	AA775378	N-acetylglucosaminyltransferase I
82.22938	87.82484	101.4247	100.3887	1.186759	0.030637	AA425861	Human peroxisomal enoyl-CoA hydratase-like protein (HPXEL) mRNA, complete cds
11.64434	13.31599	17.14451	17.83238	1.4013	0.031058	AA125981	Activin A receptor, type II
21.97884	23.2192	25.98003	26.10156	1.152297	0.031252	AA598978	Filamin 1 (actin-binding protein-280)
9.91296	10.8484	15.74301	17.88272	1.61963	0.031409	H96235	V-ets avian erythroblastosis virus E26 oncogene homolog 2
36.19658	37.39864	33.21386	33.53209	0.906933	0.031415	AA027012	Kinase insert domain receptor (a type III receptor tyrosine kinase)
29.17678	27.70456	33.35908	32.60837	1.159738	0.031524	R56638	Glutaryl-Coenzyme A dehydrogenase
14.66517	15.24825	21.08112	19.26586	1.348792	0.031808	N35888	Phosphomannomutase 2
13.8279	15.03698	18.58936	19.85551	1.331891	0.031812	AA496334	DYNAMIN-1
11.39412	12.75156	15.70726	15.94188	1.310757	0.032092	AA683520	ANTILEUKOPROTEINASE 1 PRECURSOR
9.284274	11.0507	15.55734	16.95524	1.59885	0.032557	AA180013	Human mRNA for HGF activator like protein, complete cds
120.1432	116.808	91.86152	99.60838	0.808056	0.032712	AA187148	Core-binding factor, beta subunit
29.28212	29.53973	33.69324	35.62598	1.17846	0.032813	T52362	H.sapiens mRNA for Icln protein
12.62167	12.3043	15.16462	16.35209	1.264413	0.033065	R62813	Human L-myc protein gene, complete cds
12.32508	12.00672	13.92138	13.44971	1.124911	0.033314	R89082	Homo sapiens A-kinase anchoring protein (AKAP18) mRNA, complete cds
19.14025	18.79995	27.85192	25.06118	1.394645	0.033495	T59245	S-ADENOSYLMETHIONINE SYNTHETASE GAMMA FORM

11.68684	11.55691	14.19041	15.37657	1.27204	0.033816	AA777289	Glutathione reductase
11.40516	12.89907	16.93159	16.19207	1.362877	0.033916	AA149097	Hemopoietic cell kinase
111.214	101.8281	62.51724	73.64225	0.63912	0.034024	N74956	RNA polymerase II polypeptide B (140 kD)
37.64903	32.92124	22.32711	23.01163	0.642462	0.034027	R38194	Human mRNA for LZTR-1, complete cds
459.5402	409.521	597.1828	648.7151	1.433614	0.034453	H54023	Homo sapiens monocyte/macrophage Ig-related receptor MIR-10 (MIR cl-10) mRNA, complete cds
59.87162	55.82647	32.1758	39.54386	0.619886	0.034642	H23197	Human mRNA for MOBP (myelin-associated oligodendrocytic basic protein), complete cds
19.80885	19.08847	26.37321	29.56803	1.438177	0.034996	AA419264	Homo sapiens hair and skin epidermal-type 12-lipoxygenase-related protein (ALOX12E) mRNA
29.98141	34.71095	48.09765	53.39613	1.568868	0.035285	AA701455	Human CENP-F kinetochore protein mRNA, complete cds
26.99895	30.46287	40.42197	44.43633	1.476777	0.035476	AA487460	Human mRNA for dihydropyrimidinase related protein-2, complete cds
1823.974	1897.418	1239.798	1429.806	0.717367	0.035524	AA293218	Cleavage stimulation factor, 3' pre-RNA, subunit 2, 64kD
12.29707	12.53	15.78503	17.38515	1.336049	0.035571	H86518	X-arrestin
22.55051	23.87862	27.55155	28.99762	1.217967	0.035641	AA394127	Homo sapiens NF-AT3 mRNA, complete cds
48.95605	48.2176	46.20174	45.40618	0.942724	0.035994	AA443547	TRANSCRIPTION FACTOR P65
23.36412	21.59025	28.61167	27.38745	1.245688	0.036035	AA456570	H.sapiens mRNA for interferon regulatory factor 3
12.93649	14.34749	17.32881	17.20979	1.265893	0.03605	AA430178	Homo sapiens Ran binding protein 2 (RanBP2alpha) mRNA, partial cds
35.67819	36.25628	50.52037	57.61499	1.503248	0.036556	AA446453	Human mRNA for c-myc binding protein, complete cds
58.31607	61.65066	69.13112	68.30519	1.14562	0.036563	AA157813	INTERFERON-ALPHA INDUCED 11.5 KD PROTEIN
11.50147	13.27703	16.81222	17.07402	1.367566	0.036707	AA444049	Human MAP kinase phosphatase (MKP-2) mRNA, complete cds
11.30327	12.61007	15.8655	17.07348	1.377432	0.036746	N35067	Human cdc2-related protein kinase (CHED) mRNA, complete cds
31.58377	32.25889	36.77875	35.29086	1.128863	0.037253	AA454810	Membrane component, chromosome 1, surface marker 1
24.60914	24.42533	29.79488	32.40404	1.268473	0.037283	AA180007	Protein kinase, cAMP-dependent, regulatory, type II, beta
27.87648	26.96707	34.00312	31.97973	1.203111	0.037446	AA485913	Human nuclear chloride ion channel protein (NCC27) mRNA, complete cds
12.8329	13.87053	15.94357	16.3778	1.210383	0.037828	AA708161	Human scr3 mRNA for RNA binding protein SCR3, complete cds
25.11428	24.38132	28.04803	29.48606	1.162408	0.038032	H78385	Human huntingtin interacting protein (HIP2) mRNA, complete cds
13.68521	14.87289	17.46576	18.29301	1.252141	0.038109	AA487593	Transferrin receptor (p90, CD71)
13.88883	13.36036	16.3021	17.52736	1.241485	0.038747	AA600217	CAMP-dependent transcription factor ATF-4 (CREB2)
15.99237	17.40953	21.22475	20.34448	1.244517	0.039282	AA487148	Human TBP-associated factor (hTAFII130) mRNA, partial cds
19.6487	22.8455	30.0211	32.63452	1.474451	0.039477	AA485653	Human beta-1,2-N-acetylglucosaminyltransferase II (MGAT2) gene, complete cds
12.87959	13.21833	16.66987	18.51198	1.348071	0.039981	AA447593	Homo sapiens axonemal dynein light chain (hp28) mRNA, complete cds
59.09829	60.86134	84.12417	75.99251	1.334755	0.040352	T65786	PRE-MRNA SPLICING FACTOR SF2, P33 SUBUNIT
25.22532	26.71258	22.11491	22.51497	0.859293	0.041658	AA683578	ADENOSINE DEAMINASE

26.27655	24.07382	32.948	31.05993	1.271251	0.042282	N23454	Ubiquitin-activating enzyme E1, like
46.05216	50.63513	67.22026	62.01856	1.336668	0.042488	-	-
64.51113	59.33324	74.1574	73.91723	1.195651	0.042844	-	-
12.98688	14.48746	19.47726	17.95394	1.362406	0.043156	W51760	Fibroblast growth factor 2 (basic)
219.2486	204.176	114.5668	146.362	0.616234	0.04383	-	-
10.99637	11.68638	14.47818	16.03376	1.345161	0.04414	N45141	ADENYLATE CYCLASE, TYPE II
11.70176	12.9816	15.34002	15.24312	1.239018	0.044213	R12373	Paraoxonase 1
20.60713	24.18667	31.92885	30.52933	1.394349	0.044224	AA487582	EXT1
10.39533	11.19881	13.32046	14.38266	1.2829	0.044391	AA702663	Human myosin-IXb mRNA, complete cds
571.1043	553.2296	404.8496	319.4926	0.644241	0.044394	T53298	Prostacyclin-stimulating factor [human, cultured diploid fibroblast cells, mRNA, 1124 nt]
24.2576	21.07047	35.16807	31.7123	1.475474	0.044431	R60847	H.sapiens mRNA for TFG protein
11.17431	12.77589	15.86511	16.94966	1.370125	0.04446	AA055486	Homo sapiens ataxia-telangiectasia group D-associated protein mRNA, complete cds
15.20577	13.00471	20.11916	22.30718	1.503921	0.044505	AA481554	Human ERPROT 213-21 mRNA, complete cds
52.18162	49.89176	57.6968	60.32594	1.156254	0.044612	-	-
14.32816	15.47386	20.21347	18.60559	1.302565	0.044747	AA857212	Galactose-1-phosphate uridyl transferase
15.27714	17.40102	22.64832	25.21208	1.464599	0.044874	AA488681	Human mRNA for rab GDI alpha, complete cds
124.9324	136.2994	72.31894	90.68338	0.623976	0.045098	H69561	Mannosidase, alpha type II
19.46156	19.38244	24.53968	27.43002	1.337908	0.045257	R45640	Diphtheria toxin receptor (heparin-binding epidermal growth factor-like growth factor)
53.02629	55.26104	67.47205	74.56885	1.311704	0.045313	-	-
12.36903	12.64076	16.27642	18.38896	1.386073	0.045375	AA159577	Mucin 5, subtype B, tracheobronchial
24.41258	30.30908	40.9738	40.53666	1.489547	0.045422	AA431321	Homo sapiens thyroid receptor interactor (TRIP7) mRNA, 3' end of cds
16.30796	18.26048	24.87257	22.74569	1.377507	0.045625	AA490945	Homo sapiens secretory carrier-associated membrane protein (SCAMP) mRNA, complete cds
13.14567	13.70386	17.69657	16.22872	1.263534	0.045893	H08545	Homo sapiens potassium channel homolog (KCNQ3) mRNA, partial cds
21.6216	22.01372	38.80142	32.63003	1.63701	0.046098	AA663981	Human Ig germline H-chain G-E-A region B: gamma-2 constant region, 3' end
15.62038	14.66827	17.82916	18.90073	1.212662	0.046125	AA173926	Homo sapiens mRNA for putative glucosyltransferase, partial cds
72.4865	75.75304	81.2518	81.93709	1.100846	0.046404	-	-
17.56159	16.63121	14.94582	15.05702	0.877461	0.046547	AA875888	BRAIN NEURON CYTOPLASMIC PROTEIN 1
17.94749	16.29775	20.79573	21.54375	1.236361	0.046608	R54807	Human beta-sarcoglycan A3b mRNA, complete cds
23.24825	17.70674	32.83718	32.84879	1.603858	0.046718	AA173369	Human mitochondrial ATP synthase subunit 9, P3 gene copy, mRNA
13.70688	14.02148	15.81686	16.89613	1.179767	0.047285	T63988	Human mRNA for DB1, complete cds
60.13647	65.13849	73.42034	74.57603	1.181372	0.047447	-	-

58.84769	62.85428	84.16513	76.34862	1.318908	0.04759	-	-
21.58536	22.57456	35.16831	30.41148	1.485052	0.047792	N59150	INTERFERON-ALPHA/BETA RECEPTOR ALPHA CHAIN PRECURSOR
257.6779	282.1547	205.3771	216.3273	0.781176	0.047858	AA890663	Human protein kinase PAK1 mRNA, complete cds
11.93706	14.16259	18.20345	19.69386	1.452024	0.047874	AA052960	Human Cbf5p homolog (CBF5) mRNA, complete cds
11.93086	13.51221	17.18016	19.05956	1.424346	0.048054	R23735	Human R kappa B mRNA, complete cds
11.69299	13.05967	16.11937	17.67079	1.365112	0.048557	H12338	Homo sapiens DNAX activation protein 12 (DAP12) mRNA, complete cds
21.37391	22.0031	28.41784	25.96556	1.253738	0.04905	AA433944	H.sapiens mRNA for mediator of receptor-induced toxicity
4529.848	4593.677	3008.337	3587.713	0.722972	0.049286	AA709414	Nidogen (enactin)
19.32836	18.8765	24.75206	28.11089	1.383671	0.04952	AA447761	Aminolevulinate, delta-, synthase 1
14.38522	16.87973	20.94944	21.10651	1.345147	0.049685	R56562	Human lunatic fringe mRNA, partial cds
12.90092	14.18309	19.29533	17.45546	1.356918	0.049829	N33574	Homo sapiens growth inhibitor p33ING1 (ING1) mRNA, complete cds
14.98717	17.49183	22.61318	25.1479	1.470521	0.050304	AA626867	ER LUMEN PROTEIN RETAINING RECEPTOR 2
62.02984	82.8975	122.8191	115.9648	1.647611	0.050642	R47893	TONSILLAR LYMPHOCYTE LD78 BETA PROTEIN PRECURSOR
20.47757	17.30179	25.54171	26.78405	1.385035	0.050806	R15814	Human malate dehydrogenase (MDHA) mRNA, complete cds
13.59585	11.97833	16.26887	17.14702	1.306626	0.050918	AA055979	Integrin, alpha 7B

Appendix II

Hyperlink data of interaction hits: Hybrigenics 1st screen LANA1 N-terminus aa1-337

KIAA0742
http://www.ncbi.nlm.nih.gov/entrez/query.fcgi?cmd=Retrieve&db=nucleotide&list_uids=17433931&dopt=GenBank

KIAA1513
http://www.ncbi.nlm.nih.gov/entrez/query.fcgi?cmd=Retrieve&db=nucleotide&list_uids=14736708&dopt=GenBank

KIAA0570
http://www.ncbi.nlm.nih.gov/entrez/query.fcgi?cmd=Retrieve&db=protein&list_uids=3043664&dopt=GenPept

KIAA0793
http://www.ncbi.nlm.nih.gov/entrez/query.fcgi?cmd=Retrieve&db=nucleotide&list_uids=3882306&dopt=GenBank

KIAA0120
http://www.ncbi.nlm.nih.gov/entrez/query.fcgi?cmd=Retrieve&db=nucleotide&list_uids=434762&dopt=GenBank

KIAA0045
http://www.ncbi.nlm.nih.gov/entrez/query.fcgi?cmd=Retrieve&db=nucleotide&list_uids=460710&dopt=GenBank

KIAA0057
http://www.ncbi.nlm.nih.gov/entrez/query.fcgi?cmd=Retrieve&db=nucleotide&list_uids=498149&dopt=GenBank

KIAA1119
http://www.ncbi.nlm.nih.gov/entrez/query.fcgi?cmd=Retrieve&db=nucleotide&list_uids=6329707&dopt=GenBank

NPI-1 - nucleoprotein interactor 1-SRP1 homolog
http://www.ncbi.nlm.nih.gov/entrez/query.fcgi?cmd=Retrieve&db=nucleotide&list_uids=913392&dopt=GenBank

Human hsp27 ERE-TATA-binding protein (HET) Related= SAF-B
http://www.ncbi.nlm.nih.gov/entrez/query.fcgi?cmd=Retrieve&db=nucleotide&list_uids=2828536&dopt=GenBank

Homo sapiens mRNA for CDEP
http://www.ncbi.nlm.nih.gov/entrez/query.fcgi?cmd=Retrieve&db=nucleotide&list_uids=2766164&dopt=GenBank

Homo sapiens actinin, alpha 4 (ACTN4)
http://www.ncbi.nlm.nih.gov/entrez/query.fcgi?cmd=Retrieve&db=nucleotide&list_uids=12025677&dopt=GenBank

EUROIMAGE 1654781
http://www.ncbi.nlm.nih.gov/entrez/query.fcgi?cmd=Retrieve&db=nucleotide&list_uids=17066293&dopt=GenBank

Homo sapiens similar to unnamed protein product (LOC90102)
http://www.ncbi.nlm.nih.gov/entrez/query.fcgi?cmd=Retrieve&db=nucleotide&list_uids=17435685&dopt=GenBank

Homo sapiens hypothetical gene supported by AK00209 (LOC92751)
http://www.ncbi.nlm.nih.gov/entrez/query.fcgi?cmd=Retrieve&db=nucleotide&list_uids=17487840&dopt=GenBank

HUMELIA Human structural protein 4.1
http://www.ncbi.nlm.nih.gov/entrez/query.fcgi?cmd=Retrieve&db=nucleotide&list_uids=182075&dopt=GenBank

Human putative monocarboxylate transporter (MCT)
http://www.ncbi.nlm.nih.gov/entrez/query.fcgi?cmd=Retrieve&db=nucleotide&list_uids=2463627&dopt=GenBank

Homo sapiens Fas binding protein (hDaxx)
http://www.ncbi.nlm.nih.gov/entrez/query.fcgi?cmd=Retrieve&db=nucleotide&list_uids=2724133&dopt=GenBank

Homo sapiens ras GTPase-activating-like protein (IQGAP1)
http://www.ncbi.nlm.nih.gov/entrez/query.fcgi?cmd=Retrieve&db=nucleotide&list_uids=536843&dopt=GenBank
http://www.ncbi.nlm.nih.gov/entrez/query.fcgi?cmd=Retrieve&db=PubMed&list_uids=8051149&dopt=Abstract

Homo sapiens EH-domain containing protein testilin
http://www.ncbi.nlm.nih.gov/entrez/query.fcgi?cmd=Retrieve&db=nucleotide&list_uids=5639664&dopt=GenBank

Homo sapiens cDNA FLJ11046 fis
http://www.ncbi.nlm.nih.gov/entrez/query.fcgi?cmd=Retrieve&db=nucleotide&list_uids=7023465&dopt=GenBank

Contig number	Contig member	Sequence I.D.	Percentage match vs Genbank sequence
Contig918348	2	gi|8922841|ref|NM_018309.1| Homo sapiens hypothetical protein FLJ11046 (FLJ11046), mRNA	100.0
Contig918362	2	gi|7706636|ref|NM_016166.1| Homo sapiens DEAD/H (Asp-Glu-Ala-Asp/His) box binding protein 1 (DDXBP1), mRNA	100.0
Contig918353	2	gi|7706636|ref|NM_016166.1| Homo sapiens DEAD/H (Asp-Glu-Ala-Asp/His) box binding protein 1 (DDXBP1), mRNA	99.0
Contig918329	6	gi|7662309|ref|NM_014808.1| Homo sapiens KIAA0793 gene product (KIAA0793), mRNA	99.3
Contig918257	1	gi|7662185|ref|NM_014709.1| Homo sapiens KIAA0570 gene product (KIAA0570), mRNA	100.0
Contig918240	1	gi|6912449|ref|NM_012288.1| Homo sapiens TRAM-like protein (KIAA0057), mRNA	98.8
Contig918236	1	gi|6912449|ref|NM_012288.1| Homo sapiens TRAM-like protein (KIAA0057), mRNA	98.4
Contig918260	1	gi|6329707|dbj|AB032945.1|AB032945 Homo sapiens mRNA for KIAA1119 protein, partial cds	99.1
Contig918368	1	gi|5803008|ref|NM_006795.1| Homo sapiens EH domain containing 1 (EHD1), mRNA	97.6
Contig918356	1	gi|5803008|ref|NM_006795.1| Homo sapiens EH domain containing 1 (EHD1), mRNA	100.0
Contig918333	6	gi|5031632|ref|NM_005766.1| Homo sapiens FERM, RhoGEF (ARHGEF) and pleckstrin domain protein 1 (chondrocyte-derived) (FARP1), mRNA	100.0
Contig918352	6	gi|5031632|ref|NM_005766.1| Homo sapiens FERM, RhoGEF (ARHGEF) and pleckstrin domain protein 1 (chondrocyte-derived) (FARP1), mRNA	98.7
Contig918365	1	gi|4759113|ref|NM_004696.1| Homo sapiens solute carrier family 16 (monocarboxylic acid transporters), member 4 (SLC16A4), mRNA	100.0
Contig918350	1	gi|4759113|ref|NM_004696.1| Homo sapiens solute carrier family 16 (monocarboxylic acid transporters), member 4 (SLC16A4), mRNA	95.0
Contig918241	1	gi|4758647|ref|NM_004521.1| Homo sapiens kinesin family member 5B (KIF5B), mRNA	93.8

Contig918251	1	gi|4758647|ref|NM_004521.1| Homo sapiens kinesin family member 5B (KIF5B), mRNA	99.4
Contig918279	1	gi|4758273|ref|NM_004437.1| Homo sapiens erythrocyte membrane protein band 4.1 (elliptocytosis 1, RH-linked) (EPB41), mRNA	97.9
Contig918264	2	gi|4507356|ref|NM_003564.1| Homo sapiens transgelin 2 (TAGLN2), mRNA	99.7
Contig918364	6	gi|4506786|ref|NM_003870.1| Homo sapiens IQ motif containing GTPase activating protein 1 (IQGAP1), mRNA	100.0
Contig918314	6	gi|4506786|ref|NM_003870.1| Homo sapiens IQ motif containing GTPase activating protein 1 (IQGAP1), mRNA	99.6
Contig918363	2	gi|4506778|ref|NM_002967.1| Homo sapiens scaffold attachment factor B (SAFB), mRNA	97.9
Contig918358	2	gi|4506778|ref|NM_002967.1| Homo sapiens scaffold attachment factor B (SAFB), mRNA	99.5
Contig918321	6	gi|4504894|ref|NM_002264.1| Homo sapiens karyopherin alpha 1 (importin alpha 5) (KPNA1), mRNA	98.8
Contig918345	6	gi|4504894|ref|NM_002264.1| Homo sapiens karyopherin alpha 1 (importin alpha 5) (KPNA1), mRNA	99.3
Contig918232	1	gi|4503256|ref|NM_001350.1| Homo sapiens death-associated protein 6 (DAXX), mRNA	93.4
Contig918229	1	gi|4503256|ref|NM_001350.1| Homo sapiens death-associated protein 6 (DAXX), mRNA	90.5
Contig918287	1	gi|17487840|ref|XM_047062.3| Homo sapiens hypothetical gene supported by AK002209 (LOC92751), mRNA	100.0
Contig918310	1	gi|17487840|ref|XM_047062.3| Homo sapiens hypothetical gene supported by AK002209 (LOC92751), mRNA	100.0
Contig918347	2	gi|17455349|ref|XM_047641.2| Homo sapiens high-mobility group 20B (HMG20B), mRNA	99.8
Contig918342	2	gi|17455349|ref|XM_047641.2| Homo sapiens high-mobility group 20B (HMG20B), mRNA	98.9
Contig918298	1	gi|17445723|ref|XM_033706.3| Homo sapiens erythrocyte membrane protein band 4.1 (elliptocytosis 1, RH-linked) (EPB41), mRNA	99.4
Contig918308	7	gi|17435685|ref|XM_028958.2| Homo sapiens similar to unnamed protein product (LOC90102), mRNA	99.7
Contig918233	1	gi|17433931|ref|XM_034072.3| Homo sapiens KIAA0742 protein (KIAA0742),	99.7

		mRNA	
Contig918227	1	gi|17433931|ref|XM_034072.3| Homo sapiens KIAA0742 protein (KIAA0742), mRNA	99.0
Contig918311	2	gi|17066293|emb|AJ420429.1|HSA420429 Homo sapiens mRNA full length insert cDNA clone EUROIMAGE 1654781	98.8
Contig918346	1	gi|14736714|ref|XM_043758.1| Homo sapiens KIAA1513 protein (KIAA1513), mRNA	99.4
Contig918243	1	gi|12025677|ref|NM_004924.2| Homo sapiens actinin, alpha 4 (ACTN4), mRNA	98.8
Contig918238	1	gi|12025677|ref|NM_004924.2| Homo sapiens actinin, alpha 4 (ACTN4), mRNA	99.7
Contig918369	1	gi|10863902|ref|NM_004238.1| Homo sapiens thyroid hormone receptor interactor 12 (TRIP12), mRNA	99.7
Contig918366	1	gi|10863902|ref|NM_004238.1| Homo sapiens thyroid hormone receptor interactor 12 (TRIP12), mRNA	96.5